THE EFFECTS OF EXPERIMENTAL OUTFLOW OBSTRUCTION ON THE DEVELOPING BLADDER

by

Nikesh Thiruchelvam

The Nephro-Urology Unit

Institute of Child Health

University College London

30 Guilford Street

London WC1N 1EH

A thesis submitted to the University of London

for the degree of Doctor of Medicine

2003

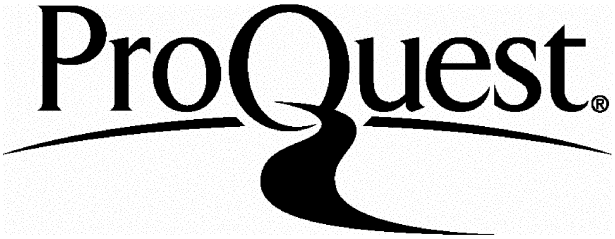

1. Abstract

In utero bladder outflow obstruction (BOO) of the human developing bladder, commonly caused by posterior urethral valves, produces significant bladder dysfunction with symptoms of urinary incontinence, poor bladder emptying and urinary tract infection. Furthermore, many of these boys suffer significant renal impairment. To investigate the antenatal events that lead to this postnatal dysfunction, I have used an experimental fetal ovine model of in utero BOO.

I found that the obstructed fetal bladder became larger, heavier and had grown; this was accompanied by an increase in proliferation and apoptosis within the detrusor muscle layer and an increase of apoptosis with no increase in proliferation within the lamina propria layer. Also documented was a downregulation of the anti-death protein Bcl-2 and an upregulation of the pro-death protein Bax. Moreover, activated caspase-3, an effector of apoptotic death, was increased in obstructed bladders.

I found the obstructed fetal bladder became hypocontractile and denervated and exhibited greater atropine-resistant contractions. Nitric oxide-mediated relaxations were also present. In addition, I observed increased compliance and reduced elasticity and viscoelasticity in the obstructed fetal bladder.

My results suggest that enhanced apoptosis in detrusor smooth muscle cells appeared to be a part of a remodelling response during compensatory hyperplasia and hypertrophy. In the lamina propria, an imbalance between death and proliferation led to a relative

depletion of cells. Furthermore, the obstructed fetal bladder became hypocontractile; in addition to denervation, this may result from a reduction in the elastic modulus that may prevent any extramuscular components from sustaining force.

These discoveries provide insight into why the fetal bladder functions poorly postnatally when exposed to bladder outflow obstruction and suggests potential molecular avenues for fetal bladder manipulation. Future strategies will characterise the in vivo pressure changes after obstruction, contractile properties of isolated detrusor myocytes and changes in the 'deobstructed' obstructed fetal bladder.

Table of Contents

List of Figures

List of Tables

Abbreviations

αSMA	alpha-smooth muscle actin
ACh	acetyl choline
ABMA	α-β methylene-ATP
ADP	adenosine diphosphate
AM	amplitude modulation
Bax	bcl-2 associated X protein
BCA	bicinchoninic acid
Bcl-2	b-cell leukaemia/lymphoma-2
BSA	Bovine serum albumin
DAB	diaminobenzidine tetrahydrochloride
BOO	bladder outflow obstruction
cGMP	cyclic guanosine 3',5'-monophosphate
d	bladder wall thickness
°C	degrees Celsius
Ca^{2+}	calcium
CO_2	carbon dioxide
DEM	data exchange matrix
DNA	deoxyribose nucleic acid
EC_{50}	concentration required to achieve $T_{max}/2$
ECL	enhanced chemiluminescence
EFS	electrical filed stimulation

ESRF	end-stage renal failure
f	frequency of stimulation
FCS	fetal calf serum
FITC	fluorescein-isothiocyanate
HEPES	N-[2-hydroxyethyl]piperazine-N'-[2-ethanesulphonic acid]
IM	immature void
$K_{1/2}$	frequency required to achieve $T_{max}/2$
HRP	horseradish peroxidase
MHC	myosin heavy chain
NaCl	sodium chloride
NO	nitric oxide
O_2	oxygen
ODQ	1H-[1,2,4]oxadiazolo[4,3-a]quinoxalin-1-one
P	luminal pressure
PARP	poly (ADP-ribose) polymerase
PBS	prune belly syndrome
PCNA	proliferating cell nuclear antigen
PI	propidium iodide
pEC_{50}	logarithmic transform of $K_{1/2}$
PGP 9.5	protein gene product 9.5
p$K_{1/2}$	logarithmic transform of $K_{1/2}$
PUV	posterior urethral valves
r_1	inner radius of the bladder

RNA	ribose nucleic acid
σ	wall stress
S	agonist concentration
SDS	sodium dodecyl sulphate
SMC	smooth muscle cell
ST	stacatto activity in trains
SV	stacatto activity pre- and post-void
SR	sarcoplasmic reticulum
τ_1 and τ_2	time constants
T	Tension
T'	visco-elastic components of the total change of stress with τ_1
T''	visco-elastic components of the total change of stress with τ_2
T_1	steady-state elastic components for the period of stretch
T_2	steady-state elastic components for the period of relaxation
T_{max}	the estimated maximum tension at high frequencies or high concentrations
$T(t)$	the visco-elastic changes of stress
T_v	bladder tissue volume
TCC	transitional cell carcinoma
TEMED	N,N,N-N-tetramethylethylenediamine
Tespa	3-aminopropyltriethoxysilane
TTX	Tetrodotoxin
TUNEL	deoxynucleotidyltransferase-mediated uridinetriphosphate (UTP) nick end-labelling

U	unstable type bladder activity
UTP	uridinetriphosphate
UV	ultra-violet
W_v	work in deforming the viscous component
W_e	work in deforming the elastic component
V	volume in bladder

2. Introduction

The urinary bladder, hereforth simply called 'the bladder' is a dynamic organ that is able to collect urine excreted by the kidneys and store it securely within the body. When the time is appropriate, contraction of the bladder muscular wall, causing a rapid rise in its internal pressure, and simultaneous relaxation of its outlet, allows urine to be expelled via the urethra. It then empties to completion before outlet closure and then relaxes again to start the next filling cycle. During fetal development, obstruction to this outlet from whatever cause, results in significant postnatal bladder dysfunction, despite antenatal and postnatal intervention. By far the commonest cause of in utero bladder outflow obstruction (BOO) is posterior urethral valves (PUV), other causes include the Prune-Belly syndrome, urethral atresia, syringocoeles and Cowper's gland cysts. In my thesis, in order to understand these postnatal events, I aim to determine the prenatal events that occur in the bladder exposed to urinary outflow obstruction. My studies were based on the hypotheses that in utero BOO results in a) significant alteration to the cell turnover with deregulation of proliferation, apoptosis and apoptotic regulatory protein expression and b) significant perturbation to contractility, neurotransmission and the physical properties of the developing fetal bladder. To do this, I aimed to procure fetal bladder samples from an experimental fetal ovine model of in utero BOO. This is a useful model as the fetus is of considerable size that is able to tolerate in utero surgery. Furthermore, numerous investigators have described how experimental fetal ovine urinary tract manipulation is able to mimic human disease. I also aimed to describe the changes to organ growth and cell turnover in the developing and obstructed fetal bladder, identify molecules involved in neurotransmission in the fetal bladder and discover the changes to

contractility, neurotransmission and the physical characteristics in the obstructed fetal bladder. In this section, I describe the primary causes of human in utero BOO, the embryological development of the human and ovine urinary tract and PUV, innervation of the human bladder, experimental strategies of determining in utero effects of BOO on the fetal bladder and current understanding of the molecular biology, in particular, cell proliferation and apoptosis, and physiology, of the developing and obstructed fetal bladder.

2.1 Posterior urethral valves

2.1.1 Definition

PUV result from a membranous obstruction (Figure 1) to the developing fetal urethra, and is unique to males. The incidence of PUV is approximately 1 in 5,000 male births (Cuckow, 1998; Woolf and Thiruchelvam, 2001) but this figure may change because i) increasing numbers are detected prenatally and ii) the most severe of these may be terminated before birth. PUV have been classified as (Figure 2): type I PUV are folds extending inferiorly from the verumontanum to the membranous urethra; type II PUV are leaflets or folds radiating from the verumontanum up to the bladder neck; type III PUV are concentric diaphragms, with a central lumen found within the prostatic urethra (Young and Frantz, 1919). However, as there is no clear difference in the presentation or management of these different types, the usefulness of such a classification system remains in doubt.

2.1.2 Diagnosis and presentation

With increased use of antenatal screening, prenatal diagnosis of PUV is made in 50 % of cases found to have to have PUV postnatally; fetal PUV ultrasonographic findings (Figure 3) are hydroureteronephrosis, a distended bladder, and a dilated posterior urethra (Hutton et al, 1997). Postnatally, the diagnosis of PUV must be confirmed by the micturating cystourethrogram (Figure 4); this contrast study, performed via a urethral or suprapubic catheter, usually shows the dilated, obstructed posterior urethra as well as hypertrophy of the bladder neck, an irregular bladder outline and any associated vesicoureteric reflux. The 'classical' presentation of PUV, however, is within the first year of life (Cuckow, 1998). Presentation at birth includes abdominal masses (distended bladder, hydronephrosis), respiratory distress from pulmonary hypoplasia (secondary to the oligohydramnios of obstructive uropathy) and urinary ascites. Others cases present within the neonatal period with urinary infection, electrolyte disturbance and dehydration. Later presentation within the first year of life includes failure to thrive, renal failure and urosepsis.

2.1.3 PUV fetal bladder morphology

Histological and prenatal ultrasound studies of PUV fetal bladders have documented varied morphological characteristics. Freedman et al (Freedman et al, 1997) in a study of human fetuses with BOO (six of the nine fetuses studied had PUV with a mean gestation of 29 weeks), documented thickened bladder walls, associated with increased smooth muscle and collagen, as assessed by computer-assisted image analysis of stained bladders sections; all but two of the fetuses studied had histologically-proven renal dysplasia. Kim

et al (1991b) studied seven obstructed fetal bladders with PUV (mean gestation 26 weeks) and using a grid and point-count technique of stained bladder sections, also reported increased muscle thickness, but with a decrease in collagen content relative to muscle. Finally, Workman and Kogan (1990) also found increased muscle thickness in their study of four human fetal PUV bladders (mean gestation 27 weeks) as determined by a grid and point-count technique of stained bladder sections, but found no increase in connective tissue deposition.

Studies suggest that the presence of oligohydramnios and megacystis (an enlarged fetal bladder) on antenatal ultrasound imaging are highly predictive of a diagnosis of fetal urethral obstruction (Oliveira et al, 2000). However, despite an increasing trend of antenatal detection of dilated bladders (Cuckow, 1998), it remains impossible to distinguish definitely, prenatal posterior urethral valves from other causes of in utero bladder distension and oligohydramnios (Callan et al, 1990; Golbus et al, 1982). Abbott et al (1998) in their study of antenatal megacystis and hydroureteronephrosis confirmed PUV postnatally in only 42 % of cases. Similarly, Holmes et al (2001) in their study of fetal intervention for presumed obstructive uropathy found, postnatally, only 39 % of cases had PUV. Other causes resulting in megacystis include PBS, urethral fibrostenosis, cloacal anomalies, ureteral duplication, vesico-ureteric reflux and urethral atresia. Interestingly, large, thinwalled bladders detected on antenatal ultrasound imaging have also been described in the megacystis-megaureter association; this pathology results in large fetal bladders due to the constant recycling of massive amounts of refluxed urine (Mandell et al, 1992). It is possible that minor forms of obstruction tend not to produce

detectable dilatation early in the second trimester and those cases detected by the fetal anomaly scan may represent the severe end of the obstructed spectrum (Thomas, 2001). This is in keeping with the histological study by Volmar et al (2001) that found that a kink in the urethra or severe valve obstruction produced thin, dilated bladders whereas typical mild PUV bladders resulted in thickened dilated bladders. This is also consistent with antenatal ultrasound investigations by McHugo and Whittle (2001) that suggest a severe obstructive insult produces a thin-walled dilated bladder whilst mild intermittent obstruction results in a dilated bladder which is thick walled.

Both histological and radiological investigations suggest that human fetal diseases of obstructive uropathy are created from a wide spectrum of severity of obstructive lesions; this spectrum appears to result in bladder dilatation with varying degrees of bladder wall thickness. These morphological differences influence the range of clinical symptoms seen in boys with PUV (Hendren, 1971).

2.1.4 Fetal management

Antenatal intervention exists in the form of vesicoamniotic shunting and fetal cystoscopy and endoscopic fulguration (Freedman et al, 1999; Herndon et al, 2000). It is, however, unclear whether any fetal intervention improves long term renal or bladder function or prevents lung hypoplasia since prospective studies randomised to control or active treatment are yet to be achieved.

2.1.5 Postnatal treatment

The mainstay of postnatal management is early bladder drainage by a urethral or suprapubic catheter; this is accompanied by, if necessary, treatment of urosepsis, renal insufficiency, dehydration and electrolyte disturbances. Once the child is stable, valve ablation by cystoscopy is performed (Smith et al, 1996).

Controversy surrounds the issue of the management of PUV in those boys with persistent renal insufficiency despite adequate catheter drainage of the bladder. Urinary diversion with vesicostomy, ureterostomy or pyelostomy has been tried to allow sufficient kidney drainage in an attempt to permit the obstructed renal parenchyma to recover. Investigators (Kim et al, 1996; Krueger et al, 1980; Podesta et al, 2002; Reinberg et al, 1992) have found contrary evidence to suggest whether urinary diversion or primary valve ablation (with expectant follow-up) provides the best renal outcome and which treatment strategy results in better urodynamic function of the bladder and as such, avoid later bladder augmentation.

2.1.6 Bladder dysfunction

Various investigations are available to evaluate bladder function (and primarily dysfunction) in the clinical setting and may be collectively referred to as urodynamics. Urodynamic evaluation includes history and examination of the patient and simple measurements of the volume and frequency of voids; non-invasive tests include bladder and urinary tract ultrasound, performed before and after voiding and uroflowmetry. Measurement of the pressure-volume relationships of the bladder involves a more

invasive approach; pressure inside the bladder is measured by a urethral (or suprapubic) catheter and a second catheter within the abdomen (in most cases placed in the rectum) allows the abdominal component of this to be measured separately and subtracted to give the pressure that is produced by the bladder muscle alone (detrusor pressure). Different types of bladder activity can be derived from these pressures to characterise bladder function and dysfunction.

Despite intervention, by various means, bladder dysfunction in PUV boys, often manifested as incontinence, persists (De Gennaro et al, 1998) (Emir et al, 2002). Three categories of bladder dysfunction have been identified in PUV: i) myogenic bladder failure, characterised by large bladder capacity, large post-micturition residual volumes and poor contractile function; ii) bladder hyperreflexia with instability and iii) small capacity bladders with hypertonia or poor compliance (Bauer et al, 1979; Peters et al, 1990). Subsequent studies have revealed not only a large overlap between these categories but also, that they appear to be time-dependent (De Gennaro et al, 2000; Holmdahl, 1997). Following valve resection, the bladders of these boys tend to be unstable and hypercontractile but later in childhood the bladder capacity increases and the unstable contractions remain and then slowly diminish. Finally, at or around puberty, following years of increased bladder workload, muscle failure sets in leading to large, floppy bladders. Other factors contributing to myogenic failure include the high fluid output caused by renal impairment (Cuckow et al, 1997) and the development of the prostate gland at puberty.

2.1.7 Renal dysfunction

The commonest cause of end-stage renal failure (ESRF) (i.e. chronic renal failure requiring dialysis or renal transplantation) in children is bilateral renal dysplasia, a term that describes organs containing undifferentiated and metaplastic tissues such as smooth muscle and cartilage (Risdon and Woolf, 1998). Just under half the cases of UK childhood ESRF caused by renal dysplasia are associated with urinary tract obstruction, with posterior urethral valves (PUV) being overwhelmingly the commonest specific diagnosis, accounting for one quarter of all boys with ESRF (Lewis, 1999).

Bladder dysfunction is implicated in the aetiology of this renal impairment. Investigators have reported that urinary incontinence after five years of age (Parkhouse et al, 1988) and poor bladder compliance and myogenic failure (Lopez et al, 2002) are closely correlated with poor long term renal outcome. Furthermore, assessments of outcome of renal transplant graft survival into PUV bladders have found variable degrees of success. Several studies report that renal transplantation in patients with PUV has less success than in transplants into patients with normal vesical function (Groenewegen et al, 1993; Reinberg et al, 1988). Others have found no decline in graft survival and long-term renal outcome between the two groups (Crowe et al, 1998; Ross et al, 1994) although graft function does appear to deteriorate.

2.2 Prune-belly syndrome

The diagnosis of prune belly syndrome, or triad syndrome, is made in infants with urinary tract dilatation associated with cryptorchidism and incomplete development of abdominal

wall muscles (Figure 5); the condition affects 1 in 40,000 births (Wheatley et al, 1996). Fetal bladder morphology, as assessed by haematoxylin and eosin stained bladder microspcopy, is variable with thick and thin walled distended bladders observed in human fetuses with PBS (Shimada et al, 2000). Whilst PBS is considered to be an 'obstructive' urinary tract, it is open to debate whether the condition represents either a case of functional urinary flow impairment, such as from a bladder neuromuscular disorder (Volmar et al, 2001), or perhaps results from a transient, fetal physical obstruction of the urethra (Jennings, 2000) (Figure 6). In 75 % of cases, there are associated malformations of the cardiopulmonary, gastrointestinal, and orthopaedic systems (Jennings, 2000) possibly secondary to the oligohydramnios that leads to a limited intrauterine space, causing fetal compression and deformity. With increased prenatal imaging, PBS may be detected antenatally, but as for PUV, in utero intervention (by vesico-amniotic shunting) results in equivocal improvements to renal and bladder function (Irwin and Vane, 2000; Perez-Brayfield et al, 2001; Shimada et al, 2000).

2.3 Embryology of the developing and obstructed urinary tract

2.3.1 Bladder development

The bladder is derived from the cloaca (Cuckow et al, 2001) which forms from the hindgut of the developing human embryo; at around 28 days of gestation, the cloaca is separated by an advancing urorectal septum to form an anterior urogenital sinus (that receives the mesonephric ducts) and a posterior rectum. When this septum reaches the cloacal membrane (during the sixth week of gestation), the latter is divided into a

posterior anal membrane and an anterior urogenital membrane that breaks down in the seventh week.

The superior urogenital sinus forms the primitive bladder and grows together with the anterior abdominal wall; the two structures are connected by the allantois (which connects the apex of the fetal bladder to the umbilical root). The latter forms the urachus which then obliterates around the third-fourth month of fetal life (Bourdelat et al, 1998). By 13 weeks of gestation, the primitive bladder mesenchyme has differentiated discernible circular and longitudinal strands of smooth muscle with distinct muscle layers visible by 16 weeks gestation (Newman and Antonakopoulos, 1989).

During the septation process, the mesonephric ducts become progressively incorporated into the posterior aspect of the primitive bladder. At this time, the ureteric orifices also become incorporated into a more proximal portion of the posterior wall of the bladder with the area between the ureteric orifices and the fused mesonephric ducts forming the bladder trigone. The distal part of the urogenital sinus then forms the posterior urethra with the anterior urethra formed by closure of the urethral folds (Figure 7).

2.3.2 Kidney development

The intermediate mesoderm on the dorsal body wall forms three pairs of developing kidneys (Cuckow et al, 2001): the pronephros, mesonephros and the metanephros; only the latter remains to form the adult kidney. The pronephros forms at day 22 and gives off the pronephric duct that becomes the mesonephric duct at the cloacal wall; the

pronephros then involutes. The mesonephros forms at 24 days of gestation and produces small quantities of urine by the tenth week that drains into the cloaca via the mesonephric duct. The majority of the mesonephros involutes with some remnants (with some of the mesonephric duct) contributing to the development of the epididymis, seminal vesicle and ejaculatory ducts in the male fetus. Prior to this involution, at around 28 days of gestation, each mesonephric duct gives off a ureteric bud. The bud elongates and penetrates the mesenchymal metanephros to form the metanephric blastema. The ureteric bud branches to form the ureter, renal pelvis, calyces and collecting tubules; the mesenchyme creates the cortex of the kidney with the first glomeruli forming by 8-9 weeks of gestation and nephrogenesis continuing until 34-36 weeks gestation (Figure 7).

2.3.3 PUV embryology

It has been hypothesised that PUV arise as a result of the mesonephric ducts entering the cloaca in a more anterior position than normal with migration of the ducts impeded by the enfolding and separation of the cloaca, thus causing the ducts to fuse in the midline anteriorly (Stephens, 1983) (Figure 8). It is also possible that valves result by a failure of complete dissolution of the urogenital membrane (Stephens, 1983) (Figure 8).

2.4 Innervation and neurotransmission in the bladder

2.4.1 Central and peripheral innervation

Micturition or voiding is the process of emptying the bladder. It is a complex chain of events involving the detrusor muscle and the urethral sphincter which are activated by

autonomic nerves in the bladder and somatic and autonomic nerves in the sphincter (the urethral sphincter has smooth as well as skeletal muscle and therefore an autonomic as well as a somatic innervation); these events are influenced by the central nervous system (George, 2001). As the bladder fills with urine, relaxation of its wall and the maintenance of tone in the sphincter allow it to contain the urine at low pressure. When it is distended, signals indicating a full bladder are transmitted to the spinal cord in sensory (afferent) nerves and ascend to the brain (Figure 9).

Neurotransmitter release in the brain results in signals being sent back down the spinal cord, to converge on the two main areas involved in spinal micturition control (George, 2001). These are the thoracolumbar region (thoracic nerves 10, 11 and 12 and lumbar nerves 1 and 2) and the sacral region (sacral nerves 2,3 and 4). The autonomic parasympathetic and sympathetic nerves (otherwise known as preganglionic fibres) pass outside the spinal cord to synapse with the cell bodies of peripheral autonomic nerves in specialised areas known as ganglia (or plexuses). Neurotransmitter release here results in impulses leaving the ganglia in postganglionic nerves to reach the bladder muscle, bladder trigone, or urethra. A further somatic outflow (from Onuf's nucleus) passes directly to supply the pelvic floor and urethral sphincter via the pudendal nerve.

Additional neurotransmitter release from postganglionic nerve endings adjacent to the bladder muscle cell results in receptor activation on its membrane and causes the release of numerous chemical messengers within the muscle cell that result in its contraction (Brading and Inoue, 1991). Similarly the somatic and autonomic supply to the sphincter

modifies its tone and may effect relaxation and opening of the bladder outlet (Gosling and Dixon, 1975).

2.4.2 Overview of bladder detrusor muscle pharmacology

There are several chemicals involved in effecting bladder contraction. These include neurotransmitters and modulators that allow communication between the central nervous system, peripheral nervous system and the lower urinary tract in the adult bladder. In addition, local trophic factors are involved in the maintenance and growth of nerves supplying the bladder (Anderson 1993).

Following receptor activation on the bladder, Ca^{2+} is released from the sarcoplasmic reticulum (SR) by a) a chain of membrane-bound reactions that lead to the production of inositol phosphate or b) calcium influx through the surface membrane (possibly ATP-mediated). Following SR release of Ca^{2+}, the latter binds to calmodulin, and via a subsequent cascade of reactions, phosphorylates and activates a portion of the myosin molecule. This promotes interaction with actin molecules (with ATP consumption) and results in an increase in muscle tension. A reduction in the intracellular Ca^{2+} causes muscle relaxation probably by SR sequestration and transmembrane calcium flux (Fry and Wu, 1998) (Figure 10).

For central and peripheral neurotransmission in the adult, acetylcholine (ACh) is released from preganglionic neurons (from the sacral spinal cord) and activates nicotinic receptors on peripheral ganglions. From here, further ACh release by parasympathetic fibres results

in excitatory activation of the bladder via muscarinic receptors (namely M_2 and M_3 receptors) (Wang et al, 1995) and bladder contraction. Other neurotransmitters postulated in adult lower urinary tract pharmacology include noradrenaline (Gosling et al, 1999; Taki et al, 1999), adenosine triphosphate (Elneil et al, 2001), neuropeptide Y, tachykinins, vasoactive intestinal peptide and calcitonin gene-related peptide (Dixon et al, 1998; Smet et al, 1996) and vasopressin (Holmquist et al, 1991). In addition, sex steroids may modulate bladder receptors and influence bladder growth (Celayir et al, 2002). Finally, nitric oxide has a role in neurologically mediated relaxation in the lower urinary tract, especially in the urethra (Andersson and Persson, 1995). Centrally acting neurotransmitters include glutamate, dopamine, serotonin, noradrenaline, gamma-amino-butyric acid, neuropeptides, enkephalins and ACh (de Groat, 1990).

2.5 Experimental strategies for investigating in utero bladder outflow obstruction

In attempt to understand fetal bladder structure and function and subsequent changes after in utero bladder outflow obstruction, investigators have examined the bladders or bladder myocytes from human fetuses (De La Rosette et al, 2002; Freedman et al, 1997; Kim et al, 1991a; Kim et al, 1991b; Newman and Antonakopoulos, 1989; Workman and Kogan, 1990) and infants (Cortivo et al, 1981; Deveaud et al, 1998), fetal sheep (Arens et al, 2000; Cendron et al, 1994; Karim et al, 1993; Kogan and Iwamoto, 1989; Levin et al, 2001; Mevorach et al, 1994; Osterhage, 1981; Peters et al, 1992b; Peters et al, 1997; Tanagho, 1972; Wlodek et al, 1989), fetal rabbits (Chiavegato et al, 1993; Rohrmann et al, 1997a; Rohrmann et al, 1997b), fetal rat (Baskin et al, 1996a; Baskin et al, 1996b;

Sutherland et al, 1997), fetal cows (Baskin et al, 1993a; Coplen et al, 1994; Koo et al, 1995), the genetically-manipulated mouse (Bassuk et al, 2000) and the fetal mouse (Park et al, 1997; Smeulders et al, 2001).

The adult pig bladder has similar anatomical and functional characteristics to the human bladder (Crowe and Burnstock, 1989; Dalmose et al, 2000; Guan et al, 1994). Although, the normal fetal porcine bladder has been studied (Olsen et al, 2001), surgical manipulation of the fetal porcine urinary tract, to produce an experimental model of in utero bladder outflow obstruction, is currently not feasible; this is primarily because of their multigravid pregnancies necessitating complex technical surgery and probable high mortalility. As such, investigators have focused principally on the fetal sheep for fetal urinary tract manipulation, of the bladder (Cendron et al, 1994; Karim et al, 1993; Levin et al, 2001; Peters et al, 1992b; Tanagho, 1972), ureters (Santis et al, 2000) and kidneys (Adzick et al, 1985; Attar et al, 1998; Beck, 1971; Bellinger et al, 1986; Bogaert et al, 1994; Carr et al, 1995; Duncombe et al, 2002; Edouga et al, 2001; Gobet et al, 1999a; Gobet et al, 1999b; Harrison et al, 1983; Kogan and Iwamoto, 1989; Peters et al, 1992a; Yang et al, 2001). The fetal sheep is a useful model because mother and fetus tolerate surgery with little morbidity or mortalility, the fetus is of considerable size as compared to small mammals, ewes are relatively easy to handle and they have well established breeding protocols. Furthermore, studies listed above reveal that experimental bladder outflow obstruction mimics human disease. Disadvantages include financial expense, requirement of a substantial holding facility and extra personnel to perform surgery (because of animal size) and the limited breeding season of some sheep strains.

2.5.1 Fetal sheep urinary tract embryology

Ovine gestation lasts for 145 days; ovine lower urinary tract development is similar to human fetal urinary development (Tanagho, 1972). Like the human fetus, the urogenital sinus in the fetal sheep is formed by division of the cloaca and later forms the primitive bladder and urethra. The bladder extends to the umbilicus and opens directly into the allantois. At mid-gestation, the ovine fetal urethra is well formed but is not used as an outflow tract from the bladder as the lumen is packed with desquamated epithelial cells and debris. At this time point, urine from the fetal kidneys pass from the bladder into the allantoic cavity via the urachus until approximately 90 days of gestation when the bladder begins to recede caudally, pulling on the allantoic stalk (Figure 11). Urine progressively passes directly into the amniotic cavity via the urethra until the urachus fully obliterates (the exact time this occurs is unknown but it may remain patent up to term). Ovine fetal allantoic and amniotic sacs remain separate cavities with the former eventually rupturing into the amniotic cavity to form one sac. This is different to the human fetus where no equivalent membranes exist; the amniotic cavity expands to obliterate the small chorionic cavity, between four-eight weeks gestation, to become the sole cavity surrounding the human fetus (Larson, 2001).

Although three types of kidney develop during human gestation, the ovine fetus does not develop a pronephros, but forms a 'giant glomerulus', consisting of approximately 15 fused glomeruli, at the cranial end of the future mesonephros (Davies, 1951). The ovine mesonephros exists for a very similar period of gestation as the human fetus, forming around day 17 of gestation, reaching a peak nephron number by day 27-30 and then

regresses from day 40 to 57 (Moritz and Wintour, 1999). As sheep have a more primitive placenta than the human placenta, the mesonephros is more highly developed than the human fetus and is able to produce a hypotonic urine from day 18 of gestation. This urine passes into the allantoic cavity which increases in volume from 3 ml at day 20 of gestation to 20 ml by day 24 (Moritz and Wintour, 1999). This rapid expansion of the allantoic membrane is important in developing contact between maternal uterine calculation and fetal blood vessels, to form placental caruncles. Ovine metanephric development begins at day 27, with ureteric bud branching. By mid-gestation, urine production is an impressive 5-6 ml per hour and urine tonicity remains hypotonic throughout ovine development (Wintour et al, 1996). Also at mid-gestation, the composition of the allantoic fluid and fetal urine differ quite significantly because of differential rates of solute removal across the allantoic membranes (Wintour et al, 1986). Metanephric formation of new nephrons is complete by day 135 of gestation and therefore complete before birth; this is similar to human development and different to many other mammals (eg mice and rats) where nephrogenesis continues past term (Matsell and Tarantal, 2002).

2.6 The molecular biology of the developing and obstructed fetal bladder

2.6.1 The developing bladder

Molecular studies in the developing fetal bladder are limited; studies have described the temporal expression of key muscle and extracellular matrix proteins in the developing

human (Kim et al, 1991a), mouse (Smeulders et al, 2001), rabbit (Chiavegato et al, 1993; Lin et al, 2000; Sakurai et al, 1996), cow (Baskin et al, 1994b; Koo et al, 1997; Koo et al, 1998) and sheep (Arens et al, 2000). With interest to my thesis, Smeulders et al (2001) described how cell proliferation, as assessed by immunohistochemistry and western blot of the proliferation marker, proliferating cell nuclear antigen, was highest at inception of the bladder in the fetal mouse and fell progressively throughout gestation; in addition, detrusor muscle cell apoptosis, determined using the TUNEL method, was only noted at embryonic day 14 with no further cell death documented. Also noted was increasing α-smooth muscle actin and vimentin protein expression throughout gestation representing increased detrusor smooth muscle differentiation. Study of the human fetal bladder revealed increasing muscle thickness and decreasing relative collagen content during development. Fetal animal studies have shown, that with increasing gestation, as assessed by western blotting of myosin heavy chain (MHC) isoforms, there was decreasing detrusor MHC isoform 1 expression and increasing MHC isoform 2 expression (Arens et al, 2000; Chiavegato et al, 1993; Lin et al, 2000; Sakurai et al, 1996), suggesting a prenatal maturation of detrusor contractile ability. Also noted, by northern and slot blot analyses and immunohistochemistry of fetal bladders, was decreasing elastin and collagen III expression and increasing microfibrillar protein and collagen I expression (Koo et al, 1997; Koo et al, 1998) possibly illustrating the development of bladder compliance and capacity (Baskin et al, 1994a).

2.6.2 Bladder growth, hypertrophy and hyperplasia in the obstructed fetal bladder

BOO in the adult rat bladder has been documented to cause detrusor muscle hypertrophy and hyperplasia (Uvelius et al, 1984). This appears to occur in a time-dependent manner that is different to the developing bladder. In the adult rabbit bladder, by nylon taping of the bladder neck and urethral catheterisation, the reported changes are temporary submucosal oedema, increased fibrocollagenous connective tissue deposition and then smooth cell mass increase (in part replacing the connective tissue) by detrusor myocyte hypertrophy followed by hyperplasia, as assessed by microscopy and point counting (Brent and Stephens, 1975). By contrast, the growing rabbit bladder exhibited smooth muscle hypertrophy preceded by smooth muscle hyperplasia (Brent and Stephens, 1975).

Similarly, growth by detrusor hypertrophy and hyperplasia has been documented in the ovine fetal bladder subjected to BOO by partial urethral obstruction and complete urachal ligation. Peters et al (1992b) produced ovine BOO at 60 days gestation and sacrificed fetuses after 35 or 85 days; a marked growth response was found in obstructed bladders as assessed by increased bladder weight, DNA and protein content, and detrusor smooth muscle cell size as calculated by computer morphometric analyses. Karim et al (1993) produced BOO at 90 – 100 days gestation and obtained bladders at term; the authors reported a significant increase in bladder weight and detrusor DNA content in the obstructed bladders. Cendron et al (1994) observed a significant increase in bladder weight at term in ovine fetuses obstructed at 90 days gestation. Finally, Levin et al (2001) documented a trend towards increased bladder weight after short-term (5 days) BOO in

ovine fetuses at 90 days gestation. However, despite these investigations of bladder growth, hypertrophy and hyperplasia, little is known of the balance between these processes and programmed cell death.

2.6.3 Apoptosis

Cell death occurs by necrosis or apoptosis (Kerr et al, 1972) (Figure 12). Necrosis is uncontrolled cell death that leads to cell swelling, mitochondrial damage and cell membrane lysis with release of intracellular contents; this results in an inflammatory response, with subsequent oedema and damage to the surrounding cells. In contrast, apoptosis, or programmed cell death, keeps the intracellular content of the dying cell sequestered; it is defined by cell shrinkage, nuclear condensation, DNA cleavage and cell membrane blebbing (containing intracellular contents such as nuclear matter and cellular organelles). These apoptotic bodies are removed by phagocytes or by neighbouring cells.

Apoptosis has been increasingly implicated in organogenesis during embryo development (Jacobson et al, 1997) (Figure 13); it is involved in organ sculpting (eg loss of webs between digits or loss of cells in solid structures to form lumina), deleting unwanted structures (eg loss of vestigial organs and involution of the mesonephros), adjusting cell numbers (eg deleting excess precursors in the metanephric kidney) and eliminating abnormal or harmful cells (eg T and B lymphocytes that develop self-reactive receptors). Furthermore, advances have been made in determining molecular death pathways.

The key steps in apoptosis is a series of activations of proteases called caspases (Hayashi and Araki, 2002), previously known as interlekin-1 beta-converting enzyme-like proteases. Caspases have been divided into three groups:

Group I caspase-1, caspase-4, caspase-5, caspase-11

Group II caspase-2, caspase-3, caspase-7

Group III caspase-6, caspase-8, caspase-9, caspase-10

Group I caspases are involved in cytokine processing, Group III caspases activate group II caspases and the latter group consist of effector proteins that are able to directly cleave substrates resulting in apoptosis. The most important of these, capsase-3, results in cell death by either activating caspase-activated DNase or directly cleaving cell surface membranes or cellular enzymes when activated. Furthermore, these caspases are able to lead to disassembly of nuclear and cytoskeletal structures, disable cell repair and label apoptotic cells for phagocytosis (primarily by macrophages) (Zhivotovsky et al, 1997).

Currently, two pathways have been described that activate caspases (Figure 14). Death factors, such as Fas ligand (Nagata, 1994), bind to death receptors and activate group III caspases, specifically caspase-8 and caspase-10. Alternatively, external stimuli, such as irradiation or chemotherapeutic agents, result in cytochrome C release from mitochondria which activates the Group III caspase, caspase-9. Subsequently, both pathways converge with activation of Group II caspases.

Members of the protein family, Bcl-2 (B-cell leukaemia/lymphoma-2), have also emerged as important in the regulation of apoptosis (Fadeel et al, 1999). Pro-death

molecules, such as Bcl-2 associated X protein (Bax) and anti-death molecules, such as Bcl-2, play key roles by acting both at the level of the mitochondria, and at pre- and postmitochondrial stages, and therefore directly influence cytochrome C release.

2.6.4 Apoptosis in the urinary tract

All studies in this section examined apoptosis by the TUNEL method and apoptosis-related proteins by immunohistochemistry, unless otherwise stated. Programmed cell death plays a significant role in renal morphogenesis. During development, a high index of proliferation, as assessed by PCNA expression, and a low index of apoptosis, accompanied with increased Bcl-2 expression (additionally determined by cytophotometry) were observed in murine and human renal metanephric cells (Lichnovsky et al, 1999; Winyard et al, 1996b); apoptosis, as documented by cell morphology, has also been observed in the nephrogenic region and medullary papilla of the developing rat kidney (Coles et al, 1993). Furthermore, fetal renal pathology is associated with aberrations of apoptosis and apoptosis-related proteins. Increased apoptosis and decreased Bcl-2 expression has been documented in the stroma of pre- and postnatal polycystic and dysplastic human kidneys (Winyard et al, 1996a). In utero urinary tract obstruction resulted in high rates of apoptosis in the developing renal pelvis and tubulointerstitium, accompanied with increased Bax and decreased Bcl-2 expression (additionally documented by in situ hybridisation) in apoptotic renal tubules, in the developing opossum (Liapis et al, 2000), and increased apoptosis in the renal cortex, in the developing sheep (Attar et al, 1998); these histopathological changes appear to be related to the gestational age at which the injury occurred (Poucell et al, 2000).

Moreover, mice with null mutations of Bcl-2 demonstrate fulminate apoptosis during metanephric development resulting in renal hypoplasia at birth and multicystic renal disease later in life (Veis et al, 1993). Similarly adult renal pathology also results in perturbation of cell turnover; urinary obstruction in the adult rat resulted in tubulointerstitial apoptosis with downregulation of Bcl-2 (Chevalier et al, 2000), upregulation of caspases (as assessed by ribonuclease protection assays and immunohistochemistry) (Truong et al, 2001) and increased apoptosis and Bax expression in smooth muscle cells of the obstructed ureter (Chuang et al, 2002). Furthermore, glomerulonephritis, also in the adult rat, resulted in increased apoptosis and caspase-3 (as assessed by substrate cleavage assays) with a shift in the Bax-Bcl-2 balance (additionally assessed by western and northern blotting) (Yang et al, 2002).

Less is known of programmed cell death in the developing fetal bladder. Apoptosis has been documented in the separation of the cloaca into the urogenital sinus in embryonic rat development (as early as embryonic day 12) (Qi et al, 2000) and has also been observed in the murine fetal bladder (at embryonic day 14 only) (Smeulders et al, 2001). In addition, immediately prior to birth, the fetal mouse bladder undergoes urothelial cell desquamation that is accompanied with apoptosis (as assessed by cell morphology and cytochemistry) (Jezernik et al, 1997) and programmed cell death is also present during the postnatal restoration of the urothelium (Erman et al, 2001). In adult pathology, bladder apoptosis has been documented to a) increase following ischaemia-reperfusion injury (Saito and Miyagawa, 2002), alpha-1 adrenoceptor antagonist treatment of benign prostatic hypertrophy (Erdogru et al, 2002), relief of bladder outflow obstruction

(Santarosa et al, 1994) and transitional cell carcinoma (TCC) of the bladder (King et al, 1996), and b) decrease in diabetes mellitus (Khan et al, 2002) and following stretch of bladder smooth muscle cells (as assessed by propidium iodide incorporation and flow cytometry) (Galvin et al, 2002). Finally, Bcl-2 expression in the bladder is associated with poorly differentiated TCC of the bladder (King et al, 1996) and immunohistochemical testing of activated caspase-3 suggests this molecule is involved in the progression of bladder carcinoma from carcinoma-in-situ to invasive bladder cancer (Burton et al, 2000). However, as there are no studies of the effects of fetal urinary pathology on fetal bladder apoptosis, I have chosen to examine programmed cell death and apoptosis-related proteins in my experimental model in utero bladder outflow obstruction.

2.7 The physiology of the developing and obstructed fetal bladder

Current methods of studying fetal bladder physiology are human fetal ultrasound and physiological measurements made in whole organ preparations, muscle strip studies and in vivo fetal bladders.

2.7.1 Ultrasound studies of the developing bladder

As early as 20 weeks of gestation, the human fetal bladder is able to store and empty urine; with increasing gestation, these functions mature as bladder capacity and effectiveness of bladder emptying increase up to term. With ultrasound imaging, the human fetal bladder can be seen to void every 30 minutes at 28 weeks of gestation and

every 60 minutes by 40 weeks gestation (Hata and Deter, 1992). The maximum fetal bladder volume increases from 1 ml at 20 weeks gestation to 36 – 54 ml by 40 weeks gestation (Rabinowitz et al, 1989) with average voiding lasting approximately 9.5 seconds; complete bladder emptying is achieved by 40 weeks gestation.

2.7.2 Ontogeny of animal fetal bladder physiology

Whole bladder studies from the fetal calf reveal that with increasing gestation, the fetal bladder demonstrates increased compliance (the bladder is able to accommodate increased urinary volume without an increase in intravesical pressure) (Coplen et al, 1994; Koo et al, 1995). This was confirmed in a study using circularly clamped fetal bladder strips (Baskin et al, 1994a). It has since been postulated that the change in compliance during gestation is associated with the documented transformation in collagen subtype expression (Kim et al, 1991a; Koo et al, 1997). Furthermore, muscle tone has also been implicated; compliance increases through gestation because the immature fetal bladder has high active smooth muscle tone that decreases with maturation allowing for this greater urine accommodation (Coplen et al, 1994; Dean et al, 1997).

Active contractile function also develops during gestation. Early gestation whole bladder preparations from the fetal calf emptied by 50 % when stimulated with the muscarinic agonist, bethanechol, whilst mid and late gestation preparations emptied to almost completion (Koo et al, 1995). These age-related differences in contractility may only relate to the upper half of the fetal bladder (Lee et al, 1994).

By documenting pressure changes within the fetal bladder using indwelling catheters, ovine fetal bladder contractions were discernable at 120 days gestation and could be pharmacologically manipulated (Kogan and Iwamoto, 1989); contractile function appeared to be under cholinergic and β-adrenergic control. By using a similar method at the same gestation, nitric oxide also appeared to be active in lower urinary tract function (Mevorach et al, 1994). Finally, during this period, ovine fetal voiding appeared to coincide with periods of electrocortical activity in the fetal brain (Wlodek et al, 1989) suggesting that descending control of bladder activity was developed.

Pressure recordings within the fetal pig also show maturation of bladder function (Olsen et al, 2001). During the second trimester, fetuses showed no sign of active storage and voiding with continuous urine flow with apparent flow increases synchronous with bladder contractions; this suggests that at this gestation in the fetal pig, the bladder acts simply as a conduit. By the third trimester, distinct periods of voiding were observed with urethral urine flow, bladder contractions (that were of higher pressure than earlier in gestation) and the development of urethral sphincter bursting activity.

2.7.3 Physiology of the obstructed fetal bladder

Physiological studies of experimental fetal BOO have been performed in the fetal rabbit and the fetal sheep. Lagomorph fetal bladder obstruction (Rohrmann et al, 1997a) led to increased compliance in whole bladder preparations that was primarily attributable to passive properties of the bladder rather than smooth muscle tone. Furthermore, they

reported hypocontractile obstructed bladder strips. In contrast, by different methodology, Peters et al (1992b) reported reduced compliance in the obstructed ovine fetus. Levin et al (2001) also described hypocontractile responses in ovine fetal bladders after short-term bladder outflow obstruction.

2.7.4 In vivo fetal cystometry

Currently, only three studies have documented pressure characteristics in the fetal bladder, in the fetal sheep and fetal pig, using externalised catheters. Kogan and Iwamoto (1989) used intravesical catheters, connected to pressure recorders, in the fetal sheep. With the ewes ambulatory, fetal bladder pressures were documented following intravenous furosemide administration or by artificially filling the bladder. Similarly, Mevorach et al (1994) documented bladder contractions in the ovine fetus by artificially filling the bladder with warm saline and pressures recorded with intravesical catheters. Finally, under maternal sedation, Olsen et al (2001) reported fetal bladder pressures in the porcine fetus using intravesical catheters but without any artificial means of bladder filling by instillation or forced diuresis. These studies, however, are not without problems: animals will try to remove catheters on their flanks, animals have imposed immobility and are stressed, there is an increased risk of infection and fetal mortality and studies tend to be of a short duration. Furthermore, ambulatory urodynamics in humans suggest that artificial filling and a stressful environment may result in nonphysiological detrusor activity; compliance remains high, unstable detrusor activity is more frequently observed, voided volumes are lower and maximum voided pressures higher (Robertson et al, 1994; Robertson et al, 1996; Vereecken and Van Nuland, 1998; Webb et al, 1990). To

overcome these difficulties, investigators have used radiotelemetry devices to monitor bladder pressure. These have a number of advantages (Mills et al, 2000): reduced stress to animals (no handling, restraining or tethering to recording machines, no anaesthesia and no invasive monitoring), monitoring can be over a prolonged period of time providing meaningful physiological data, and computer-based monitoring allows accurate mathematical analysis. Radiotelemetered cystometry had been used successfully to describe ambulatory pressure recordings in the bladder, by natural filling, in the adult pig (Mills et al, 2000) and adult monkey (El Ghoneimi et al, 1999) and the obstructed adult pig (Speakman et al, 1987); such technology has not been evaluated in the fetal bladder.

2.8 Concluding remarks

My introduction shows that in utero BOO of the human fetal bladder results in significant postnatal urinary tract dysfunction. To examine the fetal consequences of this obstruction, investigators have performed limited studies in the human fetal bladder and developed experimental models of in utero BOO, primarily using the developing sheep. These latter studies suggest that obstruction results in a large bladder with impaired contractility. However, no studies, to date, examine proliferation and apoptosis and detailed neurotransmission and viscoelasticity in the developing and obstructed fetal bladder. In the following chapters, I describe the hypotheses and aims of my thesis and the methodology used to achieve these.

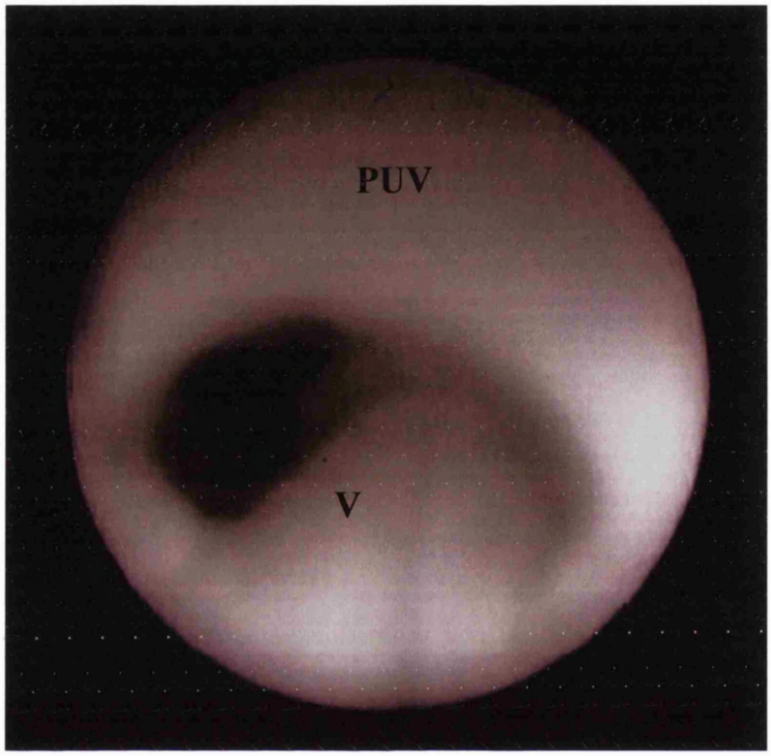

Figure 1. Cystocopic view of posterior urethral valves
View, through a cystoscope, of a male urethra, that shows the obstructive posterior urethral valve (PUV); also shown is the anatomical landmark, the verumontanum (V). Picture courtesy of Mr PM Cuckow.

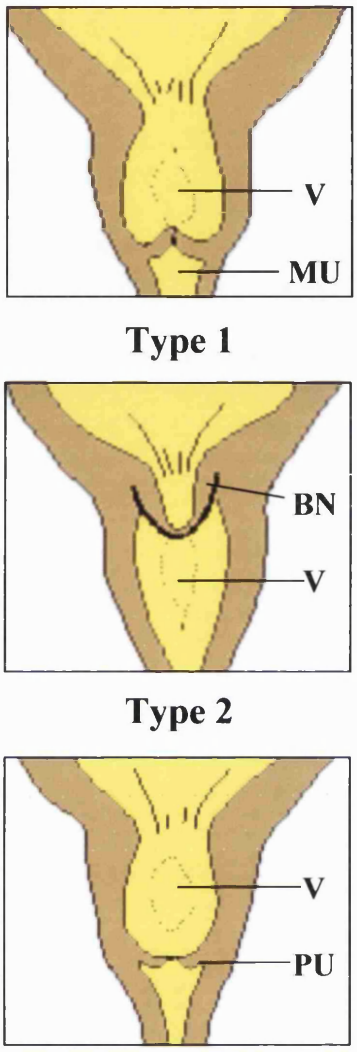

Figure 2. Posterior urethral valves classification
Type 1 PUV are folds extending inferiorly from the verumontanum (V) to the membranous urethra (MU). Type 2 PUV are leaflets or folds radiating from the verumontanum up to the bladder neck (BN) and Type 3 PUV are concentric diaphragms, with a central lumen found within the prostatic urethra (PU) below the verumontanum. Adapted from Young and Frantz, 1919.

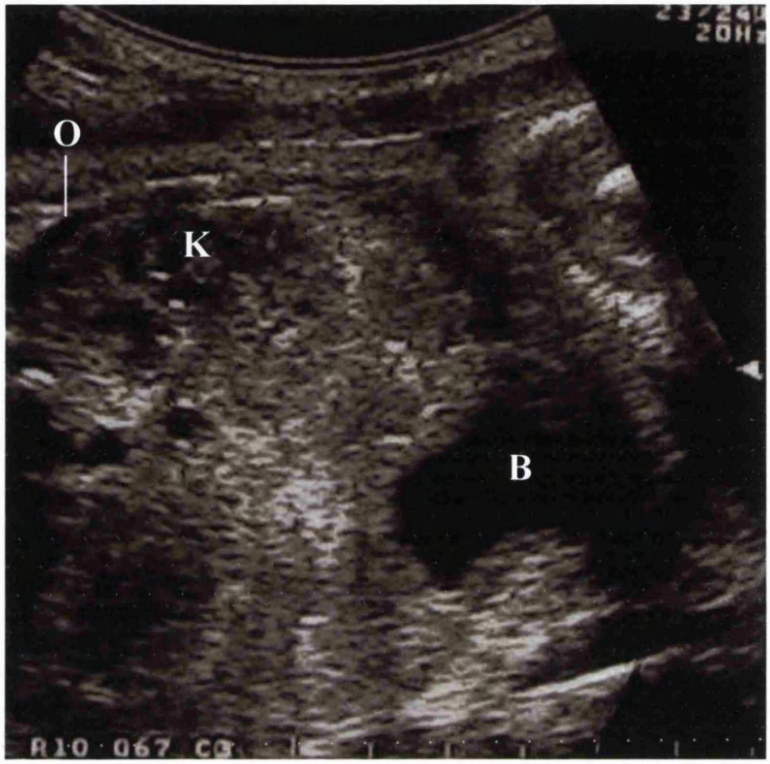

Figure 3. Antenatal ultrasound image of a fetus with PUV
Ultrasound image shows the dilated bladder (B) of a fetus with posterior urethral valves; these babies also suffer from hydronephrotic kidneys (K) and oligohydramnios (O). Picture courtesy of Mr PM Cuckow.

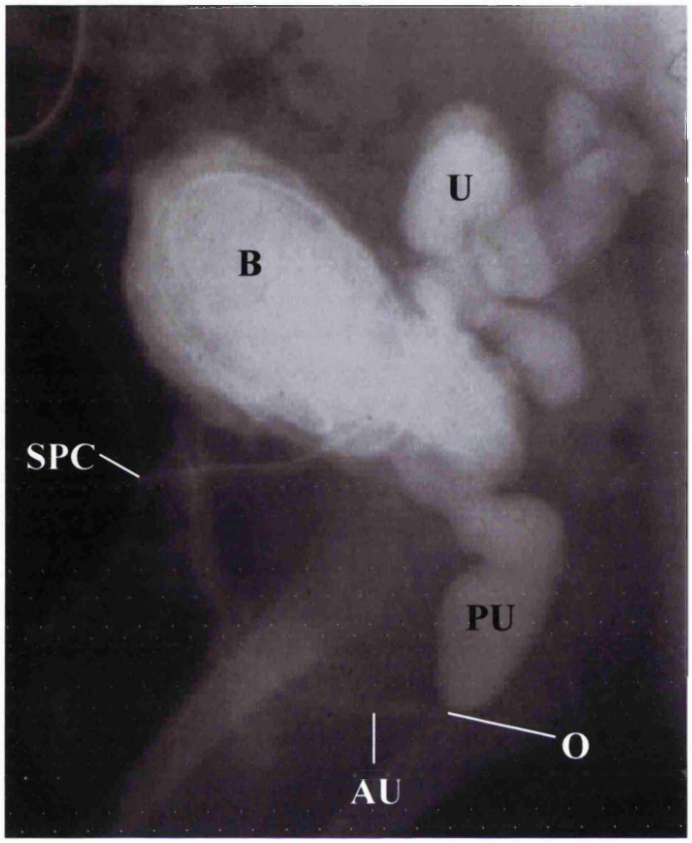

Figure 4. Micturating cystourethrogram of a boy with PUV

To perform this radiological examination, contrast is injected into the bladder (B) via a suprapubic catheter (SPC). The contrast delineates the dilated posterior urethra (PU), and after passing the site of obstruction (O), by posterior urethral valves, enters the normal calibre anterior urethra (AU). Also seen are the refluxing ureters (U) that are commonly associted with posterior urethral valves. X-ray image courtesy of Mr PM Cuckow.

Figure 5. Abdominal wall defect of Prune Belly Syndrome
Picture of a neonate with PBS. Note laxity of abdominal wall which, in conjuction with urinary tract dilatation and cryptorchidism, define the triad of PBS. Photo courtesy of Mr DT Wilcox.

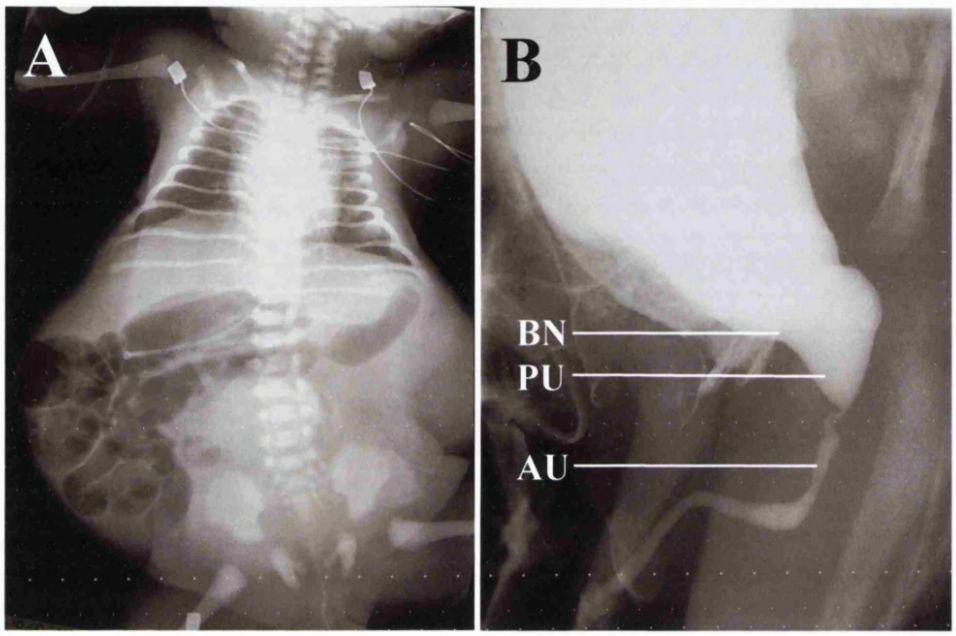

Figure 6. Radiological imaging in Prune Belly Syndrome

A: Plain abdominal radiograph of a neonate with PBS. Note the wide abdomen due to abdominal wall laxity. B: MCUG of the same neonate with PBS. The image shows a wide bladder neck (BN), a dilated posterior urethra (PU) and a normal calibre anterior urethra (AU) that suggests a possible obstruction in the posterior urethra. Xray images courtesy of Mr DT Wilcox.

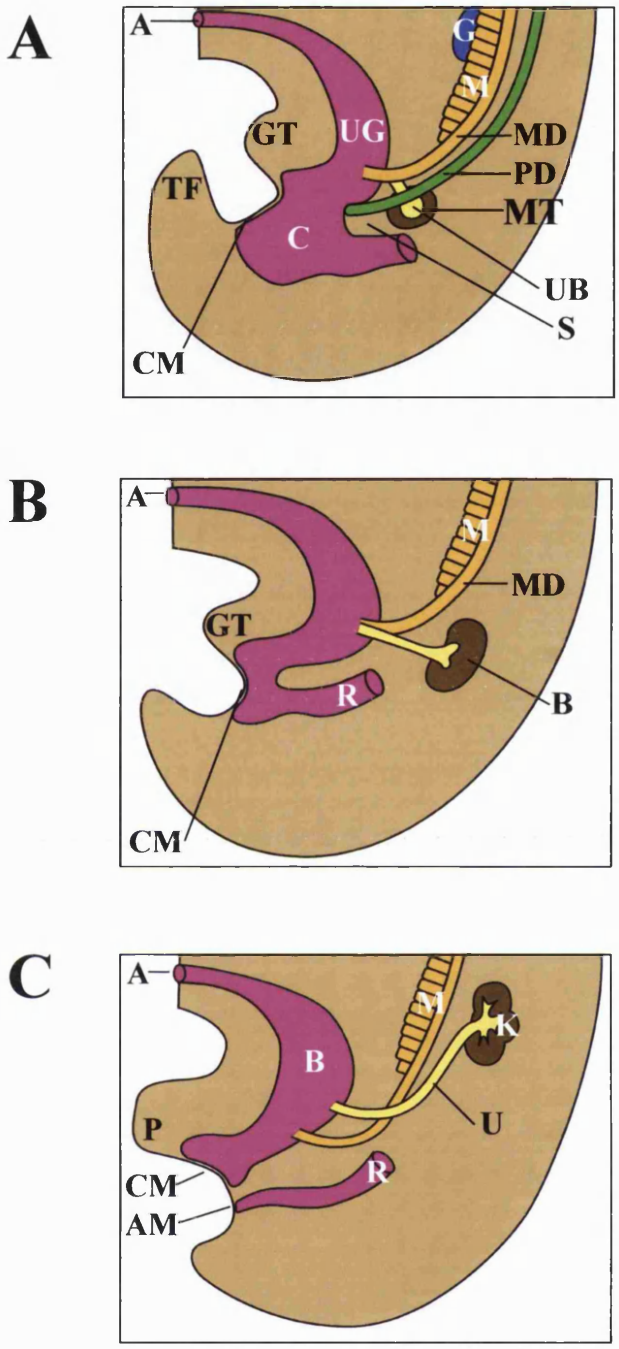

Figure 7. Human urinary tact embryology

A-C represents urinary tract embryology during the 4th (A), 5th (B) and 6th (C) of human fetal gestation. During this period, the mesonephros produces urine and then involutes, the ureteric bud penetrates the metanephros to form the metanephric blastema and subsequently the kidney and the septum divides the urogenital sinus to form the rectum and the primitive bladder. Key: *A*, allantois; *M*, mesonephros; *MD,* mesonephric duct; *B*, metanephric blastema; *G*, gonad; *UB,* ureteric bud; *S,* septum; *CM*, cloacal membrane; *TF,* tail fold; *GT*, genital tubercle; *UG,* urogenital sinus; *MT*, metanephros; *R,* rectum; *K*, kidney; *U,* ureter; *AM*, anal membrane; *P*, phallus. Adapted from Cuckow PM et al, 2001.

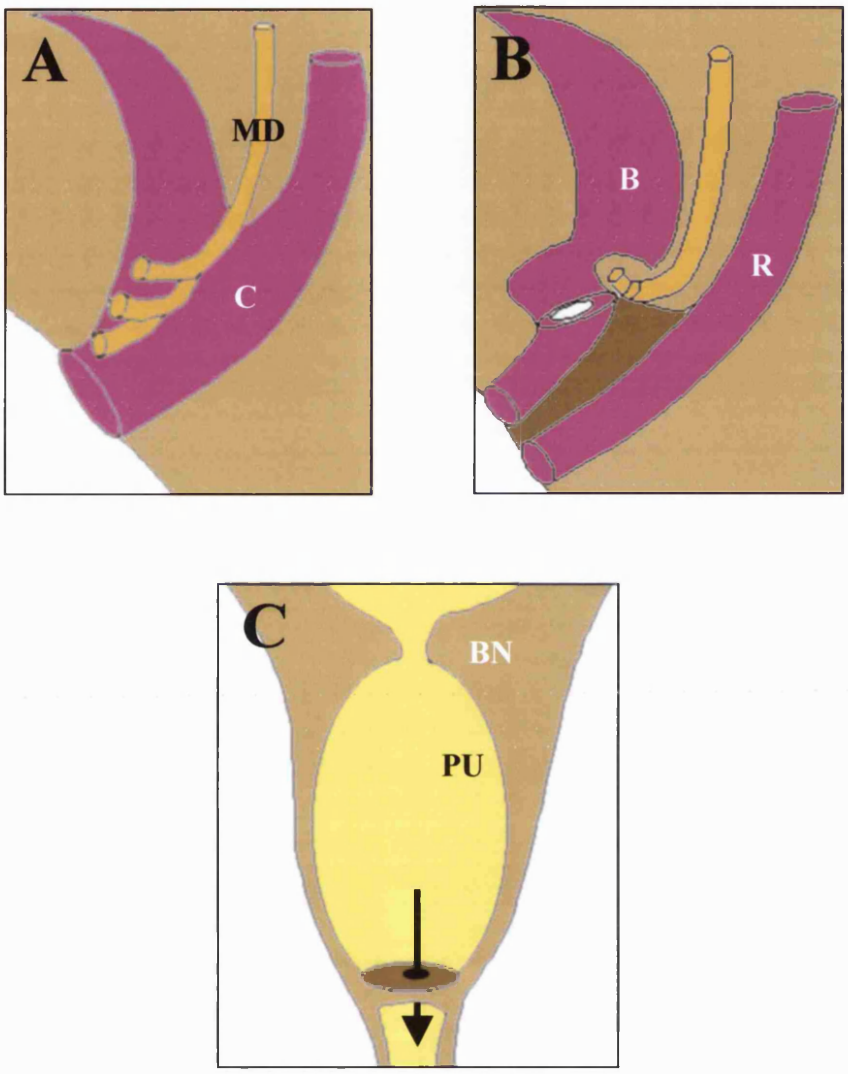

Figure 8. Posterior urethral valve embryology
PUV may arise because of abnormal anterior integration of the mesonephric duct into the cloaca (A), resulting in obliquely orientated ridges (B) that compose the valves. Alternatively, they may arise by failure of complete dissolution of the urogenital membrane (C). Key: *C*, cloaca; *MD*, mesonephric duct; *B,* bladder; *R*, rectum; *BN*, bladder neck; *PU*, prostatic urethra. Adapted from Stephens, 1983.

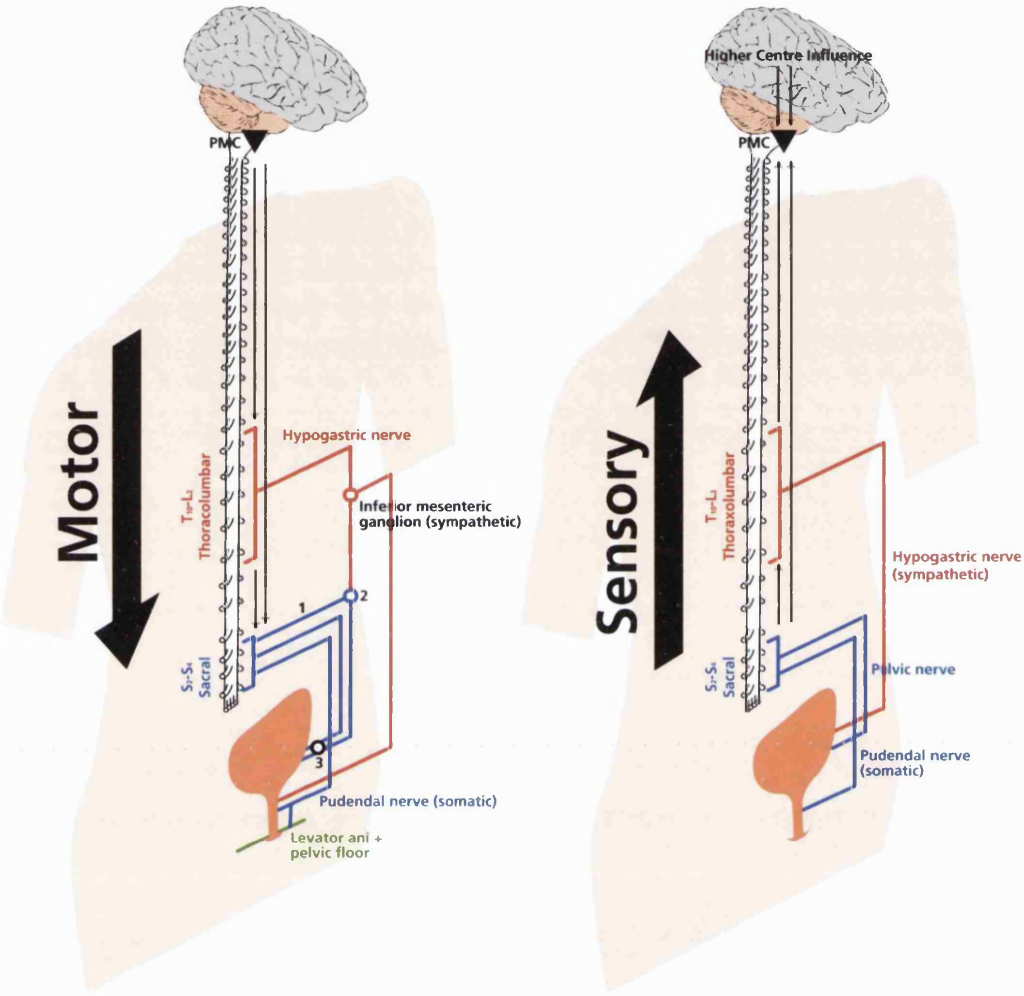

Figure 9. Innervation of the bladder

To allow for bladder filling, the bladder relaxes it's tone (by negative feedback of the sympathetic nervous system) and by maintaining bladder outflow closure by the somatic nerves. With further filling, impulses are carried up the pelvic nerve to enter into the sacral region of the spinal cord and eventually reach the pontine micturition centre (PMC) in the pons, this area may also be influenced by further higher cerebral control. Voiding is achieved by co-ordinated parasympathetic activation (impulses pass via the preganglionic parasympathetic nerves 1, the pelvic ganglion 2 to reach the bladder by the pelvic nerve 3), sympathetic activation (via the hypogastric nerve and the inferior mesenteric ganglion to cause bladder trigonal contraction) and somatic activation (to alter the tone of the levator ani and the pelvic floor). Adapted from George, 2001.

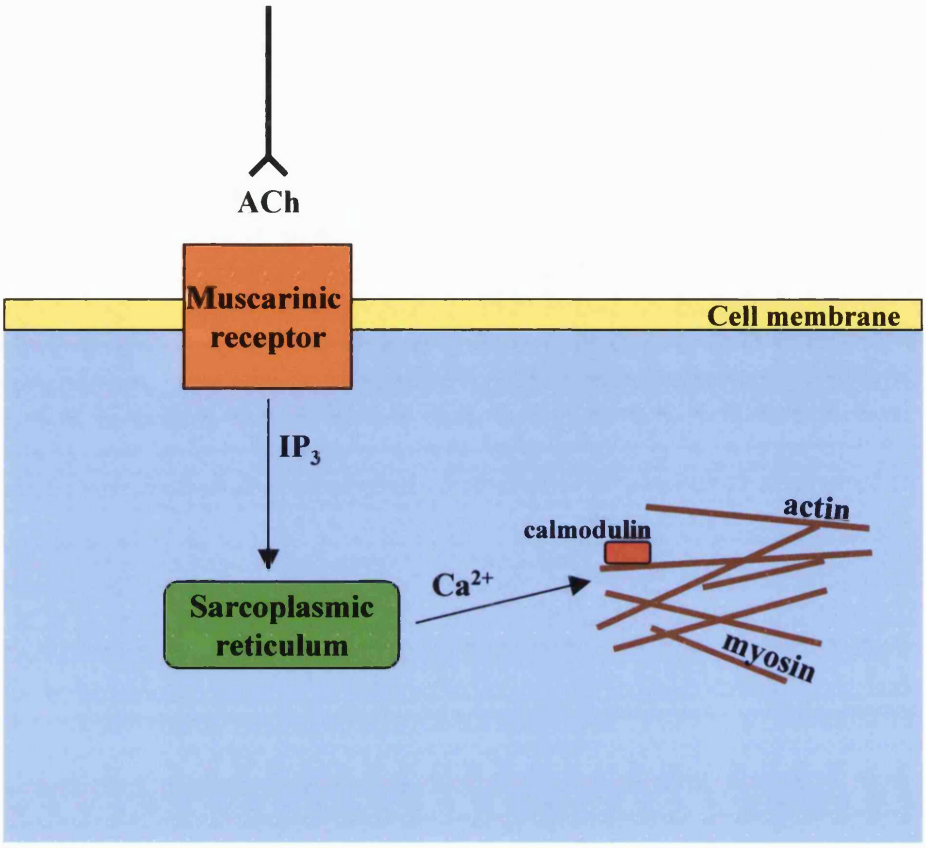

Figure 10. Bladder pharmacology
Following receptor activation on the bladder primarily by acetyl choline (ACh), calcium is released from the sarcoplasmic reticulum by a chain of reactions leading to the production of inositol phosphate (IP_3), or by calcium influx through the surface membrane. The calcium binds to calmodulin, and via a subsequent cascade of reactions, phosphorylates and activates a portion of the myosin molecule. This promotes interaction with actin molecules and results in contraction. Adapted from Fry and Wu, 1998.

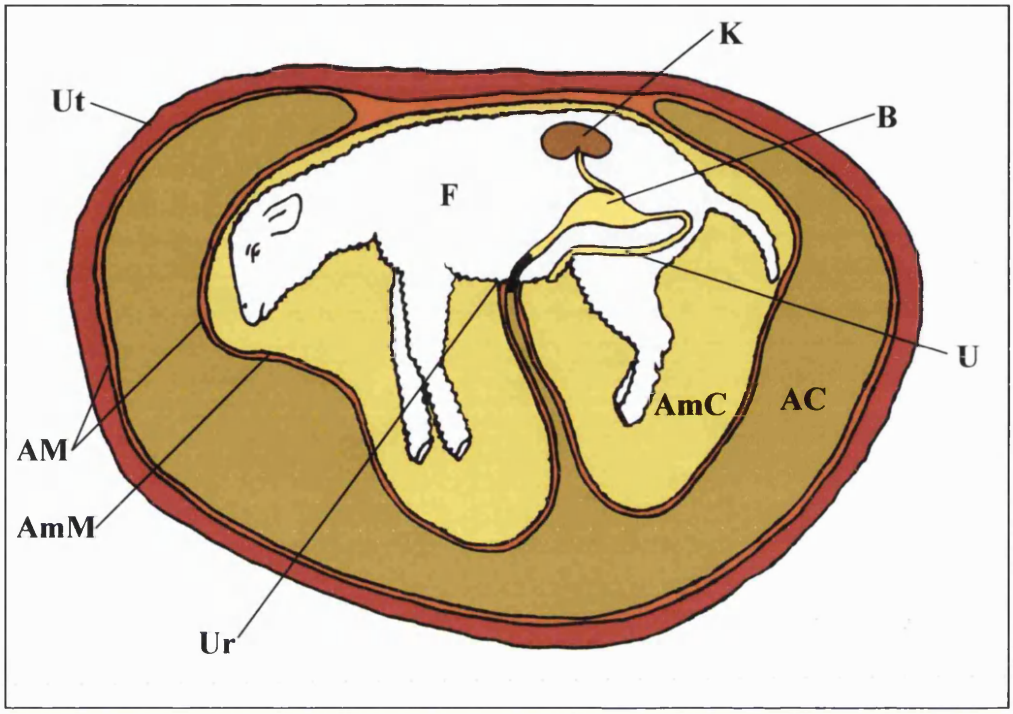

Figure 11. Fetal ovine anatomy
Figure shows anatomy of ovine fetus within maternal uterine cavity; note how bladder urine primarily drains into amniotic cavity and urachal urine flows into allantoic cavity. Key: *F*, fetus; *K*, kidney; *B*, bladder; *U*, urethra; *AC*, allantoic cavity; *AmC*, amniotic cavity; *Ur*, urachus; *AmM,* amniotic membrane; *AM*, allantoic membranes; *Ut*, uterus. Modified from Wlodek et al, 1998.

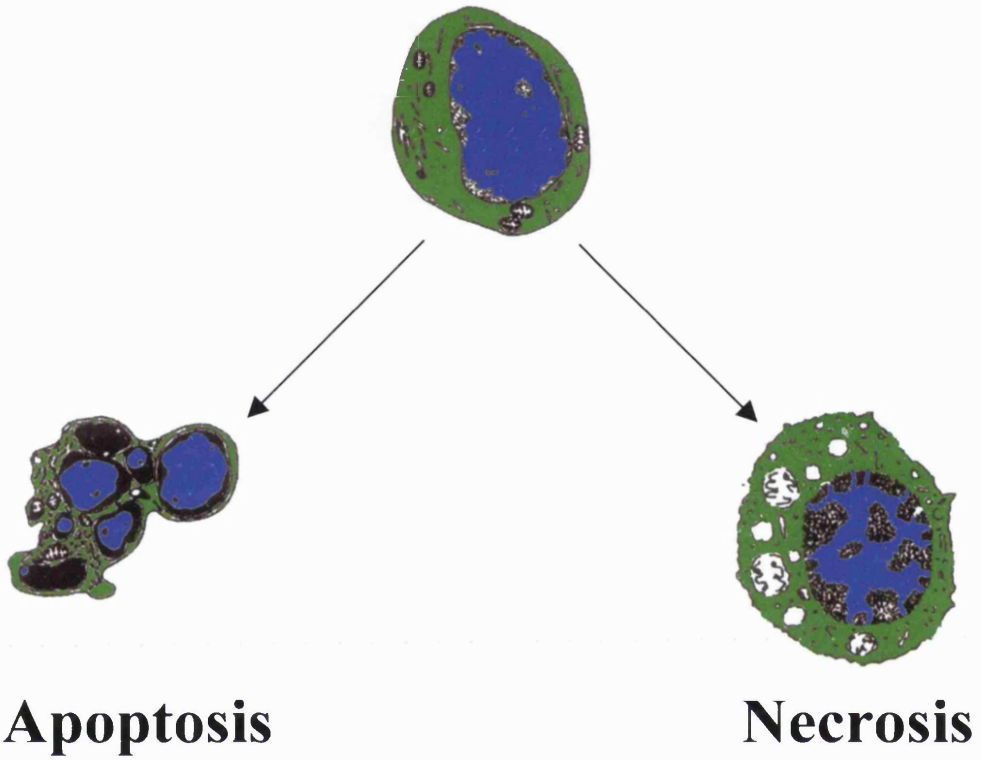

Figure 12. Apoptosis versus necrosis
Schematic diagrams of the morphological changes of apoptosis and necrosis. The apoptotic cell shows cell shrinkage, convolution and blebbing, condensation of the heterochromatin against the nuclear envelop, maintenance of organelles (especially mitochondria) and the development of membrane-bound apoptotic bodies. In contrast, the necrotic cell appears swollen, nuclear and cellular membranes and organelles are disrupted and the heterochromatin is irregularly clumped throughout the nucleus. Adapted from Gobe and Harmon, 2001.

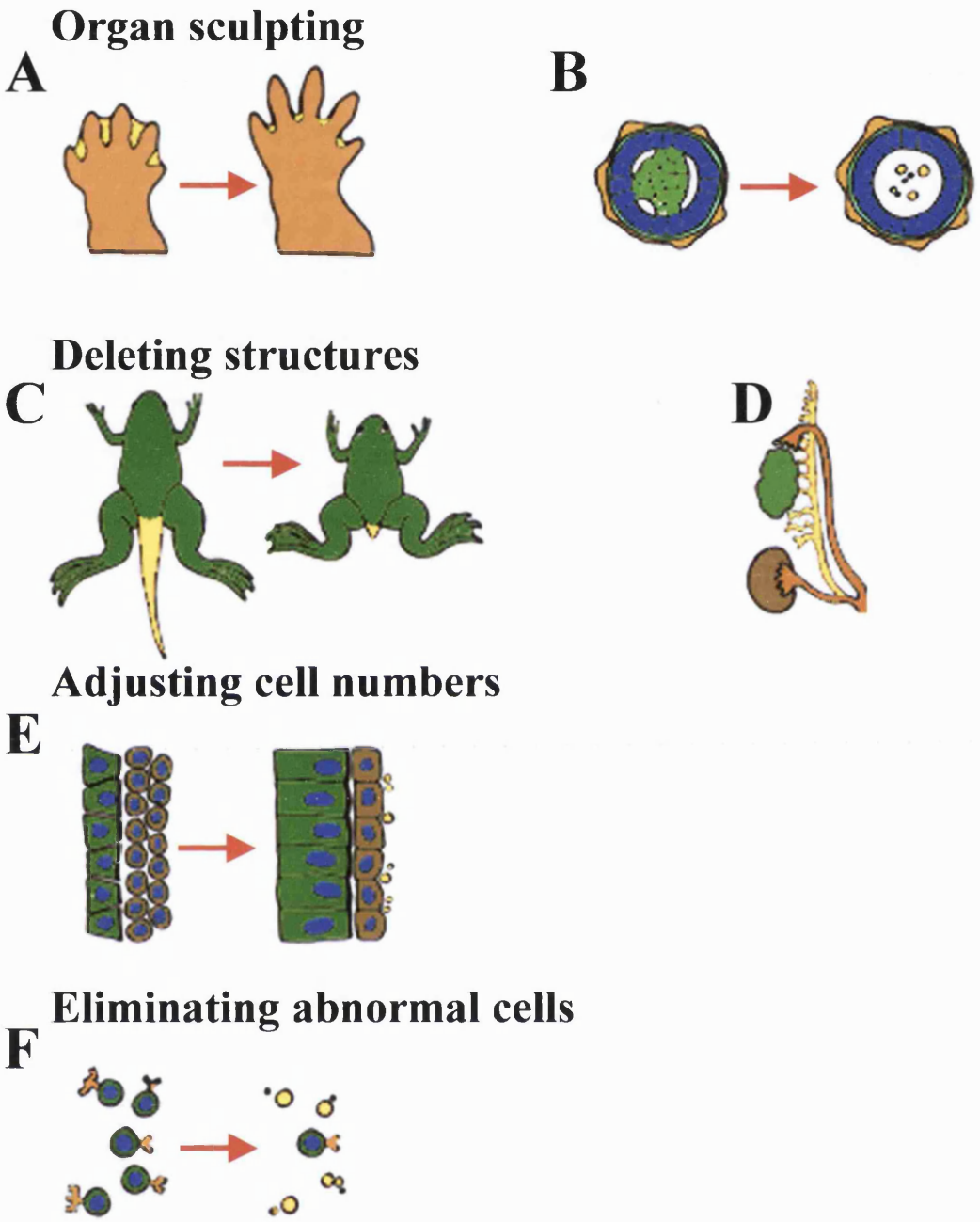

Figure 13. Apoptosis in organogenesis
Apoptosis is involved in organ sculpting, such as in eliminating cells in developing digits (A) and hollowing out solid structures to create lumina in tubes (B), in eliminating unwanted structures, such as vestigial organs (C) and the developing mesonephros (D), in adjusting cell numbers when cells are overproduced, such as deleting excess precursors in the metanephric kidney (E) and eliminating abnormal or harmful cells, such as T and B lymphocytes that develop self-reactive receptors (F). Modified from Jacobson et al, 1997.

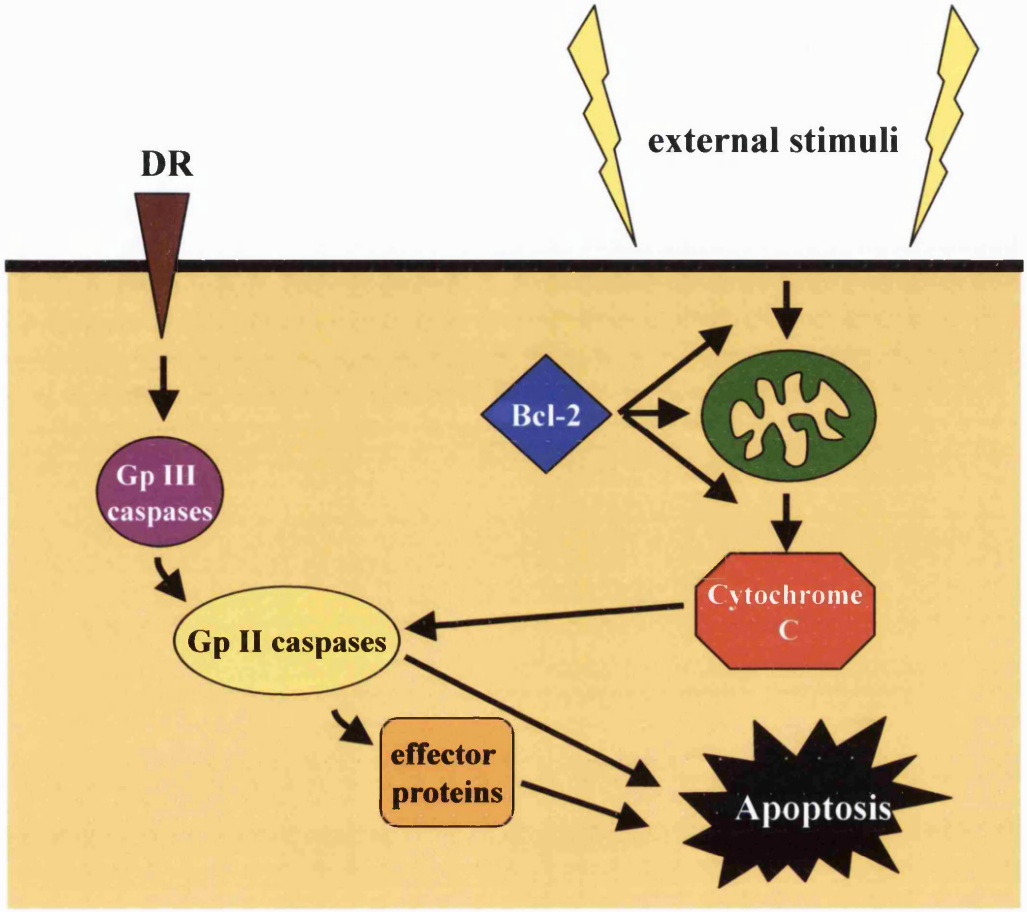

Figure 14. The caspase cascade
Apoptosis is activated by two pathways that interact. The binding of death ligands to the death receptors activate group III and subsequently group II caspases. Alternatively, external stimuli, such as irradiation or chemotherapeutic agents, cause cytochrome C release from mitochondria which activate group II caspases. Either directly, or via effector proteins such as caspase-activated DNase, group II caspases (primarily caspase-3) result in cell death by apoptosis. The Bcl-2 family of apoptotic regulatory proteins act, both at the level of the mitochondria, and at pre- and postmitochondrial stages, to influence cytochrome C release. Modified from Hayashi and Araki, 2002.

3. Experimental strategy

In utero BOO results in significant postnatal bladder dysfunction. In order to understand how the fetal bladder responds to this urinary obstruction, the aims of my thesis were to examine the following hypotheses.

3.1 Hypotheses

1) In utero bladder outflow obstruction results in significant alteration to the cell turnover of the developing fetal bladder with deregulation of proliferation, apoptosis and apoptotic regulatory protein expression.

2) In utero bladder outflow obstruction results in significant perturbation to contractility, neurotransmission and physical properties of the developing fetal bladder.

To answer these hypotheses, I aimed to perform the following experiments.

3.2 Aims

1) Obtain fetal bladder samples in an experimental fetal ovine model of in utero bladder outflow obstruction and sham control animals.

2) Document the changes to organ growth and cell turnover in the fetal bladder exposed to bladder outflow obstruction, versus sham control bladders.

3) Determine the normal maturation of the fetal bladder, with special reference to bladder growth and cell turnover.

4) Identify molecules involved in neurotransmission in the normal fetal bladder.

5) Ascertain the changes to fetal bladder contractility and neurotransmission after BOO using electrophysiological bladder strip studies.

6) Discover the changes to the physical characteristics of obstructed fetal bladders by examining the pressure-volume relationships in ex vivo whole bladders and biomechanical visco-elastic properties of bladder strips, in both experimental groups.

7) Determine the feasibility of using radiotelemetry implants to document the in vivo pressure changes in the fetal bladder.

4. Material and Methods

Unless otherwise stated, all chemicals were from Sigma (Poole, Dorset, UK).

4.1 Experimental model

4.1.1 Animals

To obtain fetuses at the required gestational age, I purchased pregnant Romney Marsh ewes from the Royal Veterinary College herd (Potters Bar, Hertfordshire, UK). For my thesis, I used 31 ewes of which 8 ewes were pregnant with twin pregnancies; the remaining ewes carried singleton fetuses. This yielded a total of 39 fetuses of which four died prior to planned post-mortem, probably from surgical or anaesthetic insult. In addition, I purchased four pregnant Pole Dorsett ewes (that yielded four fetuses) from the Royal Veterinary College to perform the in vivo radiotelemetry recording of fetal bladder pressure recording experiments; a change of breed was necessary as these latter experiments were performed outside of the normal breeding season for Romney Marsh sheep. Finally, I received by donation, four bladder samples from adult Romney Marsh sheep. All work was conducted in accordance with the UK Home Office Animals (Scientific Procedures) Act 1986.

4.1.2 Experimental Design

For the main experiments, I used 35 Romney Marsh sheep fetuses; these were used as follows:

• Eleven were sham-operated male control fetuses at 105 days gestation (the *sham* male group) and compared with *obstructed* male bladders that underwent the same analyses.

- Five bladders were analysed for *molecular biology* studies by bladder weight, protein and DNA content, caspase-3 activity and morphometric analyses, and for *physiology* studies by filling cystometry measurements, in vitro studies of contractility and biomechanical properties.

- The remaining six bladders were analysed for *molecular biology* studies by histology by Masson's trichrome and Elastin van Gieson stains, proliferating cell nuclear antigen (PCNA) immunohistochemisty, Bcl-2 and Bax immunohistochemistry and western blot and TUNEL in-situ end-labelling, and for *physiology* studies by S100 and PGP 9.5 immunohistochemistry and western blot and morphometric analyses.

• Eleven male fetuses had induced partial bladder outflow obstruction at 105 days gestation (the *obstructed* group). Bladders were analysed as for *sham* male bladders.

• Five were sham-operated female fetuses at 105 days gestation (the *sham* female group). These were used for in vitro contractility studies (and compared to the five *sham* male bladders that underwent physiological analyses) and for the maturational study (see below).

• Two (one male and one female) were fetuses at 75 days gestation; these bladders were analysed for the maturational study (see below).

• Six (3 male and 3 female) were fetuses at 145 days gestation; these bladders were analysed for the maturational study (see below).

To study the effects of in utero BOO, I compared Romney Marsh *obstructed* and *sham* male fetuses because human fetal BOO occurs almost exclusively in males (Woolf and Thiruchelvam, 2001). In addition, to examine any possible sex differences, I compared Romney Marsh *sham* males and *sham* females in the physiology experiments. Finally, I also performed a limited maturational study that examined control bladders only. This compared bladders from the two 75 day gestation fetuses, five *sham* female and five *sham* male fetuses (105 day gestation), six 145 day gestation fetuses (three male and three female) and four adults (aged four-eight years, two male and two female).

Molecular Biology

Analysis was by bladder weight, protein and DNA content, caspase-3 activity, morphometric analyses, histology by Masson's trichrome and Elastin van Gieson stains, proliferating cell nuclear antigen (PCNA) immunohistochemisty, Bcl-2 and Bax immunohistochemistry and western blot, and TUNEL in-situ end-labelling.

Analysis for the maturational study was by histology by Masson's trichrome stain, PCNA immunohistochemistry and western blot and caspase-3 activity and protein and DNA content.

Physiology

Analysis was by filling cystometry measurements, in vitro studies of contractility and biomechanical properties. In addition, fetal bladders were analysed by S100 and PGP 9.5 immunohistochemistry and western blot and morphometric analysis for innervation studies and to determine detrusor thickness, respectively.

4.1.3 Fetal surgery

Fetal surgery was performed by myself and Peter Cuckow, Consultant Paediatric Urologist and co-supervisor. Initial preliminary operations were performed by Peter Nyirady, visiting Hungarian Research Fellow and Peter Cuckow. For induction of general anaesthesia of time-mated Romney marsh ewes, I administered 1 g thiopentone sodium (Intraval Sodium; Rhone Merieux, Dublin, Ireland) intravenously, predominantly via the jugular vein. With the aid of the laryngoscope, I inserted a 10F endotracheal tube and maintained oxygenation and anaesthesia with 2-3% halothane (Fluothane^{TM}; Mallinckrodt Veterinans, Phillipsburg, USA) in a nitrous oxide and oxygen mixture. Following induction, I administered 1 g of streptomycin/penicillin (Streptopen; Schering-Plough Animal Health, Omaha, USA) intramuscularly, typically in the upper hind leg, as

a prophylactic measure against wound infection. With the ewe in a supine position (lying on her back) (see Figure 17), a laparotomy was performed, the uterine horn delivered and via a hysterotomy, the fetal hindquarters delivered. Incisions were primarily made with a cauterising diathermy probe (with the earth plate placed on the ewe's crown). For the obstructive procedure, fetal abdominal muscle were exposed by blunt dissection and carefully incised to expose the urachus. This was ligated with 3/0 silk and the abdominal wound closed with 6/0 prolene. The male urethra was exposed by a small longitudinal incision made at the perineal end of the abdomen and incompletely obstructed by snug placement of a 2 mm omega-shaped, silver ring secured with a 3/0 silk ligature (see Figure 18); this wound was also closed with 6/0 prolene. In attempt to prevent intra-amniotic infections, I administered 80 mg gentamicin (Cidomycin® Adult Injectable; Hoechst Marion Roussel, Strasbourg, Germany) and 600 mg benzylpenicillin sodium (Britannia Pharmaceuticals Limited, Redhill, Surrey, UK) into the amniotic cavity. For the sham procedure in male and female fetuses, the urethra and urachus were exposed only. The uterus was then closed in two layers with 0/0 silk followed by maternal fascia and skin closure with cloth tape (3mm Polyesterband, Catgut GmBH, Postfach, Markneukirchen, Germany) and 2/0 silk respectively. Following wound closure, I administered Vetergesic® (buprenorphine analgesia, Alstoe Animal Health, Melton Mowbray, Leicestershire, UK) intramuscularly, again in the upper hind leg, to ease the post-operative recovery. This surgical technique was associated with a 15 % mortality.

At weekly intervals, ultrasound examination using a scanner equipped with an annular array multifrequency sector transducer, centre frequency 5 MHz (Vingmed CFM 800;

Vingmed Sound, Horten, Norway) was performed by Anna David, Clinical Research Fellow, Fetal Medicine Unit, University College London. This was performed by holding the ewe placed on its hindquarters and the ultrasound probe positioned on the maternal abdomen (see Figure 19). This enabled visualisation of the fetus to check for fetal life signs (fetal heart beat and fetal movement) and to determine the extent of urinary tract dilatation.

After thirty days, the ewe was sacrificed by intravenous injection (via the jugular vein) of pentobarbitone sodium (Euthatal; Rhone Merieux, Athens, USA). Fetuses were then weighed and parameters of fetal size, occipto-snout length and femur length, were measured. Some fetal bladders then underwent filling cystometry. All fetuses then underwent post-mortem examination, dissection of the urinary tract and separate weight and size measurements of the bladder and kidneys. Samples were then removed from the bladder dome, weighed and then placed in Ca^{2+} free HEPES Tyrode's solution (see below, for composition), snap-frozen in liquid nitrogen or fixed in 10% paraformaldehyde (BDH, Poole, UK). In addition, fetal kidneys were preserved for histology.

4.2 Biochemistry and Molecular biology

4.2.1 Dry weight measurement

For dry weight measurement, samples (from *sham male* and *obstructed* groups, n=5) were slowly dehydrated by warming at 65 °C and were repeatedly weighed until a base-line weight was reached; in this way, a ratio of dry weight to wet weight was established

for each sample and then extrapolated to total bladder weight to enable total bladder dry weight measurement.

4.2.2 Protein quantification

Further samples of bladder domes were homogenised at 4 °C in radioimmunoprecipitation assay buffer containing the following protease inhibitors; 30 µl/ml aprotinin (2.2 mg/ml), 10 µl/ml phenylmethylsulfonyl fluoride (10 mg/ml) and 10 µl/ml sodium orthovanadate (100 mM in 95 % ethanol). The buffer lysed cells and promotes solubilisation of protein; proteinase inhibitors prevented protein degradation. After centrifugation at 16,600 xg at 4 °C, protein concentration in supernatants was measured using the BCA protein assay (Pierce, Rockford, USA). This assay combines the reduction of Cu^{2+} to Cu^{1+} by protein in an alkaline solution and the subsequent colormetric detection of Cu^{1+} by a reagent containing bicinchoninic acid (BCA). The combination of BCA with Cu^{1+} results in a purple-coloured reaction product that exhibits a strong absorbance at 562 nm that is linear with increasing protein concentrations over a broad working range (20-2000 µg/ml). The protein concentration of the test sample was then calculated from the colour response produced from a dilution series of an albumin standard (2 mg/ml bovine serum albumin).

Ten µl of each protein sample, as well as the albumin dilution series, were incubated with 200 µl of working reagent (50 parts reagent A with 1 part reagent B from BCA assay) in a 96 microwell plate for 30 minutes at 37 °C. Using a colorimetric microwell plate reader (Titertek Multiskan Plus, Labsystems, Vantaa, Finland), absorbance was recorded at 562

nm and protein concentrations of the samples were determined by comparison with the standard colour response curve of the albumin standard.

4.2.3 DNA extraction and quantification

For DNA extraction, I placed samples of approximately 100 mg fetal bladder (previously snap frozen in liquid nitrogen) into 750 ul of lysis buffer and left overnight at 50 °C (lysis buffer: 20 mM Tris pH 7.4, 100 mM EDTA pH 8.0 and 1mg/ml proteinase K). After vigorous vortex for 10 seconds, 0.2 M NaCl was then added to stop the proteinase reaction. An equal volume of phenol:chloroform:isoamyl alcohol (25:24:1) was added to stop any further RNAse activity and to remove any protein contaminants. After centrifugation at 16,600 xg for 15 minutes, I removed the aqueous phase and discarded the rest (middle layer of denatured proteins and organic bottom layer). To precipitate the DNA, I added an equal volume of isopropanolol to the DNA solution and left at –70 °C for 2 hours. After further centrifugation at 16,600 xg for 15 minutes, I discarded all the solution and vortexed the remaining pellet with 500 ul of 70 % ethanol to remove salts and small organic molecules. I then discarded all the solution and air-dried the remaining pellet for 5 minutes before resuspending the DNA pellet in 100 µl of Tris-EDTA.

To determine DNA quantity, the DNA concentration of the resuspended DNA solution was calculated from the emission wavelength of 260 nm using a luminescence spectrometer (Ultrospec 1000, Amersham Pharmacia Biotech, Little Chalfont, Buckinghamshire, UK). I then determined total DNA content from the calculated DNA concentration for the 100 mg bladder sample.

I determined DNA purity by the following two methods (Sambrook et al, 1987):

1) *Absorbance ratio.* I measured the emission wavelength of 280 nm (the absorbance of UV light by aromatic amino acids in protein solutions) of the DNA sample and calculated the 260:280 nm absorbance ratio; if this ratio was greater than 1.7, the sample was considered to have a high DNA purity.

2) *Agarose gel electrophoresis.* 1 % agarose was made in tris-acetate-EDTA (TAE) buffer and dissolved by microwave heating (10x TAE: 0.4 M Tris-acetate, 0.01 M EDTA, ph 8.0, 3 μl of 20 g/l ethidium bromide solution). This solution was poured into a horizontal gel mould and combs inserted. After cooling at room temperature and setting of the gel, the combs were removed and the gel transferred to a horizontal tank and covered with 1x TAE buffer. Samples of DNA were then loaded into the wells and the gel run at 80 V for 45 minutes and then visualised under ultraviolet exposure. Quality of DNA was good if bands were observed at the appropriate high molecular weight.

4.2.4 Histology

Tissue processing and embedding

Fixed bladders (in 10 % formaldehyde) were processed into a form that enabled thin microscopic sectioning using a VIP Processor. First, the bladder tissue was dehydrated with a series of alcohols, from 50 % up to and including 100 %. The next step, clearing, removes the dehydrate and is performed by placing the tissue in xylene. Finally, after exposure to four changes of wax, the tissue was placed in cartridges and set in wax.

Tissue sectioning

Once embedded, tissue blocks were kept on ice to aid even sectioning. I cut the tissues into 5 μm thin sections using a microtome; the sections were floated onto a 50 °C heated water bath (that helped to remove any wrinkles) and then picked up on TESPA (3-aminopropyltriethoxysilane)-coated glass slides and air dried. The slides were coated in TESPA (2 % TESPA in acetone for 2 minutes) to help the sections 'stick' to the glass slides.

Staining

In order to get the wax out of the tissue and allow water soluble dyes to penetrate the sections, the embedding process described above had to be reversed. I did this by running slides through histoclear (twice for 10 minutes) and decreasing concentrations of alcohols (100 % to 50 %) and then in running tap water for 10 minutes. The following stains were chosen for their ability to stain various cellular components of bladder tissue.

Masson's Trichrome

This stain was used to illustrate smooth muscle and connective tissue changes in bladder sections. Masson's Trichrome stains collagen blue, erythrocytes, muscle cell cytoplasm and keratin red and nuclei purple (Bancroft and Cook, 1994). Slides were placed in 3 % potassium dichromate for 1 hour at 60 °C and then stained with filtered Celestine blue and haematoxylin for five minutes each. Slides were then stained with filtered chromotrope green solution (0.6 % chromotrope, 0.3 % fast green, 0.6 % phosphatungstic

acid and 1 % acetic acid) for 15 minutes, and after two cycles of blotting and dehyration, slides were placed in histoclear and then mounted in dextropropoxyphene (BDH).

Elastin van Geison

I used this technique to illustrate connective tissue differences in bladder sections. The stain colours elastin black, collagen red and erythrocytes and myocyte cytoplasm yellow and nuclei purple (Bancroft and Cook, 1994). Slides were oxidized in 0.25 % acidified potassium permanganate (10 ml of 3 % H_2SO_4 and 90 ml of 0.25 % $KmnO_4$), washed in 1 % oxalic acid and then 70 % alcohol. Slides were then stained in 1 % Moore's elastin in 1 % acid alcohol for 2 hours. After hydration, slides were exposed to filtered Celestin blue for 1 minute and then counterstained with Mayer's Haematoxylin and then van Geison for 3 minutes each. Following dehydration, sections were mounted in dextropropoxyphene (BDH).

4.2.5 Morphometric analysis

Using image analysis software (KS 300, Carl Zeiss, Oberkochen, Germany), I calculated mean detrusor SMC area (μm^2) by measuring the area of detrusor muscle bundles in Masson's Trichrome stained sections, using a x20 objective, and then factoring the area for the number of nuclei in each bundle. Muscle bundles were examined from four randomly placed fields in the muscle layers of bladders from each group (n=6). I measured cell density in the lamina propria by counting the number of nuclei in a fixed square area of known size, using a 20x objective, and then correcting cell density to 1

mm^2 area; these areas were from four randomly placed fields in the lamina propria of bladders from each group (n=6).

4.2.6 Immunohistochemistry

This technique is used to identify specific proteins (antigens) within cells in tissue sections by means of antigen-antibody interactions; the site of antibody binding is identified either by direct labelling of the antibody, or by use of a secondary labelling method.

Pretreatment

In order to promote antibody penetration and blocking of antigen secondary to the fixing process, tissue sections were pretreated; I found that optimal pre-treatment was achieved by microwaving sections at high power for 10 minutes in 2.1 g/l citric acid pH 6.0 in a microwave oven (Shi et al, 1991). Section were then washed with 3 % hydrogen peroxide in methanol for 30 minutes to quench any endogenous peroxidase activity and then washed in phosphate-buffered saline (Oxoid Ltd, Basingstoke, Hampshire, UK) and phosphate-buffered saline-0.1% tween20 (BDH) for 5 minutes each. Sections were then blocked in 10 % fetal calf serum (FCS) (GIBCO BRL, Life Technologies, Paisley, Strathclyde, UK) with 2 % bovine serum albumin (BSA) and 0.1% tween20 (BDH) for ten minutes.

Antibodies and signal detection

Antibodies were obtained either by fusing immune B cells from the spleen with tumour cells to produce hybridomas that secrete a single type of antibody (monoclonal antibody), or by immunizing an animal of any one of a variety of species with a purified antigen and then isolating antibodies (polyclonal antibodies) from the animal as it develops an immune response.

Detection of antigen can be achieved by conjugating antibodies with flurorescent dyes, biotin or with enzymes. Alternatively, unconjugated primary antibodies maybe detected with specific labelled secondary antibodies. With the exception of PCNA primary antibody, all the antibodies used in my thesis were unconjugated primary antibodies that required the use of a streptavidin-biotin conjugate kit (StreptABComplex/HRP, DAKO) and biotin-conjugated secondary antibodies. This reaction works as follows. Biotin, a small vitamin molecule, will bind to one of four biotin-binding sites on the large glycoprotein, avidin (Reagent A in kit). Biotinylated secondary antibody binds to unconjugated primary antibody; the latter is bound to exposed antigen in the pre-treated tissue sections. Avidin, binds to biotinylated horseradish peroxidase (Reagent B in kit) and this complex binds to the biotin attached to the secondary antibody with subsequent amplification of the signal. Finally, peroxidase activity is detected by colormetric changes in diaminobenzidine tetrahydrochloride (DAB) (0.5 g/l in deionised water). PCNA primary antibody was conjugated with biotin and therefore did not require the addition of any biotin-conjugated secondary antibody. With all antibodies, optimal signalling was obtained by using serial concentrations of primary and secondary

antibodies and optimising exposure time to DAB. Omission of primary antibody and substitution with blocking solution acted as a negative control.

α-smooth muscle actin, PCNA, Bcl-2 and Bax immunohistochemistry

α-smooth muscle actin (αSMA) was used to identify detrusor smooth muscle in tissue sections (Baskin et al. 1993b). PCNA, an auxiliary protein for DNA polymerase-δ, was used as a surrogate marker for cellular proliferation (Prelich et al, 1987). Bcl-2, the archetypal anti-death protein and Bax, a pro-death protein, were used to illustrate the role of death proteins in apoptosis (Jacobson et al, 1993). These proteins were used to detect differences between *sham male* and *obstructed* groups. In addition, I used PCNA immunohistochemistry to illustrate differences in the developing fetal bladder and the adult bladder. Sections were prepared as follows.

Bladder sections were dewaxed in histoclear and rehydrated in a descending series of alcohols and then washed in tap water for 10 minutes. Sections were then microwaved on high power for 10 minutes in 2.1 g/l citric acid pH 6.0. Sections were then exposed to 3% hydrogen peroxide in methanol for 30 minutes and then washed in phosphate-buffered saline for five minutes and then phosphate-buffered saline-0.1% tween20 (BDH, Poole, UK) for 10 minutes. Sections were blocked in 10% FCS with 2% BSA and 1% tween20 for one hour. Sections were incubated overnight at 4°C in a humidified chamber with monoclonal anti-mouse αSMA antibody (1:4), polyclonal biotin-conjugated mouse anti-human PCNA antibody (1:50; Pharmingen, San Diego, USA), monoclonal anti-mouse Bcl-2 antibody (1:50) or polyclonal rabbit anti-human Bax antibody (1:50; Chemicon,

Temecula, USA). Omission of the primary antibody and substitution with the blocking agent acted as a negative control. After three further phosphate-buffered saline washes, biotinylated sheep anti-mouse antibody (Amersham Pharmacia Biotech, Little Chalfont, Buckinghamshire, UK) for anti-αSMA and anti-Bcl-2 sections or donkey anti-rabbit (Amersham) for anti-Bax sections at 1:200 dilution. I omitted this step for the biotin-conjugated anti-PCNA antibody. Slides were washed with phosphate-buffered saline and reacted with streptavidin-conjugated horseradish peroxidase (HRP) for one hour. Peroxidase activity was then developed with diaminobenzidine for 15 seconds for anti-αSMA, six minutes for anti PCNA and 3 minutes for anti-Bcl-2 and anti-Bax, to generate a brown colour. Sections were counterstained in haematoxylin, to detect cell nuclei, dehydrated in an ascending alcohol series and mounted in dextropropoxyphene (BDH). I examined and photographed slides on a Zeiss Axiophot II microscope (Carl Zeiss, Oberkochen, Germany).

Proliferative index

To quantify proliferation, nuclear counts were made of PCNA positively stained nuclei within each of the three layers of the fetal bladder: the detrusor muscle layer, the lamina propria and the urothelium. For the detrusor layer, by random field placement using a 20x objective, 100 cells were counted within muscle bundles and the number of PCNA positively-stained cells (cells with brown stained nuclei of any shade) were counted; this was performed ten times in different fields, so that 1000 nuclei for each fetal sample were analysed. The *Proliferative Index* for each sample was the percentage of cells positive for PCNA. For cells from lamina propria and urothelial layers, 100 nuclei were counted ten

times in randomly placed fields within these layers to generate the *Proliferative Indices*. In addition, a *Proliferative Index,* as described for urothelial and lamina propria layers, was determined for the prominent cell population which was found to surround detrusor muscle bundles in the *obstructed* group.

4.2.7 Western blot

Western blotting, or immunoblotting (Sambrook et al, 1987), is a useful method to measure protein in a semi-quantitative manner, by identifying specific antigens recognized by polyclonal or monoclonal antibodies. After protein quantification, as described above, bladder sample proteins are separated on a sodium dodecyl sulphate (SDS)-polyacrylamide gel. Proteins are then electrophoretically transferred in a semidry apparatus to a nitrocellulose membrane (polyvinylidene difluoride); uniformity of transfer can be checked with Ponceau S staining. The transferred proteins are bound to the surface of the membrane providing access for antigen detection; all remaining bindings sites are then non-specifically blocked by protein blocking agents (such as fat-free dry milk, tween-20 and BSA) (Harlow and Lane, 1988). Antigen is detected by incubation with a primary antibody and then a HRP-conjugated secondary antibody. The specific protein is then visualized by luminescent detection on radiographic film, photographed or scanned and finally, quantitated by densitometry. Potential problems with western blotting include high background, nonspecific and weak cross-reactivity of antibodies, poor protein transfer, membrane binding efficiency and sensitivity and inability of antibodies to recognize denatured forms of antigen when transferred to the membrane.

Protein electrophoresis

Proteins from fetal bladder samples were extracted and quantified as described above. Samples were then diluted down so all samples were of the same concentration and then stored at – 20 °C until later use. The proteins were separated using polyacrylamide gels created using the Mini-Protean II apparatus (Bio-Rad Laboratories, Hemel Hempstead, Hertfordshire, UK). The method employed two gels: an upper stacking gel (pH 6.8) and a lower resolving gel (pH 8.8); both contain chloride as the mobile anion.

Gels were set up according to manufacturers instructions. Two glass plates were held apart by 1.5 mm spacers and the gels poured in between. The lower resolving gel had various compositions depending on the molecular weight of the protein to be detected: 6 % gel to detect proteins of molecular weight 120-220 kDa, 8 % gel for 50-100 kDa and 15 % for 15-50 kDa. Gel composition was sterile water, 30 % acrylamide, 1.5 M Tris pH 8.8, 10 % SDS, 10 % ammonium persulphate and 1 % N,N,N-N-tetramethylethylenediamine (TEMED); proportions were altered to acquire different percentage gels. The gel formed as the polymerised acrylamide cross-linked with TEMED and ammonium persulphate with the latter providing free radicals. This gel was poured into the 1.5 mm space until the gel reached approximately 1.5 cm from the top of the smaller glass plate. A thin layer of water-saturated butan-1-ol was then added to exclude oxygen and to ensure a flat surface for the stacking gel. After allowing the gel to set for 1 hour, butan-1-ol was rinsed off with tap water, the top of the gel dried with Whatmann 3MM paper and stacking gel poured on to the top of the smaller glass plate. Ten millilitres of this 5 % stacking gel contained 6.8 ml deionised water, 1.7 ml Protogel,

1.25 ml 1.0M Tris pH 6.8, 0.1 ml 10 % SDS, 0.1 ml 10 % ammonium persulphate and 0.01 ml TEMED. A 10-well comb was then inserted into the gel so the top of the well dividers were level with the top of the smaller glass plate and the gel left to set for 1 hour.

The gels, held in place by the glass plates, were placed in a tank that held a running buffer (tris-glycine buffer, 25 mM trizma-base, 250 mM glycine, 0.1 % SDS, pH 8.8) containing glycine anions. The Laemmli discontinuous buffer system (Laemmli, 1970) was used with part of the running buffer over and between the gels and the remainder in the electrophoresis tank. As electrophoresis begins, glycine moves through the stacking gel behind the chloride ions creating an area of low conductivity; the latter moves the proteins through the large pores of the stacking gel and into narrow bands at the top of the resolving gel. Within this latter gel, the hydrophobic regions of proteins bind to the strongly anionic detergent, SDS (within the resolving gel), causing the proteins to unfold and become negatively charged. As these complexed proteins move towards the positively charged electrode, they separate and migrate differentially according to their molecular weight, thus separating out the proteins in the original sample.

Protein samples were thawed and 5-20 μg of protein (depending on the antibody used) were mixed with equal volumes of sample buffer (1 ml glycerol, 0.5 ml β-mercaptoethanol, 3 ml 10 % SDS, 1.25 ml 1 M Tris pH 6.7 and 1 mg bromophenol blue) and then denatured, as well as protein markers (Amersham), at 100 °C for 5 minutes. Denaturing and the reducing agent, β-mercaptoethanol, were used to dissociate proteins. These samples were then carefully loaded into the wells, with 10 μl of protein marker,

loaded into one of the wells, and run at 70 mV until the desired size of protein marker reached the middle of the resolving gel.

Electroblotting

After electrophoresis, glass plates were removed, the stacking gel discarded and the resolving gel placed in transfer buffer (48 mM Tris, 39 mM glycine, 0.037 % SDS and 20 % methanol). One piece of nitrocellulose membrane (Hibond P, Amersham Pharmacia Biotech) per gel and six pieces of Whatmann 3MM paper (of sufficient size to cover two gels) were cut and floated in transfer buffer. As the Mini-Protean II apparatus allowed two gels to be run simultaneously, the top right-hand corner of one gel and one nitrocellulose membrane were cut to allow for correct identification and orientation. The gels and filter paper were then placed on the anode plate of the semi-dry electroblotter (Bio Rad) as follows: three pieces of filter paper, nitrocellulose membrane, resolving gel and finally, three more pieces of filter paper; air bubbles were removed by rolling out each layer with a pipette. To prevent the upper stack of paper contacting the lower stack (and thereby causing short-circuiting), Saran Wrap ® (Dow Chemical Company, Midland, Michigan, USA) was arranged around the gels. The cathode lid of the electroblotter was then fitted and the proteins transferred at 12 V for 52 minutes for all gels.

I then confirmed uniform transfer of proteins by staining the nitrocellulose membrane with Ponceau S solution for 5 minutes (see Figure 20). After washing in deionised water, proteins were visualised as pink bands and photographed using a digital camera.

Blocking and addition of antibodies

To block non-specific binding sites, blots were incubated with 5 % fat-free milk powder, 2 % BSA and 0.2 % tween20 in phosphate-buffered saline (pH 7.4) for 2 hours on a shaker (to ensure equal exposure of membrane). The primary antibody was then applied to membranes overnight at 4 °C: polyclonal mouse anti-human PCNA antibody (1:1000; Pharmingen), monoclonal anti-mouse Bcl-2 antibody (1:1000) or polyclonal rabbit anti-human Bax antibody (1:1000; Chemicon). Antibodies were diluted in blocking solution to minimise non-specific binding.

After washing the membranes twice in 0.2 % tween20 in phosphate-buffered saline for 20 minutes each on a shaker and then 1 hour in blocking solution, blots were then exposed to HRP-coupled secondary antibodies for one hour: donkey anti-rabbit antibody, 1:1000 for Bax detection, or sheep anti-mouse antibody, 1:500 for PCNA detection or 1:1000 for Bcl-2 detection. Membranes were then washed, on a shaker, in phosphate-buffered saline-tween20 three times for 20 minutes and in phosphate-buffered saline twice for 30 minutes.

Band detection by chemiluminescence

I detected the HRP in the secondary antibody using the Enhanced Chemiluminescence system (ECL, Amersham Pharmacia Biotech). This system relies on the hydrogen peroxidase-hydrogen peroxide catalysed oxidation of luminol; the latter then develops an excited state and subsequently decays via a light-emitting pathway. The membranes were

placed on Saran Wrap and 5 ml of ECL detection reagent applied to each gel for 1 minute. Excess reagent was then drained off, the membrane wrapped in Saran Wrap and stuck into an X-ray cassette and finally, light emission detected by exposure to autoradiographic film (MXB film, Kodak, Rayne, UK) in a darkroom, for an optimised length of time, depending on intensity of signal (PCNA: 15 minutes, Bax and Bcl-2: 30 minutes). The sizes of proteins were then detected by placing the film over the membranes and denoting the molecular weights from the Rainbow marker.

β-actin control

In addition to Ponceau S staining, I also demonstrated equal loading of protein into wells prior to electrophoresis by probing for the 'house-keeping' protein, β-actin; this protein is a cytoskeletal protein that is uniformly expressed in all cells. After chemiluminescent detection of proteins, membranes were removed from the X-ray cassette and washed with blocking solution on a shaker for 2 hours. Membranes then underwent the same procedure described above for β-actin detection: mouse anti-human β-actin primary antibody (1:5000), HRP-linked sheep anti-mouse secondary antibody (1:5000) and ECL chemiluminescent detection for 10 seconds. By this method, I found that levels of β-actin were not significantly different in the experimental groups I studied.

Semi-quantification.

Intensities of bands on the X-ray film was measured by densitometry using Phoretix ID computer program (Phoretix International, Newcastle-upon-Tyne, UK). X-ray films were scanned into Adobe Photoshop and the image then loaded into the Phoretix program

which enabled me to calculate the area and intensity of each band. In the Results, protein expression for all proteins have been corrected for β-actin expression for each lane.

4.2.8 TUNEL in-situ end-labelling

To determine programmed cell death, I used the TUNEL method (Gavrieli et al, 1992); it employs a fluorescein-labelled nucleotide that attaches onto strand breaks in digested DNA found in apoptotic nuclei by in situ end-labelling (terminal deoxynucleotidyltransferase-mediated uridinetriphosphate (UTP) nick end-labelling (TUNEL) In Situ Cell Death detection kit, Boehringer Mannheim, Mannheim, Germany). After dewaxing and rehydration in water, I incubated sections with trypsin for 30 minutes at 37 °C and then exposed sections to terminal deoxytransferase and fluorescein-isothiocyanate (FITC) conjugated UTP. Control sections were exposed to FITC-conjugated UTP only. Sections were then stained with 4 mg/L propidium iodide (PI) containing 100 mg/L RNase A and finally, were mounted in Citifluor (Chemical Labs, Canterbury, UK). Sections were viewed with either a Zeiss Axiophot II microscope (Carl Zeiss) or a confocal microscope (Leica TCS SP2, Leica, Heidelberg, Germany). Using appropriate wavelengths, TUNEL labelled nuclei were detected as a green colour (515 to 565 nm) and could be confirmed as nuclear in origin by staining with PI (617 nm), a dye which intercalates with DNA.

Apoptotic index

To quantify apoptosis, apoptotic nuclei were counted as described for PCNA positive cells (see above) and expressed as the *Apoptotic Index* in each of the three layers in the *sham* and *obstructed* groups. I found that, in all samples, about two thirds of TUNEL-

labelled nuclei were also pyknotic (small, irregular and brightly-staining) as assessed by PI staining; this is explained because the molecular in-situ end-labelling methodology is likely to be more sensitive than the morphological method at detecting apoptotic cells.

4.2.9 Activated caspase-3

Since the identification of sequences that are cleaved in various caspase substrates during apoptosis (Nicholson and Thornberry, 1997), it has become possible to determine specific caspase activity using these substrates, containing the appropriate peptide, coupled to chromogenic groups. Using this methodology, the Caspase-3 Colormetric Activity Assay Kit (Chemicon) is based on the spectrophotometric detection of the chromophore *p*-nitroaniline (*p*NA) after cleavage from the labelled substrate DEVD-*p*NA; the DEVD amino acid sequence is derived from the caspase-3 cleavage site in enzyme poly (ADP-ribose) polymerase (PARP), a DNA repair enzyme.

Bladder samples were incubated at room temperature in Cell Lysis Buffer (proprietary buffer in kit) and subsequent supernatant was incubated with 1 mM ATP at 37 °C for 30 minutes. Samples were incubated with caspase-3 substrate (Ac-DEVD-*p*NA) at 37 °C for one hour and subsequent peptide cleavage measured at an emission wavelength of 405 λ using a luminescence spectrometer (Titertek Multiskan Plus). Absorbency readings were also determined for a *p*NA standard curve and for quantitative purposes, decreasing dilutions of recombinant active caspase-3 (Chemicon) was also tested by the Assay Kit. From the latter two curves, I was able to determine caspase-3 activity in the fetal bladder samples; activity was expressed in units where one unit was the amount of enzyme that

will cleave 1.0 nmol of the colorimetric substrate Ac-DEVD-*p*NA per hour at 37 °C under saturated substrate concentrations. In addition, for control purposes, two samples (one each from the *sham* and *obstructed* groups) were pre-incubated with caspase-3 inhibitor (Ac-DEVD-CHO) for 10 minutes at room temperature before adding caspase-3 substrate solution. I found that addition of inhibitor produced decreased enzyme activity in both the sham fetal bladder sample (2.3 vs 0.1 enzyme units, n=1) and the obstructed fetal bladder sample (3.3 vs 0.3 enzyme units, n=1).

4.2.10 Statistics

Group results were expressed as the mean±SD. As data sets were consistent with a normal distribution, independent samples Students t-tests were used to examine differences in values between *sham* and *obstructed* groups for comparisons of weight, protein and DNA content, detrusor SMC area, lamina propria cell density, *Proliferative Indices*, *Apoptotic Indices,* chemiluminescence of Bcl-2 and Bax (factored for β-actin) and activated caspase-3 units. The null hypothesis was rejected at $p<0.05$. One-way analysis of variance (ANOVA) was performed to compare difference in means±SD of the *Proliferative Indices* and *Apoptotic Indices* within the three layers of the fetal bladder, with a Bonferroni correction to allow for multiple comparisons. For the developing groups, statistics were not performed as there were insufficient samples (n=2) in the 75 day gestation group.

4.3 Physiology

To characterise neurotransmission in the developing and obstructed fetal bladder, I performed in vitro contractility studies, using bladder strips; this technique is based on methodology as previously described (Palfrey et al, 1984). In addition, to determine detrusor thickness and to visualise and quantify nerves in the fetal bladder, I performed histological and immunohistochemical studies, respectively, in fetal bladder sections. To determine visco-elastic properties, I performed filling cystometry experiments in whole bladders and biomechanical stretch studies in bladder strips. Although I performed the filling cystometry experiments at the time of post-mortem, prior to the strip studies, I will describe the latter first, in the Material and Methods and Results, for clarity.

4.3.1 In vitro contractility studies

At the time of post-mortem, fetal bladder samples, from mid-region of bladders, were placed in Ca^{2+} free Hepes Tyrode's solution (105 mM NaCl, 19.5 mM HEPES (N-[2-hydroxyethyl]piperazine-N'-[2-ethanesulphonic acid]), 3.6 mM KCl, 0.9 mM $MgCl_2.H_2O$, 3.6 mM $NaH_2PO_4.H_2O$, 21.5 mM $NaHCO_3$, 5.5 mM glucose, 4.5 mM Na pyruvate, pH 7.1 adjusted with 1M NaOH). Samples were transported to the laboratory at the Institute of Urology and using a dissecting microscope (x 20), I removed the urothelium and adventitia by dissection. I then excised a strip of detrusor muscle *(denuded* strip*)* attempting to keep the muscle strip diameter less than 1 mm to facilitate diffusion of substrates into the preparation. The muscle strip was then placed in an experimental chamber which was mounted on a heavy metal base that, in turn, was mounted on a heavy metal table with metal legs embedded in sand (Figure 21). The

perspex experimental chamber contains a 3 mm wide trough that contains a static hook at one end. One end of the bladder strip was tied, using 8/0 silk, to this static hook; the other end of the strip is tied to a hook attached to an isometric tension transducer (UC3, Gould Statham, GmBH, Seeheim-Ober Beerbach, Germany) that could be manipulated with a Prior micromanipulator that enabled alteration of muscle strip resting length. Strips were then superfused with normal Tyrode's solution gassed with 95% O_2 / 5% CO_2, pH 7.4, 37 °C (Tyrode's solution: 118 mM NaCl, 24 mM $NaHCO_3$, 4.0 mM KCl, 1.0 mM $MgCl_2.6H_2O$, 0.4 mM $NaH_2PO_4.H_2O$, 1.8 mM $CaCl_2$, 6.1 mM glucose and 5.0 mM Na pyruvate). The sides of the trough contained parallel platinum plate electrodes that delivered electrical field stimulation (EFS) to the strip using a Bioscience stimulator and programmer. This delivered 3 second trains of 0.1 ms square wave pulses every 90 seconds with a pulse frequency ranging from 1-60 Hz. This sequence has been shown to generate phasic contractions by direct stimulation of nerves embedded within the strip without direct muscular activation.

Pharmacological manipulation of contractile function, with various agonists and antagonists of putative neurotransmitter action, was used to characterise those involved in regulating detrusor contractility. Control steady-state contractions were obtained at 8 Hz EFS. Nerve-mediated tension was taken as the difference between total and tetrodotoxin (TTX)-resistant force. The latter was calculated by generating a force-frequency response, by stimulating between 1 and 60 Hz, in the absence and presence of TTX (1 μM), an especially potent neurotoxin that specifically blocks voltage-gated sodium channels on the surface of nerve membranes. Smooth muscle has no such sodium channel

associated with its action potential and therefore, as a small element of force remains after the addition of TTX, this must be subtracted from the EFS-generated force to determine true nerve-mediated force.

Muscarinic neurotransmission

In addition to EFS, contractures were elicited by carbachol, a muscarinic agonist (1 μM, 3 μM, 10 μM and 30 μM).

Purinergic neurotransmission

Strips were stimulated by EFS at 8 Hz in the presence of atropine (1 μm), a competitive antagonist of muscarinic receptors. Atropine-resistant contractions were taken as the difference between nerve-mediated responses in the absence or presence of atropine and reflected the proportion of nerve-mediated contraction elicited by acetyl choline release. The purinergic component of contraction was obtained by eliciting contraction in the absence and presence of 10 μm α-β-methylene ATP (ABMA), a purinergic receptor (P2X) agonist that elicits a contracture in muscle strips. However, continued presence causes desensitisation of this receptor to prevent any further activation by neurally released ATP. In addition, strips were stimulated at 8 Hz in the presence of adenosine (1 mM) and, after steady-state baseline contractions at 8 Hz, contractures were elicited in unstimulated preparations by carbachol (1 μM), carbachol (1 μM) plus adenosine (1 mM), and then subsequently with carbachol (1 μM) alone. The latter experiments were performed to establish the effect of adenosine on pre-contracted strips; the mean force

generated by the carbachol contracture was determined from the pre- and post-adenosine experiment.

Nitrergic neurotransmission

Strips were maximally stimulated with carbachol (10 μM) and after two test EFS responses, elicited at 8 Hz, a force frequency relation was determined. After return to control solutions and achieving steady-state baseline contractions at 8 Hz, a repeat carbachol contracture was elicited in the presence of 1H-[1,2,4]oxadiazolo[4,3-a]quinoxalin-1-one (ODQ), an agent that has been shown to reduce the relaxant effect of cyclic guanosine 3',5'-monophosphate (cGMP) that is generated by the release of nitric oxide (NO) (Garthwaite et al, 1995).

At the end of all experiments, the muscle was weighed and contractile force expressed in units of $mN.mg^{-1}$ wet weight of tissue. Force-frequency relations and dose-response relations were fitted to the empirical equations (Bayliss et al, 1999):

$$T = \frac{T_{max} \cdot f^n}{K_{1/2}^n + f^n} \qquad T = \frac{T_{max}\,[S]^n}{EC_{50}^n + [S]^n}$$

where T is the tension, T_{max} is the estimated maximum tension at high frequencies or high concentrations, f is the frequency of stimulation, [S] is the agonist concentration, $K_{1/2}$ and EC_{50} are the frequency and concentration respectively required to achieve $T_{max}/2$ and n is a constant. In the Results, I expressed $K_{1/2}$ and EC_{50} as their logarithmic transforms $pK_{1/2}$ ($-\log_{10}K_{1/2}$) and pEC_{50} ($-\log_{10}EC_{50}$) as these have been shown to be normally distributed parameters (Bayliss et al, 1999).

The effect of the mucosa

To determine the effect of mucosa on detrusor muscle contractility, I also determined force-frequency relations for full thickness bladder wall strips *(mucosal* strip*)* and corrected force generated to the wet weight of the detrusor in the preparation. The latter was calculated by histological study (see below). In addition, these strips were also stimulated in the presence of ODQ (1 μM) to determine the role, if any, of nitric oxide.

Detrusor thickness calculation

So that mucosal bladder strips could be corrected for wet weight of muscle (to allow direct comparison with *denuded* muscle strips), I calculated the percentage thickness of the detrusor smooth muscle layer in bladder sections stained with Masson's trichrome. Histology and Masson's trichrome stain were performed as previously described in Section 4.2.4. Using the KS 300 computer program (Carl Zeiss), I calculated detrusor thickness and whole wall thickness for bladders from *sham* and *obstructed* groups (n=5 both groups) to calculate the relative proportions.

Neuronal protein immunohistochemistry and western blot

To visualise nerves within fetal bladders, I performed immunohistochemistry of two key neuronal proteins. S100 is a calcium-binding protein, found in neuroepithelial and neural crest derived cells; it is present in all Schwann cells and in most neurons (Stefansson et al, 1982). Protein gene product 9.5 (PGP 9.5) is a cytosolic protein that is highly expressed in neurons (Gulbenkian et al, 1987). Immuniohistochemistry was performed as previously described in section 4.2.6. In brief, the primary antibodies used were anti-

S100 antibody (1:500; DAKO, Ely, UK) or anti-PGP 9.5 antibody (1:500; DAKO) and the secondary antibody used was biotinylated goat anti-rabbit antibody (1:200; Amersham Pharmacia Biotech, Little Chalfont, Buckinghamshire, UK).

To quantify any change of innervation in the *sham* and *obstructed* fetal bladders, I performed western blot of PGP 9.5, as described in section 4.2.7. In brief, the primary antibody used was anti-PGP 9.5 antibody (1:1000; DAKO) or β-actin (1:10000), a 'house-keeping' protein and the secondary antibodies were either HRP-linked goat anti-rabbit antibody (1:1000), for PGP 9.5 detection, or HRP-linked sheep anti-mouse antibody (1:5000), for β-actin detection. Bands were detected by chemiluminescence, for 30 seconds (PGP 9.5) or 10 seconds (β-actin). S100 protein binds calcium and as such, also reacts with calcium-binding proteins such as calmodulin and myosin light chain (Baudier, Glasser, & Gerard 1986) found in detrusor muscle; hence, it was appropriate only for immunohistochemistry.

4.3.2 Filling cystometry

I used ex vivo filling cystometry to determine the relationship between storage volume and luminal pressure in *sham* and *obstructed* fetal bladders. At the time of postmortem, with the urinary tract in situ, the urethra and the urachus were clipped to avoid any urine loss (this was necessary as the obstruction was incomplete); the ureters were also clipped close to the vesico-ureteric junctions. I then placed a double lumen catheter into the bladder, one lumen for filling and the other for pressure recording (see Figure 22). Access was by a cut-down technique either through the urethra or the urachus and the

catheter held with 2/0 silk ligatures. Intravesical pressure was recorded with reference to air (i.e. atmospheric pressure = zero) by a water-filled transducer (PDCR 75, Druck Ltd, Groby, Leicestershire, UK) placed level with the bladder and connected, via a bridge amplifier, to a chart recorder (Lectromed, Letchworth, Hertfordshire, UK). The pressure at the outset was recorded, and the bladder then drained noting the volume. The bladder was intermittently hand-filled by syringe with Ca^{2+} free HEPES Tyrode's solution at room temperature using step-wise increments of 0.1 to 1.0 ml for sham bladders and increments of up to 5.0 ml for obstructed bladders. Intravesical pressure was recorded continuously and documented from stable plateaux following stress-relaxation. I stopped filling the bladder when the initial bladder volumes were reached or when the bladder became tense on visual observation: over-distending the bladder was avoided to prevent tissue damage, as samples were subsequently used for in vitro studies. The complete procedure took approximately 10 minutes. There was no significant difference in results obtained from contractility studies between fetal bladders that were or were not exposed to filling cystometry.

Wall stress

To examine further the compliance of the bladder wall and take account of disparate bladder volumes between the two groups, wall stress was derived. Wall stress, σ, was measured using a modified Laplace relation: $\sigma = P.r_1/2.d$, where P is luminal pressure, r_1 inner radius of the bladder and d the wall thickness; r_1 was calculated from the volume V in the bladder from the relation $V = (4\pi/3).r_1^3$. The tissue volume, T_v, of the bladder wall (bladder weight/density; density=1.05 $g.ml^{-1}$) was used to calculate wall thickness

assuming the tissue formed a concentric sphere around the bladder lumen and using the relation:

$$d = \sqrt[3]{[(3T_v/4\pi)+r_1^3]} - \sqrt[3]{[3V/4\pi]}$$

4.3.3 Biomechanical stretch studies

To examine further the visco-elastic properties of detrusor from the fetal bladder wall, I performed biomechanical stretch studies of bladder strips. Bladder muscle strips were cut from the bladder dome as described in section 4.3.1. and placed in an experimental chamber, with a trough similar in design to that described for the electrophysiological contractility studies (see Figure 23). For these experiments, the mucosa was removed as this influences overall visco-elastic parameters (Susset and Regnier, 1981). Strips were superfused with normal Tyrode's solution gassed with 95% O_2 / 5% CO_2, pH 7.4, 37 °C. The muscle strips were tied at one end to an isometric force transducer (UC3, Gould Statham) and the other end tied to a fixed hook; the position of this hook could be adjusted in the horizontal plane by a voltage-operated solenoid (308B Lever Arm System, Cambridge Technology Inc, Watertown, MA, USA). Changes of muscle strain (up to 1.6 mm in 0.3 mm increments) were generated by imposing square voltage waves on the solenoid for 50 seconds duration and then return to steady state length with continuous force measurement throughout this period (100 seconds). The resultant changes to muscle stress (tension) were recorded, and after measuring muscle strip length and wet weight, expressed as tension per cross-section area ($mN.mm^{-2}$). Ramp steps (frequency <0.01 Hz, 50 seconds stretch and 50 seconds relaxation to original steady-state length) were also examined to determine any steady-state hysteresis in the stress-strain relationships.

Control experiments used a metal bar or a rubber band in place of the muscle strip. With a metal bar, the experimental system exhibited a steady-state settling time of <50 μs to an instantaneous length change, i.e. several orders of magnitude faster than changes to muscle stress. A linear stress-strain relation was recorded with a rubber band, demonstrating no intrinsic hysteresis in the experimental system. The visco-elastic changes of stress, *T(t)*, were fitted to the following equations:

$T(t) = T' (\exp (- t / \tau_1)) + T_1$ for the period of stretch

$T(t) = T'' (1 - (\exp (- t / \tau_2))) + T_2$ for the period of relaxation

where *T'* and *T''* are the magnitudes of the visco-elastic components of the total change of stress with time constants τ_1 and τ_2. T_1 and T_2 are the steady-state elastic components. Work involved in changing muscle length was calculated for the formula:

Work/time=force x distance shorted (per unit time).

Thus, the work in deforming the viscous component, W_v, was calculated from the integral of the time-dependent component of the tension change during the period of stretch or relaxation, *t*.

$W_v = T't - T'\tau [\exp (- t / \tau)$

The work to deform the elastic component, W_e, was calculated from:

$W_e = T_1 \bullet t.$

When hysteresis loops were calculated, the area between the curves was determined using Simpson's rule (this allows approximation of the integral; in this case, by the summation of areas of 25 columns under each curve).

4.3.4 Radiotelemetered fetal bladder cystometry

These preliminary experiments were performed in four control fetuses to determine the feasibility of fetal bladder cystometry in an experimental model of in utero bladder outflow obstruction. All radiotelemetry equipment was purchased from Data Sciences International, MN, USA.

Radiotelemetry equipment

Fetal bladder and abdominal pressures were recorded using dual pressure D70PCP radiotelemetry implants (PhysioTel ® Multiplus ^{TM} TL Series Implants) (see Figure 24) that employ two fluid-filled 1.2 mm catheters that have a thin walled biocompatible tip and a noncompressible fluid that communicates with pressure sensors within the body of the implant. The first two experiments (Experiments 1 and 4) used implants with a 30 cm catheter and a 25 cm catheter with a plastic cuff. The remaining two experiments used implants with two 30 cm catheters with no cuffs. Within the implant (covered with a biocompatible outer layer), was a micropower electronics module that processed the pressure information received from the pressure sensors and then transmitted this digitised data using a radio frequency transmitter (that can transmit up to a 50 cm radius). The implants also had two biopotential leads, capable of measuring electrocardiographic and electromyographic data that were not used in these preliminary studies.

Data was then received by a remote receiver (RMC-1) that interfaced with a Data Exchange Matrix (DEM) and also received information of the ambient pressure from an ambient pressure recorder (APR-1). The DEM then transferred and stored the data in the

Dataquest A.R.T. system (a computer-based data acquisition system) that allowed visualization of pressure recordings, accurate measurement of parameters and export of data to Microsoft Office Excel to derive traces by subtraction. A diagram of the setup is shown in Figure 25A.

Study design and implantation

We used four fetuses and used different methods of catheter placement to optimise the technique. Sheep anaesthesia, fetal exposure at surgery, uterine and wound closure, antibiotic usage, post-operative care and euthanasia were performed as previously described in section 4.1.3. Fetal hindquarters were delivered and catheters were placed as follows:

Experiment 1: Male fetus, 105 days gestation, bladder catheter placed in bladder directly through bladder wall and abdominal catheter placed within fetal abdomen.

Experiment 2: Female fetus, 105 days gestation, as above

Experiment 3: Male fetus, 105 days gestation, as above except bladder catheter placed through the urachus.

Experiment 4: Male fetus, 75 days gestation, bladder catheter placed through the urachus and abdominal catheter tip sutured to fetal skin.

All catheters were tunnelled (except in experiment 4) and anchored to fetal skin with 2/0 silk. All implants were then sutured to the uterine wall with 2/0 silk.

When the ewe was placed in the appropriate pen (with a receiver fixed onto one of the walls) (Figure 25B), radiotelemetry recording of pressure was performed. I recorded pressures for about two hours (at approximately the same time of day) two or three times per week for 25-30 days. The implants house batteries that last for three months of continuous use and can be switched on and off by passing a magnet over the implant (the 'on' position can be determined by detecting a high-pitched noise when holding an amplitude modulation (AM) radio near the animal). Originally, I hoped to preserve battery life, and therefore cost, by only turning the implant on when I was recording pressures. However, as the implant was deep inside the maternal abdomen in all animals, I was unable to do this. After 25-30 days post-implantation, I terminated the experiment by sacrificing the maternal ewe. Apart from a few minor adhesions around the implant body, all implants and catheters were easily retrieved and batteries turned to the off position. During one post-mortem, I found that the magnet could turn the implant on and off if it was placed under the maternal skin (as recommended for use in adult experiments by the manufacturer) or fixed onto the inside of the maternal wall in this one animal; such information may be useful in planning future experiments.

Validation by simultaneous filling cystometry

At post-mortem, experiments 1 and 4 underwent simultaneous radiotelemetry and filling cystometry pressure recordings to validate the pressures recorded by the radiotelemetry implants. To do this, at post-mortem, in addition to radiotelemetry catheters in situ, filling cystometry catheters were placed into the bladder as previously described in section 4.3.2 and the bladder intermittently hand-filled with saline. Results were then compared for the

pressure-volume recordings from the paper chart recordings from filling cystometry and the computer-generated images from the radiotelemetry implants.

4.3.5 Statistics

Results are expressed as the mean±SD unless otherwise stated; independent samples Student's t-tests were used to examine differences in mean values between *sham* and *obstructed* groups and between male and female *sham* groups. To determine whether percentage changes to data sets were different from 100% (nitrergic neurotransmission and the effect of mucosa on force generation) a Mann-Whitney U-test was used; with the latter test, results are expressed as the median and the interquartile range. The null hypothesis was rejected if $p<0.05$.

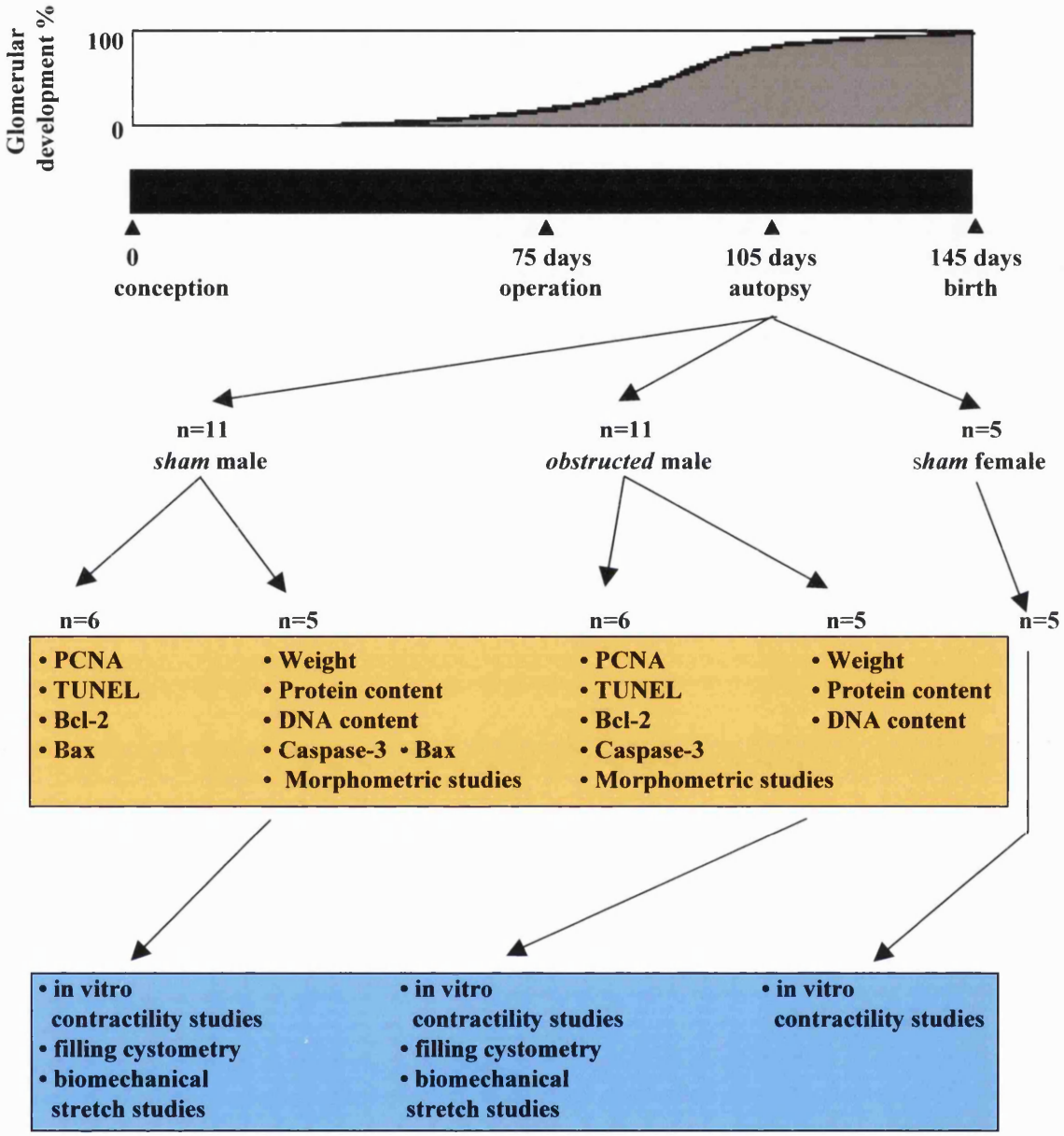

Figure 15. Experimental design of in utero bladder obstruction study

Scheme of fetal sheep gestation, from conception to birth, with timing of *sham* and *obstructed* group operations and analyses of urinary bladders (molecular biology in the orange box and physiology studies in the blue box). In order to place these procedures in relation to upper renal tract development, the percent glomerular complement of the developing sheep metanephric kidney is also shown (adapted from results in Edouga et al, 2001).

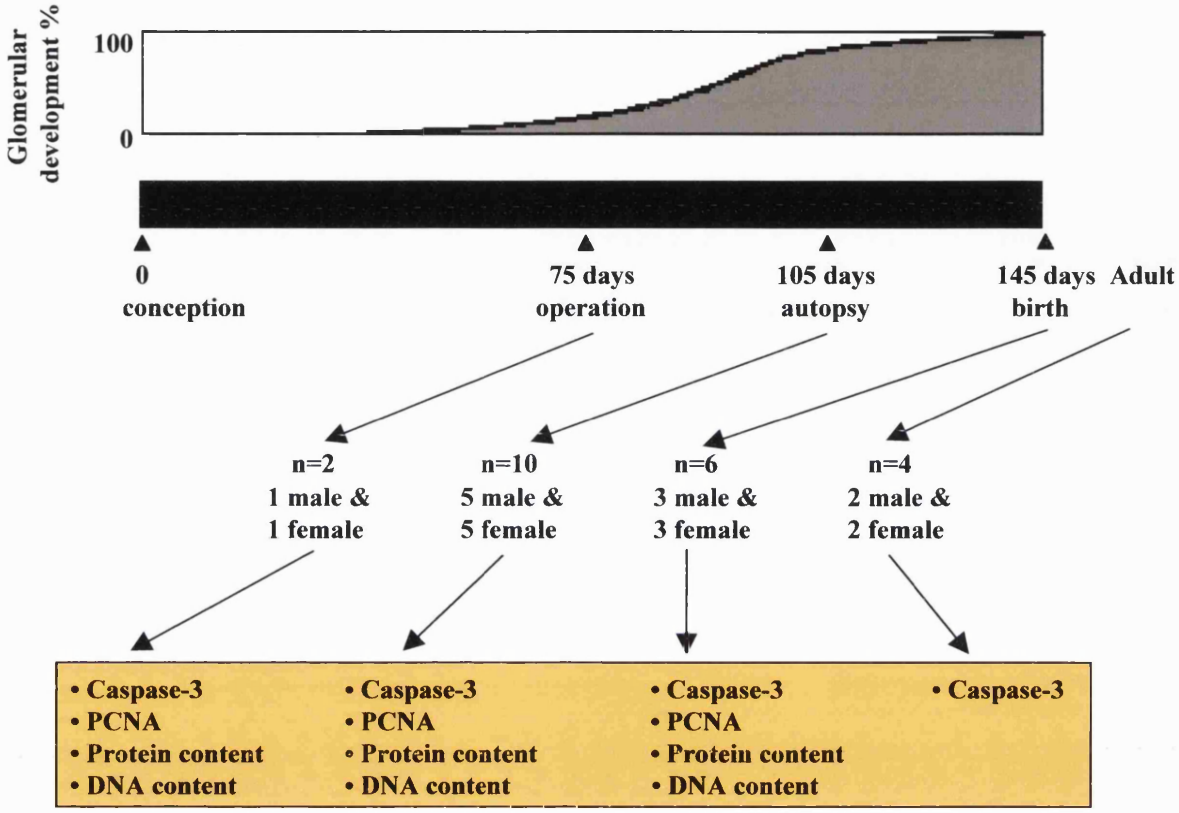

Figure 16. Experimental design of maturation study
Scheme of fetal sheep gestation, from conception to birth, with timing of collected bladder samples and analyses for selected molecular biology studies (in the orange box)

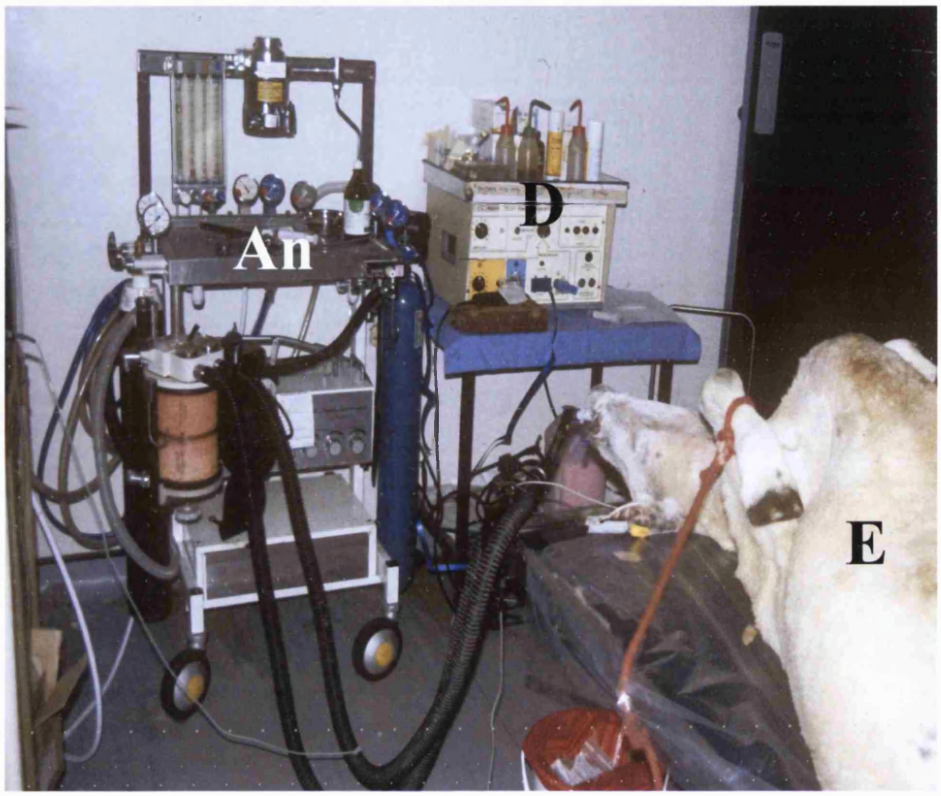

Figure 17. Sheep surgery
Pregnant ewe (E) is shown lying prone on the operating table, with legs held by rope. The ewe has been intubated and anaesthesia maintained by 2-3% halothane and oxygen by the anaesthetic circuit (An). Also seen to the right of the anaesthetic machine is the diathermy unit (D), used to cauterize tissue.

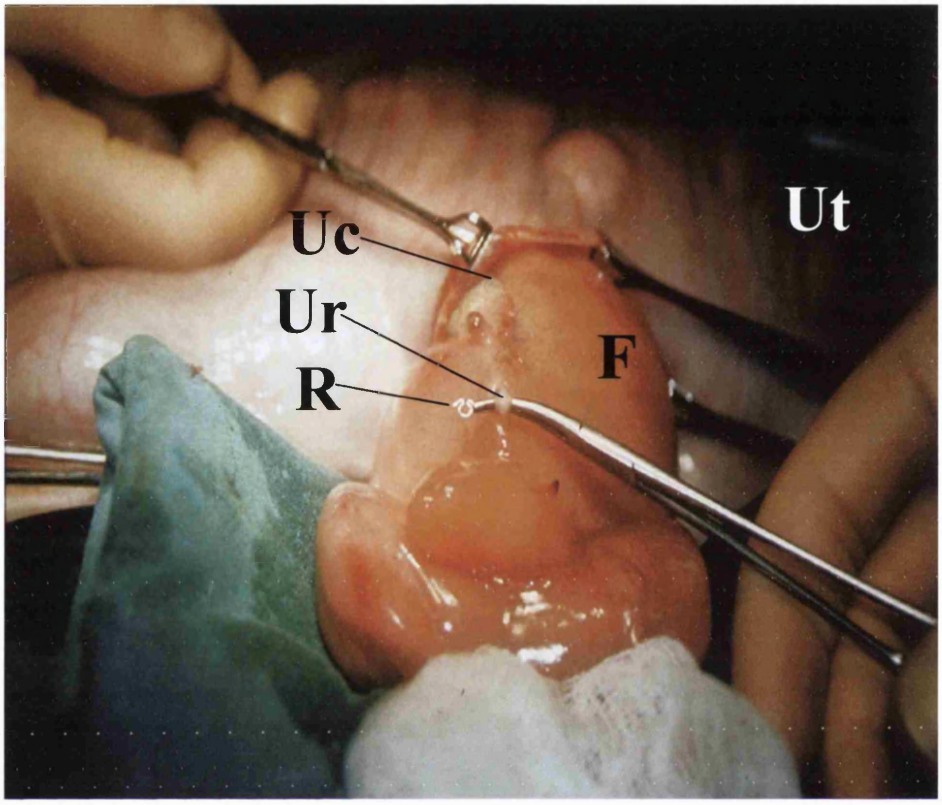

Figure 18. Fetal sheep surgery
The fetus (F) have been delivered from the maternal uterus (Ut). In this figure, bladder outflow obstruction was induced by placement of a 2mm omega-shaped silver ring (R) around the fetal sheep urethra (Ur) and ligation of the urachus (Uc, shows anatomical site of urachus).

Figure 19. Fetal ultrasound
For fetal ultrasound, the ewe is placed on her hindquarters and held whilst the ultrasound probe is placed on the maternal abdomen, over the site of the maternal uterus.

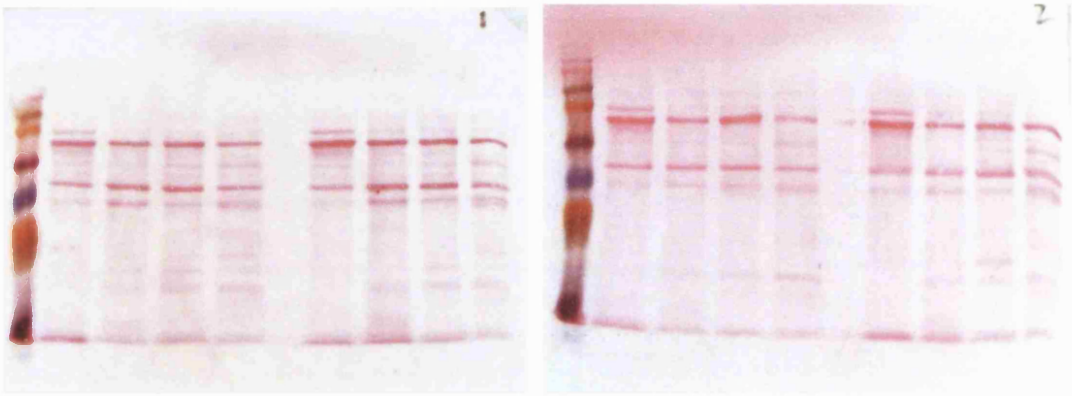

Figure 20. Ponceau S staining
Ponceau S was used to show uniform transfer of proteins from gels to nitrocellulose membranes after electroblotting. In this example, membranes show (from left to right) a lane containing the rainbow marker, four lanes of proteins, an empty lane and then a further four lanes of proteins. Note membrane 1 has top right corner removed to aid identification (as the Mini-Protean II apparatus allowed two gels to be run simultaneously).

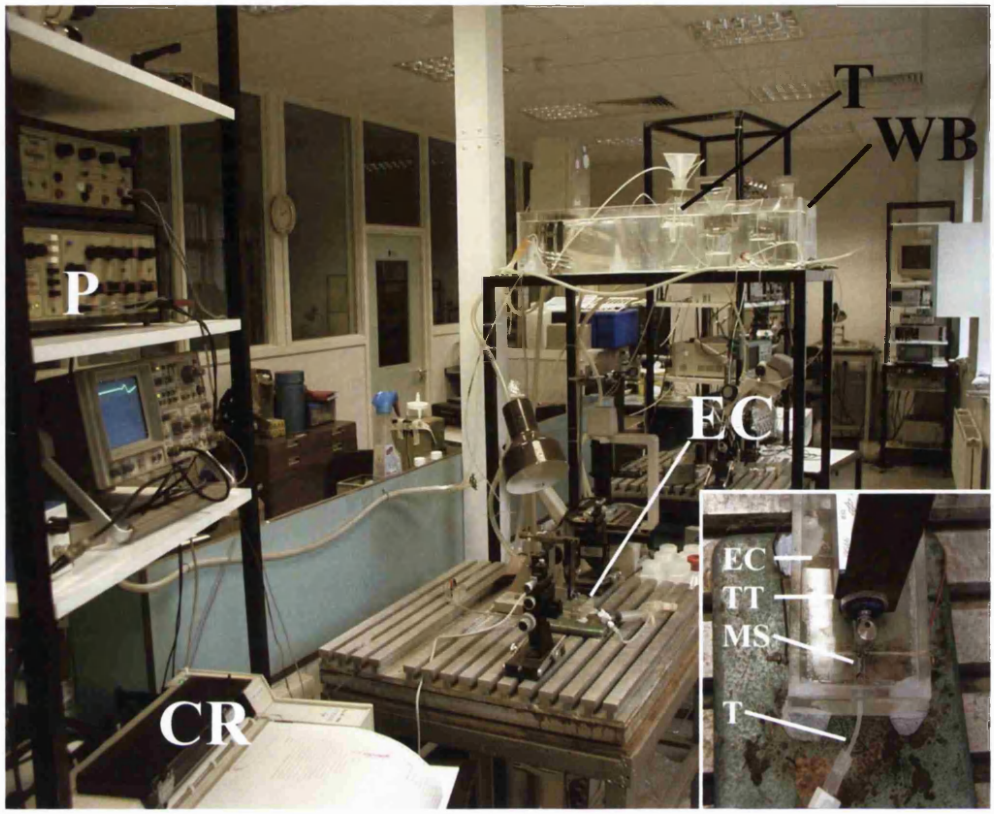

Figure 21. Electrophysiology contractility rig setup
Experimental chamber (EC), held on a metal table, contains muscle strip that is supefused with gassed Tyrodes solution (T) kept at 37 °C by the water bath (WB). Stimulator and programmer (P) determines sequence of electrical field stimulation delivered to muscle strip, tension produced recorded on chart recorder (CR). Insert shows high power image of experimental chamber with tension transducer (TT), muscle strip (MS, with adjacent plate electrodes) and Tyrodes superfusate.

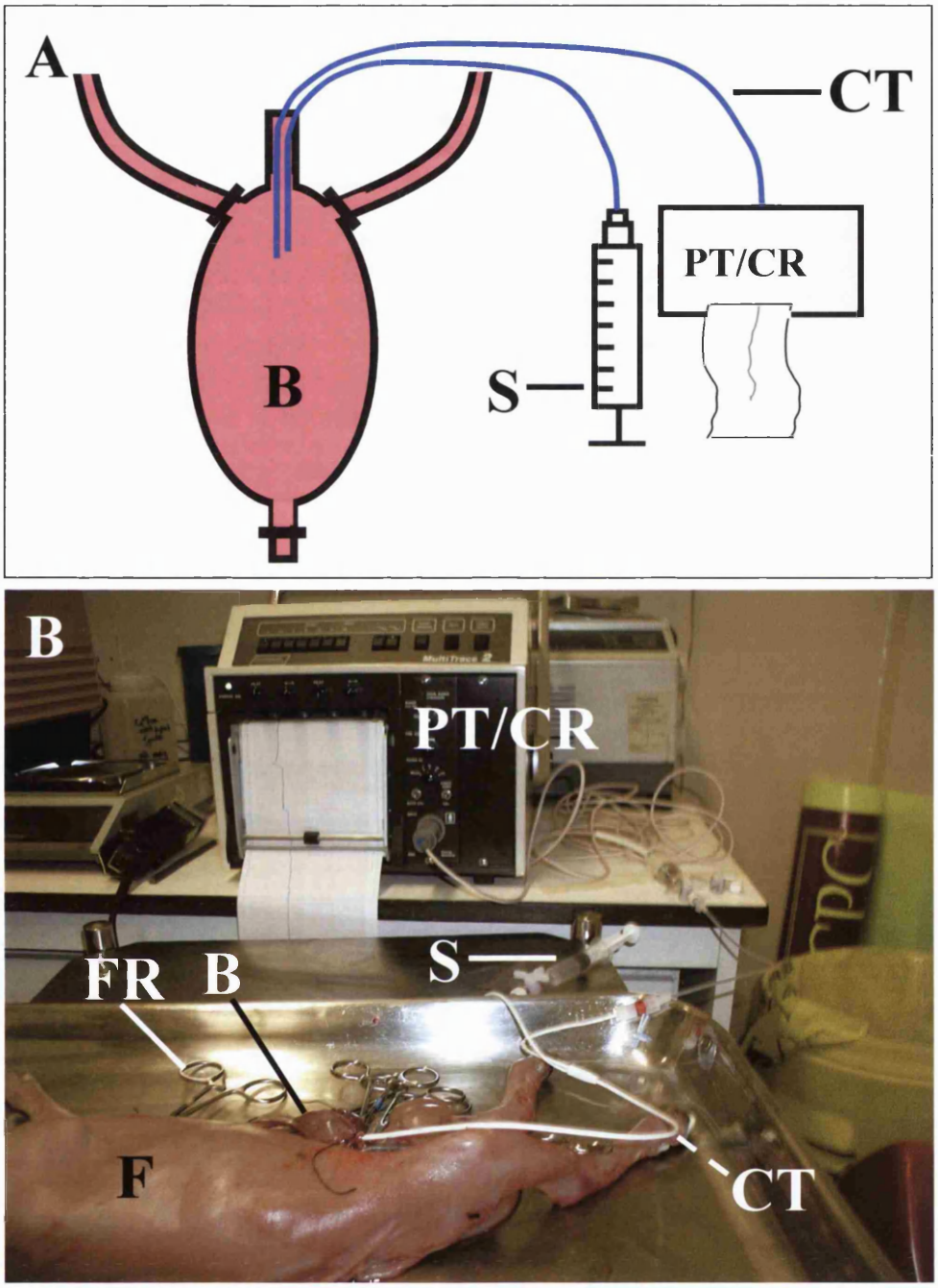

Figure 22. Filling cystometry
A: Diagram representing bladder (B) with outflow tracts clipped, a double lumen catheter (CT), in this example, through the urachus, with the ends of the catheter attached to a syringe (S) and pressure transducer (PR) and chart recorder (CR). B: Photograph of procedure with double lumen catheter, in this case, entering through the urethra of the bladder (B) of the fetus (F); forceps (FR) were used to clip the outflow tracts.

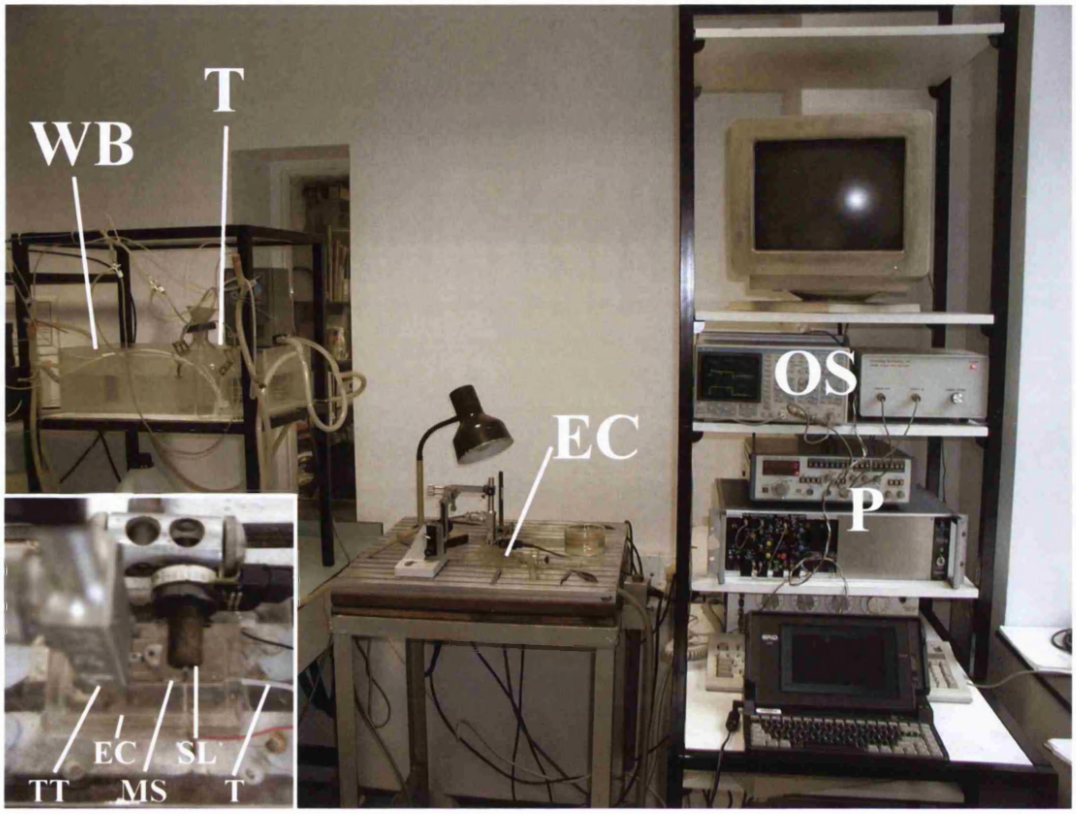

Figure 23. Biomechanical stretch rig setup
Experimental chamber (EC), held on metal table, contains muscle strip that is supefused with gassed Tyrodes solution (T) kept at 37 °C by the water bath (WB). Programmer (P) alters voltage to produce various lengths of stretch by the solenoid. Voltage changes of tension and stretch are produced on the oscilloscope (OS). Insert shows high power image of experimental chamber (EC) with tension transducer (TT), muscle strip (MS), voltage-gated solenoid (SL) and Tyrodes superfusate.

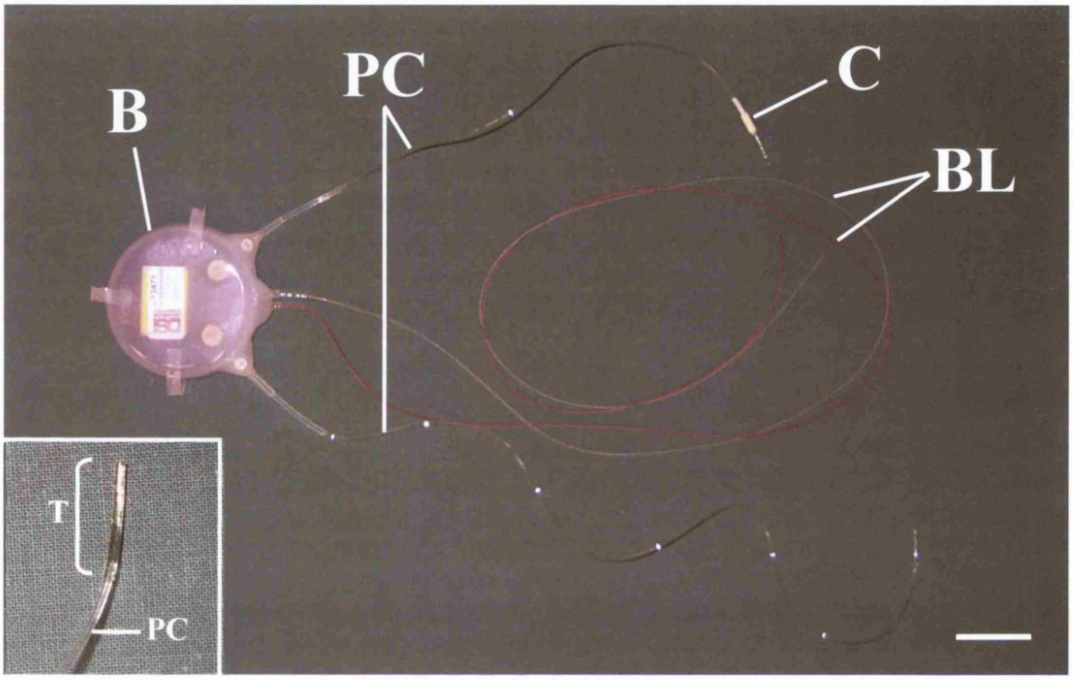

Figure 24. D70PCP radiotelemetry implant
Body of implant (B, with a biocompatible cover) has two 1.2 mm catheters (PC, in this figure, one catheter is 30 cm and the other, with a plastic cuff, C, is 25 cm) that transmit pressure. In addition, the implant has two biopotential leads (BL) that were not used in my thesis. Insert shows high power image of distal end of pressure catheter; at the very end is a biocompatible tip that contains a pressure-sensitive gel, the remainder of the catheter is filled with a noncompressible gel. Bar is 2.7 cm.

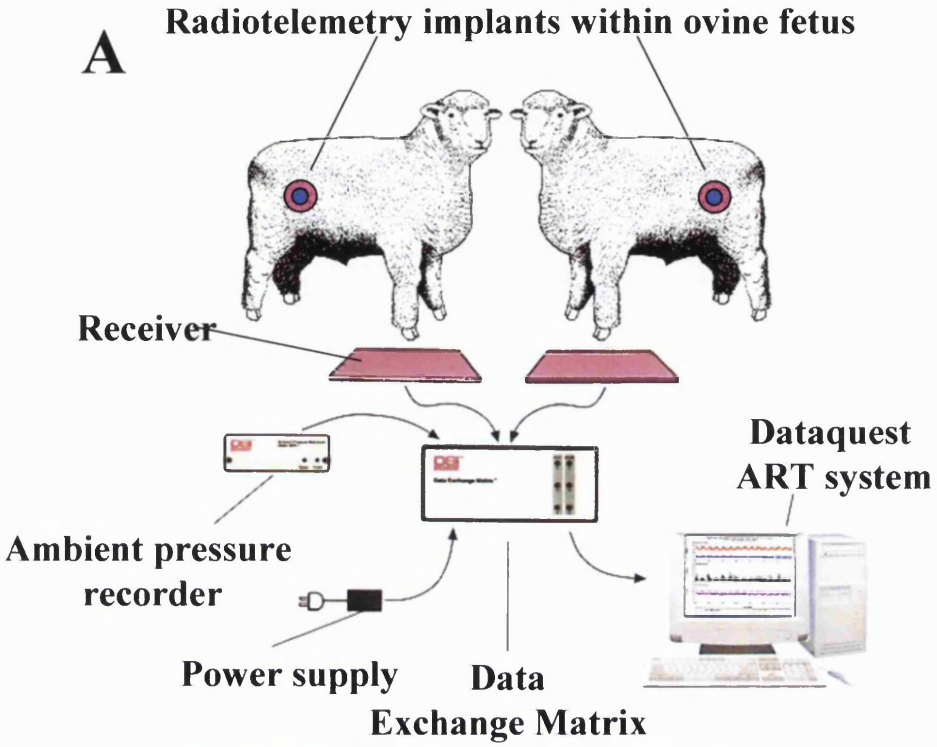

Figure 25. Setup of radiotelemetry recording equipment
A: Radiotelemetry implants within ovine fetus transmit bladder and abdominal pressure to a receiver on the sheep pen. The receiver interfaces with a Data Exchange Matrix (DEM) that also receives information of the ambient pressure from an ambient pressure recorder. The DEM then transfers and stores the data in the Dataquest A.R.T. system. The system used was able to monitor two experiments simultaneously. B: Recording of fetal pressures, note maternal ewe (E) is untethered, not stressed and has no exiting catheters or tubes; the receiver (R) is housed on one side of the pen, the cable from the receiver then enters DEM.

5. Results

5.1 Experimental model

5.1.1 Gross changes of the fetal bladder after BOO

At weekly intervals following surgery, ultrasonography showed no hydronephrosis in *sham* fetal kidneys (Figure 26A), and *sham* fetal bladders were of insufficient size to be definitively demonstrated. In the *obstructed* group, all fetal kidneys became hydronephrotic and bladders were dilated (Figure 26B); this appearance was evident at the first ultrasound examination and the severity progressed during the 30 days of observation. This appearance was also found at post-mortem performed at 105 days of gestation (Figure 27) which confirmed the increased size of the partially obstructed fetal bladder, with dilatation of the ureters and increased size of the kidneys that were hydronephrotic on sectioning (Figure 27 insert).

Table 1 shows the fetal bladder and body weights and bladder-to-body weight ratio (BBR). Both body (2.07±0.41 kg versus 1.38±0.29 kg, n=5 both groups) and bladder weights (7.28±4.41 g versus 1.14±0.25 g, n=5 both groups) were significantly increased ($p<0.05$) in the *obstructed* versus *sham* male group. However, the increase in bladder weight was greater than that of body weight as demonstrated by the increase of BBR (3.39±1.78 g/kg versus 0.82±0.11 g/kg, n=5 both groups, $p<0.05$). Although, fetal weight was significantly increased in the *obstructed* group, the femur length (6.4±0.8 cm versus 5.5±0.3 cm, n=5 both groups, $p>0.05$) and occipito-snout length (14.6±1.6 cm versus

12.7±0.8 cm, n=5 both groups, $p>0.05$) were the same in the *obstructed* and *sham* male groups. This suggests that there was no overall size difference but there may have been fluid accumulation in the *obstructed* group. There were no differences ($p>0.05$) between male and female *sham* fetuses in body (1.49±0.29 kg) or bladder weights (1.09±0.16 g).

5.1.2 Summary

- In utero BOO resulted in a change to the macroscopic features of the urinary tract.

- Ultrasound and post-mortem features of obstructed urinary tracts revealed hydroureteronephrosis and a dilated bladder.

- The *obstructed* bladder was significantly heavier than the *sham* bladder.

5.2 Molecular biology

5.2.1 Histology, αSMA expression and morphometric analyses

Histological examination of kidneys from *sham* fetuses which had undergone the same protocol (Figure 28) had revealed a prominent nephrogenic zone, with normal calibre tubules and developing glomeruli. By contrast, in *obstructed* kidneys, a perturbation of nephrogenesis had been noted, with morphological disruption of the nephrogenic cortex and subcortical cysts.

Masson's trichrome histological stain showed that, at 105 days gestation, *sham* fetal bladders were well-developed, with a urothelial layer covering the lamina propria; detrusor muscle bundles were apparent, with a trilaminar appearance, and with little connective tissue between individual muscle bundles (Figure 29A). High power images (Figure 29C and D) reveal a detrusor muscle layer containing discrete muscle bundles with few cells between bundles, a lamina propria containing cells surrounded by collagen and a urothelium which was three-four cell layers thick. By contrast, *obstructed* bladder walls were thinner, their urothelium was flattened and the cellularity of the lamina propria appeared decreased (Figure 29B). High power images (Figure 29E and F) show that *obstructed* bladders had a detrusor layer with muscle bundles separated by prominent spaces containing collagen and cells, a lamina propria layer that appeared to have a lower density of cells, and an attenuated, predominantly single cell-layered, urothelium. Furthermore, these images suggested that myocytes in *obstructed* bladders were larger than cells found in the *sham* group; this was confirmed by measuring a significant increase ($p<0.001$) in the average area of detrusor SMC by morphometric analysis ($132\pm59\mu m^2$ versus $64\pm15\mu m^2$, n=5 each group). The impression of a relatively acellular lamina propria was confirmed by morphometric analysis, with a significantly lower ($p<0.001$) cell density in this layer ($3144\pm1101/mm^2$ versus $4718\pm946/mm^2$, n=5 each group).

Similar observations of morphological disruption of the *obstructed* fetal bladder were made by staining histological sections with Elastin van Geison (Figure 30). Moreover, this stain revealed that, not only was there increased collagen deposition throughout the

obstructed bladder, but there was increased elastin deposition in addition. As noted previously, this increased extracellular matrix deposition was observed around obstructed muscle bundles and throughout the lamina propria of the *obstructed* fetal bladder.

Finally, there was prominent immunolocalisation of αSMA (Figure 31) to myocytes within smooth muscle bundles within *sham* and *obstructed* fetal bladders. This confirmed that detrusor SMC had differentiated into smooth muscle cells at this stage of gestation in the fetal ovine bladder and that this differentiation had also occurred in the *obstructed* bladder.

5.2.2 Dry weight, protein content and DNA content

Concomitant with the observed increase in wet weight of the *obstructed* fetal bladder, an increase ($p<0.05$) of dry weight was also recorded (1.07±0.57g versus 0.16±0.06g, n=5 each group). There was no difference ($p=0.65$) in the dry/wet weight ratio between *obstructed* (15.8±2.7%, n=5) and *sham* (14.2±7.0%, n=5) groups. Total protein was significantly greater ($p<0.005$) in *obstructed* versus *sham* bladders (303.4±114.9mg versus 64.0±6.0mg, n=5 each group). Extracted DNA from *obstructed* and *sham* samples were of sufficient quality as confirmed by an appropriate absorbance ratio (1.87±0.20 arbitrary units, for all samples) and appropriate bands after agarose gel electrophoresis (Figure 32). Laddering of DNA as often seen in apoptosis (Miyake et al, 2000) was not observed; this may have been due to low *apoptotic indices* in sham and obstructed bladders (see later). Quantification revealed that total DNA content was significantly greater ($p<0.05$) in *obstructed* versus *sham* bladders (5.60±3.08mg versus 1.49±0.47mg,

n=5 each group). There was a nonsignificant (p=0.21) increase in the protein/DNA ratio of full-thickness bladder samples (0.06±0.03 versus 0.05±0.03, n=5 each group). There was only a trend suggesting cellular hypertrophy, but it is important to note that this ratio is of DNA and protein contents of whole bladder wall specimens and not exclusively of the detrusor muscle layer. To summarise, after BOO, the average increase in fetal bladder wet weight was 539%, in dry weight was 569%, in protein content was 374% and in DNA content was 276%.

5.2.3 Proliferation

As assessed by immunostaining of proliferating cell nuclear antigen (Figure 33), all three layers in *sham* and *obstructed* bladders at 105 days gestation contained proliferating cells. Quantification, as determined by counting PCNA-immunolocalised cells, is shown in Figure 33E. In the *sham* controls (n=6), there were no significant differences in *Proliferative Indices* between the cells in the three main layers of the bladder wall (44±17 % in detrusor SMC, 45±4 % in lamina propria layer and 46±8 % in urothelium; $p>0.05$, ANOVA). In contrast, in the *obstructed* group (n=6), there was a significantly lower *Proliferative Index* in lamina propria cells (40±5 %) versus detrusor SMC (68±2 %; $p<0.001$, ANOVA) and versus urothelial cells (57±1 %; $p<0.05$, ANOVA). Furthermore, there was a significant increase ($p<0.05$) in the *Proliferative Index* in detrusor SMC of the *obstructed* versus the *sham* group but there were no significant differences of *Proliferative Indices* of lamina propria or urothelial cells between these two groups. Lastly, a prominent proliferating cell population was observed around *obstructed* muscle

cell bundles (Figure 34A) which were not evident in *sham* bladders; the *Proliferative Index* of these cells was 50±10 % (n=6) (Figure 34B).

5.2.4 Apoptosis

TUNEL in-situ end-labelling (Figure 35) revealed that some cells were undergoing death by apoptosis in all layers in both *sham* and *obstructed* bladders at 105 days gestation. In Figures 35A-C, the numbers of apoptotic nuclei were higher than average and as such, I had to count 1000 cells per fetal bladder to calculate the mean *Apoptotic Index*. Quantification of apoptosis is shown in Figure 35D. I found that there were no significant differences between *Apoptotic Indices* in cells of the three layers from either the *sham* (n=6) (0.14±0.09 % in detrusor SMC, 0.11±0.06 % in lamina propria layer and 0.04±0.05 % in urothelium; $p>0.05$, ANOVA) or *obstructed* (n=6) (0.31±0.07 % in detrusor SMC, 0.29±0.07 % in lamina propria layer and 0.09±0.09 % in urothelium; $p>0.05$, ANOVA) groups. As depicted in Figure 35D, the *Apoptotic Index* was significantly increased in the *obstructed* versus *sham* bladders in detrusor SMC ($p<0.001$) and also lamina propria cells ($p<0.001$); there was no significant difference in apoptosis between *obstructed* and *sham* urothelial cells. Apoptosis was not observed in the population of proliferating cells located between muscle bundles in the *obstructed* bladders.

5.2.5 Activated caspase-3 quantification

By a substrate cleavage assay, activated caspase-3 was detected in the *sham* bladder at 105 days gestation (2.0±0.4 enzyme units, n=5) and was significantly increased ($p<0.005$) in time-matched *obstructed* bladders (4.2±0.5, enzyme units, n=5) (Figure 36).

One unit was the amount of enzyme that will cleave 1.0 nmol of the colorimetric substrate Ac-DEVD-*p*NA per hour at 37 °C under saturated substrate concentrations.

5.2.6 Bcl-2 and Bax expression

Bcl-2 immunohistochemistry revealed this anti-death protein was present within the cytoplasm of most cells within each layer of the *sham* (Figure 37A and B) and *obstructed* (Figure 37C and D) bladders at 105 days gestation. Western blot of full thickness bladder samples showed a band at 26 kDa (Figure 38), as previously reported (Oltvai et al, 1993), and quantification, using Bcl-2/β actin ratios, showed a significant down-regulation (approximately 50%) of Bcl-2 protein in *obstructed* versus *sham* bladders (10.0±4.9 arbitrary units versus 20.0±6.5 arbitrary units, n=6 each group, $p<0.05$). Bax immunohistochemistry revealed that this pro-death protein was also present within the cytoplasm of cells within all layers of the *sham* (Figure 37E and F) and *obstructed* (Figure 37G and H) fetal bladders at 105 days gestation; moreover, the staining intensity was subjectively increased in the *obstructed* versus *sham* detrusor SMC and lamina propria (e.g. compare Figures 37E and F with G and H). Western blot of full thickness bladder samples showed a band at 22 kDa (Figure 38), as previously reported (Kulig et al, 1999), and quantification, using Bax/β actin ratios, showed a significant up-regulation (approximately 200%) of Bax protein in *obstructed* versus *sham* bladders (54.9±8.1 arbitrary units versus 18.2±14.0 arbitrary units, n=6 each group, $p<0.001$).

5.2.7 The developing fetal bladder

To examine the maturational changes that occur in the bladder during normal fetal development, I performed selected studies in fetal bladders at four time points: 75 days gestation, 105 days gestation, 145 days gestation and the adult sheep bladder. Staining with Masson's trichrome (Figure 39) revealed progressive thickening of the fetal bladder wall from 75 days gestation through 105 and 145 days. Detrusor muscle bundles were present at all three time points, but appear to become increasingly organised with increasing gestation. During this period, the bladder grows, as assessed by the total content of protein (57.0 mg, n=2; 68.7±22.4 mg, n=10; 126.9±48.6 mg, n=6, at 75, 105 and 145 days gestation respectively) and DNA (1.36 mg, n=2; 1.44±0.37 mg, n=10; 2.97±2.13 mg, n=6, at the same time points).

PCNA immunohistochemistry (Figure 40) revealed all three layers in fetal bladders at all three gestational time points contained proliferating cells with very little immunolocalisation of PCNA within nuclei of any layer within the adult bladder. Western blot of full thickness bladder samples harvested from these fetuses, and also from adult sheep, showed a band at 36 kDa (Figure 41), as previously reported (Attar et al, 1998); as assessed by PCNA/β-actin ratios (Figure 41), there was a progressive fall in levels of PCNA protein.

Finally, using activated caspase-3 activity as a surrogate marker of apoptotic death (Figure 42), a similar downward trend was found between 75 and 145 days gestation.

5.2.8 Summary

- *Sham* fetal bladders, at 105 days gestation, were well developed with discrete layers of the urothelium, lamina propria and detrusor muscle. *Obstructed* fetal bladders were thinner, their urothelium was flattened, cellularity of the lamina propria appeared decreased and muscle bundles were separated by prominent spaces containing collagen, elastin and cells.

- Morphometry confirmed detrusor myocytes in *obstructed* bladders were larger with a lower cell density in the lamina propria of these bladders.

- Dry weight, total protein and total protein content were significantly increased in the *obstructed* bladder.

- The *Proliferative index* was significantly increased in the detrusor layer of the *obstructed* bladder.

- The *Proliferative Index* of cells around *obstructed* muscle cell bundles was 50 %.

- The *Apoptotic Index* was significantly increased in the detrusor and lamina propria layers of the *obstructed* bladder.

- Full thickness bladder wall samples revealed increased activated caspase-3 in the *obstructed* bladder.

- Bcl-2 and Bax protein expression were evident within cells from all layers from both *sham* and *obstructed* fetal bladders.

- Bcl-2 protein expression was significantly decreased and Bax protein expression was significantly increased in full thickness bladder wall samples from the *obstructed* bladder.

- From 75 days gestation through to 145 days gestation, the fetal bladder becomes thicker and grows and exhibits decreased cell proliferation and apoptosis.

5.3 Physiology

5.3.1 Contractility studies

Muscle strips

The lengths (5.8±1.0 mm *sham* males, 5.2±0.6 mm *sham* females, 6.5±0.6 mm *obstructed* males) and weights (4.5±1.9 mg, 4.4±1.5 mg, 10.6±4.2 mg, respectively) of the denuded bladder strips used in the contractility studies were not significantly different between groups; however, for all *denuded* muscle strip experiments, tension was normalised to unit muscle weight. *Mucosal* strips were heavier than *denuded* strips (12.4±2.7 mg, 14.3±4.0 mg, 11.5±3.0 mg, respectively) but as above, tension was normalised to unit muscle weight. Preparations did not exhibit spontaneous contractions when experiments were being carried out; however, in a small number from *sham* bladders, spontaneous contractions developed in the later stages when recordings were terminated. Force-

frequency relations and dose-response relations could be fitted to empirical equations (see Material and Methods section 4.3.1) (Figure 43).

Contractile properties of bladder strips – nerve-mediated contractions and muscarinic responses.

Force-frequency relationships were generated by varying the tetanic stimulation frequency between 1-60 Hz in normal Tyrode's solution, and then in the presence of 1 μM TTX. Nerve-mediated tension was taken as the difference between total and TTX-resistant force. Figure 44A shows that the estimated maximum tension at high frequencies, T_{max}, was significantly reduced in the *obstructed,* versus *sham,* group (1.12±0.46 mN.mg^{-1} versus 5.21±2.43 mN.mg^{-1}, n=5 both groups). The frequency required for half maximum tension ($K_{1/2}$) was not different in the two groups (Figure 44B) - p$K_{1/2}$ values 1.28±0.06 versus 1.24±0.13, respectively (mean $K_{1/2}$'s 19.1 Hz and 17.4 Hz, n=5 both groups). In addition, *sham* male and female parameters (T_{max}: 5.12±1.37 mN.mg^{-1} and p$K_{1/2}$ 1.04±0.16; n=5) were not significantly different.

The inotropic response to carbachol in electrically unstimulated preparations was also reduced in the obstructed group. The T_{max} derived from dose-response curves (Figure 44C) was significantly reduced (4.70±1.73 mN.mg^{-1} versus 10.30 ± 2.38 mN.mg^{-1}, $p<0.05$, n=5 both groups). However, the potency of carbachol was unchanged (Figure 44D) as estimated EC_{50} values were similar (pEC_{50} values 5.58±0.29 and 5.79±0.41, respectively; mean EC_{50} values 2.63 μM and 1.62 μM, respectively, n=5 both groups).

The responses to carbachol were not significantly different in the *sham* male and female groups (T_{max} 7.77±1.61 $mN.mg^{-1}$, pEC_{50} 5.63 ± 0.19).

Although both interventions revealed a reduced contractile response in the *obstructed* group, the magnitude of force decline was greater for the nerve-mediated responses compared to the carbachol-evoked contractions. The ratio of T_{max} values from the force-frequency relationship and the carbachol dose-response curve was calculated for each preparation. For *sham* animals, this was 0.68±0.30 (n=5) and was significantly less in the *obstructed* group (0.28±0.16; n=5, $p<0.05$) – Figure 44E. This may be explained by a reduction not just of the force-generating capacity of the detrusor in the obstructed bladder, but also by a denervation to the tissue. The ratio of nerve-mediated and carbachol T_{max} values were similar in the *sham* male and female (0.50±0.12, n=5) groups.

Neuronal protein expression

The contractility experiments implied that obstruction in the fetal bladder led to denervation. This was further examined by determining the expression of two key neuronal proteins, S100 and PGP 9.5. In the *sham* male bladder, S100 (Figure 45A) and PGP 9.5 (Figure 45C) immunolocalised, most prominently, to nerve bundles between and within muscle fascicles and in the serosal layer. By contrast, there was an observed reduction of neuronal immunostaining with S100 (Figure 45B) and with PGP 9.5 (Figure 45D) in the detrusor muscle layers of the *obstructed* bladder. Western blot of PGP 9.5 showed an appropriate band at 25 kDa, as previously reported (Martin et al, 2000), in all bladders (Figure 45E), but densitometry confirmed a significant ($p<0.05$) reduction of

signal intensity, factored for β actin protein, in *obstructed* compared to *sham* bladders (respectively, 81±11 arbitrary units versus 61±11 arbitrary units, n=8 in each group) (Figure 45F).

Contractile properties of bladder strips – the effect of adenosine, ABMA and atropine-resistant contractions.

The role of the purinergic system in the developing *sham* and *obstructed* fetal bladder was examined. Figure 46A shows that 1 mM adenosine significantly reduced tension produced by 8 Hz electrical field stimulation in both the *sham* male group (0.66±0.24 $mN.mg^{-1}$ to 0.30±0.22 $mN.mg^{-1}$, n=5; $p<0.05$) and the *obstructed* group (0.24±0.12 $mN.mg^{-1}$ to 0.08±0.07 $mN.mg^{-1}$, n=5; $p<0.05$). The percentage reduction of force by adenosine was similar in the *sham* male (60±25 %) and *obstructed* groups (58±30 %). However the reduction of force was significantly greater ($p<0.05$) in the *sham* female group (1.85±1.67 $mN.mg^{-1}$ to 0.10±0.04 $mN.mg^{-1}$, n=5; 94±8 % reduction) versus the *sham* male group.

To investigate the site of action of adenosine, its effect on the carbachol contracture in electrically unstimulated preparations was measured (Figure 46B). 1 mM adenosine had no significant effect on the magnitude of the carbachol (1 μM) contracture – 107±21 %, 88±10 % and 102±16 % of control with adenosine for *sham* male, *sham* female and *obstructed* male groups, respectively. This implies that adenosine has no direct effect on muscle contractility but acts on earlier steps in the generation of contraction.

Atropine-resistant contractions were recorded in the presence of 1 μM atropine. Three of five strips from *obstructed* bladders, none from *sham* male and one from *sham* female bladders revealed atropine resistance. Figure 46C shows an example of force-frequency curves in the presence and absence of 1 μM atropine. The atropine-resistant response (51±27 %, n=4 at 8 Hz) peaked at low frequencies.

Following purinoreceptor sensitisation and subsequent inhibition with ABMA, the force frequency relation was significantly smaller ($p<0.05$) in the presence of ABMA in the *sham* group (Figure 46D) - T_{max} EFS 5.16±1.86 mN.mg tissue wet weight^{-1} versus T_{max} EFS in presence of ABMA 1.86±1.15 mN.mg tissue wet weight^{-1}. Male and female (n=10) data has been combined as there was no significant difference between *sham* male and *sham* female groups in T_{max} EFS (5.11±1.37 mN.mg tissue wet weight^{-1} versus 5.21±2.43 mN.mg tissue wet weight^{-1}, n=5 both groups, $p>0.05$) or T_{max} EFS in presence of ABMA (3.63±0.62 mN.mg tissue wet weight^{-1} versus 3.14±1.56 mN.mg tissue wet weight^{-1}, n=5 both groups, $p>0.05$). This fall of the force frequency relation in the presence of ABMA was not evident in the *obstructed* group (1.12±0.46 vs 1.04±0.49, $p>0.05$ paired t-test).

Contractile properties of bladder strips – the nitrergic system.

ODQ was used to examine the possible role of a nitrergic component to fetal bladder neurotransmission, as this agent has been shown to reduce the relaxant effect of cGMP that is generated by release of nitric oxide (NO) (Garthwaite et al, 1995). Preparations were electrically stimulated when the muscle was contracted by 1 μM carbachol to record

any relaxation that might be evoked by release of NO. Figure 47A shows transient relaxations to electrical field stimulation in a muscle contracted with carbachol, at higher frequencies the responses became biphasic. 1 μM TTX abolished these responses confirming that responses were nerve-mediated (Figure 48).

Figure 47B also shows that in the presence of 1 μM ODQ, the relaxant responses were diminished. The reduction in response was significant in both *sham* male and *obstructed* bladders (Figure 47C – 43 %, 42-99 % and 17 %, 10-19 respectively, n=5 both groups; $p<0.05$, Mann Whitney rank test; figure and text show median and interquartile range). The effect of ODQ was variable in different preparations in any group, so that no significance in the magnitude of the effect was seen in muscles from both groups. A similar trend of diminished response with ODQ was seen in three preparations from *sham* females. 0.1 % (v/v) chloroform, used as a solvent for ODQ, had no effect on the relaxant responses.

The effect of the mucosa

Figure 49 shows that the presence of mucosa had a significant ($p<0.05$, Mann-Whitney U test; figure 49 and text show median and interquartile range) dampening effect on muscle contractility in the *sham* male group (T_{max} EFS full thickness strip 79 %, 48-80 % of *denuded* strip force) and the *sham* female group (T_{max} EFS full thickness strip 59 %, 63-75 % of *denuded* strip force). With *mucosal* strips, ODQ significantly elevated tension in the *sham* male and *female* groups (116 %, 112-119 %; 112 %, 111-120 % respectively, n=5 both groups). In the *obstructed* group, the presence of mucosa had no significant

effect on T_{max} EFS (105 %, 93-184 %, n=5) although the variability of the data was relatively large. Furthermore, ODQ did not affect the force produced by the *mucosal* strip in the *obstructed* group (120±20 %control).

Detrusor thickness

Using the KS 300 computer program, I found that the *obstructed* fetal bladder wall was significantly ($p<0.05$) thinner than their *sham* counterparts (1.77±0.22 mm versus 2.60±0.45 mm, n=5 both groups). Similarly, I found that the *obstructed* detrusor widths were significantly ($p<0.05$) thinner than those of the *sham* detrusor muscle (1.07±0.15 mm versus 1.45±0.27 mm, n=5 both groups). However, there was a similar proportion of detrusor comprising the bladder wall when corrected for this difference in wall thickness (60.8±9.7 % versus 56.3±6.3 %, n=5 both groups). The detrusor component as a proportion of the whole wall was used to calculate the relative muscle weight of *mucosal* bladder strips (above).

5.3.2 Filling cystometry

Intravesical volumes found at post-mortem examination were greater ($p<0.05$) in the *obstructed* group than in the *sham* male group (49.8±32.0 ml versus 5.7±3.9 ml, n=5 both groups). After removal of this volume, the total volumes instilled in the *obstructed* bladders for the cystometry measurements (52.0±31.7 ml, n=5) were greater ($p<0.05$) than those instilled into *sham* bladders (6.4±2.6 ml, n=5) for similar increases in pressure (12.2±5.0 cm H_2O versus 10.6±1.8 cm H_2O, n=5 both groups, $p>0.05$). Both the *sham* and the *obstructed* bladders demonstrated stress-relaxation of the pressure change after an

injection of fluid, i.e. pressure rose rapidly and partially recovered over several seconds to a stable level (Figure 50A). The steady-state pressure values were used to calculate compliance. Figure 50B shows representative examples of pressure-volume curves from a *sham* and an *obstructed* bladder. The fitted straight-line is equivalent to 1/C (C = compliance $=\Delta V/\Delta P$), these fits were made over the initial linear portions of the curve only; over the complete range of volumes, the relationship appeared to be curvilinear. I found that compliance was significantly greater ($p<0.05$) in the *obstructed* bladders (mean 6.69±5.47 ml.cm H_20^{-1}, n = 5) compared to those in the *sham* group (0.64±0.25 ml.cm H_20^{-1}, n=5).

To examine further the compliance of the bladder wall and take account of disparate bladder volumes between the two groups, wall stress was derived. A plot of wall stress versus bladder volume is shown in Figure 50C with examples from a *sham* and an *obstructed* bladder. Wall stress was a linear function of volume (at low volumes) and revealed that bladders from the *obstructed* group were significantly more ($p<0.05$) flaccid than *sham* bladders (2.7±2.7 $kN.m^{-2}.ml^{-1}$ versus 13.5±2.2 $kN.m^{-2}.ml^{-1}$, n=5 both groups). Calculation of wall stress was of benefit as the relationship appeared more linear over a greater range of values and therefore allowed for improved analysis and comparison between the two groups.

5.3.3 Biomechanical stretch studies

Muscle strips

The lengths (5.9±0.3 mm *sham* males, 6.1±0.4 mm sham females and 6.2±1.2 mm *obstructed* males), weights (5.2±1.1 mg, 4.7±0.9 mg and 6.7±1.5 mg, respectively) and cross-sectional areas (0.7±0.2 mm^3, 0.8±0.2 mm^3 and 1.0±0.4 mm^3, respectively) of bladder strips were not significantly different between groups; however, for all experiments, tension was normalised to unit cross-sectional area.

Stress-strain relationships of isolated preparations

Figure 51 shows the change of stress (tension) when a muscle strip from a *sham* male or *obstructed* male bladder was subjected to a step change of strain (length). The preparation demonstrated a rapid increase of stress upon stretch followed by a partial time-dependent relaxation throughout the maintenance of the strain. On cessation of the step response, muscle stress overshot before recovering to the initial resting level. The stress-strain relationship of a rubber strip showed the latter to be purely elastic with virtually no visco-elastic component during strain and no overshoot following cessation of strain (Figure 51 insert).

Table 2 shows the elastic and visco-elastic properties of *denuded* muscle strips from the three groups. The steady-state elasticity was significantly lower in the *obstructed* group versus *sham* male, group. In addition, steady-state elastic work and visco-elastic work (as calculated from the respective areas from the stress-strain relationships, Figure 52) were also significantly lower ($p<0.005$) in the *obstructed,* versus *sham* male, group.

However, the proportion of total work carried out by the elastic element (and hence the visco-elastic element) as well as the time constant of stress-relaxation (τ) was not different in the two groups. There was no difference in any parameter for the *sham* male and *female* groups, except a prolongation of the stress-relaxation time constant in the sham *female* group. Similar conclusions were obtained if the stress response on a return to the control strain from the stretched state ('off' response) was analysed indicating that the magnitude of the strain changes did not exceed the plastic limit of the preparations.

Hysteresis

Steady-state stress-strain relationships were generated by imposing ramp stretches to 120 % of resting length with a total cycle length of 100 seconds (50 seconds stretch, 50 seconds release). The rate of change of length was approximately 5-times slower than the visco-elastic time constant so that such ramps generated stress-strain relationships could be considered to reflect only the elastic properties of the tissue. Figure 53A and B show such relationships for strips from *sham* male and *obstructed* bladders. Both relationships showed hysteresis, i.e. the stretch and relaxation plots were not identical. The area within the loop is work lost during the ramp experiment (presumably as heat) and was less in strips from *obstructed,* versus *sham*, bladders (183±50 $mN.mg^{-1}.mm^{-1}$ versus 305±17 $mN.mg^{-1}.mm^{-1}$, n=3 and 5 respectively). The elastic rubber strip showed no hysteresis (Figure 53C) indicating that the behaviour was inherent to the force-transducer or attachments, with no intrinsic hysteresis to the experimental system.

5.3.4 Radiotelemetered fetal bladder cystometry

Recordings were possible in three of the four experiments; in Experiment 3, the urachal catheter displaced on the seventh day. This was considered to be the case during recordings as no voids were observed after day 7 post-implantation in this experiment; at the time of post-mortem, the fetus suffered large urinary ascites and a hole was observed at the site of urachal entry for the catheter. The catheter had pulled out of this hole but had remained intra-abdominal during the last three weeks of observation.

Apart from minor adhesions around the body of the implant, all implants were retrieved at post-mortem with relative ease, no adhesions or fibrosis were found around catheters. All implants were turned off, cleaned and were ready for re-use. Apart from experiment 3, all fetuses appeared normal for their gestational age with no gross changes in fetal morphology.

Experiments 1 and 4 underwent simultaneous ex vivo filling cystometry and radiotelemetry recording at the time of post-mortem. Filling cystometry showed identical pressure recordings to the pressures recorded by the radiotelemetry method (Figure 54). In Figure 54B, the upper trace was the pressure recorded from within the bladder (P_{ves}) and the lower trace refers to abdominal pressure (P_{abdo}).

Patterns of activity

During the 30 days of observation, I noted that there were (in all three experiments):

1) Quiet periods with no abdominal or bladder pressure rises

2) Synchronous activity in the bladder and abdomen (Figure 55)

3) Discriminate activity, associated with bladder activity only (see definitions below).

Calculation of detrusor pressure

Baseline pressure could be high because of variations in the catheter tip position in relation to the implant body; therefore, the detrusor pressure could be derived by exporting data to Microsoft Excel and subtracting abdominal pressure from vesical pressure to calculate detrusor pressure ($P_{det} = P_{ves} - P_{abdo}$) (Figure 56).

Definitions of discriminate bladder activity

Four patterns of bladder activity were recorded, and as voids were not directly observed, were defined by me as;

1) Void (105-140 days gestation): sustained elevations of detrusor pressure with superimposed high frequency, low amplitude activity (see Figure 56 for an example).

2) Immature void (75-105 days gestation): episodes of high frequency, low amplitude activity with or without elevations of baseline pressure (Figure 57).

3) Staccato activity: short (20-40 seconds) phasic elevations of pressure that were a) discrete, b) in trains (Figure 58) or c) observed pre- and post-void (Figure 59).

4) 'Unstable' type activity: very short (<5 seconds) elevations of pressure (Figure 60).

Summary of bladder activity (Table 3)

During all experiments, there were no changes in abdominal pressure during periods of discriminate bladder activity.

Experiment 1 (male fetus, 105-145 days gestation, bladder catheter through bladder wall, abdominal catheter intra-abdominal): during the period of observation, the mean number of voids per hour decreased from 2.5-3.0 to 1.5, the mean maximum detrusor pressure remained unchanged from 28 mmHg to 27 mmHg, the mean duration of each void increased from 60 seconds to 100 seconds and the other events noted were staccato activity in trains at 105 days gestation and staccato activity pre- and post-voids near term.

Experiment 2 (female fetus, 105-145 days gestation, bladder catheter through bladder wall, abdominal catheter intra-abdominal): during the period of observation, the mean number of voids decreased from 3.0-4.0 to 1.5-2.0 per hour, the mean maximum detrusor pressure increased from 21 mmHg to 40 mmHg, the mean duration of each void decreased from 180 seconds to 140 seconds; no other events were noted early in recording but near term, staccato activity pre- and post-voids were observed. No discernible voids were noted at day 22 of recording; at this time, there was high background noise that may account for this finding; alternatively, voids may have been too infrequent to be observed during the two-hour recording session.

Experiment 4 (male fetus, 75-110 days gestation, bladder catheter through urachus, abdominal catheter fixed onto fetal skin): during the initial period of observation, the mean number of immature voids were 4 per hour and by day 32 of recording, this had changed to 2 voids per hour, the mean maximum detrusor pressure increased from 15 mmHg to 25 mmHg, the mean duration of each void increased from 25 seconds to 135

seconds. Unstable type activity was noted early in recording and by the end of recording, staccato activity pre- and post-voids were observed.

5.3.5 Summary

- Muscle strips from *obstructed* bladders were hypocontractile after EFS and muscarinic stimulation. Sensitivity to EFS and muscarinic stimulation was unchanged. The magnitude of force decline was greater for nerve-mediated responses compared to carbachol-evoked contractions suggesting denervation of the *obstructed* bladder.

- There was reduced expression of neural proteins, S100 and PGP 9.5, in the *obstructed* bladder.

- The effect of adenosine appeared not to directly effect muscle contractility but had effects on earlier steps in the generation of contraction.

- Three of the five *obstructed* bladders and one of ten *sham* bladders exhibited atropine-resistant contractions.

- ABMA reduced the force of contractility in *sham* bladders.

- Nitric oxide-mediated relaxant forces were evident in bladders from *sham* and *obstructed* bladders.

- The presence of mucosa caused a negative inotropic effect in *sham* bladders that was nitric oxide-mediated.

- The *obstructed* bladder was significantly more compliant and exhibited reduced wall stress compared to the *sham* bladder.

- The *obstructed* bladder exhibited significantly lower elasticity, elastic work and visco-elastic work. The proportion of total work carried out by the elastic element (and the visco-elastic element) and the time constant of stress-relaxation remained unchanged between groups.

- Hysteresis was evident in all fetal bladders; the work lost during the ramp experiment was less in strips from *obstructed* bladders.

- Radiotelemetry cystometry was feasible in experimental fetuses with consistent 'voiding' patterns recorded.

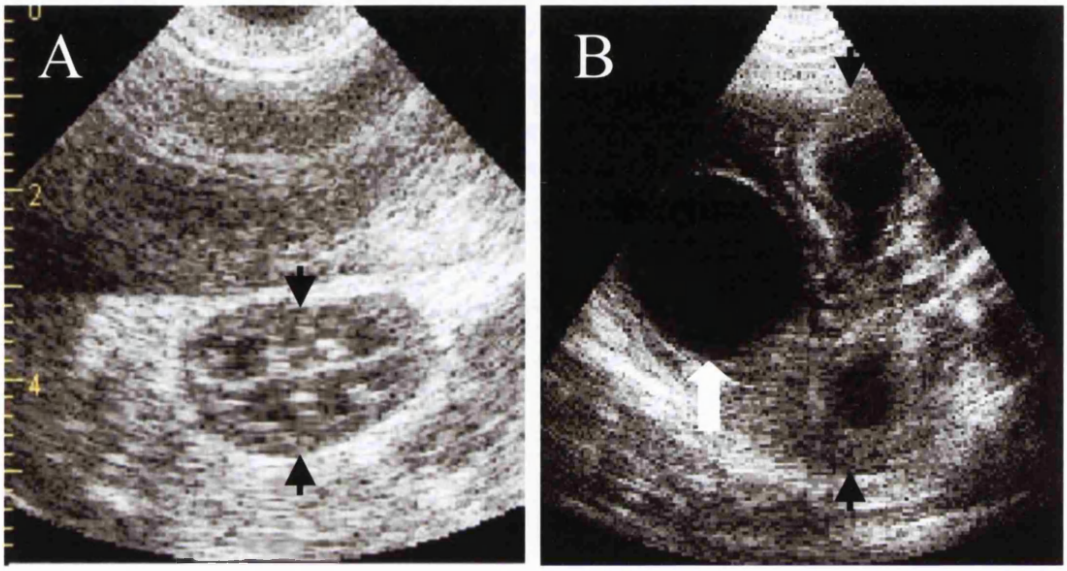

Figure 26. Ultrasonography of the developing urinary tract
A: Ultrasound of a sham male fetal kidney (black arrows), four weeks after surgery. Normal renal parenchyma is evident with no dilatation of calyces, pelvis or ureter. B: Ultrasound of a time-matched obstructed male fetal urinary tract. Note the dilated urinary bladder (white arrow) and an enlarged kidney (black arrows) with dilated calyces.

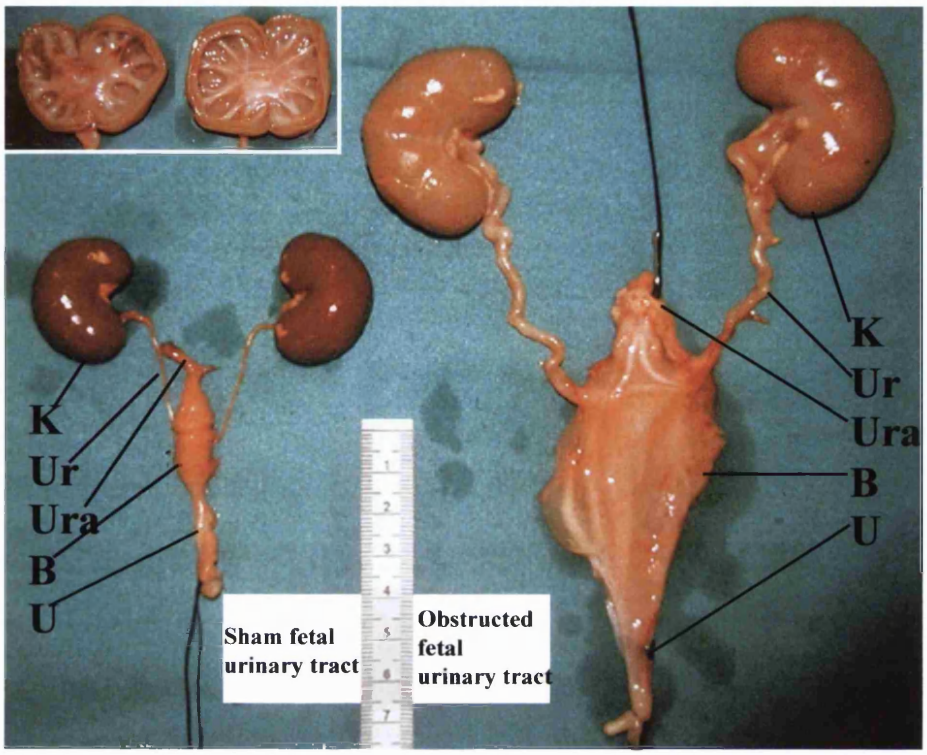

Figure 27. Post-mortem specimens

Sham urinary tract (left) and o*bstructed* specimen (right) at 105 days gestation. In the latter, note the increased size of the bladder, the dilatation of the ureters and the increased size of the kidneys which were hydronephrotic upon sectioning (see insert). These appearances were representative of 11 fetuses in each experimental group. Black thread was used for orientation following dissection. Key: *K*, metanephric kidney; *Ur*, ureter; *Ura*, urachus; *B,* bladder; *U*r urethra.

	Sham males	*Sham* females	*Obstructed* males
Bladder weight, g	1.14± 0.25	1.09±0.16	7.28±4.41*
Fetal weight, kg	1.38±0.29	1.49±0.29	2.07±0.41*
Bladder/fetal weight ratio, $g.kg^{-1}$	0.82±0.11	0.74±0.10	3.39±1.78*
Femur length, cm	5.5±0.3	5.2±0.4	6.4±0.8
Occipto-snout length, cm	12.7±0.8	13.2±0.8	14.6±1.6

Table 1. Bladder and fetal dimensions
Bladder and fetal dimensions, in *sham* male, *obstructed* male and *sham* female groups. *$p<0.05$ versus *sham* males.

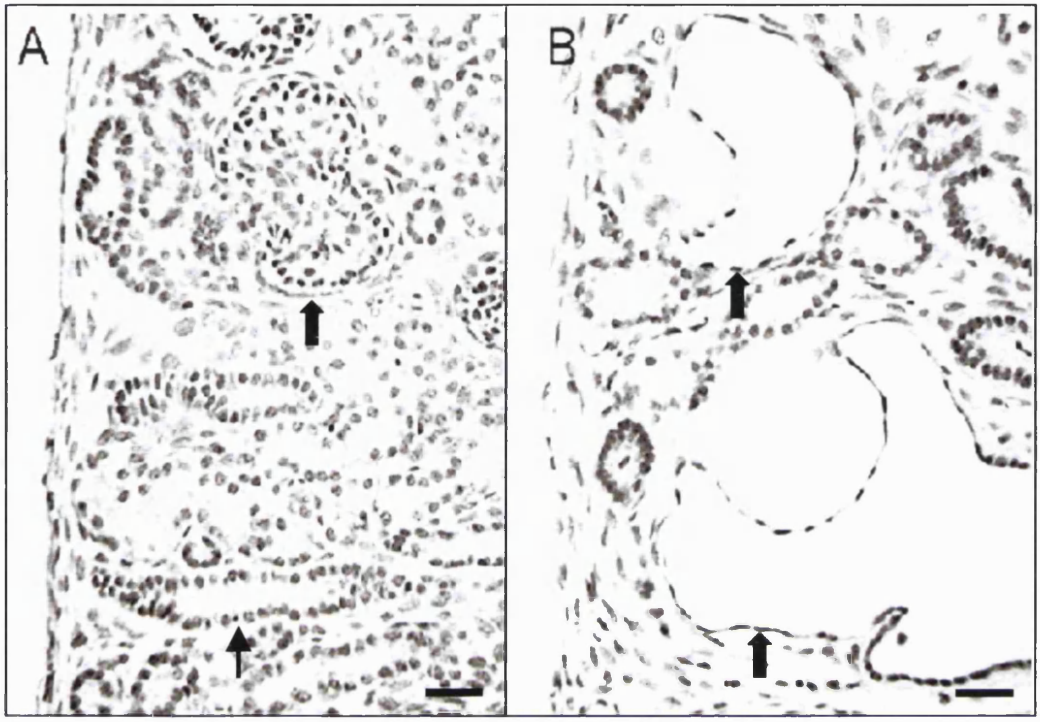

Figure 28. Histology of nephrogenic cortex of fetal kidney
Sections stained with hematoxylin. A: Sham male fetal kidney contains a nephrogenic zone with normal calibre tubules (thin arrow) and nascent glomeruli (thick arrow). B: Obstructed male fetal kidney contains cystically dilated tubules (thick arrow) and there was a lack of glomeruli. Bar is 15 μm. Picture courtesy of Dr P Nyirady.

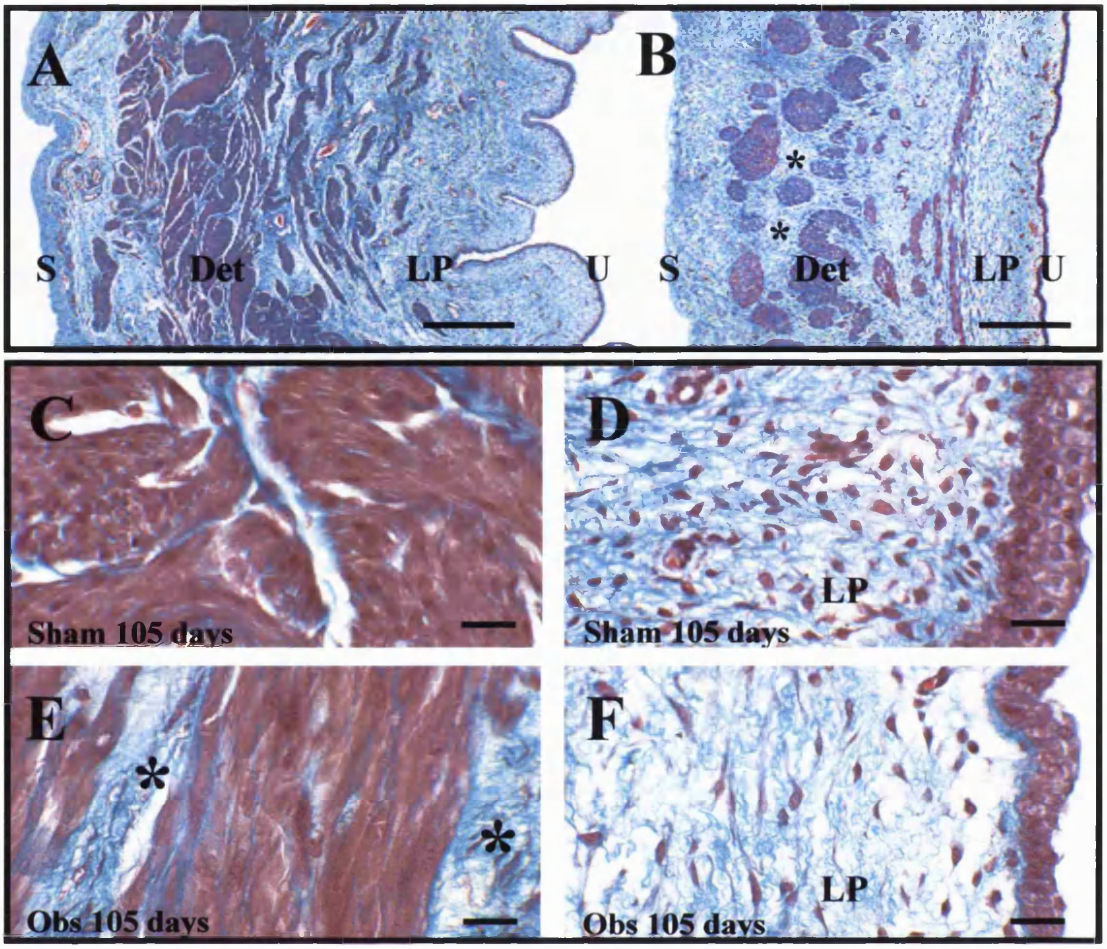

Figure 29. Histology of experimental fetal bladders – *Masson's Trichrome*

Masson's Trichrome stains collagen blue, muscle cytoplasm purple-red and erythrocytes bright red. A and B: low power images of the *sham* and *obstructed* fetal bladders, respectively. Note in the *obstructed* fetal bladder, the urothelium is flattened, lamina propria cellularity appears decreased and the detrusor muscle is disrupted with increased collagen deposition (indicated by *) in this layer. Bar is 400 μm. C-F: high power images of *sham* (C and D) and *obstructed* (E and F) fetal bladders. In the detrusor layer (C and E), distinct muscle bundles stain red and collagenous tissues between bundles stain blue; note the apparent increase in detrusor smooth muscle cell size and increased collagenous material (indicated by *) in the *obstructed* group. D and F show the lamina propria and the urothelium; note the apparent decrease in cell density in the lamina propria in the *obstructed* group. Note also the change in urothelial anatomy from 3-4 cell layers thick in the *sham* bladder to a predominantly single-layer in the *obstructed* bladder.Bars are 50 μm. Key: *S*, serosa; *Det*, detrusor muscle; *LP*, lamina propria and *U*, urothelium.

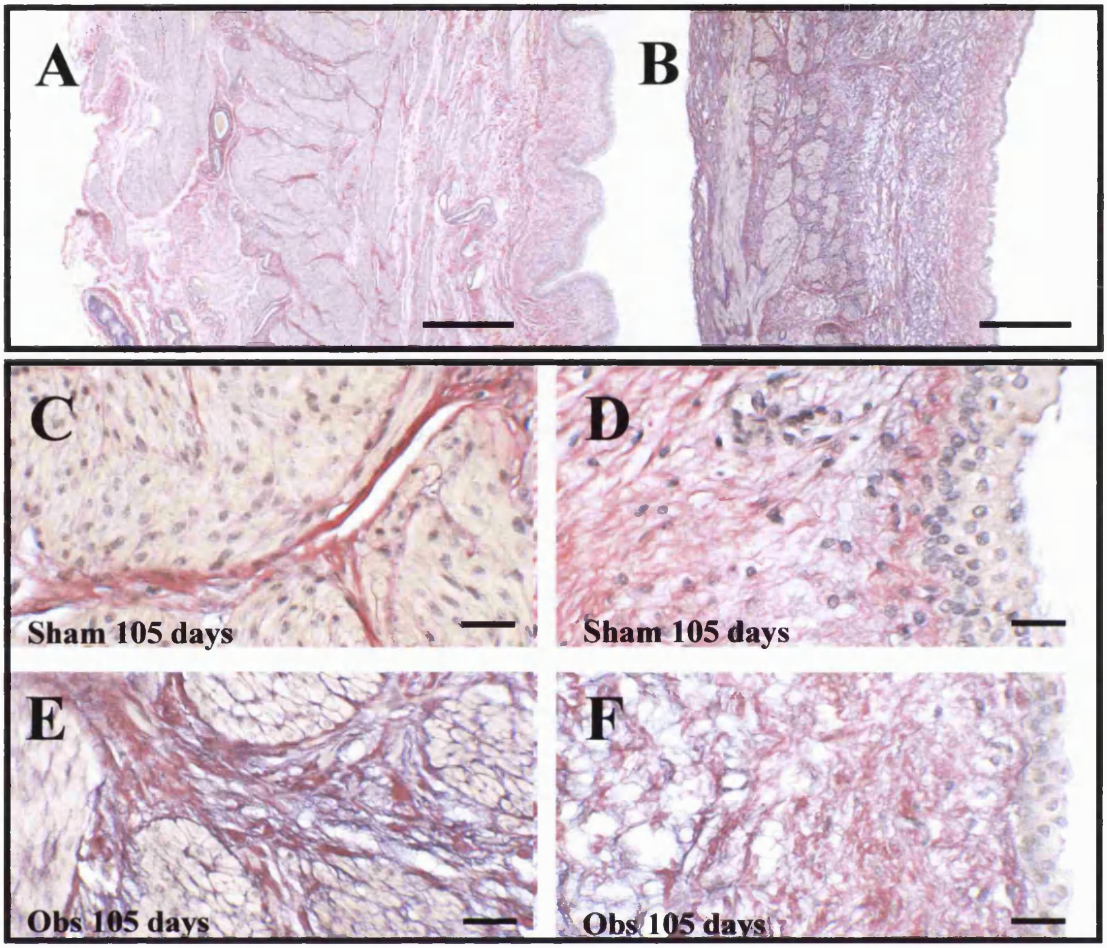

Figure 30. Histology of experimental fetal bladders – *Elastin van Geison*

Elastin van Geison stains collagen red, elastin black and muscle cytoplasm yellow. A and B are low power images of the *sham* and *obstructed* fetal bladders, respectively. Note in the *obstructed* fetal bladder, the apparent increase in elastin deposition. This is seen more clearly in high power images of *sham* (C and D) and *obstructed* (E and F) fetal bladders with apparent increase in collagen and elastin deposition around muscle bundles and within the lamina propria of the *obstructed* fetal bladder. Bars are 400 μm in A and B and bars are 50 μm in C-F.

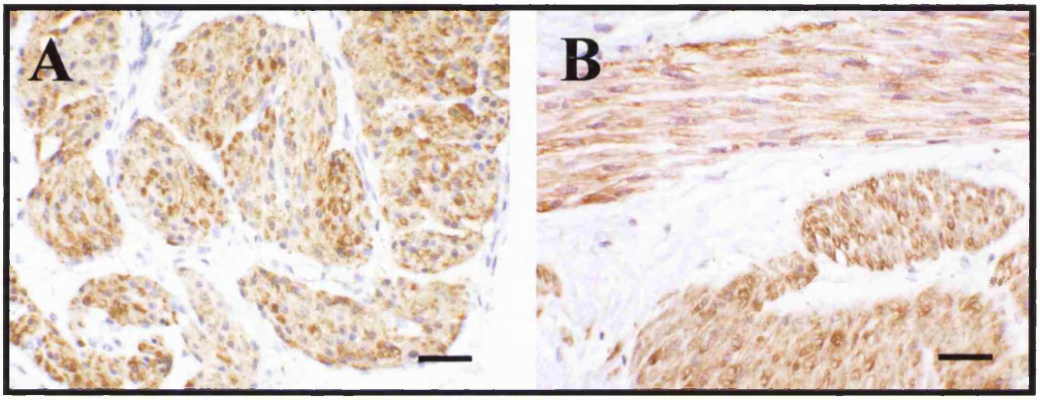

Figure 31. αSMA expression in experimental fetal bladders
A and B, from *sham* and *obstructed* bladders respectively, show prominent immunolocalisation of αSMA within detrusor muscle cells. Sections were counterstained with haematoxylin. Bars are 50 μm.

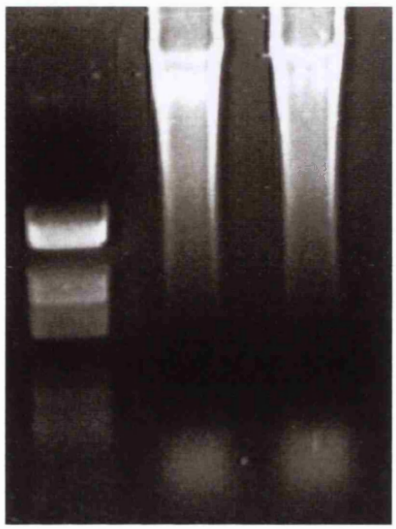

Figure 32. Agarose gel electrophoresis
Agarose gel, visualised under ultraviolet exposure, shows molecular weight marker (M) and example samples from a sham (Sh) and obstructed (Ob) bladder with bands at appropriate molecular weight of DNA.

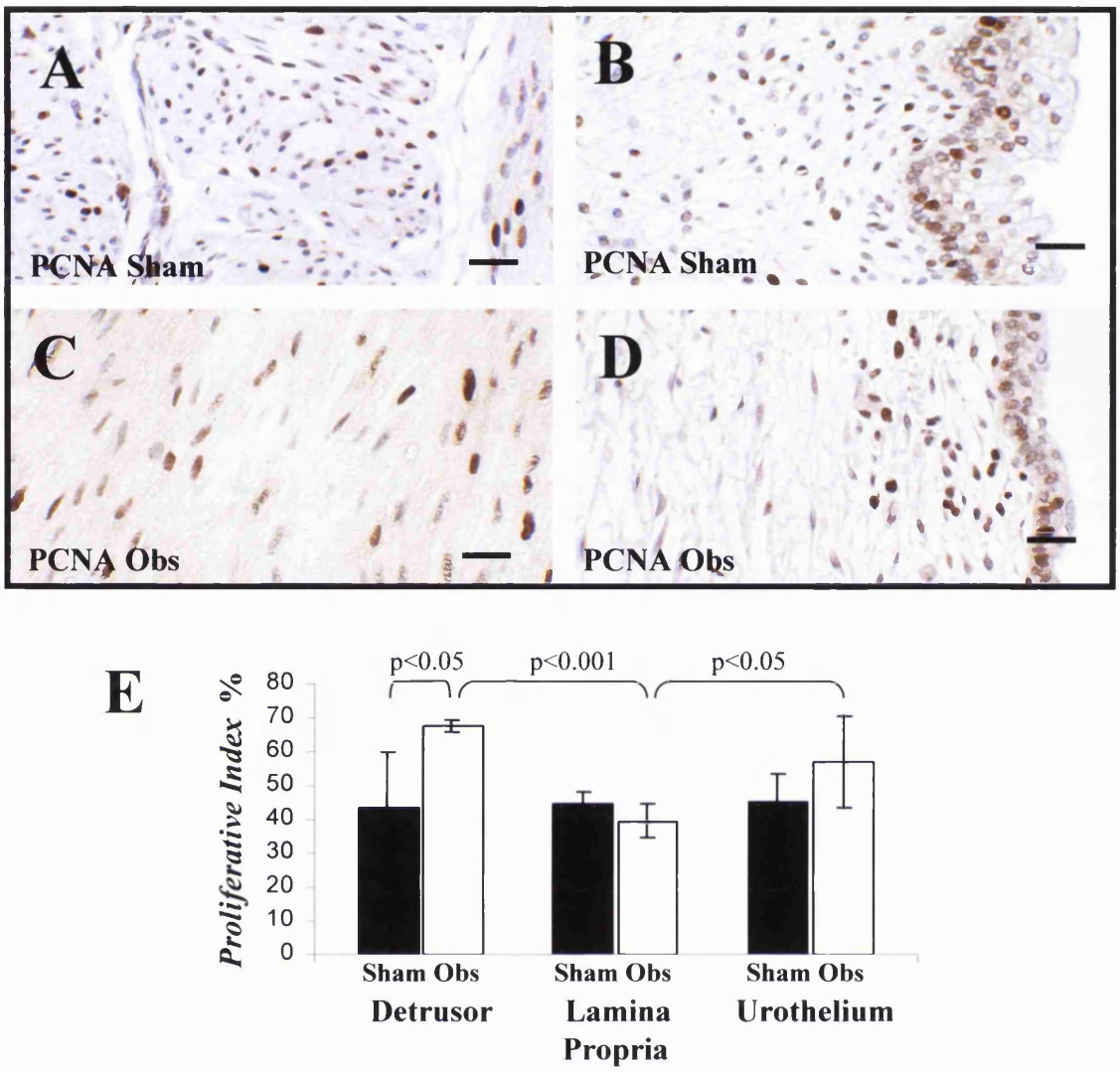

Figure 33. Cell proliferation in experimental bladders

A-D. Immunohistochemistry for PCNA in *sham* (A and B) and *obstructed* bladders (C and D) in the detrusor layer (A and C) and lamina propria and urothelial layers (B and D) at 105 days gestation. Sections were counterstained with haematoxylin. Note PCNA-positive nuclei in all three main layers of the bladders in both experimental groups. E. *Proliferative Index* in *sham* (closed bars, n=6) and *obstructed* (open bars, n=6) detrusor SMC, lamina propria cells and urothelial cells. There was a significant increase in detrusor SMC *Proliferative Index* in the *obstructed* versus the *sham* group, and there was a significantly lower *Proliferative Index* in lamina propria cells versus both detrusor SMC and also urothelial cells in the *obstructed* group. Bars are 30 μm.

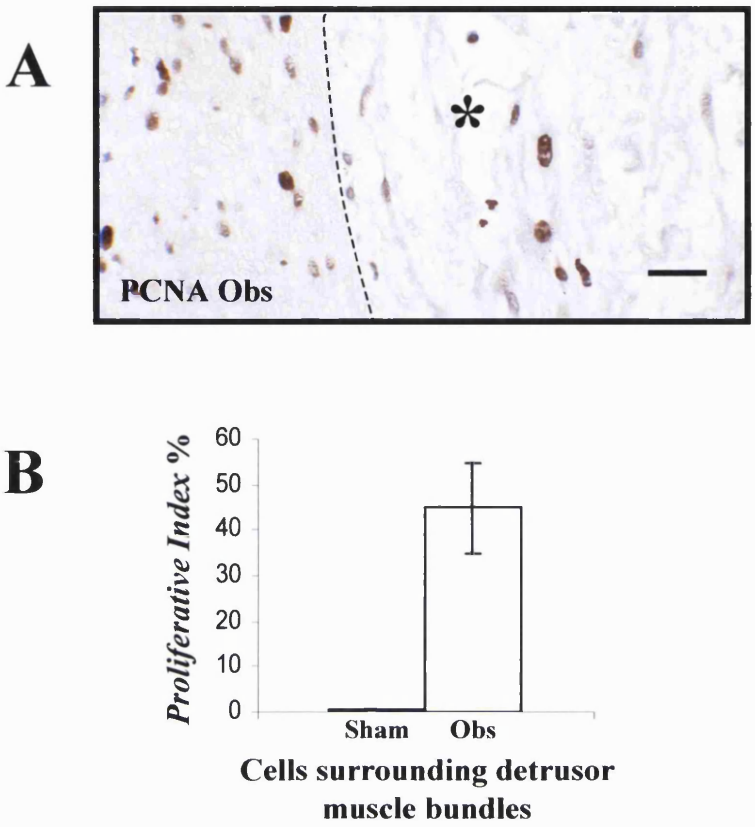

Figure 34. Proliferation of cells around muscle bundles in the *obstructed* group

A: In the *obstructed* group, a proliferating population of cells was noted between muscle bundles (to the right of the dotted line, indicated by *); no proliferation was found in the *sham* group in this location). Section stained by immunohistochemistry for PCNA and counterstained with haematoxylin. B: The *Proliferative Index* of the cell population described in A was about 48 %. Bar is 30 μm.

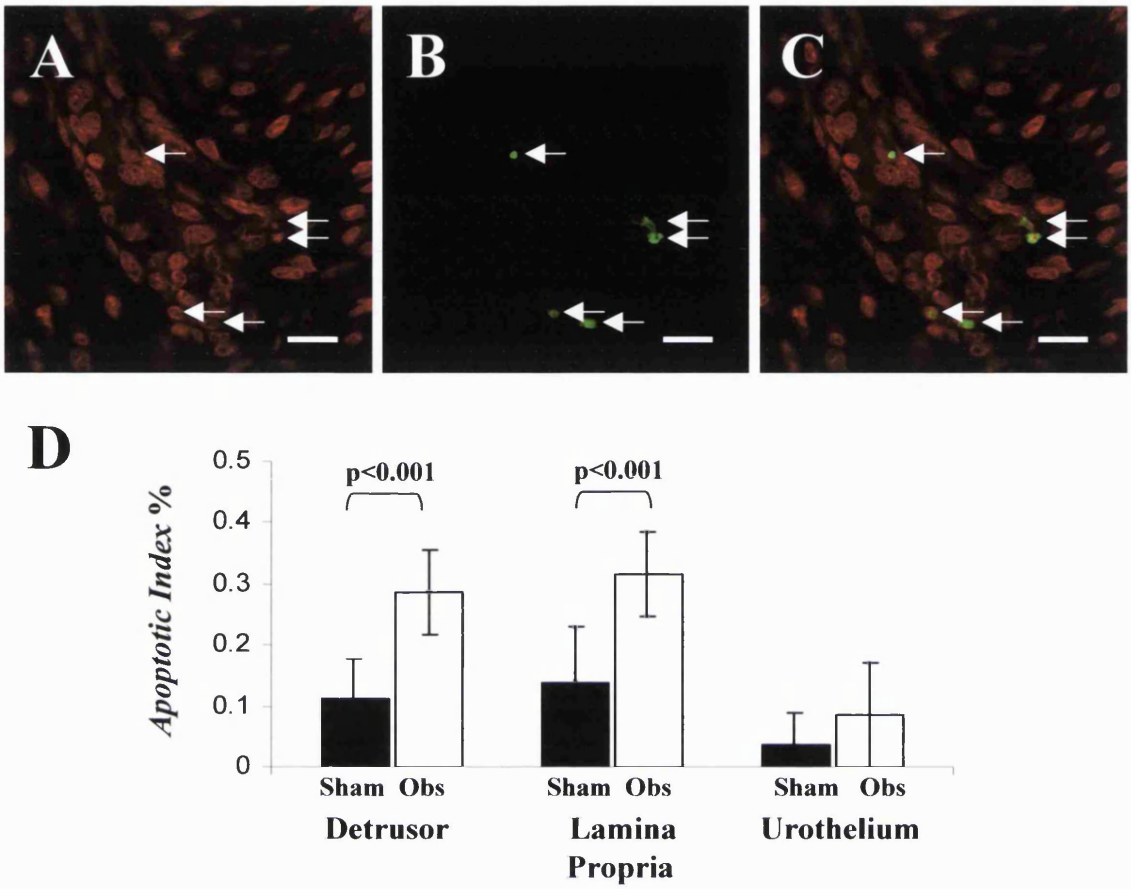

Figure 35. Apoptosis in experimental fetal bladders

A-C is the same field from an *obstructed* muscle bundle visualised in appropriate wavelengths for propidium iodide (A) and TUNEL-FITC (B), with C representing the merged image. Five TUNEL-labelled nuclei are indicated (arrows). In this field, the numbers of apoptotic nuclei were higher than average; these images were used to illustrate the TUNEL technique. Bars are 10 μm. D. The *Apoptotic Index* in *sham* (closed bars, n=6) and *obstructed* (open bars, n=6) bladders in detrusor SMC, lamina propria cells and urothelial cells. Note the significant increase of death in *obstructed* versus *sham* detrusor SMC and lamina propria cells.

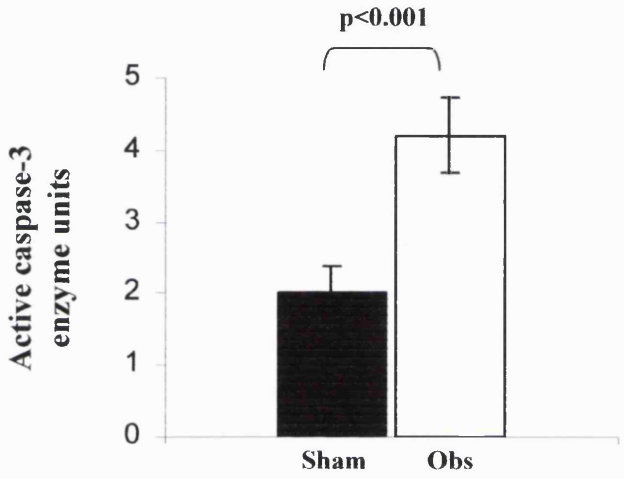

Figure 36. Activated caspase-3 in experimental fetal bladders
Increased caspase-3 enzyme activity in full thickness samples from *obstructed* bladders (closed bars, n=5) versus *sham* bladders (open bars, n=5). One unit was the amount of enzyme that will cleave 1.0 nmol of the colorimetric substrate Ac-DEVD-*p*NA per hour at 37 °C under saturated substrate concentrations.

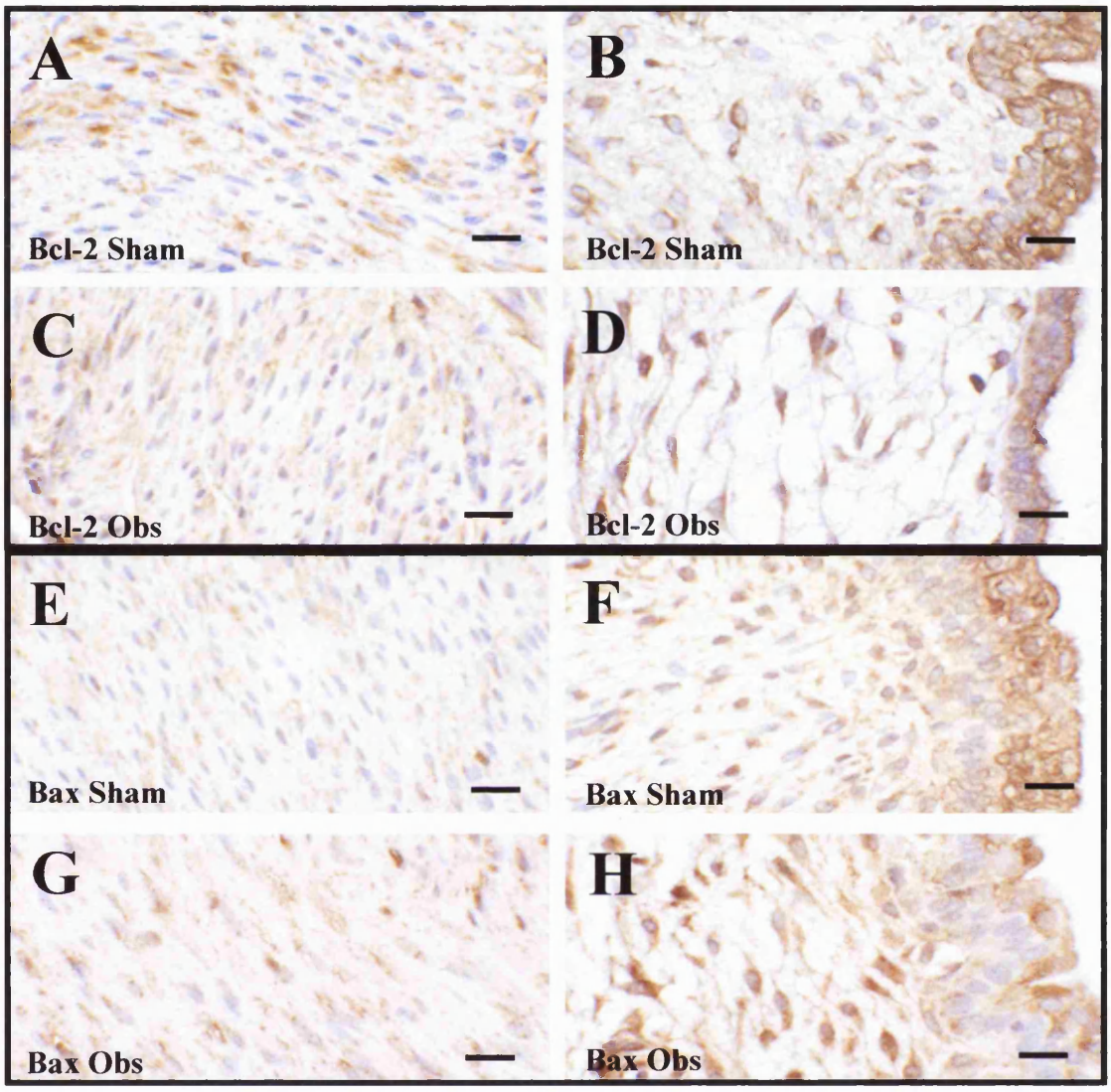

Figure 37. Bcl-2 and Bax proteins in experimental fetal bladders - *immunohistochemistry*

A-D show Bcl-2 and D-H show Bax immunohistochemistry with haemotoxylin counterstaining, representative from 6 samples in each group. A, B, E and F are *sham* bladders at 105 days gestation, while C, D, G and H are time-matched *obstructed* bladders. Note cytoplasmic staining of these two apoptotic-regulatory proteins in all bladder layers in both experimental groups; Bax immunostaining appeared more prominent in the detrusor and lamina propria layers of the *obstructed* bladders. Bars are 30 μm.

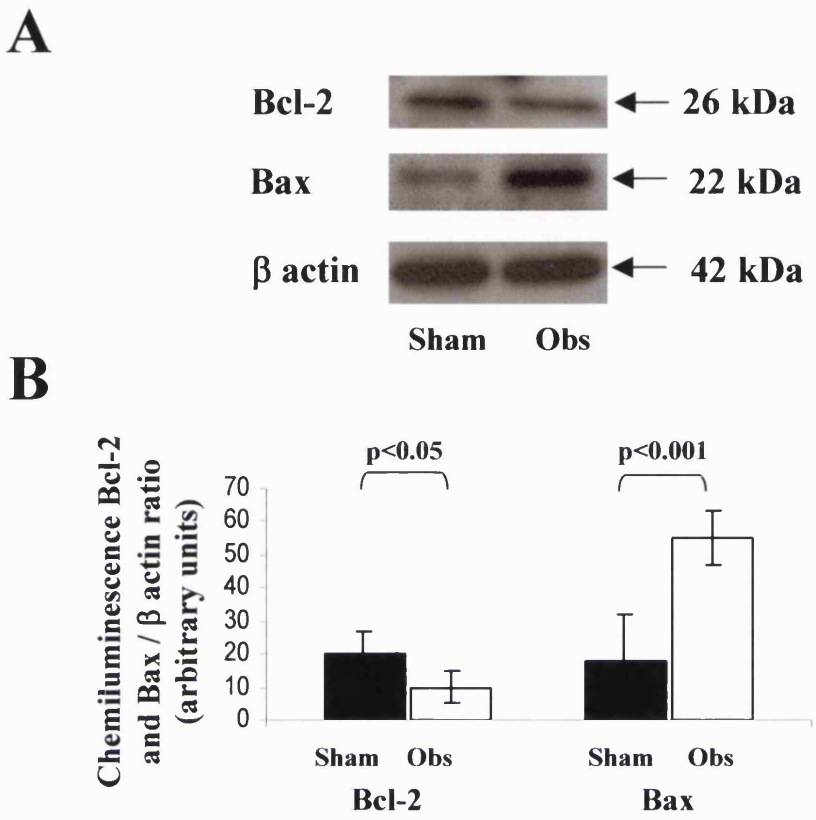

Figure 38. Bcl-2 and Bax proteins in experimental fetal bladders – *western blot*

A: Western blot of Bcl-2 (26 kDa), Bax (22 kDa) and β-actin (42 kDa) from representative *sham* and *obstructed* bladders (representative of six full thickness bladder samples in each group). B: Bcl-2/β actin and Bax/β actin ratios; closed bars for *sham* (n=6) and open bars for *obstructed* bladders (n=6). Note significant down-regulation in Bcl-2 expression and significant up-regulation in Bax expression in *obstructed* samples.

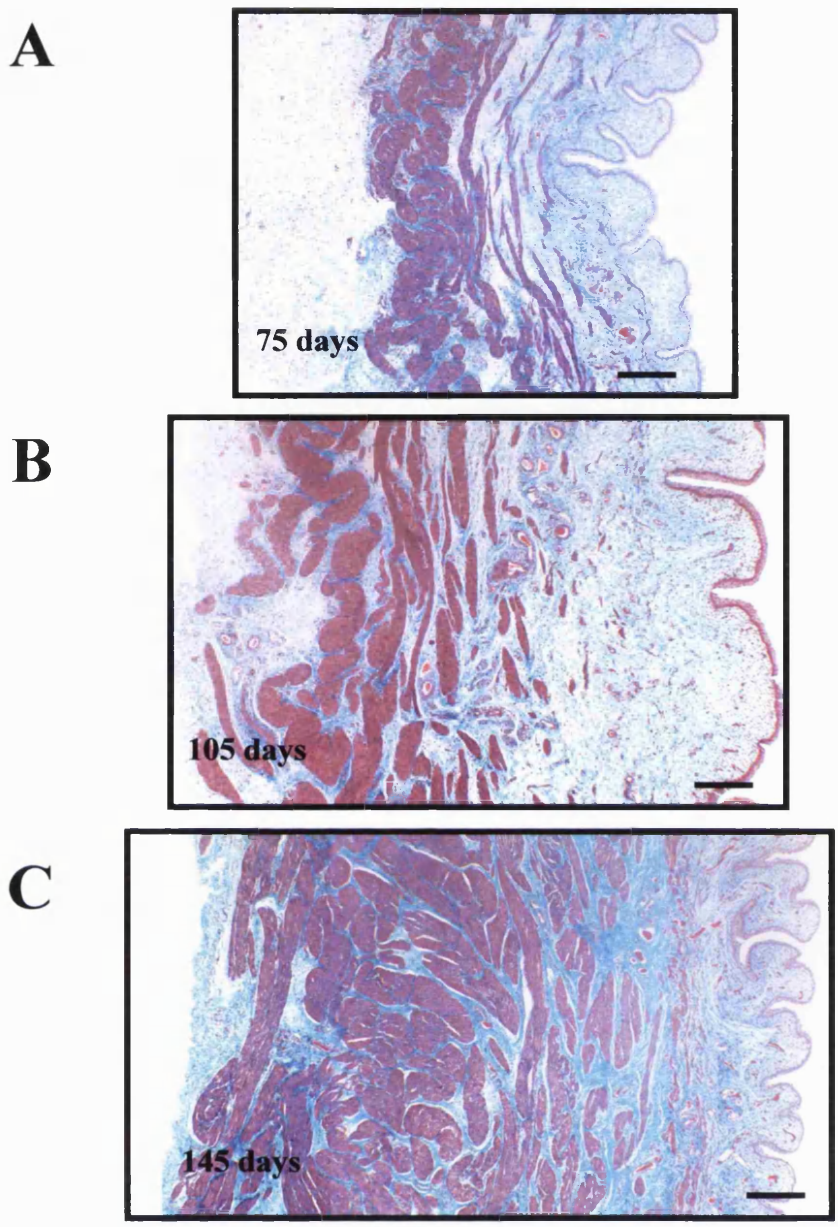

Figure 39. Histology of the developing fetal bladder
A-C depict Massons' trichrome stained sections at 75 (A), 105 (B) and 145 (C) days gestation, representative of 2, 11 and 6 fetal bladders, respectively. Note increasing thickness of the fetal bladder through gestation. Bars are 400 μm.

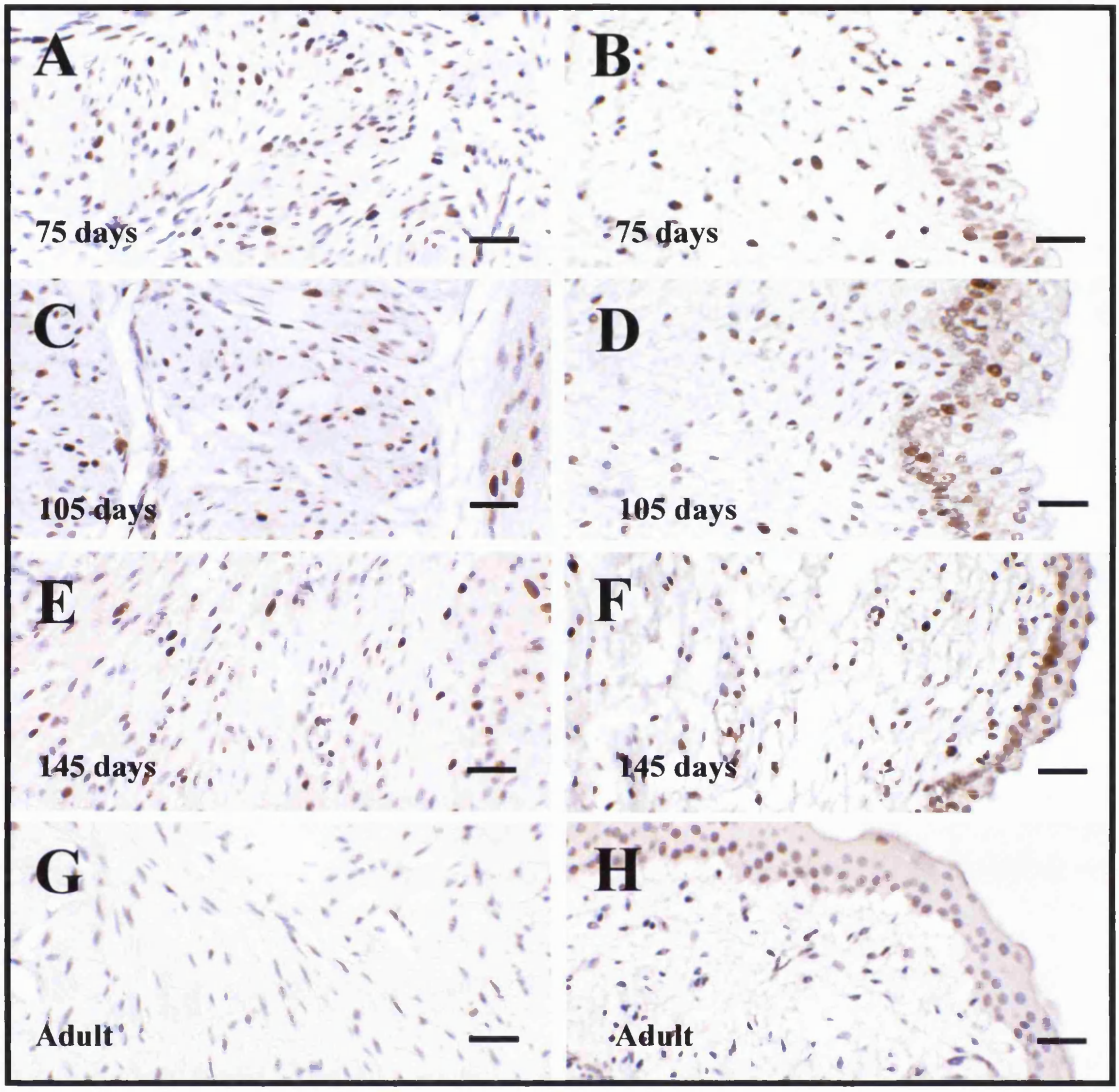

Figure 40. Proliferation in the developing bladder - *immunohistochemistry*

A-H depict immunohistochemistry for PCNA in sections at 75 (A and B), 105 (C and D) and 145 (E and F) days gestation and the adult bladder (G and H), representative of 2, 11 and 6 fetal bladders and 4 adult bladders, respectively in the detrusor layer (A, C, E and G) and lamina propria and urothelial layers (B, D, F and H). Sections were counterstained with haematoxylin. Note PCNA-positive nuclei in all three main layers of fetal bladders with minimal proliferating nuclei in the adult bladder. Bars are 30 μm.

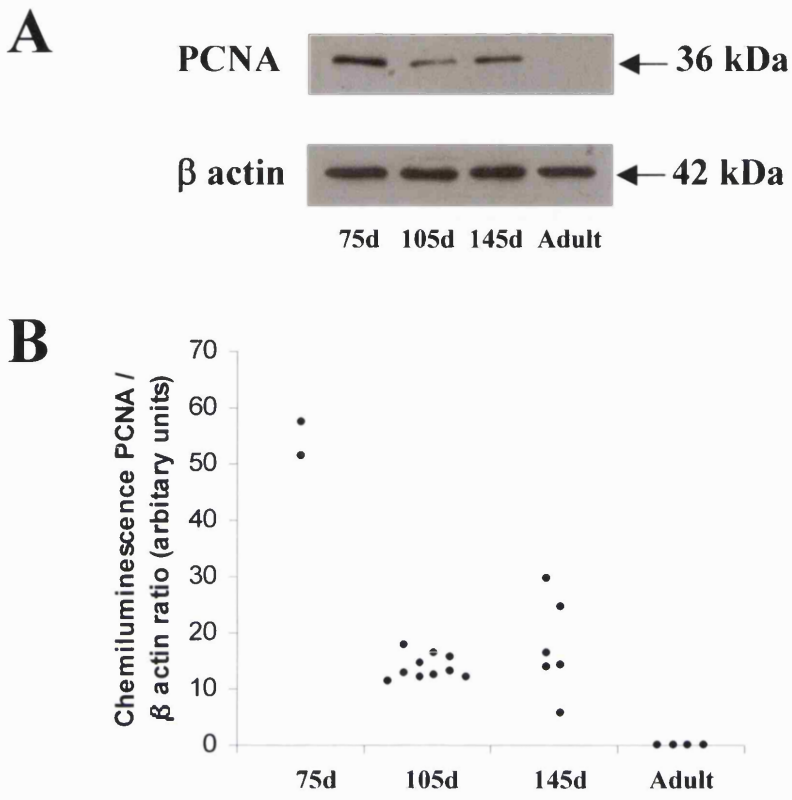

Figure 41. Proliferation in the developing bladder – *western blot*

Western blot (A) for PCNA (36 kDa) and β-actin (42 kDa) of full thickness bladder samples from 75, 105 and 145 days gestation and the adult bladder, representative of 2, 11 and 6 fetal bladders and 4 adult bladders, respectively; note the trend to down-regulation of PCNA expression through gestation into adulthood. This impression was confirmed by PCNA/β-actin ratios (B); each dot represents a single bladder sample.

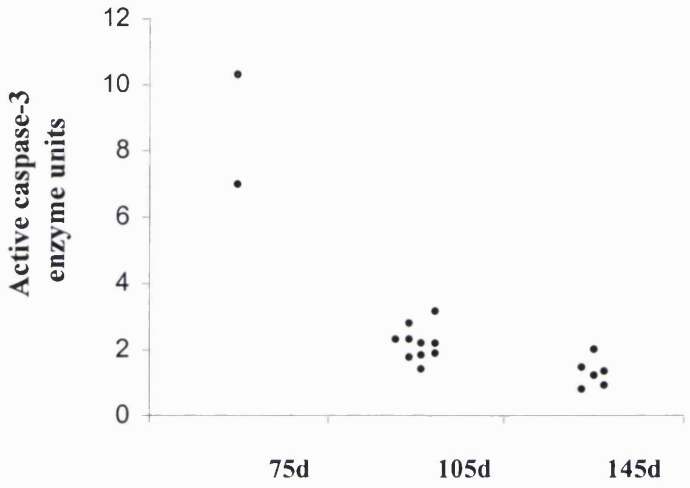

Figure 42. Cell death in the developing bladder
Activated caspase-3 in full thickness bladder samples from 75, 105 and 145 days gestation and the adult bladder; note the trend to decreased caspase-3 through gestation. One unit was the amount of enzyme that will cleave 1.0 nmol of the colorimetric substrate Ac-DEVD-*p*NA per hour at 37 °C under saturated substrate concentrations. Each dot represents a single bladder sample.

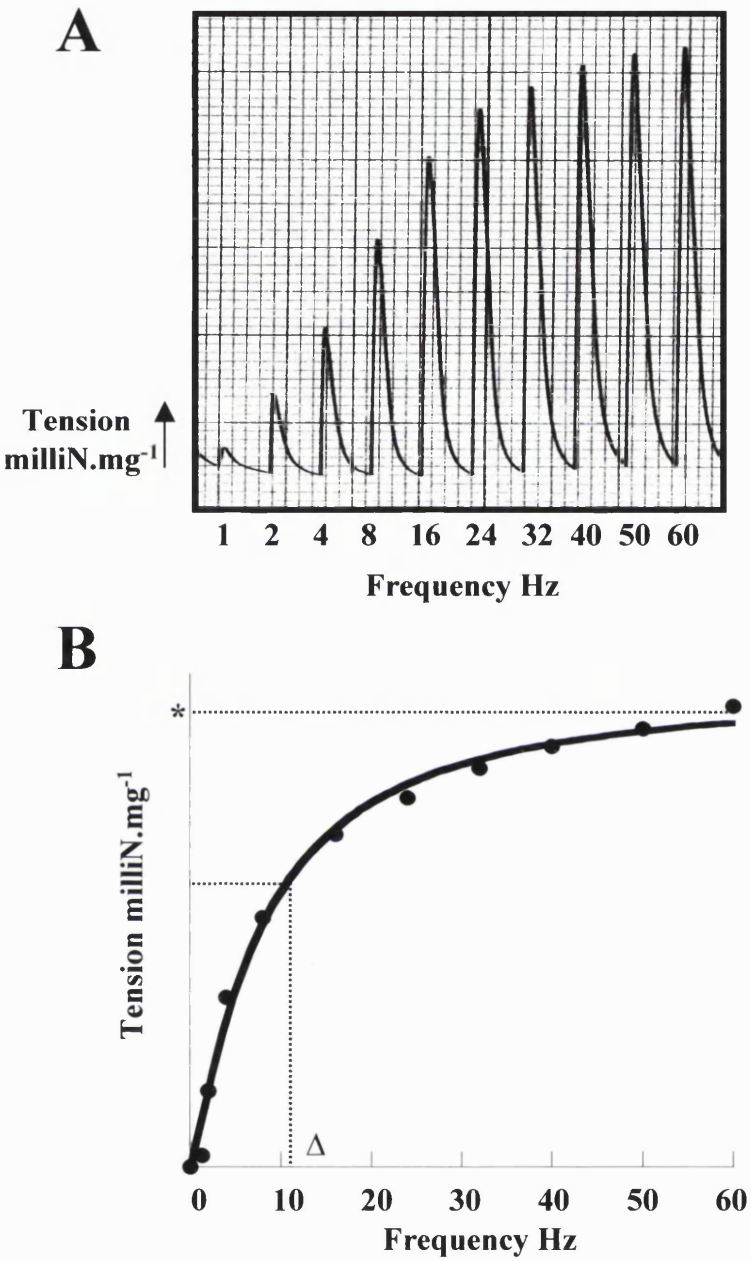

Figure 43. Force-frequency relations
A: representative example of a force-frequency relation with electrical field stimulation of increasing frequency. B: by fitting the relation to the empirical formula, T_{max} (*), the estimated maximum tension at high frequencies and $K_{1/2}$ (Δ), the frequency required to achieve $T_{max}/2$, can be calculated.

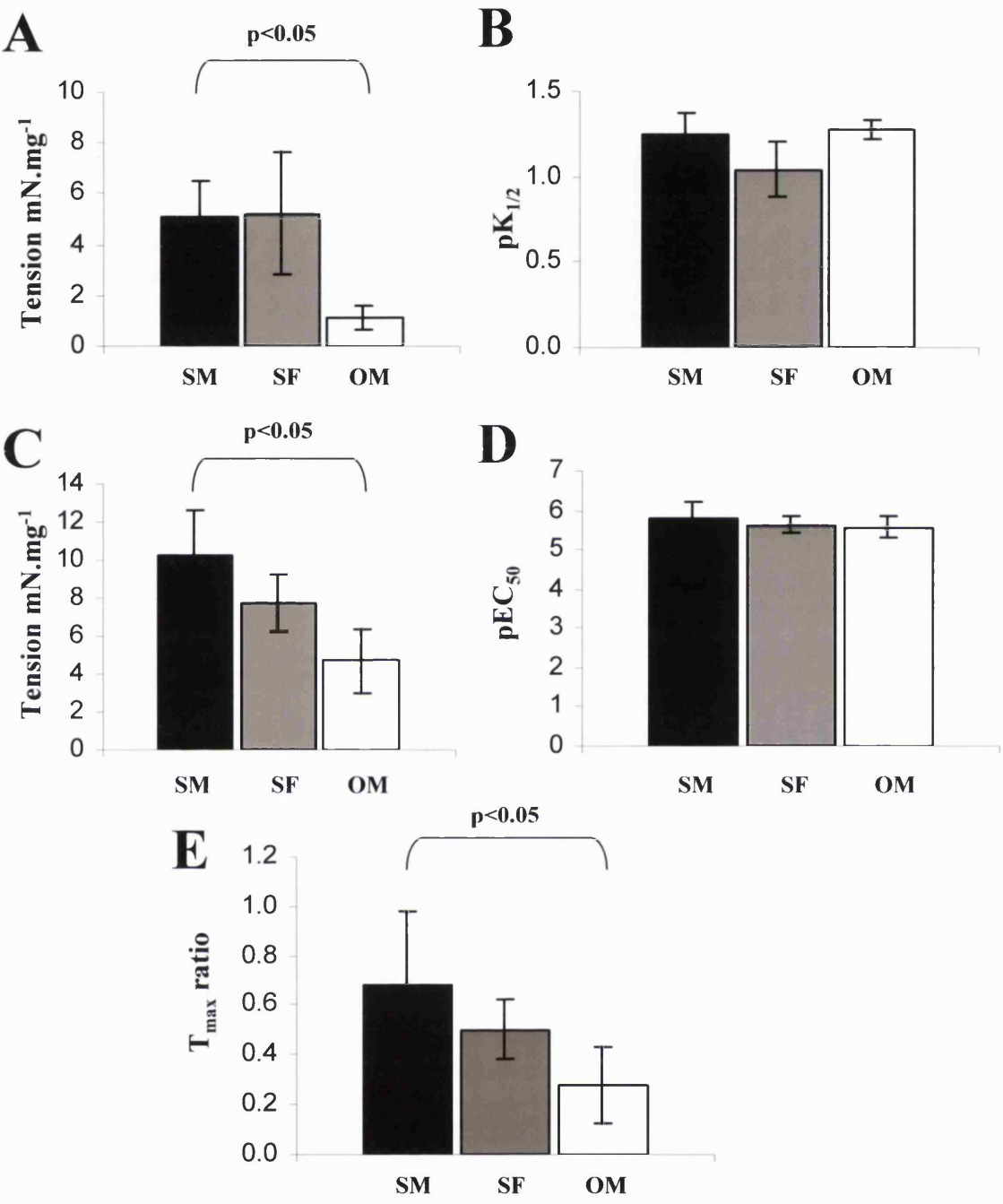

Figure 44. Contraction characteristics to nerve-mediated and carbachol stimulation

Data for *sham* male (SM), *sham* female (SF) and *obstructed* male (OM) groups. A: T_{max}, values for nerve-mediated stimulation. B: $pK_{1/2}$, values for nerve-mediated stimulation. C: T_{max} values for carbachol stimulation. D: pEC_{50} values for carbachol stimulation. E: ratio of T_{max} values for nerve-mediated and carbachol stimulation. Note $p<0.05$ *obstructed* male versus *sham* male.

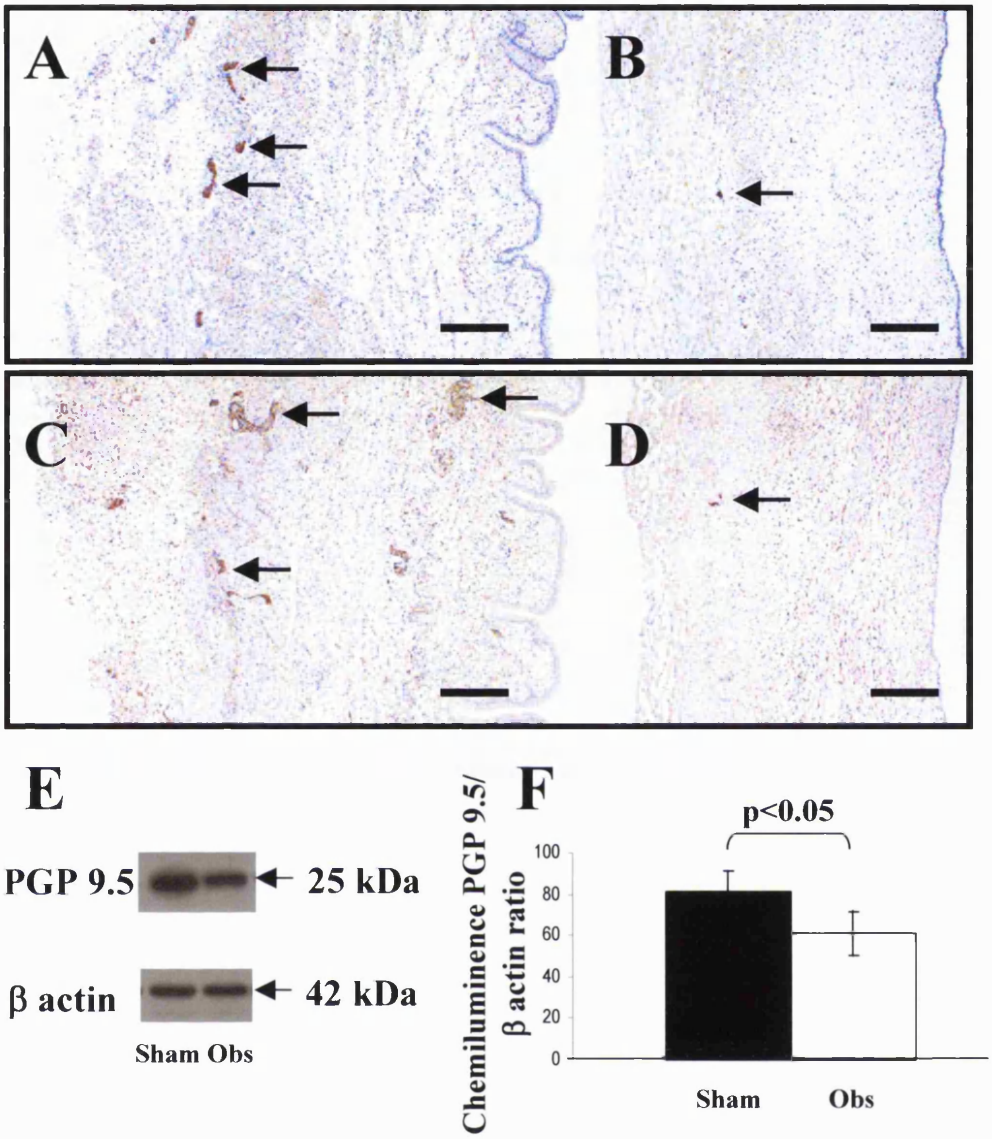

Figure 45. Innervation in experimental bladders

A and C: *sham* male bladders at 105 days gestation; B and D: time-matched *obstructed* male organs. A and B were immunostained for S100 and counterstained with haematoxylin; C and D were immunostained for PGP 9.5 and counterstained with haematoxylin. Nerves (arrowed) are immunostained brown with S100 and PGP 9.5; note in *obstructed* bladders, neuronal-pattern S100 and PGP 9.5 is diminished versus *sham* bladders. Bar is 400 μm. E: Western blot for PGP 9.5 (25 kDa) and β-actin (42 kDa) in a representative *sham* and *obstructed* (Obs) male bladder. B: Histogram showing PGP 9.5/β actin protein; closed bars from *sham* and open bars from *obstructed* bladders. Note significant ($p<0.05$) reduction in PGP 9.5 expression in *obstructed* bladders.

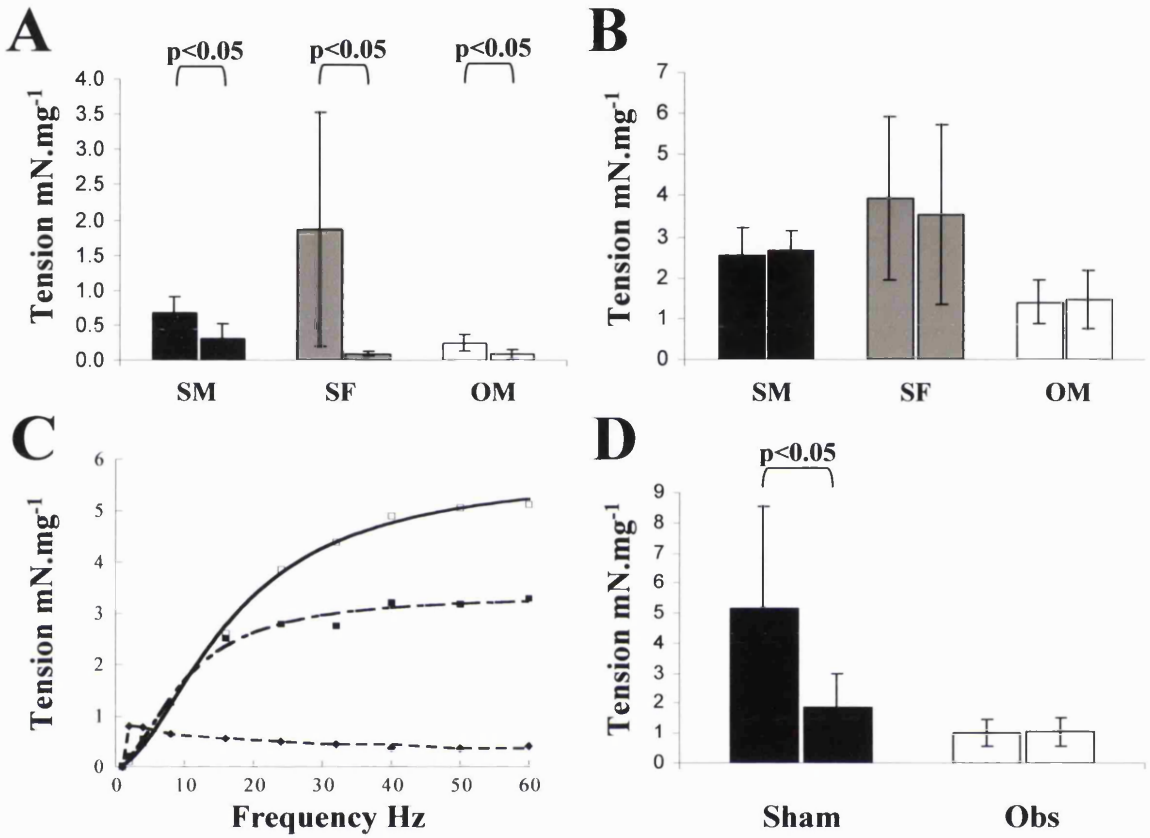

Figure 46. The effect of adenosine, ABMA and atropine-resistant contractions

Data for *sham* male (SM), *sham* female (SF) and *obstructed* male (OM) groups. A: The reduction of 8 Hz nerve-mediated contractions by 1 mM adenosine – left bar before adenosine, right bar after adenosine. B: The effect of 1 mM adenosine on carbachol contractures. C: A nerve-mediated force-frequency relation (open squares), after the addition of 10 μM ABMA (closed squares) and after the addition of 1 μM atropine (closed diamonds). D: T_{max}, values for nerve-mediated stimulation before (left column) and after (right column) addition of 10 μM ABMA in *sham* bladders (male and female *sham* data combined) and *obstructed* bladders.

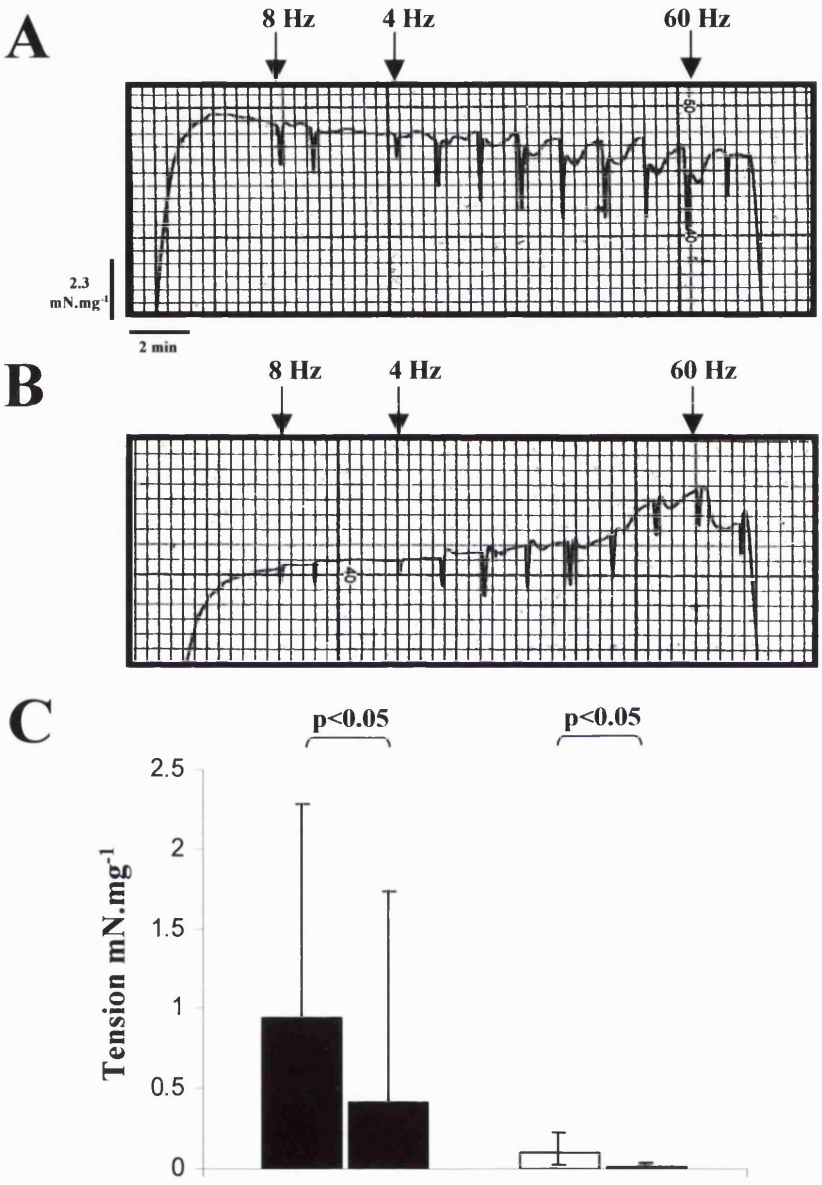

Figure 47. Nitrergic neurotransmission

Nerve-mediated contractile responses in preparations pre-contracted with 10 μM carbachol in the absence (A) or presence (B) of 1 μM ODQ. Preparations were twice test stimulated at 8 Hz followed by increasing frequencies of stimulation from 4 Hz to 60 Hz. C. Absolute magnitude of maximum estimated relaxation, T_{max}, at high frequencies in the presence and absence of 1 μM ODQ in *sham* male (SM) and *obstructed* (OM) bladder.

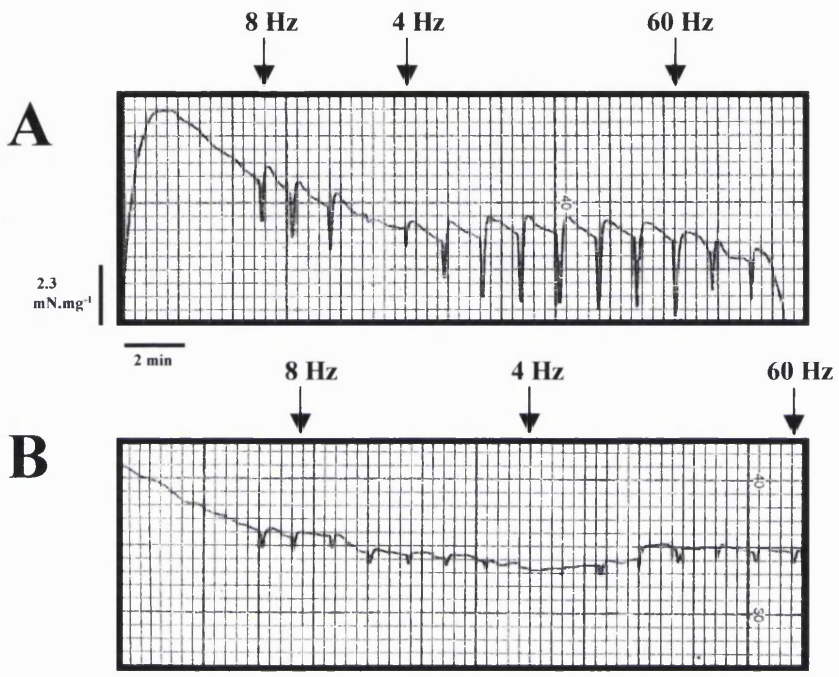

Figure 48. Nitrergic neurotransmission was nerve-mediated

Nerve-mediated contractile responses in preparations pre-contracted with 10 μM carbachol in the absence (A) and presence (B) of 1 μM TTX. Preparations were test stimulated at 8 Hz followed by increasing frequencies of stimulation from 4 Hz to 60 Hz.

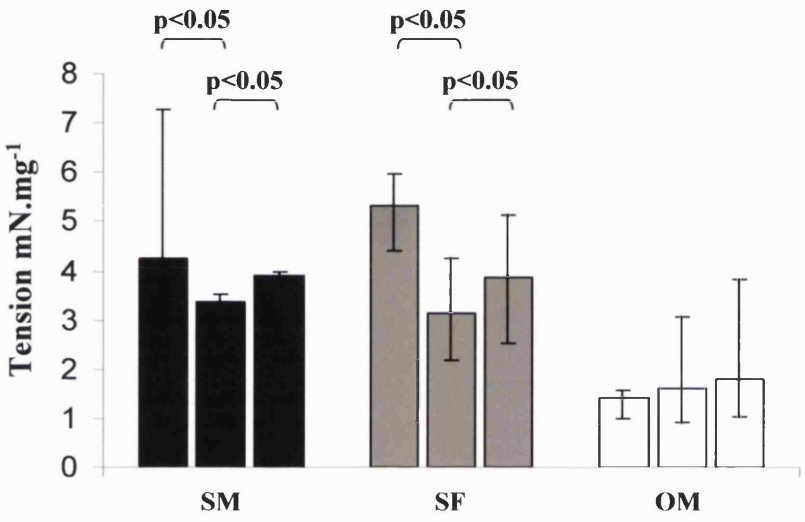

Figure 49. The effect of the mucosa

T_{max} values of *denuded* bladder strips, *mucosal* strips and *mucosal* strips in the presence of 1 μM ODQ, respectively, in *sham* males (SM), *sham* females (SF) and *obstructed* males (OM).

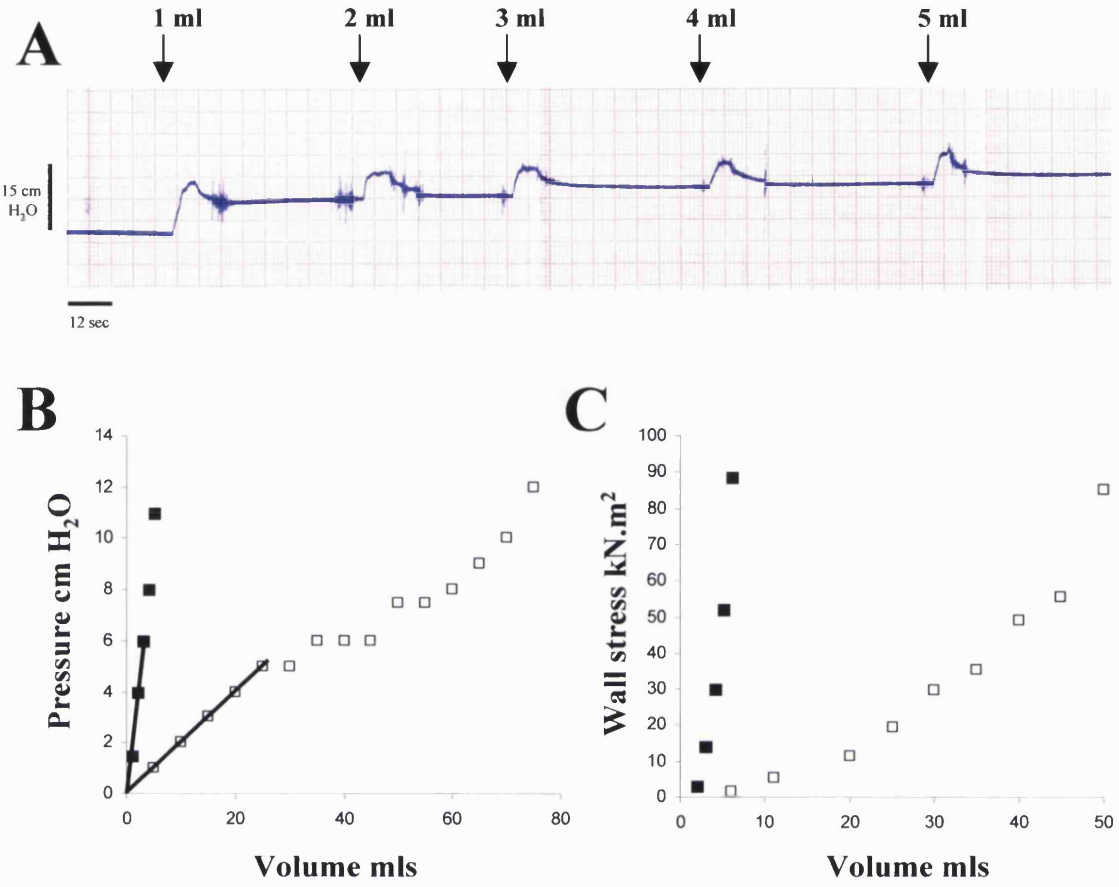

Figure 50. Filling cystometry

A: Filling cystometry in a representative *sham* male bladder that demonstrates stress-relaxation of the pressure change after injection of fluid (in 1 ml increments in the control bladders). B: Representative examples of pressure-volume curves in *sham* (closed square) and *obstructed* (open square) bladders. Fitted straight line is equivalent to 1/compliance, the latter equals $\Delta V / \Delta P$). C: Representative examples of pressure-wall stress curves. Note how wall stress appears to be linear before limit is reached when the relationship becomes curvilinear.

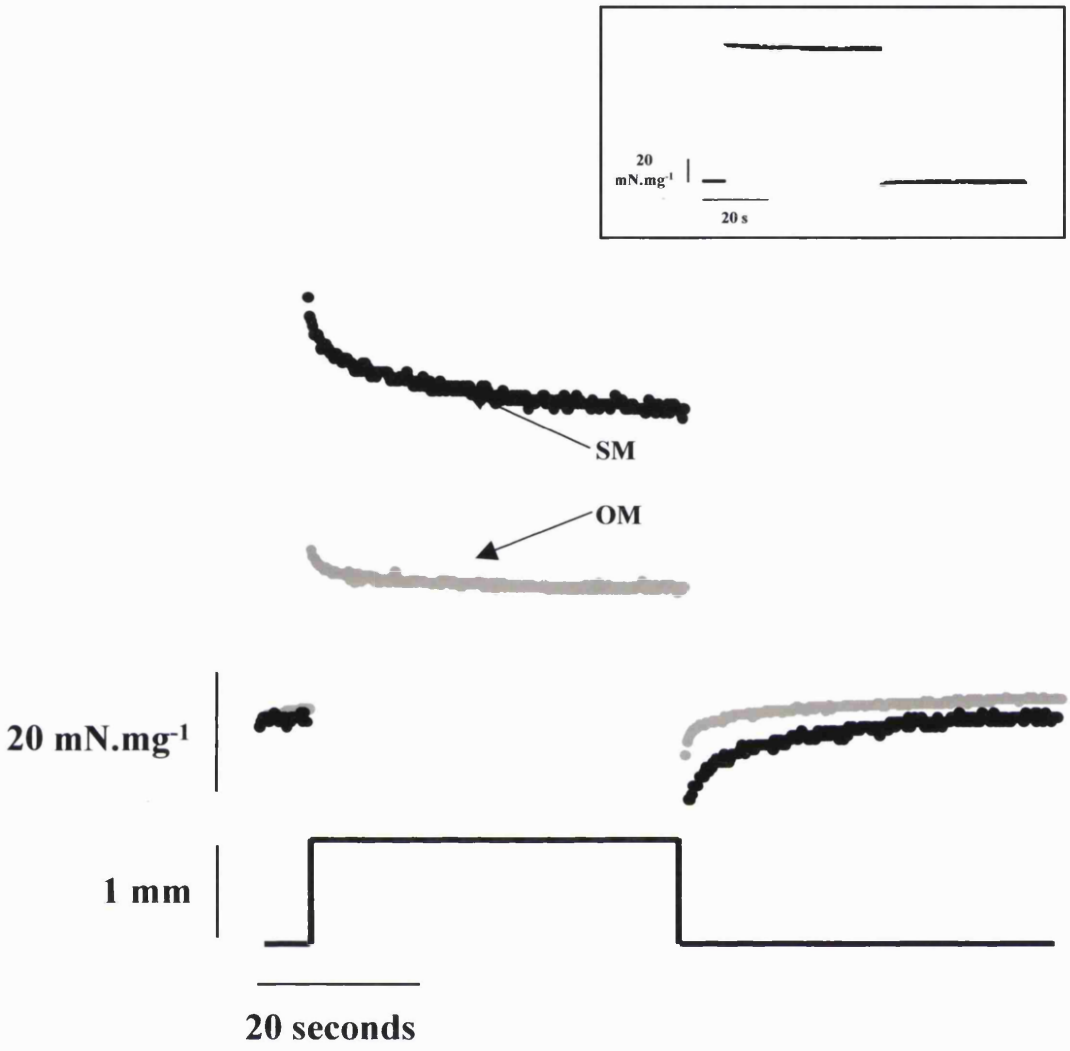

Figure 51. Stress-strain relationships of the fetal bladder
Examples of the stress responses to stretch (change of strain) in preparations from *sham* (SM, black) and *obstructed* (OM, grey) groups. Insert shows equivalent stress responses from a strip of rubber.

	Sham males	*Sham* females	*Obstructed* males
Elasticity, $mN.mm^{-3}$	143.3±173.8	183±196	38.9±39.1*
Elastic work, W_E, $mN.s.mg^{-1}$	2942±757	4168±491	881±181*
Visco-elastic work during stretch, W_V, $mN.s.mg^{-1}$	243±295	243±26	40±16
Visco-elastic work during relaxation, $mN.s.mg^{-1}$	311±330	123±86	79±68*
W_E / W_V x 100 %	90.0±12.0	96.0±0.5	95.5±2.0
τ, seconds	11.1±5.0	21.4±2.51*	12.0±3.8

Table 2. Biomechanical properties in experimental bladders

Steady-state elasticity and visco-elastic properties of muscle strips taken from *sham* and *obstructed* fetal bladders and *sham* female bladders.
*$p<0.05$ versus *sham* males.

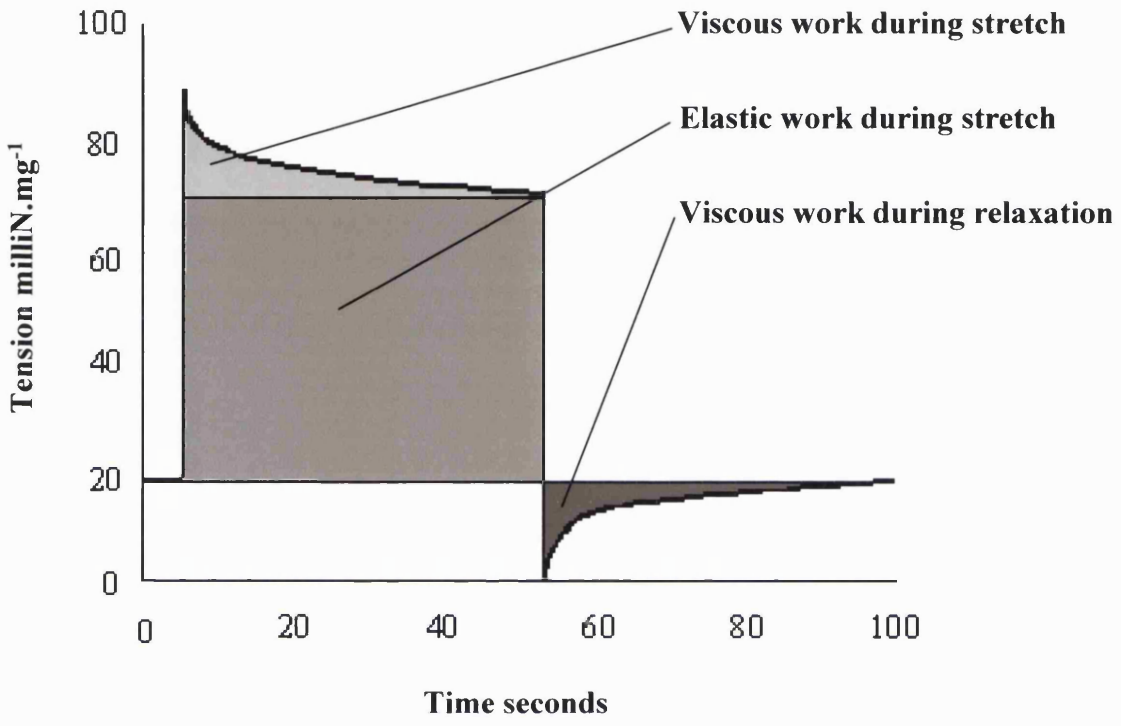

Figure 52. Elastic and viscous work

Diagrammatic representation of a stress-strain relationship in a fetal bladder preparation to illustrate areas of viscous work performed during stretch, elastic work and viscous work during relaxation.

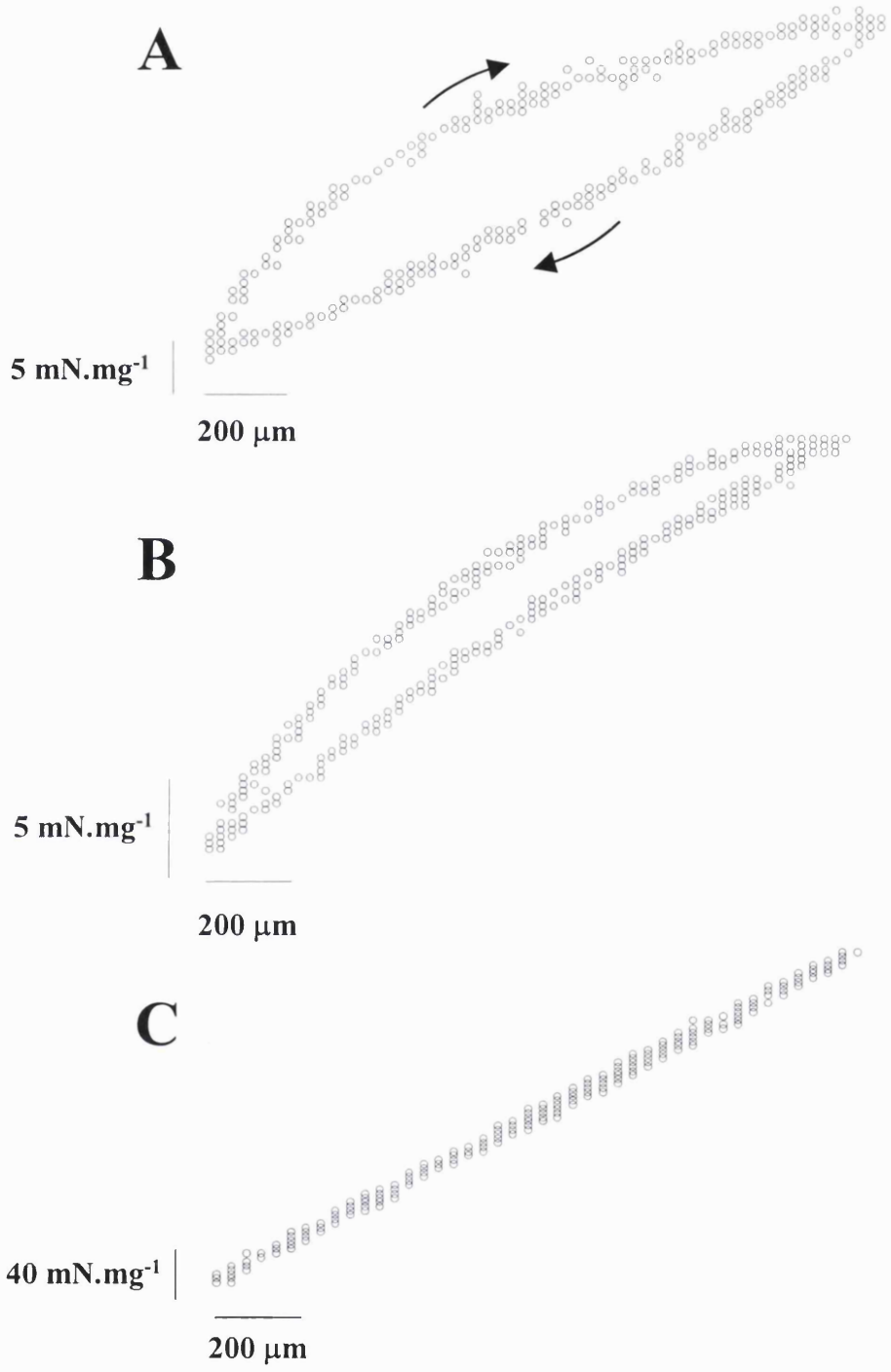

Figure 53. Hysteresis

Hysteresis loops for steady-state stress relationships of preparations from *sham* male (A) and *obstructed* (B) bladders and in a rubber strip (C). Arrows in A illustrate direction of hysteresis during stretch (upper arrow) and relaxation (lower arrow).

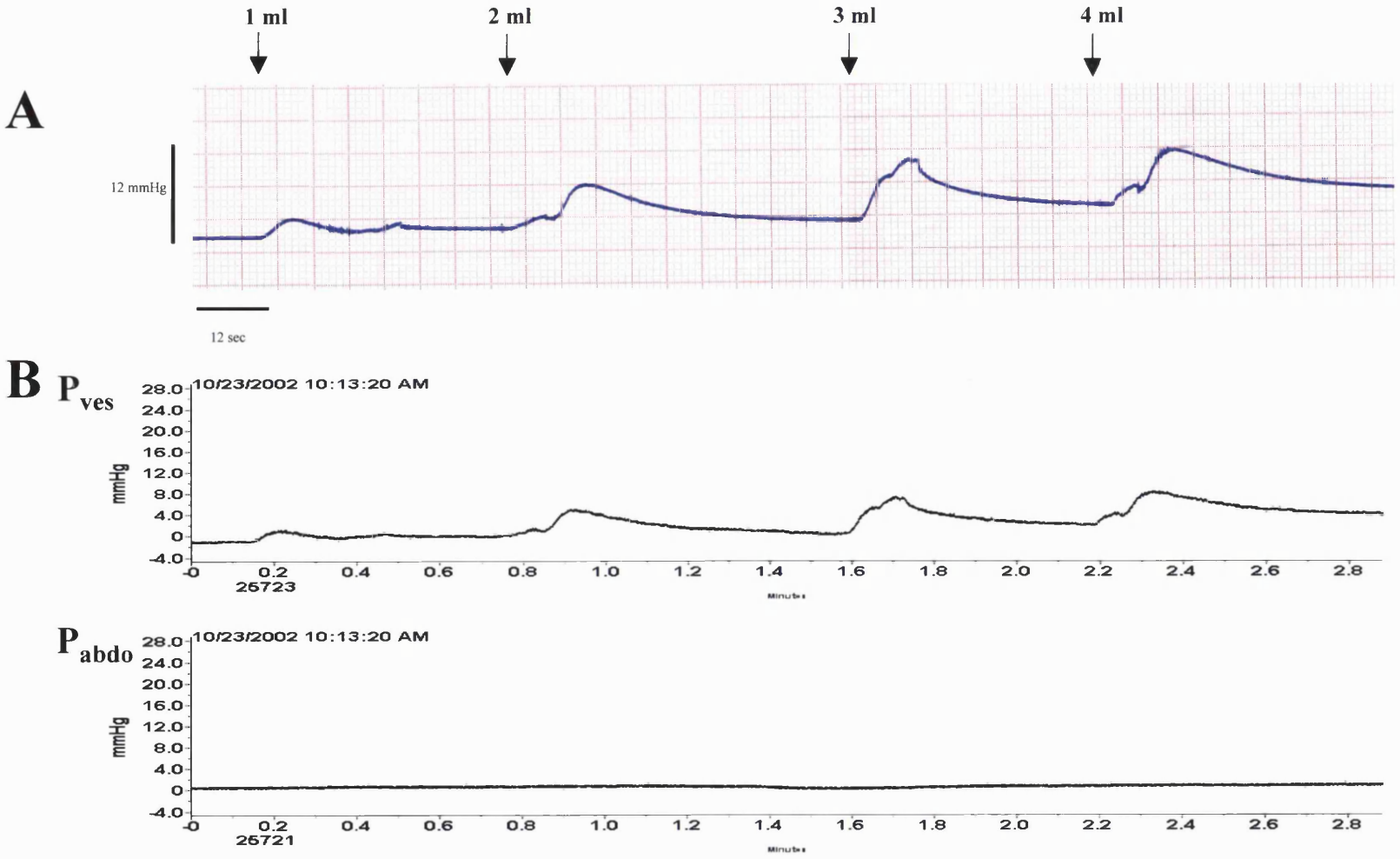

Figure 54. Simultaneous pressure recording by filling cystometry and radiotelemetered cystometry
Note conventional filling cystometry showed identical pressure recordings to the pressures recorded by the radiotelemetry method following filling of the bladder (ex vivo) at increments of 1 ml. In B, the upper trace was the pressure recorded from within the bladder (P_{ves}) and the lower trace refers to abdominal pressure (P_{abdo}).

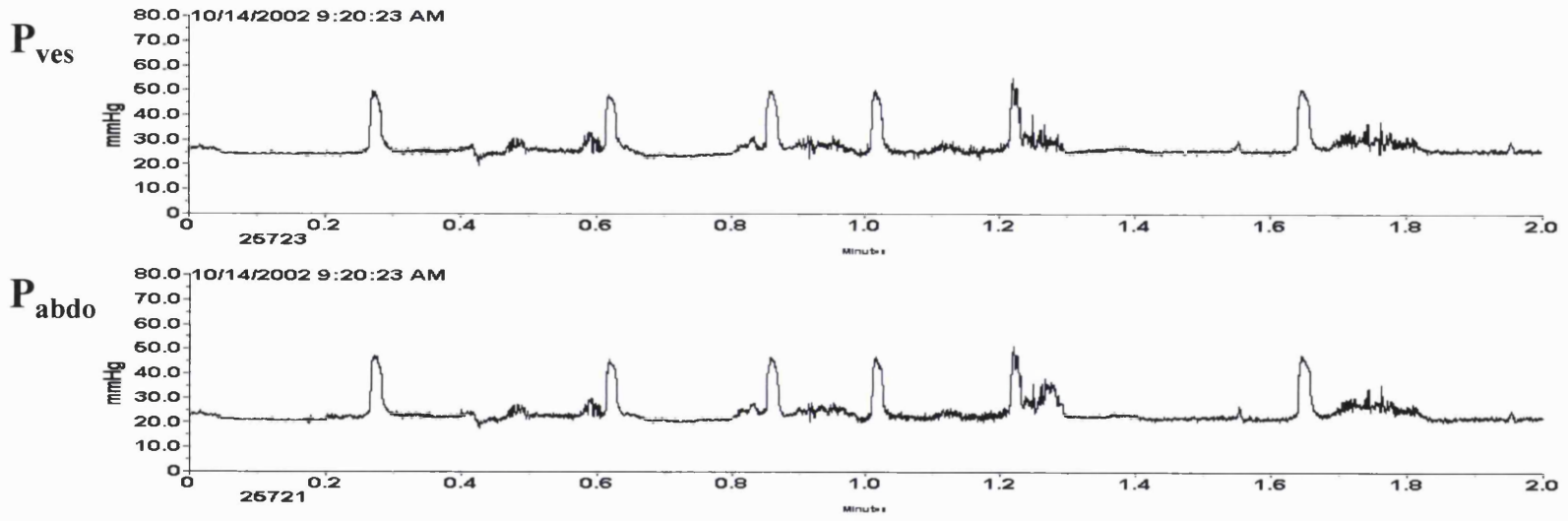

Figure 55. Synchronous bladder and abdominal activity

P_{ves}: vesical pressure, P_{abdo}: abdominal pressure; in an example radiotelemetry pressure recording. Numbers above graph refer to date and time of recording, numbers below graph refers to animal identification and pressure channel number.

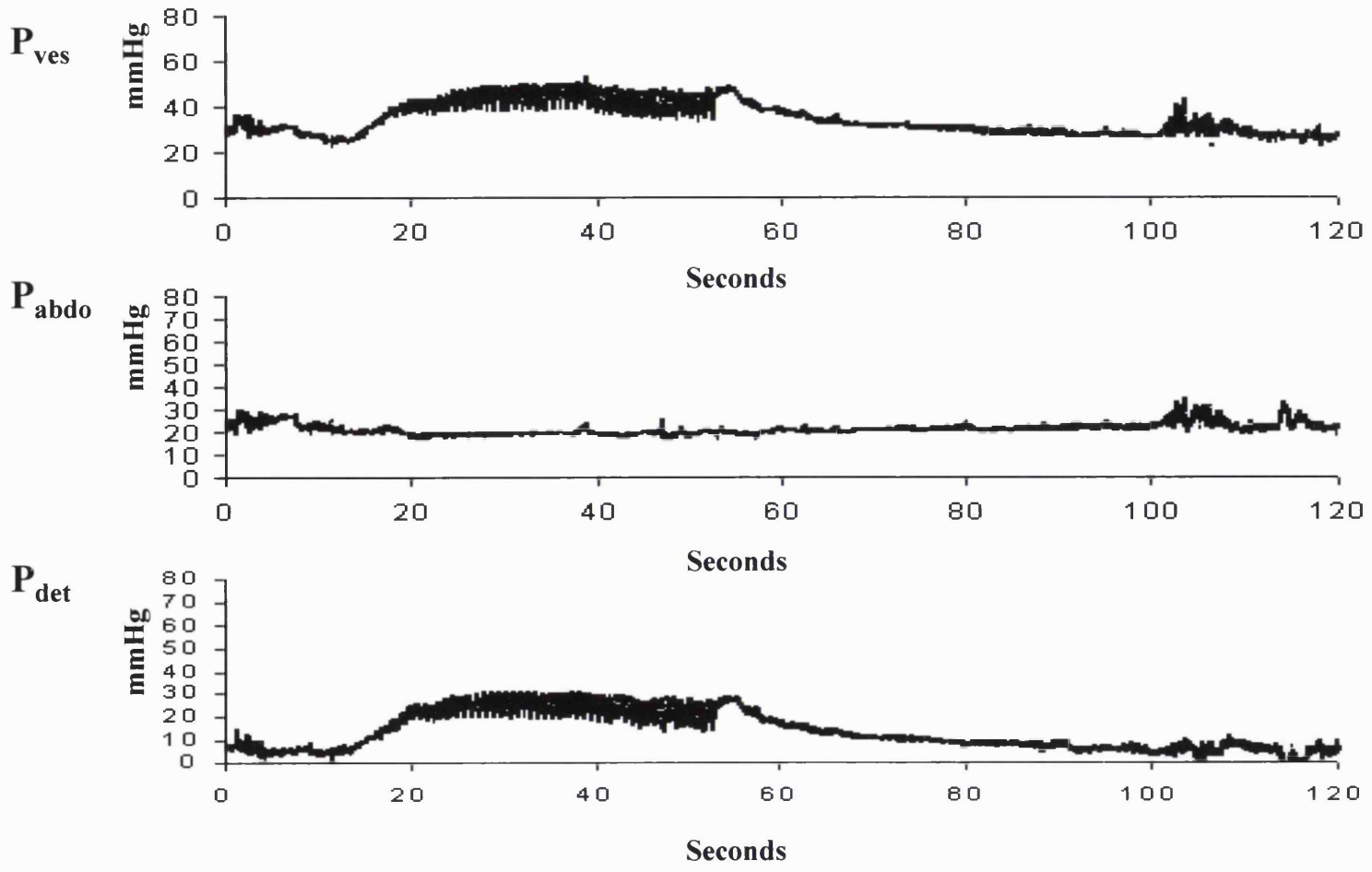

Figure 56. Calculation of detrusor pressure

Detrusor pressure (P_{det}) can be calculated by subtracting abdominal pressure (P_{abdo}) from vesical pressure (P_{ves}). Figure shows an example void in a fetus from a 105-140 gestational age group.

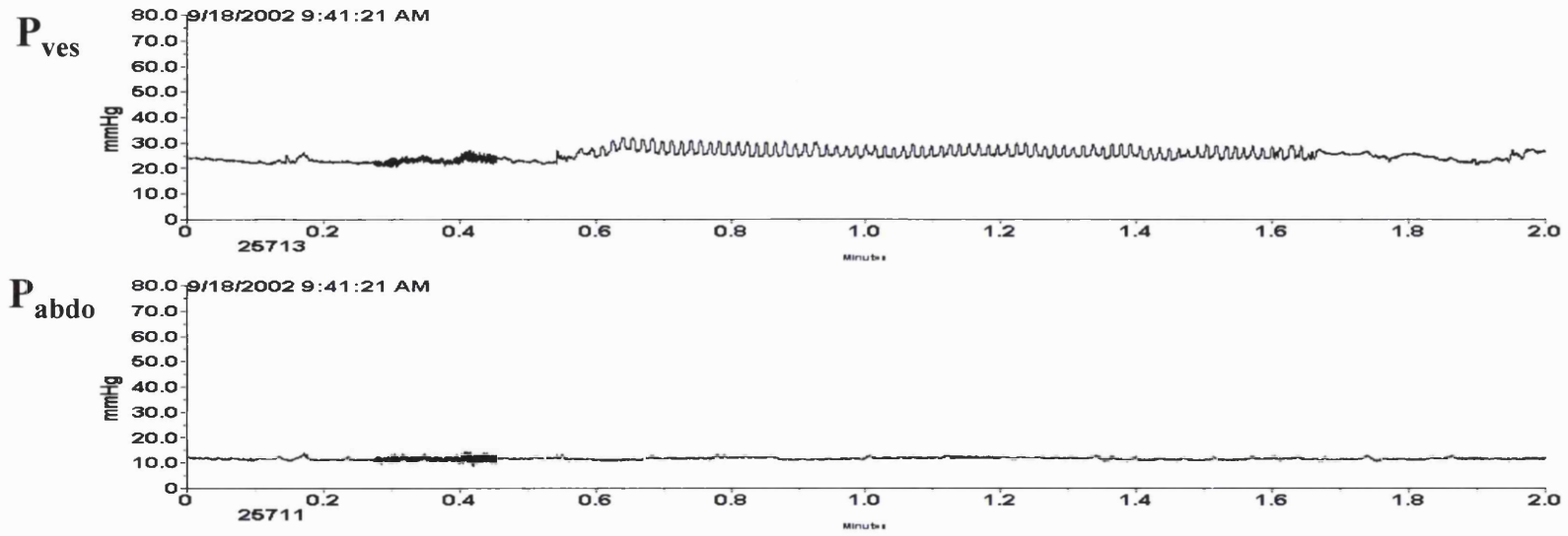

Figure 57. Immature void

Note in vesical pressure trace, high frequency, low amplitude activity with, in this example, no elevation of baseline pressure (example from experiment 4); P_{ves}: vesical pressure, P_{abdo}: abdominal pressure.

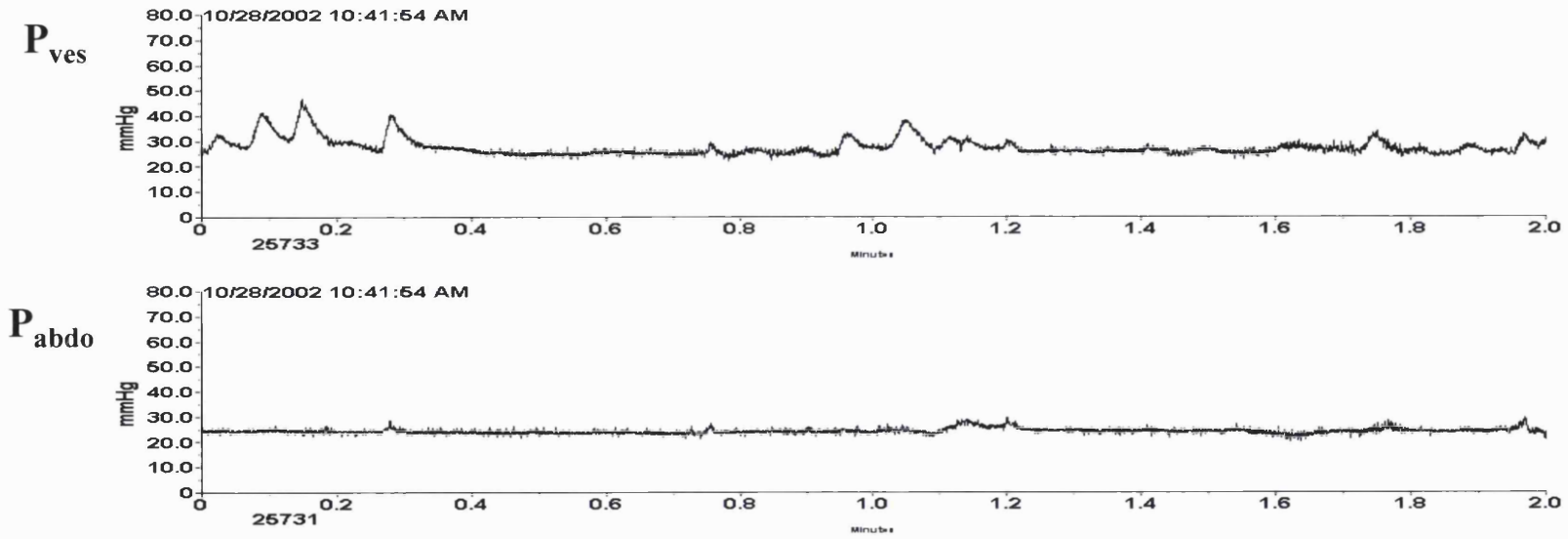

Figure 58. Staccato activity in trains

Note in vesical pressure trace, short (20-40 seconds) phasic elevations of pressure that were in trains (example from experiment 2); P_{ves}: vesical pressure, P_{abdo}: abdominal pressure.

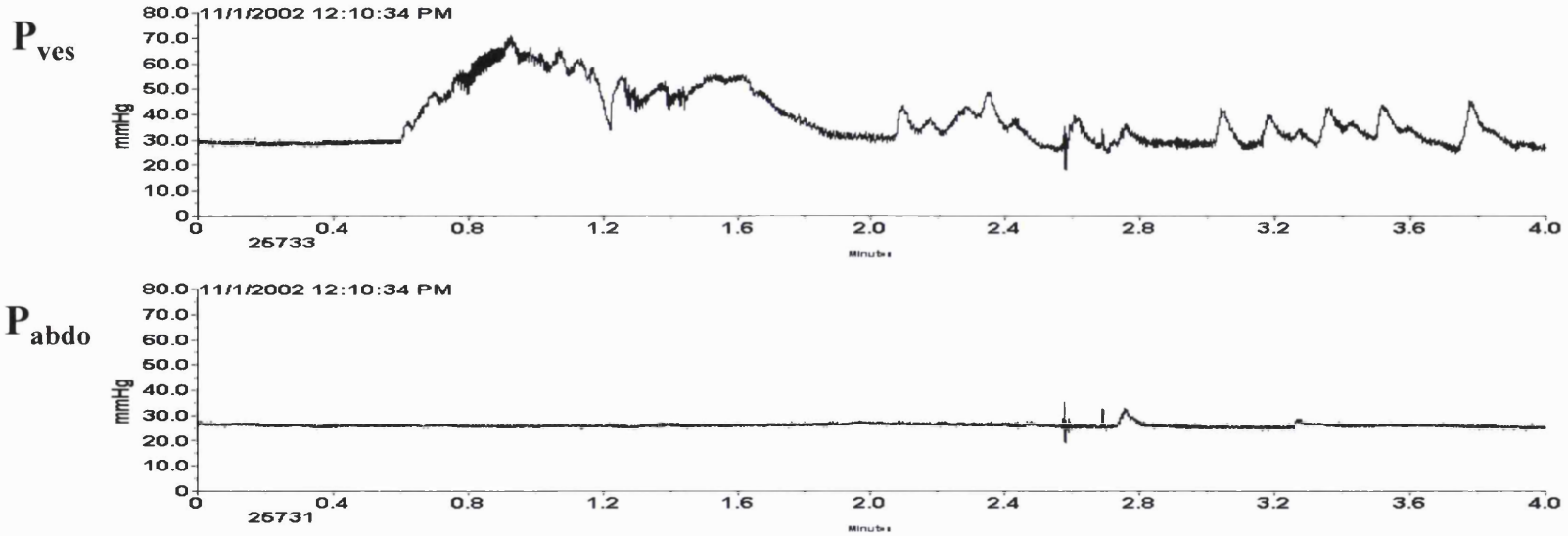

Figure 59. Staccato activity pre- and post-void

Note in vesical pressure trace, short (20-40 seconds) phasic elevations of pressure that were observed pre- and post-void (only post void activity shown, example from experiment 2); P_{ves}: vesical pressure, P_{abdo}: abdominal pressure.

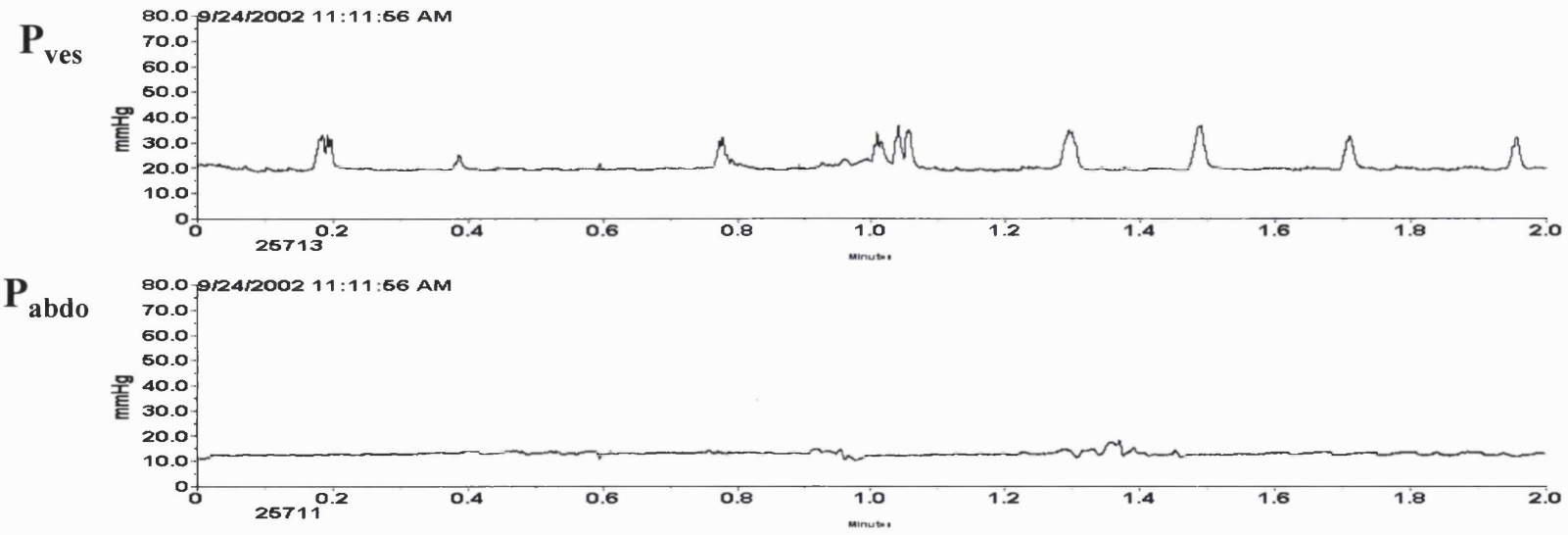

Figure 60. 'Unstable' type activity

Note in vesical pressure trace, very short (<5 seconds) elevations of pressure (example from experiment 4); P_{ves}: vesical pressure, P_{abdo}: abdominal pressure.

Experiment	Day	Mean voids/ hr	Mean P_{det} max (mmHg)	Mean Phase time (s)	Mean P_{abdo} max (mmHg)	Other events
1	1	2.5	28	60	0	Long ST
	3	3	20	75	0	2 ST
	7	2	32	95	0	2 SV
	14	2	25	105	0	2 SV
	22	1.5	27	100	0	2 SV
2	1	3	21	180	0	-
	3	4	23	235	0	-
	7	2.5	27	143	0	2 ST
	14	1.5	40	105	0	2 SV
	18	2	40	140	0	3 SV
	22	No discernible voids				
4	2	4 IM	15	25	0	U
	10	2 IM	0-5	20-40	0	3 U
	16	4 IM	10-15	20	0	4 U
	26	2.5	15	115	0	1 SV
	32	2	25	135	0	1 SV

Table 3. Discriminate bladder activity in experimental groups
Summary of discriminate bladder activity. Key*: IM*, immature void; *ST*, staccato activity in trains; *SV*, staccato activity pre- and post-void; *U*, 'unstable' type activity.

6. Discussion

In my thesis, a number of novel observations were documented. I found that the fetal bladder obstructed between 75 and 105 days gestation became larger and heavier and had grown; I found an increase in cellular proliferation and cellular apoptosis within the detrusor muscle layer and an increase of apoptosis but no proliferation within the lamina propria layers. This was accompanied by a downregulation of Bcl-2 (the anti-death protein) and an upregulation Bax (the pro-death protein) and activated caspase-3 (the effector of apoptotic death). This appeared against a background of growth and decreased cell turnover (both proliferation and apoptosis) during normal maturation of the fetal bladder between 75 days gestation and term. I also found the obstructed fetal bladder became hypocontractile, denervated, exhibited greater atropine-resistant contractions and lost the negative inotropic effect that the urothelium exerted on the detrusor muscle. I also observed increased compliance and reduced elasticity and viscoelasticity in the obstructed fetal bladder. I will now discuss these findings in detail.

6.1 The experimental model of ovine fetal BOO and human disease

The fetal sheep model I used in my thesis generated BOO at 75 days gestation by partial urethral obstruction (by placement of an omega-shaped ring) and complete urachal ligation. After 30 days, this experimental BOO produced gross changes to the macroscopic features of the fetal urinary tract; ultrasound and post-mortem examinations revealed hydroureteronephrosis and a dilated bladder. This was associated with a disruption to nephrogenesis. Such histological changes in the developing kidney have

also been documented after complete ureteric obstruction between 90 and 100 days gestation in the ovine fetus (Attar et al, 1998; Yang et al, 2001) and after experimental ovine fetal BOO (Gobet et al,1999a; Peters et al, 1992a). These changes to kidney maturation are similar to the changes in human fetal kidneys exposed to BOO (Risdon and Woolf, 1998) and suggest that this experimental model successfully mimics human disease. Furthermore, the model resulted in changes to fetal bladder structure and function. Although changes to kidney development are clinically very important, my thesis has focused on the aberrations to fetal bladder maturation.

At 105 days gestation, sham fetal bladders were well-developed, with a urothelial layer covering the lamina propria; detrusor muscle bundles were apparent, with a trilaminar appearance, and with little connective tissue between individual bundles. I found that ovine fetal BOO resulted in a large dilated, hypocontractile fetal bladder; obstructed bladders walls were thinner, their urothelium was flattened and the cellularity of the lamina propria appeared decreased. Although the muscular layer showed an increase of connective tissue between muscle bundles, there appeared to be no apparent change to αSMA expression within the detrusor muscle (this was not formally assessed).

Human fetal bladder structural changes to BOO remain uncertain (Freedman et al, 1997; Kim et al, 1991b; Workman and Kogan,1990), infants with PUV typically suffer thickwalled, hypercontractile bladders (that progress to a large hypocontractile bladder) (Holmdahl, 1997). This would imply that many of these children develop thickened, dilated bladders in utero, as detected by prenatal ultrasound examination (Agarwal and

Fisk, 2001). However, not only is the pathophysiological progression of the fetal bladder to BOO poorly understood but dilated bladders have been described in human fetal bladders which suffer in utero BOO by PUV (McHugo and Whittle, 2001; Suwanrath et al, 2001) and the possible bladder 'obstruction' associated with PBS (Volmar et al, 2001).

A number of possibilities exist for the development of a large, dilated, hypocontractile bladder in my experimental model. Firstly, the model may represent severe obstruction resulting in a severe bladder phenotype. Alternatively, the hypocontractile bladder may represent one end of a spectrum of changes that the fetal bladder undergoes in response to in utero obstruction. In response to in utero BOO, the fetal bladder may initially produce a compensatory response (with evidence of bladder thickening and hypercontractility) followed by a decompensation of bladder function, resulting in a large, ineffectual, 'floppy' organ, as observed in my results. This would mimic the spectrum of response of the mature heart when exposed to ouflow tract obstruction (Wagoner and Walsh, 1996). On the other hand, it is not inconceivable that the fetal bladder becomes dilated and poorly contractile after 30 days of in utero BOO and only later, possibly nearer term, becomes thickwalled and hypercontractile (and remains dilated). Only by obtaining fetal bladder samples at earlier and later time points, and by in vivo fetal bladder cystometry in the obstructed bladder (see later), will the pathophysiological progression of fetal BOO be determined. Finally, it is of note that contractility studies, taken from an empty or decompressed bladder, as in my thesis, may differ from in vivo whole organ physiology; this offers a further possible explanation for contractile differences in the obstructed experimental model.

6.2 The molecular biology of the developing and obstructed fetal bladder

A summary of my findings are illustrated in Figure 61.

6.2.1 BOO deregulates proliferation and apoptosis in the developing bladder

Cell proliferation in the fetal bladder

I found that 30 days of BOO resulted in enhanced growth of the fetal bladder as assessed by whole bladder weight, protein and DNA measurements. This is similar to the growth observed in the obstructed fetal bladder by other investigators in the fetal sheep (Karim et al, 1993; Peters et al, 1992b). Assessing PCNA protein expression, a surrogate marker of cell proliferation, I found that experimental fetal BOO was associated with a significantly increased percentage of proliferating detrusor SMC, versus *sham* controls, with no significant difference in the lamina propria or urothelial cells between the two groups. In addition, the average area of detrusor SMC was increased after 30 days of BOO. Furthermore, in *obstructed* bladders only, a prominent population of proliferating cells was noted between muscle bundles; these cells probably represent fibroblast-like cells which may be implicated in the increased collagen in this area, as seen by Masson's trichrome and elastin van Geison staining in *obstructed* bladders. If these alterations in proliferation and hypertrophy have occurred for a significant period during BOO, my results are consistent with the conclusion that both proliferation and hypertrophy of detrusor SMC, and also proliferation of interstitial cells between muscle bundles, make an important contribution to bladder growth after BOO. It is probable that the generation

of the new, larger SMC may be an adaptation in the fetal bladder that attempts to overcome the urinary flow impairment in my experimental model.

Apoptosis in the fetal bladder detrusor

The response to BOO, in terms of cell turnover, however, appears more complex when programmed cell death is also considered. Within detrusor muscle bundles, I found that BOO was associated with a significant increase in the percentage of apoptotic SMC; if the assumption that the clearance of cells undergoing programmed cell death is equal in the *sham* and *obstructed* groups is correct, the extent of apoptosis is approximately three times higher after BOO. This upregulation of apoptosis may occur for a number of reasons. First, it may represent a deletion of 'excess' cells in a rapidly proliferating population. Such a phenomenon has been observed as a strategy to control cell numbers in metanephric kidney development (Coles et al, 1993; Welham et al, 2002) and during embryogenesis and epidermal development in the fruit fly (Li et al, 1999; Namba et al, 1997). Such a function may allow (Welham et al, 2002) some detrusor SMC to be deleted as their neighbouring SMC hypertrophy and fill the limited space. Conversely, the apoptosis I documented may represent a pathological loss of potentially functional muscle cells which might help to overcome BOO. Overall, it appears the balance of growth in the fetal bladder is mediated by cell proliferation and hypertrophy with this process modified by programmed cell death. Further studies are necessary to determine what factors are involved in controlling the fine balance of proliferation and apoptosis; investigations of the proto-oncogene, c-myc (Rohn et al, 1998), show this protein can stimulate cell proliferation in the presence of appropriate survival factors and trigger

apoptosis in their absence. Such dual capacity may have an important impact on cell turnover in the obstructed fetal bladder and warrant further investigation.

Apoptosis in the fetal bladder lamina propria

In the lamina propria layer, I documented a significant, approximately, three-fold increase in apoptosis in *obstructed* bladders, whereas, unlike the detrusor layer, the percentage of proliferating cells was not different from *sham* controls. Furthermore, the number of cells per unit area significantly decreased in this layer. Collectively, these observations suggest that enhanced death may have led to a decrease in cell density in the lamina propria.

In the early stages of murine bladder development, the organ is relatively simple, with a prominent mesenchymal layer enveloping a simple epithelial layer (Baskin et al, 2001; Smeulders et al, 2001). Through a poorly-understood process of mutual inductive events (Baskin et al, 2001), murine bladder mesenchyme differentiates into the detrusor muscle layer and the lamina propria, while the epithelium acquires a complex, multi-layered phenotype. While it is not established whether ovine lamina propria or adjacent epithelium have similar inductive roles in the experimental period of observation in my thesis, it is interesting to note that attenuation of the lamina propria layer was accompanied by 'simplification' of the urothelium, which had only one or two layers of cells in *obstructed* bladders versus three to four layers in *sham* controls. Such attenuation of the lamina propria in *obstructed* bladders may therefore also prevent complete differentiation and maturation of fetal ovine detrusor muscle. Consideration should also

be made of the possibility that the simplification of the urothelium may also result directly from the mechanical effects of increased urine volume within the obstructed bladder. Furthermore, as the bladder matures, neurovascular bundles traverse the lamina propria (Levy and Wight, 1990); while I did not formally localise apoptotic nuclei to particular cell types in the lamina propria, my impression was that most dying cells were not in vessel walls and they were therefore likely to be interstitial cells of the lamina propria.

6.2.2 Molecular correlates of increased apoptosis in fetal BOO

Apoptosis is the end result of a cascade of molecular events (Hayashi and Araki, 2002). Caspases play central roles in apoptosis, and can be activated by via specific cell-surface receptors (e.g. Fas ligand stimulation) or a mitochrondrial cascade (e.g. activated by irradiation and diverse other stimuli). Capase-3 lies at the convergence of these two pathways, and the activated molecule is able to cleave several cellular substrates, including structural proteins and cellular enzymes, resulting in apoptosis (Wilson, 1998). Furthermore, members of the Bcl-2 family interact with these pathways, with Bcl-2 favouring survival; Bax heterodimerizes with Bcl-2, and favours cell death (Yin et al, 1994). I discovered that 30 days fetal BOO led to an average two-fold increase of caspase-3 activity in fetal bladders. This was associated with an average 50% reduction in Bcl-2 protein level and an average three-fold increase in Bax protein level in whole bladders as assessed by immunohistochemistry and western blot. To my knowledge, my

results are the first descriptions that such mechanisms exist in the developing and obstructed fetal bladder.

Other studies have examined apoptosis in experimental urinary tract obstruction in vivo, although none of these studies addressed fetal bladder apoptosis. Santarosa et al (1994) found that BOO caused bladder hypertrophy in adult rabbits, with an increase of apoptosis following relief of obstruction. Chuang et al (2002) reported that apoptosis and Bax were upregulated in smooth muscle of obstructed ureters in adult rats. Several studies have, however, examined the effects of experimental urinary tract obstruction on the developing kidney. Attar et al (1998) and Matsell et al (2002) reported that fetal ureteric obstruction, in the ovine and monkey respectively, was associated with increased apoptosis in the tufts of developing glomeruli. Furthermore, Chevalier et al (2000) found that ureteric obstruction in neonatal rats caused apoptosis in some tubules which correlated with decreased Bcl-2 protein immunostaining. Finally, Liapis et al (2000), using ureteric obstruction in the developing opossum, reported a complex picture, with enhanced apoptosis and proliferation in the renal interstitium but a predominantly apoptotic response in tubules; enhanced death was accompanied by increased Bax, and decreased Bcl-2 immunostaining.

6.2.3 Growth and cell turnover in normal maturation of the fetal bladder

The novel observations I have made regarding the effects of BOO on bladder proliferation and death should be taken in the context of an insult to an actively growing

organ. This is emphasised in my limited surveys of whole bladder PCNA protein levels, which were found to show a downward trend between 75 days gestation and adulthood, and activated caspase-3 levels, which were found to show a downward trend from between 75 days gestation and term. These findings are consistent with the only other investigation of cell turnover in the developing murine bladder (Smeulders et al, 2001), where multiple bladder samples from different time points are more readily available. This study showed that cell division and programmed death, based on PNCA protein levels and TUNEL labelling, significantly reduced at each time point from the inception of the bladder at embryonic day 14, through gestation and up to maturity at six weeks after birth. It is therefore possible that ovine fetal BOO may shift bladder cell turnover to a more embryonic pattern. Further experiments would be necessary to establish whether similar degrees of BOO elicit the same, or different, responses in more mature sheep bladders.

6.2.3 Possible mechanisms by which BOO leads to altered fetal bladder cell turnover

A number of possible explanations exist to account for the altered cell turnover in the obstructed fetal bladder. One possibility is that BOO leads to increased pressure within the fetal urinary tract and that this physical stress, perhaps through increased axial strain, somehow triggers the aberrations of bladder cell biology. There have been several such studies on detrusor, and other, cells harvested from adults. Orsola et al (2002) reported that cyclic stretch and relaxation of human detrusor SMC led to increased DNA and protein synthesis but apoptosis was not examined. Galvin et al (2002) reported similar

findings; in addition, apoptosis was decreased with stretch. On the other hand, there are reports that mechanical stretch does lead to increased apoptosis of both vascular smooth muscle (Sotoudeh et al, 2002) and renal epithelial (Miyajima et al, 2000) cells. Furthermore, the variant response observed, of cell proliferation and cell death within different layers of the obstructed bladder in my experiments, may be dependent on the different shapes of cells in these layers provoking diverse physical forces induced by the mechanical stretch produced by urinary obstruction. These forces may induce a switch between growth and cell death, as have been shown in other anchorage-dependent cells (Wang et al, 2002). However, I know of no in vitro studies which have examined the effects of stretch on isolated populations of fetal bladder cells.

Angiotensin II signalling through its type 1 receptor (AT1) has been implicated in the biology (eg proliferation) of stretched detrusor SMC (Park et al, 1998). In the developing embryo, however, another angiotensin II receptor, AT2, is prominently expressed in the urinary tract and is implicated in transducing a death signal (Nishimura et al, 1999). It may be possible that this signalling pathway might be important in the bladder apoptotic response to BOO described in the current study. Furthermore, the expression of cysteine-rich protein 61 (Cyr61), implicated in cell migration, adhesion and proliferation, is upregulated in cyclically-stretched detrusor smooth muscle cells (Tamura et al, 2001) and suggests a possible role in cell signalling in the obstructed fetal bladder. Further, functional, studies should therefore address the effects of stretch on isolated fetal bladder cells, and focus on the possible expression of Cyr61 and the activity of receptors such as AT2. Finally, hypoxia (Ghafar et al, 2002) and increased fibrosis (Peters et al, 1997) have

been observed in the obstructed adult and fetal bladder, respectively; both these pathological processes are associated with aberrant apoptosis (Misao et al, 1996; Razzaque et al, 2002).

6.2.4 Possible therapeutic manipulation of apoptosis and apoptotic correlates

The potential exists for apoptosis to be manipulated for therapeutic gain (Reed 2002) and therefore offers a prospective, non-surgical, highly targeted treatment modality for fetal bladders exposed to BOO. Although no descriptions of fetal bladder manipulation exist, pharmacological agents have been described that are associated with changes to cell turnover in the adult urinary tract. Erdogru et al (2002) showed that pre-operative administration of an α-1 receptor antagonist (traditionally used to pharmacologically decrease smooth muscle tone to the bladder outflow tract) increased apoptosis within the adult human bladder. Kurita et al (2001) found that ablation of androgens were able to promote apoptosis within the epithelia of the murine prostate; furthermore, they demonstrated prevention of apoptosis was possible by the addition of the sex steroids, testosterone and dihydrotestosterone.

It is also possible to differentially manipulate proliferation and apoptosis in the urinary tract, which would be especially useful in my model. Chueh et al (2001) found that low concentrations of the sodium-potassium pump inhibitor, ouabain, was able to induce proliferation in prostatic smooth muscle cells whilst high concentrations was able to induce apoptosis in the same cells, offering the potential for dual manipulation.

Furthermore, in the developing fetus, specific cytokines, such as tumour necrosis factor-α, are capable of inducing apoptosis in fetal kidneys (Cale et al, 1998).

Finally, it is also possible to manipulate apoptosis-related proteins. A member of the Bcl-2 family, Bad, is able to directly bind to Bcl-2 and block its survival function (Zha et al, 1996); furthermore, administration of specific growth factors can activate the serine-threonine kinase, Akt, which is able to phosphorylate and deactivate Bad, thereby preventing cell death (Datta et al, 1997). Caspases may also be manipulated; Van Molle et al (1999) showed how caspase-3 was influenced by the acute phase proteins, α1-acid glycoprotein and α1-antitrypsin, to inhibit apoptosis in their experimental murine model of hepatitis.

6.3 The physiology of the developing and obstructed fetal bladder

A summary of my findings are illustrated in Figure 62.

6.3.1 Cholinergic neurotransmission

I found that BOO produced a hypocontractile response both to electrical field stimulation and muscarinic stimulation (with carbachol); this diminished response was greater with electrical field stimulation supporting the possibility of denervation. The latter finding was confirmed by decreased expression of two key neural markers, S100 and PGP 9.5. Interestingly, Peters et al (1992b) noted an increase in cholinergic receptor number (when normalized to smooth muscle cell number) in their obstructed fetal sheep model; a

finding consistent with increased accumulation of muscarinic receptors in denervated muscle, as originally described by Brockes and Hall (1975). Bladder innervation is also decreased in response to outlet obstruction in the adult model in other species. A reduction of cholinergic and adrenergic innervation of human obstructed bladders was observed by Gosling et al (1986); Malkowicz et al (1986) found a similar reduction in the obstructed rabbit. Cumming and Chisholm (1992) found that infravesical obstruction in human adults caused a significant decrease in detrusor innervation compared to controls. In addition, following relief of obstruction, there was an increase in innervation back to pre-obstruction levels; explained by axonal impairment without neuronal cell body damage, thereby leaving the potential for axonal regeneration.

Finally, I found the stimulation frequency producing a half-maximal nerve-mediated contraction, $K_{1/2}$, and the half maximal carbachol concentration, EC_{50}, were similar in strips from *obstructed* and *sham* bladders. This shows that changes to the excitablility of muscle strips to nerve-mediated stimulation or detrusor muscarinic sensitivity could not explain the hypocontractility. The lack of denervation supersensitivity to muscarinic agonists is in contrast to observations made in the obstructed adult pig bladder (Speakman et al, 1987) but is in keeping with studies using guinea-pig, rabbit, rat, sheep or human tissue (Eaton and Bates, 1982; Harrison et al, 1987). Furthermore, to my knowledge, there have been no conclusive demonstration of denervation supersensitivity in the obstructed fetal bladder, although this was implied in a fetal rabbit preparation (Rohrmann et al, 1997a).

6.3.2 Purinergic neurotransmission

Although not statistically significant, I found that atropine-resistant contractions were primarily observed in the *obstructed* group, in keeping with reports of similar responses in detrusor from overactive human bladders (idiopathic or secondary to obstruction) (Bayliss et al, 1999). The *sham* bladders had little atropine resistance in contrast to many other animal bladders, but similar to normal human detrusor (Burnstock et al, 1978; Creed et al, 1994; Suzuki and Kokubun, 1994; Zhao et al, 1996). It has been proposed that atropine-resistant contractions occur in obstructed bladders due to decreased ectoATPase activity, so that neurally released ATP is more likely to activate detrusor smooth muscle (Harvey et al, 2002). I also found that atropine-resistant contractions were evoked more readily at lower stimulation frequencies. It is possible that neural ATP is depleted at higher frequencies and that at greater frequencies, ectoATPase release itself may be enhanced (Westfall et al, 2000). It is important to note that the similarity of the atropine-resistance responses to human detrusor makes the ovine model of direct relevance to understanding the pathophysiology of human fetal bladder obstruction.

The breakdown product of purinergic neurotransmission, adenosine, reduced significantly the magnitude of the nerve-mediated contraction in both *sham* and *obstructed* groups. However, no effect was observed on contractions evoked by direct muscarinic receptor activation. This suggests that in the ovine fetal bladder, adenosine acts on presynaptic, possibly P_1, receptors as has been previously described in other species (Nicholls et al, 1992; Suzuki and Kokubun, 1994; Theobald, 1992). There was no difference in the sensitivity of this response in the *sham* and *obstructed* groups. However, of note, I found

that detrusor from female *sham* animals was significantly more sensitive but the mechanism for this remains unknown.

The addition of ABMA, a purinergic receptor (P2X) agonist, caused a reduction in the nerve-mediated force-frequency relation in the *sham* group. However, as there is little, if any, atropine-resistant contractions in this group, this would suggest that ATP is released but is hydrolysed by ectoATPases prior to postsynaptic purinoceptor activation. This possibility is in keeping with Westfall et al's (1997) study that showed that the postjunctional action of ATP was attenuated by enzymatic degradation. I found no evidence for the dampening effect of ABMA in the *obstructed* group and a number of possibilities exist for this explanation. It is possible that there are decreased postsynaptic P2X purinoreceptors or the desensitisation of P2X purinoreceptors by ABMA may occur in a dose-dependent manner. This could be investigated by performing an ABMA dose-response relationship. This dampening effect of ABMA is consistent with Lluel et al's findings (Lluel et al, 2002) that ABMA did not diminish the force generated (except at the very high concentration of 300 μM) in an obstructed rat model.

6.3.3 Nitregic neurotransmission

Evidence is now accumulating of a role for nitric oxide-mediated relaxation in the lower urinary tract (Bennett et al, 1995; Bridgewater et al, 1993; Moon, 2002; Triguero et al, 1993). Nitric oxide produces a relaxant response in the urethra and bladder neck suggesting a role in bladder outlet relaxation during micturition. Evidence supporting the relaxant role of nitric oxide in detrusor smooth muscle remains less convincing despite

evidence of nitrergic innervation within fetal detrusor muscle (Dixon et al, 1998). I found that electrical field stimulation of maximally pre-contracted detrusor strips produced either a relaxation or a biphasic relaxation-contraction response; the latter responses occurred at higher frequencies. Stimulation of pre-contracted *obstructed* bladder detrusor strips produced a smaller absolute relaxation, in keeping with the decreased force produced by other activators. TTX abolished these electrically stimulated relaxant forces confirming their neural origin, similar observations have also been made in fetal sheep (Levin et al, 2001) and cow models (Lee et al, 1994).

The guanylate cyclase inhibitor, ODQ, attenuated relaxations in both groups and is consistent with the hypothesis that relaxation was nitric-oxide mediated. However, responses were abolished incompletely by ODQ suggesting either that it may not be totally effective or that other neurotransmitters may be involved (Fovaeus et al, 1999). I found that in utero obstruction did not alter the percentage attenuation of the relaxations by ODQ in the *sham* and *obstructed* groups; this is similar to findings in the obstructed fetal sheep bladder (Levin et al, 2001) and obstructed rat bladder (Sutherland et al, 1998) but in contrast to mice models of bladder dysfunction (Burnett et al, 1997; Lemack et al, 1999). Interestingly, fetal bladder studies of the nitrergic system did not find concomitant relaxant forces in the adult bladder of the same species (Lee et al, 1994; Levin et al, 2001) so that these relaxant forces may be necessary for the protection of renal maturation during development.

The effect of the mucosa on nitrergic neurotransmission

The nitrergic system may be associated with the bladder urothelium (Birder et al, 1998). Force-frequency relations for *mucosal* bladder strips (corrected for wet weight of muscle) examined any effect of the urothelium and these were repeated in the presence of ODQ. I found that the urothelium significantly reduced the force developed by detrusor muscle strips and this reduction was partially reversed by ODQ, suggesting nitric oxide mediation. The partial effect of ODQ again may suggest other mediators are involved (Downie and Karmazyn, 1984; Hawthorn et al, 2000); it is also possible (Downie and Karmazyn, 1984) that the dampening effect of the mucosa may be due, at least in part, to a direct mechanical effect. The presence of mucosa in the *obstructed* fetal bladder strips did not decrease the force of contraction and ODQ had no effect. This suggests that any mediator released from the urothelium may not be released following in utero obstruction; this is consistent with my histological description of an attenuated urothelium and lamina propria after obstruction.

6.3.4 Filing cystometry

The normal *sham* bladder at 105 days gestation was a well-developed compliant organ with a mean capacity of 6.4 ml associated with an end-fill pressure of 10.6 cm H_2O. The bladders exhibited partial stress-relaxation with intermittent filling but with a steady-state increase of pressure after each volume increment. In order to quantify the elastic properties of the bladder wall, pressure values were converted to wall stress by use of the Laplace relation. Using this transform, wall stress increased linearly with increasing

volume at low volumes; at higher volumes, there was deviation from this linear behaviour indicating that the elastic limit had been reached.

Bladders from the *obstructed* group had increased capacity to 52 ml for the same low pressure, 12.2 cm H_2O, as the *sham* group. Steady-state pressures also increased in a curvilinear fashion with volume and stress-relaxation was observed during intermittent filling. Pressure versus volume plots demonstrated an increased compliance ($\Delta V/\Delta P$) in the *obstructed* bladder that was mirrored as a decreased elasticity in the wall stress versus volume plots. These observations are consistent with a large, flaccid organ that, not surprisingly, is consistent with the isolated muscle contractility results showing hypocontractility. It is of interest that the wall-stress versus volume plots showed that both the *sham* and *obstructed* bladders attained elastic limits but in *obstructed* bladders, it was at a lower pressure and was achieved at a considerably greater volume. It may be proposed, therefore, that exceeding the elastic limit (either chronically throughout the obstructive period or following the acute onset of BOO) may result in irreversible changes to the properties of the bladder wall, although this will occur at greatly different volumes in the normal and post-obstructed bladder. It is important to emphasise that these elastic properties were obtained from bladders with no neuronal input and thus reflect the physical properties of the bladder wall. Interestingly, Peters et al (1992b) also observed stress-relaxation during cystometry in their obstructed ovine fetal bladders. They noted that stress-relaxation was slowed in obstruction and they suggested this was due to decreased compliance of the bladder wall. Whilst there were similarities in the experimental model, the difference in results may be explained by differences in

cystometry methodology and in the methodological derivation of bladder wall compliance.

6.3.5 Biomechanical studies

These experiments were performed to measure the visco-elastic properties of the developing and obstructed fetal bladder. The purpose was two-fold: to complement the findings from filling cystometry that showed the *obstructed* fetal bladder was more compliant and exhibited less wall stress than the *sham* counterpart; and to examine whether the hypocontractile state of the obstructed bladder may in part result from a change to the passive visco-elastic properties of the bladder wall.

Linear steady-state stress-strain relationships were generated from which an elastic modulus was calculated. I found that in strips from *obstructed* bladders, elasticity was significantly smaller than in the *sham* counterparts, showing that the tissue was more flaccid and corroborated qualitatively the cystometry findings. A reduction of elastic modulus in a tissue strip would generate the appearance of a hypocontractile preparation as tension generated by the muscular elements would generate less tension in the whole preparation. Thus reduced contractile force in an isolated muscle strip or reduced wall stress in an intact bladder, upon activation by an agonist, may not reflect any derangement of muscle function but may be simply due to the relative inability of the extramuscular components within the *obstructed* detrusor muscle to sustain that force. This is generally overlooked when attempting to explain the causes of contractile failure and can explain the relative ineffectiveness of positive inotropic agents to reverse the

problem on occasion. This explanation is not the only cause for the hypocontractility of the *obstructed* fetal bladder as nerve-mediated force was reduced more than carbachol-mediated contraction and suggests partial denervation also contributed to the smaller nerve-evoked response. However, these two factors may be sufficient to explain the reduced contractility of the obstructed bladder without the necessity of evoking significant muscle failure. This corroborates other findings (Wu et al, 1999) that show little difference in the ability of isolated cells from normal and obstructed bladders to generate agonist-mediated intracellular Ca^{2+} transients.

However, an increase of the viscous component of the overall stress-strain relationship may also attenuate transient contractile responses, due to damping of the generated tension. For this reason, I quantified the viscous work as a proportion of total work during a step change of strain and found that this was unchanged in the *obstructed* bladders. This observation, coupled with the fact that the time constant of visco-elastic relaxation was also unaltered, suggests that the physical properties of the extracellular matrix are unchanged in the *obstructed* bladder (Wagg and Fry, 1999). Differences in muscle fibre arrangement and rates of preceding stretch can influence visco-elastic properties (Susset and Regnier, 1981); I therefore took strips from the same area of the bladder and maintained constant rates and magnitudes of stretch in all experiments to minimise these problems.

Clockwise and symmetrical steady-state hysteresis loops were recorded in muscle strips from *sham* and *obstructed* groups; this is a phenomenon characteristic of inert substances

such as rubber and not organic material such as the lung. This suggests that elastic elements will absorb energy when stretched, which is released in a non-elastic way when relaxed. As the elastic modulus (the tangent to the hysteresis loop) is not a constant but depends on the magnitude of stretch, constant magnitudes of stretch were used to calculate the elastic modulus above.

6.3.6 Radiotelemetered fetal cystometry

My preliminary studies of radiotelemetry fetal cystometry show that this technique is feasible in the experimental fetus without inducing mortality or morbidity or inhibition of growth. The one experiment that failed was because one of the catheters was of insufficient length and pulled out of the bladder during in utero growth; this could be overcome by using implants with longer catheters.

The method appeared to be useful for determining fetal detrusor pressure because there was excellent synchrony between bladder and abdominal pressures (thus allowing for detection of genuine detrusor activity) and reproducible types of bladder activity were discernible. By exporting data to Microsoft Excel, I was able to subtract the abdominal pressure activity from the vesical pressure activity to reveal detrusor pressure. During observation, I detected four voiding types: staccato activity, unstable type activity, immature voids (in the fetus of gestational age 75 to 105 days) and mature voids (in the fetuses of gestational ages 105 to 145 days). The latter type of voiding has also been observed by cystometry in the fetal sheep (Mevorach et al, 1994) and fetal pig (Olsen et al, 2001). In these published studies and during my observations, high frequency, low

amplitude activity was observed during voiding. It is not known what this activity represents but possibilities include a 'burst' type activity of the urethral sphincter (Olsen et al, 2001), a urethral pump mechanism (to aid detrusor voiding) and maturation of spinal interneuronal circuitry that co-ordinates bladder contraction (de Groat et al, 2001).

Maturational differences and sex differences appeared to be detected by radiotelemetry cystometry, although this requires greater investigation as observations were only made in three experiments. My preliminary observations suggest that from 75 days to 105 days gestation, voiding patterns change from an immature type (high frequency, low amplitude activity with no or minimal elevations in baseline pressure) to a mature type (high frequency, low amplitude activity with significant elevations in pressure) and associated events change from unstable type activity (very short, less than 5 seconds, elevations of pressure) to staccato activity (short, 20-40 seconds, phasic elevations of pressure). Furthermore, from 105 days to 145 days gestation, male fetal bladder mean voids per hour, mean maximum detrusor pressure and mean duration of void decreased, remained static and increased respectively. In contrast, during the same gestational age period, the same female bladder parameters decreased, increased and decreased respectively.

6.3.7 Sex differences

Despite the possible sex differences observed in fetal bladder cystometry, by radiotelemetry, there was no significant difference between the fetal weights and bladder weights in the *sham* male and *sham* female fetuses 30 days post-operation and only a small number of functional differences, ie. the significantly greater effect of adenosine on

reducing the nerve-mediated contraction and the prolonged time-constant during visco-elastic. The lack of sex differences may be surprising as male and female fetal bladders are exposed to different sex hormones during in utero development (Thomson et al, 2002) and sex differences have been observed during voiding function studies in human neonates (Hiraoka et al, 1999). Nonetheless, the lack of sex differences in the in vitro studies may be useful in planning future fetal bladder experiments.

6.4 Biological causes of fetal bladder hypocontractility

My results suggest a number of possibilities for the development of fetal bladder decompensation after in utero BOO. It is possible that proliferation of the fibroblast-like cells around the muscle bundles in the detrusor layer leads to increased extracellular matrix deposition in the detrusor muscle layer that results in a net reduction in muscle contractility. Increased apoptosis and the associated decrease in lamina propria density may prevent lamina propria function. As described by Baskin et al (Baskin et al, 2001), this may prevent normal bladder mesenchymal differentiation and result in a poorly developed muscle that contracts poorly. This speculation is supported by my observations of normal bladder maturation that suggests the after exposure to BOO, fetal bladder cell turnover shifts to a more embryonic pattern of high rates of proliferation and apoptosis, again resulting in a poorly contracting muscle. Finally, the combination of reduced innervation, increased compliance and decreased elasticity combine to inhibit detrusor muscle contractile function.

6.5 Ovine bladder maldevelopment and human in utero BOO

My thesis has documented a number of novel observations in the ovine fetal bladder after exposure to BOO. However, it is not known if such events occur in the human fetal bladder when obstructed. Such investigation is potentially feasible. The procurement of stored human fetal bladders (embedded sections and frozen samples) would allow the molecular studies I have used in my thesis to be investigated in normal and pathological human fetal bladder maturation; it would be of interest to determine whether such aberration to cell turnover occurs in the obstructed human fetal bladder. Physiological experiments, however, although theoretically possible, would be very difficult to perform in human fetal samples; the requirement to use tissue within 24 to 48 hours in my physiological experiments would make human fetal studies impractical and strengthens the argument for using experimental animal models to study fetal bladder pathophysiology.

It is of note that my results describe the changes that occur at one time point (105 days gestation) in the ovine fetal bladder after BOO. However, it is not known if my observations occur at different time points during fetal bladder maldevelopment and of particular relevance to human disease, whether such changes persist following intervention. Experimental models would also be useful in describing any beneficial effects of overcoming fetal BOO by in utero treatment. As described in the Introduction, the outcome of human in utero intervention remains equivocal. To overcome this, the effect of in utero bladder drainage in experimental models of fetal BOO has been explored. By decompressing the obstructed fetal ovine bladder, investigators have

described partial improvement to renal development (as assessed by glomeruli number and PAX2 expresssion) (Duncombe et al, 2002; Edouga et al, 2001). Such experiments to determine the potential benefit to bladder maldevelopment, to my knowledge, have not been performed in experimental models of BOO but would be of great clinical value; this sort of manipulation will be addressed in future studies.

6.6 Future strategies

My thesis has documented molecular and physiological changes to the fetal bladder after 30 days of in utero BOO and described preliminary experiments of fetal bladder radiotelemetry cystometry. Future work should address the following:

1) Mapping the pathophysiological progression of bladder dysfunction in the experimental model of in utero BOO by observing the changes to fetal bladder cystometry during the obstructive period.

2) Obtaining fetal bladder samples after shorter periods of obstruction to determine if the fetal bladder undergoes a compensatory period of hypertrophy, hyperplasia and hypercontractility prior to the hypocontractility observed in my thesis after 30 days of in utero BOO; the earlier time points could be guided by the radiotelemetry findings.

3) Deobstructing the obstructed fetal bladder during the compensatory phase (possibly by vesico-amniotic shunting) to assess, by molecular and physiological studies, if such a procedure will prevent future bladder dysfunction.

4) Assess contractile function in individual myocytes to test the hypothesis that contractile dysfunction arises from functional muscle cells in a poorly supporting matrix.

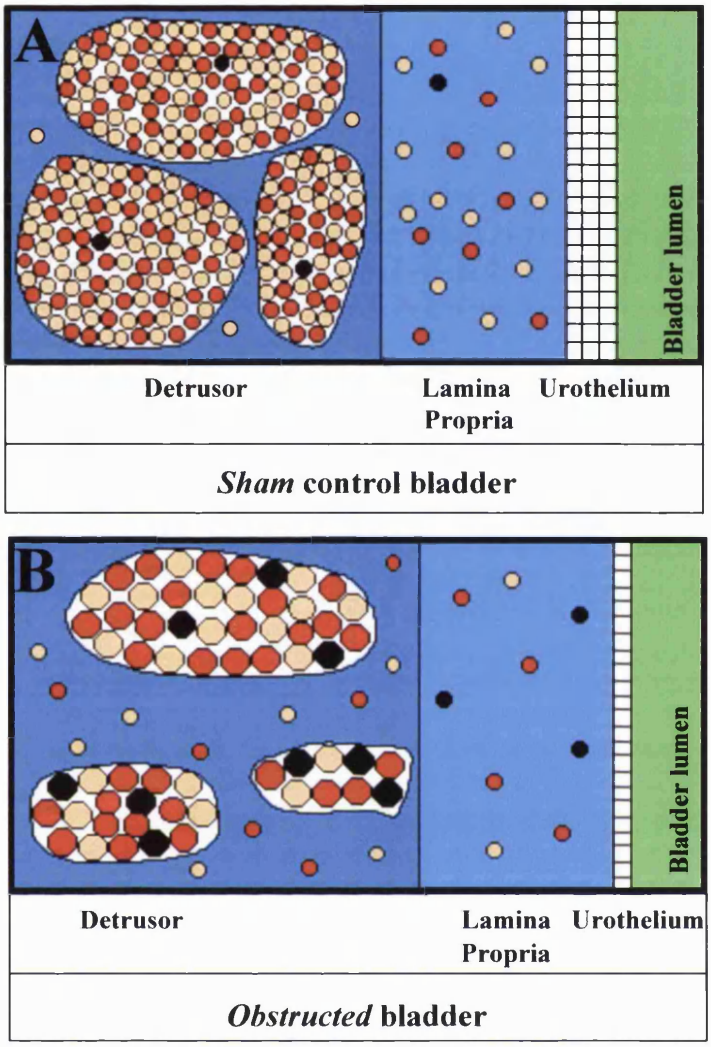

Figure 61. Cell turnover summary

A. *Sham* bladder, with proliferating (red) and apoptotic (black) cells within the detrusor and lamina propria layers. Yellow cells are non-proliferative and non-apoptotic. B. *Obstructed* bladder, with increase in proportions of proliferating and apoptotic cells in the detrusor layer and increase in apoptotic cells only in the lamina propria layer. Note also i. the larger SMC in the muscle bundles which are separated by widened spaces containing proliferating cells, ii. the lower cell density in the lamina propria and iii. the single-layered urothelium in the *obstructed* bladder.

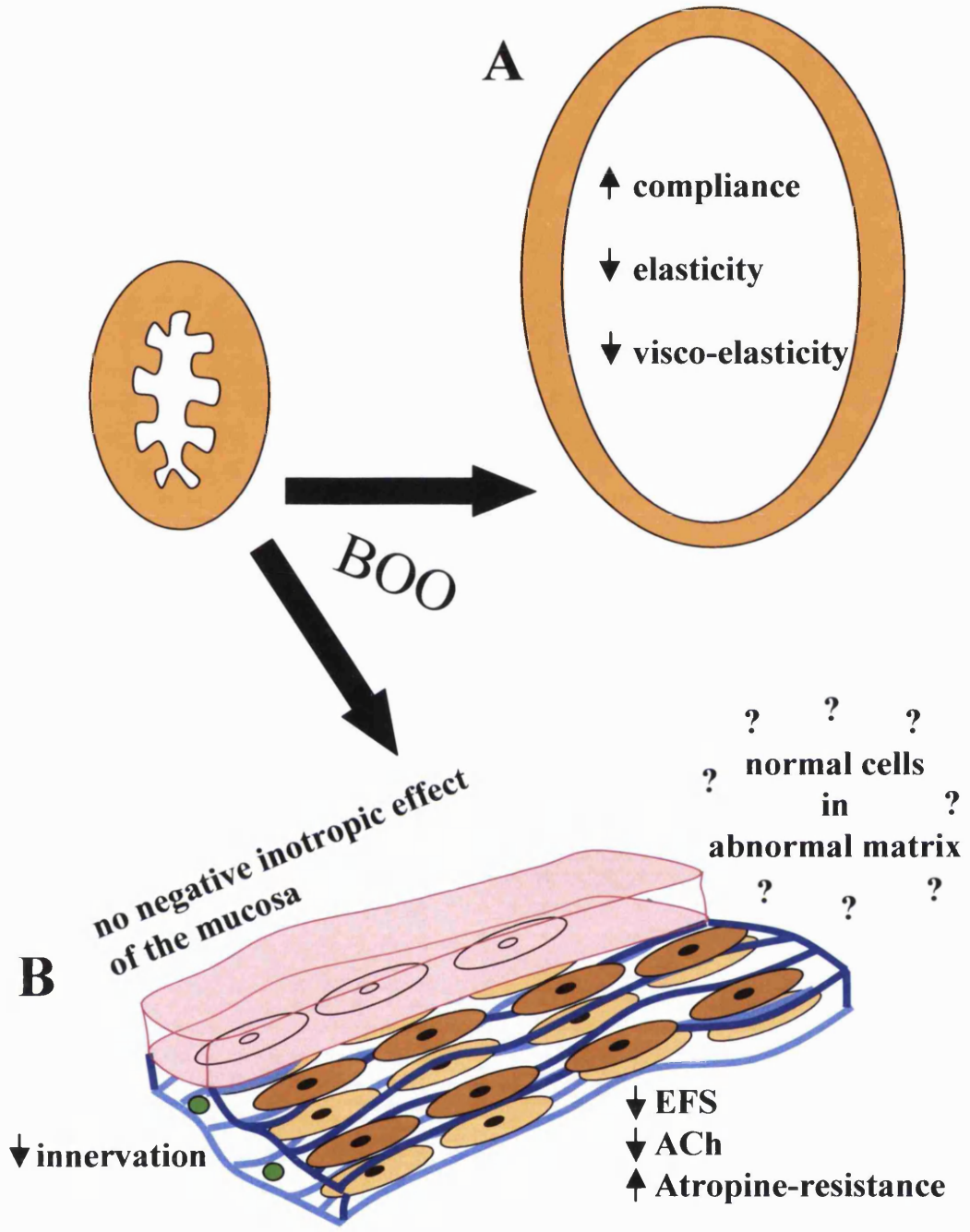

Figure 62. Physiology summary

After BOO, the fetal bladder became larger (A) and exhibited increased compliance and decreased elasticity and visco-elasticity. Contractility studies (B) reveal decreased responses to electrical filed stimulation (EFS) and acetyl choline (Ach). There appeared to be increased atropine-resistant contractions in the *obstructed* bladders. Although nitric-oxide mediated relaxation was present in the *obstructed* detrusor muscle, the nitric-oxide mediated negative inotropic effect of the mucosa was absent in full thickness bladder strips from the *obstructed* group. Decreased innervation (green) was also documented. One possible explanation for these results are that myocytes from *obstructed* bladders can contract normally but are supported by an abnormal supporting matrix.

7. Conclusion

In my thesis, I used a reproducible model of in utero BOO in the fetal sheep. Using bladders from this group, and as compared to sham control fetal bladders, I made a number of novel observations.

I found that the obstructed fetal bladder became larger and heavier and had grown; I found an increase in cellular proliferation and cellular apoptosis within the detrusor muscle layer and an increase of apoptosis only, within the lamina propria layers. This was accompanied by a downregulation of Bcl-2 and an upregulation Bax and activated caspase-3. I also found the obstructed fetal bladder became hypocontractile and denervated and exhibited greater atropine-resistant contractions. I also observed increased compliance and reduced elasticity and viscoelasticity in the obstructed fetal bladder.

My results suggest that enhanced apoptosis in detrusor smooth muscle cells was part of a remodelling response during compensatory hyperplasia and hypertrophy; in the lamina propria, an imbalance between death and proliferation, led to a relative depletion of cells. Furthermore, the obstructed fetal bladder became hypocontractile; in addition to denervation, this may result from a reduction in the elastic modulus that may prevent any extramuscular components from sustaining force, produced by the detrusor smooth muscle.

Finally, I was able to determine in vivo pressure relations of normal voiding in the fetal ovine bladder using novel radiotelemetry pressure-recording catheters. Future studies will

monitor the pathophysiological progression of in utero BOO using this method and determine the molecular and physiological changes in the fetal bladder after shorter periods of obstruction and in the 'deobstructed' obstructed fetal bladder.

8. References

Abbott JF, Levine D and Wapner R. 1998. Posterior urethral valves: inaccuracy of prenatal diagnosis. *Fetal Diagn Ther*, **13** 179-183.

Adzick NS, Harrison MR, Glick PL and Flake AW. 1985. Fetal urinary tract obstruction: experimental pathophysiology. *Semin Perinatol* **9** 79-90.

Agarwal SK and Fisk NM. 2001. In utero therapy for lower urinary tract obstruction. *Prenat Diagn.***21** 970-976.

Anderson KE. 1993. Pharmacology of lower urinary tract smooth muscles and penile erectile tissues. *Pharmacol Rev* **45** 253-308.

Andersson KE and Persson K. 1995. Nitric oxide synthase and the lower urinary tract: possible implications for physiology and pathophysiology. *Scand J Urol Nephrol Suppl* **175** 43-53.

Arens YH, Rosenfeld CR and Kamm KE. 2000. Maturational differences between vascular and bladder smooth muscle during ovine development. *Am J Physiol Regul Integr Comp Physiol* **278** R1305-R1313.

Attar R, Quinn F, Winyard PJ, Mouriquand PD, Foxall P, Hanson MA and Woolf AS. 1998. Short-term urinary flow impairment deregulates PAX2 and PCNA expression and cell survival in fetal sheep kidneys. *Am J Pathol* **152** 1225-1235.

Bancroft D and Cook HC. 1994. *Manual of Histological Techniques and Their Diagnostic Application.* Churchill Livingstone, Edinburgh, UK.

Baskin L, DiSandro M, Li Y, Li W, Hayward S and Cunha, G. 2001. Mesenchymal-epithelial interactions in bladder smooth muscle development: effects of the local tissue environment. *J Urol* **165** 1283-1288.

Baskin L, Howard PS and Macarak E. 1993a. Effect of physical forces on bladder smooth muscle and urothelium. *J Urol* **150** 601-607.

Baskin LS, Howard PS, Duckett JW, Snyder HM and Macarak E. 1993b. Bladder smooth muscle cells in culture: I. Identification and characterization. *J Urol* **149** 190-197.

Baskin L, Meaney D, Landsman A, Zderic SA and Macarak E. 1994a. Bovine bladder compliance increases with normal fetal development. *J Urol* **152** 692-695.

Baskin LS, Constantinescu S, Duckett JW, Snyder HM and Macarak E. 1994b. Type III collagen decreases in normal fetal bovine bladder development. *J Urol* **152** 688-691.

Baskin LS, Hayward SW, Young PF and Cunha GR. 1996a. Ontogeny of the rat bladder: smooth muscle and epithelial differentiation. *Acta Anat* **155** 163-171.

Baskin LS, Sutherland RS, Thomson AA, Hayward SW and Cunha GR. 1996b. Growth factors and receptors in bladder development and obstruction. *Lab Invest* **75** 157-166.

Bassuk JA, Grady R and Mitchell M. 2000. Review article: The molecular era of bladder research. Transgenic mice as experimental tools in the study of outlet obstruction. *J Urol* **164** 170-179.

Baudier J, Glasser N and Gerard D. 1986. Ions binding to S100 proteins. *J Biol Chem* **261** 8192-8203.

Bauer SB, Dieppa RA, Labib KK and Retik AB. 1979. The bladder in boys with posterior urethral valves: a urodynamic assessment. *J Urol* **121** 769-773.

Bayliss M, Wu C, Newgreen D, Mundy AR and Fry CH. 1999. A quantitative study of atropine-resistant contractile responses in human detrusor smooth muscle, from stable, unstable and obstructed bladders. *J Urol* **162** 1833-1839.

Beck AD. 1971. The effect of intra-uterine urinary obstruction upon the development of the fetal kidney. *J Urol* **105** 784-789.

Bellinger MF, Ward RM, Boal DK, Zaino RJ, Sipio JC and Wood MA. 1986. Renal function in the fetal lamb: a chronic model to study physiological effects of ureteral ligation and deligation. *J Urol* **136** 225-228.

Bennett BC, Kruse MN, Roppolo JR, Flood HD, Fraser M and de Groat WC. 1995. Neural control of urethral outlet activity in vivo: role of nitric oxide. *J Urol* **153** 2004-2009.

Birder LA, Apodaca G, de Groat WC and Kanai AJ. 1998. Adrenergic and capsaicinevoked nitric oxide release from urothelium and afferent nerves in urinary bladder. *Am J Physiol* **275** F226-F229.

Bogaert GA, Mevorach RA and Kogan BA 1994. Renal hemodynamic and functional effects of 10 days' partial urinary obstruction in the fetal lamb. *J Urol* **152** 220-225.

Bourdelat D, Husson S, Soisic F and Vrsansky P. 1998. Embryological study of the mechanism of antenatal lower urinary tract obstruction. *Ann Urol* **32** 253-268.

Brading AF and Inoue R. 1991. Ion channels and excitatory transmission in the smooth muscle of the urinary bladder. *Z Kardiol* **80** 47-53.

Brent L and Stephens FD. 1975. The response of smooth muscle cells in the rabbit urinary bladder to outflow obstruction. *Invest Urol* **12** 494-502.

Bridgewater M, MacNeil HF and Brading AF. 1993. Regulation of tone in pig urethral smooth muscle. *J Urol* **150** 223-228.

Brockes JP and Hall ZW. 1975. Synthesis of acetylcholine receptor by denervated rat diaphragm muscle. *Proc Natl Acad Sci USA* **72** 1368-1372.

Burnett AL, Calvin DC, Chamness SL, Liu JX, Nelson RJ, Klein SL, Dawson VL, Dawson TM and Snyder SH. 1997. Urinary bladder-urethral sphincter dysfunction in mice with targeted disruption of neuronal nitric oxide synthase models idiopathic voiding disorders in humans. *Nat Med* **3** 571-574.

Burnstock G, Cocks T, Crowe R and Kasakov L. 1978. Purinergic innervation of the guinea-pig urinary bladder. *Br J Pharmacol* **63** 125-138.

Burton PB, Anderson CJ and Corbishly CM. 2000. Caspase 3 and p27 as predictors of invasive bladder cancer. *N Engl J Med* **343** 1418-1420.

Cale CM, Klein NJ, Morgan G and Woolf AS. 1998. Tumor necrosis factor-α inhibits epithelial differentiation and morphogenesis in the mouse metanephric kidney in vitro. *Int J Dev Biol* **42** 663-674.

Callan NA, Blakemore K, Park J, Sanders RC, Jeffs RD and Gearhart JP. 1990. Fetal genitourinary tract anomalies: evaluation, operative correction, and follow-up. *Obstet Gynecol* **75** 67-74.

Carr MC, Schlussel RN, Peters CA, Uchida T, Mandell J and Freeman MR. 1995. Expression of cell growth regulated genes in the fetal kidney: relevance to in utero obstruction. *J Urol* **154** 242-246.

Celayir S, Ilce Z and Dervisoglu S. 2002. The sex hormone receptors in the bladder in childhood. *Eur J Pediatr Surg* **12** 312-317.

Cendron M, Horton CE, Karim OM, Takishima H, Haberlik A, Mostwin JL and Gearhart JP. 1994. A fetal lamb model of partial urethral obstruction: experimental protocol and results. *J Pediatr Surg* **29** 77-80.

Chevalier RL, Smith CD, Wolstenholme J, Krajewski S and Reed JC. 2000. Chronic ureteral obstruction in the rat suppresses renal tubular Bcl-2 and stimulates apoptosis. *Exp Nephrol* **8** 115-122.

Chiavegato A, Scatena M, Roelofs M, Ferrarese P, Pauletto P, Passerini-Glazel G, Pagano F and Sartore S. 1993. Cytoskeletal and cytocontractile protein composition of smooth muscle cells in developing and obstructed rabbit bladder. *Exp Cell Res* **207** 310-320.

Chuang YH, Chuang WL, Huang SP and Huang CH. 2002. Over-expression of apoptosis-related proteins contributes to muscular damage in the obstructed ureter of the rat. *BJU Int* **89** 106-112.

Chueh SC, Guh JH, Chen J, Lai MK and Teng CM. 2001. Dual effects of ouabain on the regulation of proliferation and apoptosis in human prostatic smooth muscle cells. *J Urol* **166** 347-353.

Coles HS, Burne JF and Raff MC. 1993. Large-scale normal cell death in the developing rat kidney and its reduction by epidermal growth factor. *Development* **118** 777-784.

Coplen DE, Macarak EJ and Levin RM. 1994. Developmental changes in normal fetal bovine whole bladder physiology. *J Urol* **151** 1391-1395.

Cortivo R, Pagano F, Passerini G, Abatangelo G and Castellani I. 1981. Elastin and collagen in the normal and obstructed urinary bladder. *Br J Urol* **53** 134-137.

Creed KE, Callahan SM and Ito Y. 1994. Excitatory neurotransmission in the mammalian bladder and the effects of suramin. *Br J Urol* **74** 736-743.

Crowe A, Cairns HS, Wood S, Rudge CJ, Woodhouse CR and Neild GH. 1998. Renal transplantation following renal failure due to urological disorders. *Nephrol Dial Transplant* **13** 2065-2069.

Crowe R and Burnstock G. 1989. A histochemical and immunohistochemical study of the autonomic innervation of the lower urinary tract of the female pig. Is the pig a good model for the human bladder and urethra? *J Urol* **141** 414-422.

Cuckow PM. 1998. Posterior urethral valves. In *Pediatric Surgery and Urology: Long Term Outcomes.* Stringer MD, Oldham KT, Mouriquand PDE and Howard ER. WB Saunders, London. 487-500.

Cuckow PM, Dinneen MD, Risdon RA, Ransley PG and Duffy PG. 1997. Long-term renal function in the posterior urethral valves, unilateral reflux and renal dysplasia syndrome. *J Urol* **158** 1004-1007.

Cuckow PM, Nyirady P and Winyard PJ. 2001. Normal and abnormal development of the urogenital tract. *Prenat Diagn* **21** 908-916.

Cumming JA and Chisholm GD. 1992. Changes in detrusor innervation with relief of outflow tract obstruction. *Br J Urol* **69** 7-11.

Dalmose AL, Hvistendahl JJ, Olsen LH, Eskild-Jensen A, Djurhuus JC and Swindle MM. 2000. Surgically induced urologic models in swine. *J Invest Surg* **13** 133-145.

Datta SR, Dudek H, Tao X, Masters S, Fu H, Gotoh Y and Greenberg ME. 1997. Akt phosphorylation of BAD couples survival signals to the cell- intrinsic death machinery. *Cell* **91** 231-241.

Davies J. 1951. Nephric development in the sheep with reference to the problem of the ruminant pronephros. *J Anat* **85** 6-11.

De Gennaro M, Capitanucci ML, Capozza N, Caione P, Mosiello G and Silveri M. 1998. Detrusor hypocontractility in children with posterior urethral valves arises before puberty. *Br J Urol* **81** 81-85.

De Gennaro M, Capitanucci ML, Mosiello G, Caione P and Silveri M. 2000. The changing urodynamic pattern from infancy to adolescence in boys with posterior urethral valves. *BJU Int* **85** 1104-1108.

de Groat WC. 1990. Central neural control of the lower urinary tract. *Ciba Found.Symp* **151** 27-44.

de Groat WC, Fraser MO, Yoshiyama M, Smerin S, Tai C, Chancellor MB, Yoshimura N and Roppolo JR. 2001. Neural control of the urethra. *Scand J Urol Nephrol Suppl* **207** 35-43.

De La Rosette J, Smedts F, Schoots C, Hoek H and Laguna P. 2002. Changing patterns of keratin expression could be associated with functional maturation of the developing human bladder. *J Urol* **168** 709-717.

Dean GE, Cargill RS, Macarak E, Snyder HM, Duckett JW and Levin R. 1997. Active and passive compliance of the fetal bovine bladder. *J Urol* **158** 1094-1099.

Deveaud CM, Macarak EJ, Kucich U, Ewalt DH, Abrams WR and Howard PS. 1998. Molecular analysis of collagens in bladder fibrosis. *J Urol* **160** 1518-1527.

Dixon JS, Jen PY and Gosling JA. 1998. Immunohistochemical characteristics of human paraganglion cells and sensory corpuscles associated with the urinary bladder. A developmental study in the male fetus, neonate and infant. *J Anat* **192** 407-415.

Downie JW and Karmazyn M. 1984. Mechanical trauma to bladder epithelium liberates prostanoids which modulate neurotransmission in rabbit detrusor muscle. *J Pharmacol Exp Ther* **230** 445-449.

Duncombe GJ, Barker AP, Moss TJ, Gurrin LC, Charles AK, Smith NM and Newnham JP. 2002. The effects of overcoming experimental bladder outflow obstruction in fetal sheep. *J Matern Fetal Med* **11** 130-137.

Eaton AC and Bates CP. 1982. An in vitro physiological study of normal and unstable human detrusor muscle. *Br J Urol* **54** 653-657.

Edouga D, Hugueny B, Gasser B, Bussieres L and Laborde K. 2001. Recovery after relief of fetal urinary obstruction: morphological, functional and molecular aspects. *Am J Physiol Renal Physiol* **281** F26-F37.

El Ghoneimi A, Desgrippes A, Luton D, Macher MA, Guibourdenche J, Garel C, Muller F, Vuillard E, Lottmann H, Nessmann C, Oury JF and Aigrain Y. 1999. Outcome of posterior urethral valves: to what extent is it improved by prenatal diagnosis? *J Urol* **162** 849-853.

Elneil S, Skepper JN, Kidd EJ, Williamson JG and Ferguson DR. 2001. Distribution of P2x(1) and P2x(3) receptors in the rat and human urinary bladder. *Pharmacology* **63** 120-128.

Emir H, Eroglu E, Tekant G, Buyukunal C, Danismend N and Soylet Y. 2002. Urodynamic findings of posterior urethral valve patients. *Eur J Pediatr Surg* **12** 38-41.

Erdogru T, Gulkesen KH, Kukul E, Yalcinkaya M, Karpuzoglu G and Baykara M. 2002. Increased Bladder Apoptosis with alpha-1 Adrenoceptor Antagonists in Benign Prostatic Hyperplasia. *Scand J Urol Nephrol* **36** 188-193.

Erman A, Jezernik K, Stiblar-Martincic D, Romih R and Veranic P. 2001. Postnatal restoration of the mouse urinary bladder urothelium. *Histochem Cell Biol* **115** 309-316.

Fadeel B, Zhivotovsky B and Orrenius S. 1999. All along the watchtower: on the regulation of apoptosis regulators. *FASEB J* **13** 1647-1657.

Fovaeus M, Fujiwara M, Hogestatt ED, Persson K and Andersson KE. 1999. A non-nitrergic smooth muscle relaxant factor released from rat urinary bladder by muscarinic receptor stimulation. *J Urol* **161** 649-653.

Freedman AL, Johnson MP, Smith CA, Gonzalez R and Evans MI. 1999. Long-term outcome in children after antenatal intervention for obstructive uropathies. *Lancet* **354** 374-377.

Freedman AL, Qureshi F, Shapiro E, Lepor H, Jacques SM, Evans MI, Smith CA, Gonzalez R and Johnson MP. 1997. Smooth muscle development in the obstructed fetal bladder. *Urology* **49** 104-107.

Fry CH and Wu C. 1998. The cellular basis of bladder instability. *Br J Urol* **81** 1-8.

Galvin DJ, Watson RW, Gillespie JI, Brady H and Fitzpatrick JM. 2002. Mechanical stretch regulates cell survival in human bladder smooth muscle cells in vitro. *Am J Physiol Renal Physiol* **283** F1192-F1199.

Garthwaite J, Southam E, Boulton CL, Nielsen EB, Schmidt K and Mayer B. 1995. Potent and selective inhibition of nitric oxide-sensitive guanylyl cyclase by 1H-[1,2,4]oxadiazolo[4,3-a]quinoxalin-1-one. *Mol Pharmacol* **48** 184-188.

Gavrieli Y, Sherman Y and Ben Sasson SA. 1992. Identification of programmed cell death in situ via specific labeling of nuclear DNA fragmentation. *J Cell Biol* **119** 493-501.

George NJR. 2001. Bladder and urethra: function and dysfunction. In *Comprehensive Urolog.* Weiss RM, George NJR, O'Reilly PH. Mosby, London. 67-79.

Ghafar MA, Anastasiadis AG, Olsson LE, Chichester P, Kaplan SA, Buttyan R and Levin RM. 2002. Hypoxia and an angiogenic response in the partially obstructed rat bladder. *Lab Invest* **82** 903-909.

Gobe G and Harmon B. 2001. Apoptosis: morphological criteria and other assays. In *Encyclopedia of Life Sciences.* Atlas RM, Bynum UF, Cox MM, Delves PJ, Gilbert SF, Matsudaira PT, Roberts JW, Roberts K, Roitt I, Silverton JW and Wood BA. Nature Publishing Group, London. 1-6.

Gobet R, Bleakley J, Cisek L, Kaefer M, Moses MA, Fernandez CA and Peters CA. 1999a. Fetal partial urethral obstruction causes renal fibrosis and is associated with proteolytic imbalance. *J Urol* **162** 854-860.

Gobet R, Park JM, Nguyen HT, Chang B, Cisek LJ and Peters CA. 1999b. Renal renin-angiotensin system dysregulation caused by partial bladder outlet obstruction in fetal sheep. *Kidney Int* **56** 1654-1661.

Golbus MS, Harrison MR, Filly RA, Callen PW and Katz M. 1982. In utero treatment of urinary tract obstruction. *Am J Obstet Gynecol* **142** 383-388.

Gosling JA and Dixon JS. 1975. The structure and innervation of smooth muscle in the wall of the bladder neck and proximal urethra. *Br J Urol* **47** 549-558.

Gosling JA, Dixon JS and Jen PY. 1999. The distribution of noradrenergic nerves in the human lower urinary tract. A review. *Eur Urol* **36** Suppl 1 23-30.

Gosling JA, Gilpin SA, Dixon JS and Gilpin CJ. 1986. Decrease in the autonomic innervation of human detrusor muscle in outflow obstruction. *J Urol* **136** 501-504.

Groenewegen AA, Sukhai RN, Nauta J, Scholtmeyer RJ and Nijman RJ. 1993. Results of renal transplantation in boys treated for posterior urethral valves. *J Urol* **149** 1517-1520.

Guan Z, Kiruluta G, Coolsaet B and Elhilali M. 1994. Conscious minipig model for evaluating the lower urinary tract. *Neurourol Urodyn* **13** 147-158.

Gulbenkian S, Wharton J and Polak JM. 1987. The visualisation of cardiovascular innervation in the guinea pig using an antiserum to protein gene product 9.5 (PGP 9.5). *J Auton Nerv Syst* **18** 235-247.

Harlow E and Lane D. 1988. *Antibodies: A Laboratory Manual.* Cold Harbor Spring Laboratory Press, Cold Harbor Spring, NY, USA. 471-510.

Harrison MR, Ross N, Noall R and de Lorimier AA. 1983. Correction of congenital hydronephrosis in utero. I. The model: fetal urethral obstruction produces hydronephrosis and pulmonary hypoplasia in fetal lambs. *J Pediatr Surg* **18** 247-256.

Harrison SC, Hunnam GR, Farman P, Ferguson DR and Doyle PT. 1987. Bladder instability and denervation in patients with bladder outflow obstruction. *Br J Urol* **60** 519-522.

Harvey RA, Skennerton DE, Newgreen D and Fry CH. 2002. The contractile potency of adenosine triphosphate and ecto-adenosine triphosphatase activity in guinea pig detrusor and detrusor from patients with a stable, unstable or obstructed bladder. *J Urol* **168** 1235-1239.

Hata T and Deter RL. 1992. A review of fetal organ measurements obtained with ultrasound: normal growth. *J Clin Ultrasound* **20** 155-174.

Hawthorn MH, Chapple CR, Cock M and Chess-Williams R. 2000. Urothelium-derived inhibitory factor(s) influences on detrusor muscle contractility in vitro. *Br J Pharmacol* **129** 416-419.

Hayashi M and Araki T. 2002. Caspase in renal development. *Nephrol Dial Transplant* **17** Suppl 9 8-10.

Hendren WH. 1971. Posterior urethral valves in boys. A broad clinical spectrum. *J.Urol* **106** 298-307.

Herndon CD, Ferrer FA, Freedman A and McKenna PH. 2000. Consensus on the prenatal management of antenatally detected urological abnormalities. *J Urol* **164** 1052-1056.

Hiraoka M, Hori C, Tsukahara H, Kasuga K, Kotsuji F and Mayumi M. 1999. Voiding function study with ultrasound in male and female neonates. *Kidney Int* **55** 1920-1926.

Holmdahl G. 1997. Bladder dysfunction in boys with posterior urethral valves. *Scand J Urol Nephrol* **188** 1-36.

Holmes N, Harrison MR and Baskin LS. 2001. Fetal surgery for posterior urethral valves: long-term postnatal outcomes. *Pediatrics* **108** E7.

Holmquist F, Lundin S, Larsson B, Hedlund H and Andersson KE. 1991. Studies on binding sites, contents, and effects of AVP in isolated bladder and urethra from rabbits and humans. *Am J Physiol* **261** R865-R874.

Hutton KA, Thomas DF and Davies BW. 1997. Prenatally detected posterior urethral valves: qualitative assessment of second trimester scans and prediction of outcome. *J Urol* **158** 1022-1025.

Irwin BH and Vane DW. 2000. Complications of intrauterine intervention for treatment of fetal obstructive uropathy. *Urology* **55** 774.

Jacobson MD, Weil M and Raff MC. 1997. Programmed cell death in animal development. *Cell* **88** 347-354.

Jennings RW. 2000. Prune belly syndrome. *Semin.Pediatr Surg* **9** 115-120.

Jezernik K, Sterle M and Batista U. 1997. The distinct steps of cell detachment during development of mouse uroepithelial cells in the bladder. *Cell Biol Int* **21** 1-6.

Karim OM, Cendron M, Mostwin JL and Gearhart JP. 1993. Developmental alterations in the fetal lamb bladder subjected to partial urethral obstruction in utero. *J Urol* **150**1060-1063.

Kerr JF, Wyllie AH and Currie AR. 1972. Apoptosis: a basic biological phenomenon with wide-ranging implications in tissue kinetics. *Br J Cancer* **26** 239-257.

Khan MA, Thompson CS, Calvert RC, Mikhailidis DP and Morgan RJ. 2002. Decreased urinary bladder apoptosis in a rabbit model of diabetes mellitus. *Urol Res* **30** 79-83.

Kim KM, Kogan BA, Massad CA and Huang YC. 1991a. Collagen and elastin in the normal fetal bladder. *J Urol***146** 524-527.

Kim KM, Kogan BA, Massad CA and Huang YC. 1991b. Collagen and elastin in the obstructed fetal bladder. *J Urol* **146** 528-531.

Kim YH, Horowitz M, Combs A, Nitti VW, Libretti D and Glassberg, KI. 1996. Comparative urodynamic findings after primary valve ablation, vesicostomy or proximal diversion. *J Urol* **156** 673-676.

King ED, Matteson J, Jacobs SC and Kyprianou N. 1996. Incidence of apoptosis, cell proliferation and bcl-2 expression in transitional cell carcinoma of the bladder: association with tumor progression. *J.Urol* **155** 316-320.

Kogan BA and Iwamoto HS. 1989. Lower urinary tract function in the sheep fetus: studies of autonomic control and pharmacologic responses of the fetal bladder. *J Urol* **141** 1019-1024.

Koo HP, Howard PS, Chang SL, Snyder HM, Ducket JW and Macarak EJ. 1997. Developmental expression of interstitial collagen genes in fetal bladders. *J Urol* **158** 954-961.

Koo HP, Macarak EJ, Chang SL, Rosenbloom J and Howard PS. 1998. Temporal expression of elastic fiber components in bladder development. *Connect Tissue Res* **37** 1-11.

Koo HP, Macarak EJ, Zderic SA, Duckett JW, Synder HM and Levin RM. 1995. The ontogeny of bladder function in the fetal calf. *J Urol* **154** 283-287.

Krueger RP, Hardy BE and Churchill BM. 1980. Growth in boys and posterior urethral valves. Primary valve resection vs upper tract diversion. *Urol Clin North Am* **7** 265-272.

Kulig E, Jin L, Qian X, Horvath E, Kovacs K, Stefaneanu L, Scheithauer BW and Lloyd RV. 1999. Apoptosis in nontumorous and neoplastic human pituitaries: expression of the Bcl-2 family of proteins. *Am J Pathol* **154** 767-774.

Kurita T, Wang YZ, Donjacour AA, Zhao C, Lydon JP, O'Malley BW, Isaacs JT, Dahiya R and Cunha GR. 2001. Paracrine regulation of apoptosis by steroid hormones in the male and female reproductive system. *Cell Death Differ* **8** 192-200.

Laemmli UK. 1970. Cleavage of structural proteins during the assembly of the head of bacteriophage T4. *Nature* **227** 680-685.

Larson WJ. 2001. *Human Embryology.* 3rd edn, Churchill Livingstone, New York.

Lee JG, Coplen D, Macarak E, Wein AJ and Levin RM. 1994. Comparative studies on the ontogeny and autonomic responses of the fetal calf bladder at different stages of development: involvement of nitric oxide on field stimulated relaxation. *J Urol* **151** 1096-1101.

Lemack GE, Burkhard F, Zimmern PE, McConnell JD and Lin VK. 1999. Physiologic sequelae of partial infravesical obstruction in the mouse: role of inducible nitric oxide synthase. *J Urol* **161** 1015-1022.

Levin RM, Macarak E, Howard P, Horan P and Kogan BA. 2001. The response of fetal sheep bladder tissue to partial outlet obstruction. *J Urol* **166** 1156-1160.

Levy BJ and Wight TN. 1990. Structural changes in the aging submucosa: new morphologic criteria for the evaluation of the unstable human bladder. *J Urol* 1044-1055.

Lewis M. 1999. Report of the paediatric renal registry. In *The UK Renal registry. The second annual report.* Ansell D and Feest T. 175-187.

Li QJ, Pazdera TM and Minden JS. 1999. Drosophila embryonic pattern repair: how embryos respond to cyclin E- induced ectopic division. *Development* **126** 2299-2307.

Liapis H, Yu H and Steinhardt GF. 2000. Cell proliferation, apoptosis, Bcl-2 and Bax expression in obstructed opossum early metanephroi. *J Urol* **164** 511-517.

Lichnovsky V, Erdosova B, Punkt K and Zapletal M. 1999. Expression of BCL-2 in the developing kidney of human embryos and fetuses qualitative and quantitative study. *Acta Univ Palacki Olomuc Fac Med* **142** 61-64.

Lin VK, Robertson JB, Lee IL, Zimmern PE and McConnell JD. 2000. Smooth muscle myosin heavy chains are developmentally regulated in the rabbit bladder. *J Urol* **164** 1376-1380.

Lluel P, Barras M and Palea S. 2002. Cholinergic and purinergic contribution to the micturition reflex in conscious rats with long-term bladder outlet obstruction. *Neurourol Urodyn* **21** 142-153.

Lopez PP, Martinez Urrutia MJ, Espinosa L, Lobato R, Navarro M and Jaureguizar E. 2002. Bladder dysfunction as a prognostic factor in patients with posterior urethral valves. *BJU Int* **90** 308-311.

Malkowicz SB, Wein AJ, Elbadawi A, Van Arsdalen K, Ruggieri MR and Levin RM. 1986. Acute biochemical and functional alterations in the partially obstructed rabbit urinary bladder. *J Urol* **136** 1324-1329.

Mandell J, Lebowitz RL, Peters CA, Estroff JA, Retik AB, Benacerraf BR. 1992. Prenatal diagnosis of the megacystis-megaureter association. *J Urol* **148** 1487-1489.

Martin R, Fraile B, Peinado F, Arenas MI, Elices M, Alonso L, Paniagua R, Martin JJ and Santamaria L. 2000. Immunohistochemical localization of protein gene product 9.5, ubiquitin, and neuropeptide Y immunoreactivities in epithelial and neuroendocrine cells from normal and hyperplastic human prostate. *J Histochem Cytochem* **48** 1121-1130.

Matsell DG, Mok A and Tarantal AF. 2002. Altered primate glomerular development due to in utero urinary tract obstruction. *Kidney Int* **61** 1263-1269.

Matsell DG and Tarantal AF. 2002. Experimental models of fetal obstructive nephropathy. *Pediatr Nephrol* **17** 470-476.

McHugo J and Whittle M. 2001. Enlarged fetal bladders: aetiology, management and outcome. *Prenat Diagn* **21** 958-963.

Mevorach RA, Bogaert GA and Kogan BA. 1994. Role of nitric oxide in fetal lower urinary tract function. *J Urol* **152** 510-514.

Mills IW, Noble JG and Brading AF. 2000. Radiotelemetered cystometry in pigs: validation and comparison of natural filling versus diuresis cystometry. *J Urol* **164** 1745-1750.

Misao J, Hayakawa Y, Ohno M, Kato S, Fujiwara T and Fujiwara H. 1996. Expression of bcl-2 protein, an inhibitor of apoptosis, and Bax, an accelerator of apoptosis, in ventricular myocytes of human hearts with myocardial infarction. *Circulation* **94** 1506-1512.

Miyajima A, Chen J, Lawrence C, Ledbetter S, Soslow RA, Stern J, Jha S, Pigato J, Lemer ML, Poppas DP, Vaughan ED and Felsen D. 2000. Antibody to transforming growth factor-beta ameliorates tubular apoptosis in unilateral ureteral obstruction. *Kidney Int* **58** 2301-2313.

Miyake H, Hara I, Hara S, Arakawa S and Kamidono S. 2000. Synergistic chemosensitization and inhibition of tumor growth and metastasis by adenovirus-mediated P53 gene transfer in human bladder cancer model. *Urology* **56** 332-336.

Moon A. 2002. Influence of nitric oxide signalling pathways on pre-contracted human detrusor smooth muscle in vitro. *BJU Int* **89** 942-949.

Moritz KM and Wintour EM. 1999. Functional development of the meso- and metanephros. *Pediatr Nephrol* **13** 171-178.

Nagata S. 1994. Apoptosis regulated by a death factor and its receptor: Fas ligand and Fas. *Philos Trans R Soc Lond B Biol Sci* **345** 281-287.

Namba R, Pazdera TM, Cerrone RL and Minden JS. 1997. Drosophila embryonic pattern repair: how embryos respond to bicoid dosage alteration. *Development* **124** 1393-1403.

Newman J and Antonakopoulos GN. 1989. The fine structure of the human fetal urinary bladder. Development and maturation. A light, transmission and scanning electron microscopic study. *J Anat* **166**135-150.

Nicholls J, Hourani SM and Kitchen I. 1992. Characterization of P1-purinoceptors on rat duodenum and urinary bladder. *Br J Pharmacol* **105** 639-642.

Nicholson DW and Thornberry NA. 1997. Caspases: killer proteases. *Trends Biochem Sci* **22** 299-306.

Nishimura H, Yerkes E, Hohenfellner K, Miyazaki Y, Ma J, Hunley TE, Yoshida H, Ichiki T, Threadgill D, Phillips JA, Hogan BM, Fogo A, Brock JW, Inagami T and Ichikawa I. 1999. Role of the angiotensin type 2 receptor gene in congenital anomalies of the kidney and urinary tract, CAKUT, of mice and men. *Mol Cell* **3** 1-10.

Oliveira EA, Diniz JS, Cabral AC, Pereira AK, Leite HV, Colosimo EA and Vilasboas AS. 2000. Predictive factors of fetal urethral obstruction: a multivariate analysis. *Fetal Diagn Ther* **15** 180-186.

Olsen LH, Dalmose AL, Swindle MM, Jorgensen TM and Djurhuus JC. 2001. Male fetal pig lower urinary tract function in mid second and early third trimester of gestation. *J Urol***165** 2331-2334.

Oltvai ZN, Milliman CL and Korsmeyer SJ. 1993. Bcl-2 heterodimerizes in vivo with a conserved homolog, Bax, that accelerates programmed cell death. *Cell* **74** 609-619.

Orsola A, Adam RM, Peters CA and Freeman MR. 2002. The decision to undergo DNA or protein synthesis is determined by the degree of mechanical deformation in human bladder muscle cells. *Urology* **59** 779-783.

Osterhage HR. 1981. Effect of urethral stenoses on the urinary tract. *Fortschr Med* **99** 824-828.

Palfrey EL, Fry CH and Shuttleworth KE. 1984. A new in vitro microsuperfusion technique for investigation of human detrusor muscle. *Br J Urol* **56** 635-640.

Park JM, Borer JG, Freeman MR and Peters CA. 1998. Stretch activates heparin-binding EGF-like growth factor expression in bladder smooth muscle cells. *Am J Physiol* **275** C1247-C1254.

Park JM, Yang T, Arend LJ, Smart AM, Schnermann JB and Briggs JP. 1997. Cyclooxygenase-2 is expressed in bladder during fetal development and stimulated by outlet obstruction. *Am J Physiol* **273** F538-F544.

Parkhouse HF, Barratt TM, Dillon MJ, Duffy PG, Fay J, Ransley PG, Woodhouse CR and Williams DI. 1988. Long-term outcome of boys with posterior urethral valves. *Br J Urol* **62** 59-62.

Perez-Brayfield MR, Gatti J, Berkman S, Eller D, Broecker B, Massad C, Kirsch A and Smith E. 2001. In utero intervention in a patient with prune-belly syndrome and severe urethral hypoplasia. *Urology* **57** 1178.

Peters CA, Bolkier M., Bauer SB, Hendren WH, Colodny AH, Mandell J and Retik AB. 1990. The urodynamic consequences of posterior urethral valves. *J Urol* **144** 122-126.

Peters CA, Carr MC, Lais A, Retik AB and Mandell J. 1992a. The response of the fetal kidney to obstruction. *J Urol* **148** 503-509.

Peters CA, Vasavada S, Dator D, Carr M, Shapiro E, Lepor H, McConnell J, Retik AB and Mandell J. 1992b. The effect of obstruction on the developing bladder. *J Urol* **148** 491-496.

Peters CA, Freeman MR, Fernandez CA, Shepard J, Wiederschain DG and Moses MA. 1997. Dysregulated proteolytic balance as the basis of excess extracellular matrix in fibrotic disease. *Am J Physiol* **272** R1960-R1965.

Podesta M, Ruarte AC, Gargiulo C, Medel R, Castera R, Herrera M, Levitt SB and Weiser A. 2002. Bladder function associated with posterior urethral valves after primary valve ablation or proximal urinary diversion in children and adolescents. *J Urol* **168** 1830-1835.

Poucell HS, Huang M, Bannykh S, Benirschke K and Masliah E. 2000. Fetal obstructive uropathy: patterns of renal pathology. *Pediatr Dev Pathol* **3** 223-231.

Prelich G, Tan CK, Kostura M, Mathews MB, So AG, Downey KM and Stillman B. 1987. Functional identity of proliferating cell nuclear antigen and a DNA polymerase-delta auxiliary protein. *Nature* **326** 517-520.

Qi BQ, Williams A, Beasley S and Frizelle F. 2000. Clarification of the process of separation of the cloaca into rectum and urogenital sinus in the rat embryo. *J Pediatr Surg* **35** 1810-1816.

Rabinowitz R, Peters MT, Vyas S, Campbell S and Nicolaides KH. 1989. Measurement of fetal urine production in normal pregnancy by real-time ultrasonography. *Am J Obstet Gynecol* **161** 1264-1266.

Razzaque MS, Ahsan N and Taguchi T. 2002. Role of apoptosis in fibrogenesis. *Nephron* **90** 365-372.

Reed JC. 2002. Apoptosis-based therapies. *Nat Rev Drug Discov* **1** 111-121.

Reinberg Y, de Castano I and Gonzalez R. 1992. Influence of initial therapy on progression of renal failure and body growth in children with posterior urethral valves. *J Urol* **148** 532-533.

Reinberg Y, Gonzalez R, Fryd D, Mauer SM and Najarian JS. 1988. The outcome of renal transplantation in children with posterior urethral valves. *J Urol* **140** 1491-1493.

Risdon RA and Woolf AS. 1998. Developmental defects and cystic diseases of the kidney. In *Heptinstall's Pathology of the Kidney*, 5th edn. Jeanette JC, Olson JL, Schwartz MM and Silva FG. Lippincott-Raven, Philadelphia, USA. 67-84.

Robertson AS, Griffiths C and Neal DE. 1996. Conventional urodynamics and ambulatory monitoring in the definition and management of bladder outflow obstruction. *J Urol* **155** 506-511.

Robertson AS, Griffiths CJ, Ramsden PD and Neal DE. 1994. Bladder function in healthy volunteers: ambulatory monitoring and conventional urodynamic studies. *Br J Urol* **73** 242-249.

Rohn JL, Hueber AO, McCarthy NJ, Lyon D, Navarro P, Burgering BM and Evan GI. 1998. The opposing roles of the Akt and c-Myc signalling pathways in survival from CD95-mediated apoptosis. *Oncogene* **17** 2811-2818.

Rohrmann D, Monson FC, Damaser MS, Levin RM, Duckett JW and Zderic SA. 1997a. Partial bladder outlet obstruction in the fetal rabbit. *J Urol* **158** 1071-1074.

Rohrmann D, Zderic SA, Duckett JW, Levin RM and Damaser MS. 1997b. Compliance of the obstructed fetal rabbit bladder. *Neurourol Urodyn* **16** 179-189.

Ross JH, Kay R, Novick AC, Hayes JM, Hodge EE and Streem SB. 1994. Long-term results of renal transplantation into the valve bladder. *J Urol* **151** 1500-1504.

Saito M and Miyagawa I. 2002. N(G)-nitro-L-arginine methylester, a nitric oxide synthase inhibitor, diminishes apoptosis induced by ischemia-reperfusion in the rat bladder. *Neurourol Urodyn* **21** 566-571.

Sakurai H, Matsuoka R, Furutani Y, Imamura S, Takao A and Momma K. 1996. Expression of four myosin heavy chain genes in developing blood vessels and other smooth muscle organs in rabbits. *Eur J Cell Biol* **69** 166-172.

Sambrook J, Fritsch EF and Maniatis T. 1987. *Molecular Cloning: a laboratory manual.* 2nd edn. Cold Spring Harbor Laboratory Press, Cold Spring Harbor, NY, USA.

Santarosa R, Colombel MC, Kaplan S, Monson F, Levin RM and Buttyan R. 1994. Hyperplasia and apoptosis. Opposing cellular processes that regulate the response of the rabbit bladder to transient outlet obstruction. *Lab Invest* **70** 503-510.

Santis WF, Sullivan MP, Gobet R, Cisek LJ, McGoldrick RJ, Yalla SV and Peters CA. 2000. Characterization of ureteral dysfunction in an experimental model of congenital bladder outlet obstruction. *J Urol* **163** 980-984.

Shi SR, Key ME and Kalra KL. 1991. Antigen retrieval in formalin-fixed, paraffin-embedded tissues: an enhancement method for immunohistochemical staining based on microwave oven heating of tissue sections. *J Histochem Cytochem* **39** 741-748.

Shimada K, Hosokawa S, Tohda A, Matsumoto F and Johnin K. 2000. Histology of the fetal prune belly syndrome with reference to the efficacy of prenatal decompression. *Int J Urol* **7** 161-166.

Smet PJ, Edyvane KA, Jonavicius J and Marshall VR. 1996. Neuropeptides and neurotransmitter-synthesizing enzymes in intrinsic neurons of the human urinary bladder. *J Neurocytol* **25** 112-124.

Smeulders N, Woolf AS, and Wilcox DT. 2001. Smooth muscle differentiation and cell turnover in mouse detrusor development. *J Urol* **167** 385-390.

Smith GH, Canning DA, Schulman SL, Snyder HM and Duckett JW. 1996. The long-term outcome of posterior urethral valves treated with primary valve ablation and observation. *J Urol* **155** 1730-1734.

Sotoudeh M, Li YS, Yajima N, Chang CC, Tsou TC, Wang Y, Usami S, Ratcliffe A, Chien S and Shyy JY. 2002. Induction of apoptosis in vascular smooth muscle cells by mechanical stretch. *Am J Physiol Heart Circ Physiol* **282** H1709-H1716.

Speakman MJ, Brading AF, Gilpin CJ, Dixon JS, Gilpin SA and Gosling JA. 1987. Bladder outflow obstruction-a cause of denervation supersensitivity. *J Urol* **138** 1461-1466.

Stefansson K, Wollmann RL and Moore BW. 1982. Distribution of S-100 protein outside the central nervous system. *Brain Res* **234** 309-317.

Stephens FD. 1983. *Congenital malformations of the urinary tract.* Praeger Publishers, New York, USA.

Susset JG and Regnier CH. 1981. Viscoelastic properties of bladder strips: standardization of a technique. *Invest Urol* **18** 445-450.

Sutherland RS, Baskin LS, Elfman F, Hayward SW and Cunha GR. 1997. The role of type IV collagenases in rat bladder development and obstruction. *Pediatr Res* **41** 430-434.

Sutherland RS, Baskin LS, Kogan BA and Cunha G. 1998. Neuroanatomical changes in the rat bladder after bladder outlet obstruction. *Br J Urol* **82** 895-901.

Suwanrath C, Suntharasaj T, Leetanaporn R and Mitarnun W. 2001. Prenatal diagnosis of fetal bladder outlet obstruction at Songklanagarind Hospital: report of 5 cases. *J Med Assoc Thai* **84** 1365-1371.

Suzuki H and Kokubun S. 1994. Subtypes of purinoceptors in rat and dog urinary bladder smooth muscles. *Br J Pharmacol* **112** 117-122.

Taki N, Taniguchi T, Okada K, Moriyama N Muramatsu I. 1999. Evidence for predominant mediation of alpha1-adrenoceptor in the tonus of entire urethra of women. *J Urol* **162** 1829-1832.

Tamura I, Rosenbloom J, Macarak E and Chaqour B. 2001. Regulation of Cyr61 gene expression by mechanical stretch through multiple signaling pathways. *Am J Physiol Cell Physiol* **281** C1524-C1532.

Tanagho EA. 1972. Surgically induced partial urinary obstruction in the fetal lamb. II. Urethral obstruction. *Invest Urol* **10** 25-34.

Theobald RJ. 1992. Subclasses of purinoceptors in feline bladder. *Eur J Pharmacol* **229** 125-130.

Thomas DF. 2001. Prenatal diagnosis: does it alter outcome? *Prenat Diagn* **21** 1004-1011.

Thomson AA, Timms BG, Barton L, Cunha GR and Grace OC. 2002. The role of smooth muscle in regulating prostatic induction. *Development* **129** 1905-1912.

Triguero D, Prieto D and Garcia-Pascual A. 1993. NADPH-diaphorase and NANC relaxations are correlated in the sheep urinary tract. *Neurosci Lett* **163** 93-96.

Truong LD, Choi YJ, Tsao CC, Ayala G, Sheikh-Hamad D, Nassar G and Suki WN. 2001. Renal cell apoptosis in chronic obstructive uropathy: the roles of caspases. *Kidney Int* **60** 924-934.

Uvelius B, Persson L and Mattiasson A. 1984. Smooth muscle cell hypertrophy and hyperplasia in the rat detrusor after short-time infravesical outflow obstruction. *J Urol* **131** 173-176.

Van Molle W, Denecker G, Rodriguez I, Brouckaert P, Vandenabeele P and Libert C. 1999. Activation of caspases in lethal experimental hepatitis and prevention by acute phase proteins. *J Immunol* **163** 5235-5241.

Veis DJ, Sorenson CM, Shutter JR and Korsmeyer SJ. 1993. Bcl-2-deficient mice demonstrate fulminant lymphoid apoptosis, polycystic kidneys, and hypopigmented hair. *Cell* **75** 229-240.

Vereecken RL and Van Nuland T. 1998. Detrusor pressure in ambulatory versus standard urodynamics. *Neurourol Urodyn* **17** 129-133.

Volmar KE, Fritsch MK, Perlman EJ and Hutchins GM. 2001. Patterns of congenital lower urinary tract obstructive uropathy: relation to abnormal prostate and bladder development and the prune belly syndrome. *Pediatr Dev Pathol* **4** 467-472.

Wagg A and Fry CH. 1999. Visco-elastic properties of isolated detrusor smooth muscle. *Scand J Urol Nephrol Suppl* **201** 12-18.

Wagoner LE and Walsh RA. 1996. The cellular pathophysiology of progression to heart failure. *Curr Opin Cardiol* **11** 237-244.

Wang N, Ostuni E, Whitesides GM and Ingber DE. 2002. Micropatterning tractional forces in living cells. *Cell Motil Cytoskeleton* **52** 97-106.

Wang P, Luthin GR and Ruggieri MR. 1995. Muscarinic acetylcholine receptor subtypes mediating urinary bladder contractility and coupling to GTP binding proteins. *J Pharmacol Exp Ther* **273** 959-966.

Webb RJ, Griffiths CJ, Ramsden PD and Neal DE. 1990. Measurement of voiding pressures on ambulatory monitoring: comparison with conventional cystometry. *Br J Urol* **65** 152-154.

Welham SJ, Wade A and Woolf AS. 2002. Protein restriction in pregnancy is associated with increased apoptosis of mesenchymal cells at the start of rat metanephrogenesis. *Kidney Int* **61** 1231-1242.

Westfall TD, Kennedy C and Sneddon P. 1997. The ecto-ATPase inhibitor ARL 67156 enhances parasympathetic neurotransmission in the guinea-pig urinary bladder. *Eur J Pharmacol* **329** 169-173.

Westfall TD, Sarkar S, Ramphir N, Westfall DP, Sneddon P and Kennedy C. 2000. Characterization of the ATPase released during sympathetic nerve stimulation of the guinea-pig isolated vas deferens. *Br J Pharmacol* **129** 1684-1688.

Wheatley JM, Stephens FD and Hutson JM. 1996. Prune-belly syndrome: ongoing controversies regarding pathogenesis and management. *Semin Pediatr Surg* **5** 95-106.

Wilson MR. 1998. Apoptosis: unmasking the executioner. *Cell Death Differ* **5** 646-652.

Wintour EM, Alcorn D, Butkus A, Congiu M, Earnest L, Pompolo S and Potocnik SJ. 1996. Ontogeny of hormonal and excretory function of the meso- and metanephros in the ovine fetus. *Kidney Int* **50** 1624-1633.

Wintour EM, Laurence BM and Lingwood BE. 1986. Anatomy, physiology and pathology of the amniotic and allantoic compartments in the sheep and cow. *Aust.Vet J* **63** 216-221.

Winyard PJ, Nauta J, Lirenman DS, Hardman P, Sams VR, Risdon RA and Woolf AS. 1996a. Deregulation of cell survival in cystic and dysplastic renal development. *Kidney Int* **49** 135-146.

Winyard PJ, Risdon RA, Sams VR, Dressler GR and Woolf AS. 1996b. The PAX2 tanscription factor is expressed in cystic and hyperproliferative dysplastic epithelia in human kidney malformations. *J Clin Invest.* **98** 451-459.

Wlodek ME, Challis JR and Patrick J. 1988. Urethral and urachal urine output to the amniotic and allantoic sacs in fetal sheep. *J Dev Physiol* **10** 309-319.

Wlodek ME, Thorburn GD and Harding R. 1989. Bladder contractions and micturition in fetal sheep: their relation to behavioral states. *Am J Physiol* **257** R1526-R1532.

Woolf AS and Thiruchelvam N. 2001. Congenital obstructive uropathy: Its origin and contribution to end- stage renal disease in children. *Adv Ren Replace Ther* **8** 157-163.

Workman SJ and Kogan BA. 1990. Fetal bladder histology in posterior urethral valves and the prune belly syndrome. *J Urol* **144** 337-339.

Wu C, Bayliss M, Newgreen D, Mundy AR and Fry CH. 1999. A comparison of the mode of action of ATP and carbachol on isolated human detrusor smooth muscle. *J Urol* **162** 1840-1847.

Yang B, Johnson TS, Thomas GL, Watson PF, Wagner B, Furness PN and El Nahas AM. 2002. A shift in the Bax/Bcl-2 balance may activate caspase-3 and modulate apoptosis in experimental glomerulonephritis. *Kidney Int* **62** 1301-1313.

Yang SP, Woolf AS, Quinn F and Winyard PJ. 2001. Deregulation of renal transforming growth factor-β1 after experimental short-term ureteric obstruction in fetal sheep. *Am J Pathol* **159** 109-117.

Yin XM, Oltvai ZN and Korsmeyer SJ. 1994. BH1 and BH2 domains of Bcl-2 are required for inhibition of apoptosis and heterodimerization with Bax. *Nature* **369** 321-323.

Young HH and Frantz WA. 1919. Congenital obstruction of the posterior urethra. *J Urol.***3** 289-365.

Zha J, Harada H, Yang E, Jockel J and Korsmeyer SJ. 1996. Serine phosphorylation of death agonist BAD in response to survival factor results in binding to 14-3-3 not BCL-X(L). *Cell* **87** 619-628.

Zhao M, Bo X, Neely CF and Burnstock G. 1996. Characterization and autoradiographic localization of [3H] alpha,beta- methylene ATP binding sites in cat urinary bladder. *Gen Pharmacol* **27** 509-512.

Zhivotovsky B, Burgess DH, Vanags DM and Orrenius S. 1997. Involvement of cellular proteolytic machinery in apoptosis. *Biochem Biophys Res Commun* **230** 481-488.

9. Acknowledgements

I would primarily like to thank my three supervisors, Professor Adrian S Woolf, Mr Peter M Cuckow and Professor Chris H Fry. Professor Woolf has been a constant source of knowledge and encouragement; he has taught me many scientific principles, how to interpret data and the importance of meticulous attention to detail and consistency. Mr Cuckow has been full of enthusiasm and ingenuity and a source of passion for the project and my ideas; his expert surgical skills have also been incredibly valuable. Profeesor Fry has been very generous and thorough with his teaching of physiology and tissue physics; his intelligence is often hard to keep up with. I thank all three for their approachability and support during my research fellowship.

Special thanks also to Margaret Godley. An excellent and thorough clinical scientist, she has always shown a keen interest in the project and my research fellowship. She has provided her time and expertise for many valuable discussions. Special mention should also go to Dr Peter Nyirady who performed the initial set of experiments and got the ball rolling. I also acknowledge the help of Donald Peebles and Anna David of the Department of Obstetrics and Gynaecology, University College London, for their collaboration in the project and for teaching me sheep husbandry and anaesthesia, Clare Taylor for assistance during sample collection and urine biochemistry and Lectromed for loan of the equipment used in the filling cystometry experiments.

I would also like to thank my funding bodies. I thank The Special Trustees of Great Ormond Street Hospital and the Royal College of Surgeons of England for funding me

during my research training. In addition, I am grateful for the awards of The Great Ormond Street Hospital for Children NHS Trust/Institute of Child Health Science Development Initiative Pump-priming award and the Royal College of Surgeons of England Pump-priming award that enabled the purchase of the radiotelemetry equipment.

Thanks also goes to those I have worked with in the laboratories of the Nephro-Urology Unit, Institute of Child Health and the Division of Applied Physiology, Institute of Urology, for teaching me laboratory techniques and for enjoyable discussions of research findings. Particular thanks go to Shuman Haq, David Long, Liam McCarthy, Karen Price, Naima Smeulders, Vanita Shah, Simon Welham, Paul Winyard, Richard Wu and Hai Tao Yuan.

Finally, I would like to thank the technicians at the Royal Veterinary College for providing advice and an excellent standard of care.

10. Appendices

10.1 Preliminary experiments

Initial experiments were performed by Dr Peter Nyirady and Mr Peter Cuckow. These experiments provided me with preliminary fetal ovine bladder samples (n=6 *sham* male and n=6 *obstructed* male) that allowed me to perform my initial molecular biology experiments. Remaining samples and experiments, and all work described in this thesis, was performed by myself.

10.2 Publications

10.2.1 Papers

The following papers were accepted for publication during my research fellowship. Reprints, and any future publications, are/will be enclosed at the end of the thesis.

1. Nyirady P, Thiruchelvam N, Fry CH , Godley ML, Winyard PJD, Peebles DM, Woolf AS, Cuckow PM. The effect of fetal sheep in utero bladder outflow obstruction on detrusor contractility, compliance and innervation. *J Urol* 2002 168 1615-1620

2. Woolf AS, Thiruchelvam N. Congenital obstructive uropathy – its origin and contribution to end-stage renal failure in children. *Advances in Renal Replacement Therapy* 2001 8 157-163

3. Thiruchelvam N, Nyirady P, Peebles D, Fry CH, Cuckow PM, Woolf AS. Urinary outflow obstruction increases apoptosis and deregulates Bcl-2 and Bax expression in the fetal ovine bladder. *Am J Path, in press*

4. Thiruchelvam N, Wu C, David A, Woolf AS, Cuckow PM, Fry CH. Neurotransmission and visco-elasticity in the ovine fetal bladder after in utero bladder outflow obstruction. *Am J Physiol, in press*

10.2.2 Abstracts

The following have been presented or accepted for presentation. The full abstracts follow.

1. Thiruchelvam N, Nyirady P, Fry CH, Peebles DM, Godley ML, Winyard PJD, Woolf AS, Rodeck CH, Cuckow PM. Posterior urethral valves in an animal model: electromechanical properties of detrusor smooth muscle. *British Journal of Urology* 2001 88 Suppl 1 66-67

2. Thiruchelvam N, Nyirady P, Fry CH, Peebles DM, Cuckow PM, Woolf AS. Cell turnover in the developing and obstructed fetal bladder. *British Journal of Urology* 2002 89 Suppl 2 69

3. Nyirady P, Thiruchelvam N, Fry CH, Cuckow P. Electromechanical properties of detrusor smooth muscle in the developing experimental animal model. *European Urology Suppl* 2002 1 p24

4. Wu C, Thiruchelvam N, Sui G, Fry CH. Effect of bladder outflow obstruction on the carbachol-induced $[Ca^{2+}]_i$ rise in a fetal sheep model. *The Journal of Physiology (London)* 2002 543P p75

5. Experimental fetal urinary flow impairment disrupts cell turnover, extracellular matrix and innervation in the developing urinary bladder. Thiruchelvam N, Nyirady P, Peebles D, Cuckow PM, Woolf AS. Plenary Session, The Renal Association, London

6. Biochemical outcomes in a fetal sheep model of bladder outlet obstruction. Taylor C, Thiruchelvam N, Nyirady P, Cuckow P, Foxall P. Presented at the Urological Research Society, London, 2002.

7. Natural fill, radiotelemetered fetal sheep cystometry. Thiruchelvam N, Godley M, Farrugia MK and Cuckow PM. Presented at the Urological Research Society, London, 2003.

8. Perturbation of (cholinergic, purinergic and nitrergic) neurotransmission in the ovine fetal bladder after in utero bladder outflow obstruction. Thiruchelvam N, Cuckow PM, Wu C, David A, Woolf AS, Fry CH. Accepted for the European Association of Paediatric Urology, Madrid, 2003.

PUV in an animal model - electromechanical properties of detrusor smooth muscle

N. Thiruchelvam, P. Nyirady, C.H. Fry, D.H. Peebles, M.L. Godley, P.J.D. Winyard, A.S. Woolf, C.H. Rodeck and P.H. Cuckow *Institute of Child Health, Institute of Urology and Nephrology, and Department of Obstetrics and Gynaecology, UCL, London, UK*

Introduction: PUV leads to prenatal infravesical obstruction that causes developmental abnormalities to the upper and lower urinary tracts. This study examined the fetal pathophysiology of this condition, with reference to the electromechanical properties of the bladder. **Materials and methods** A fetal lamb model with induced partial infravesical obstruction was used. In three fetuses BOO was induced in mid-gestation (78-80 days) and detrusor smooth muscle function examined *in vitro* 4 weeks later. Four sham-operated fetuses underwent a similar procedure. Smooth muscle function was characterized by: (i) constructing nerve-mediated (sensitive to 1 μmol/L tetrodotoxin) force-frequency relationships in the presence and absence of atropine (1 μmol/L) or α-β-methylene-ATP (ABMA, 10 μmol/L); and (ii) contractures elicited by KCl (120 mmol/L) and carbachol (10 μmol/L). **Results** Nerve-mediated atropine-resistant contractions were absent in either group. The absolute force (mN/mg) developed by obstructed bladder strips was significantly ($P < 0.05$) less than that from sham-operated fetuses. This was the case when electrical stimulation (0.65, SD 0.18 vs 2.98, 11.66), KCl (0.60, 0.21 vs 2.39, 0.66), carbachol (2.91, 1.03 vs 8.28, 0.54) or ABMA (0.63 vs 2.94, 2.15) were used. The ratio of tension generated by carbachol and electrical stimulation was significantly ($P < 0.05$) greater in strips from obstructed fetuses (2.3, 0.40 vs 1.3, 0.19). There was no difference in ratio of the tension produced by carbachol and KCl (5.5, 3.2 vs 3.6, 0.8; obstructed vs sham). **Conclusion** In the obstructed fetus, detrusor smooth muscle contractility is significantly impaired. The greater proportional decrease of nerve-mediated contractions suggests that there is a relative denervation of the tissue. These findings are similar to those from experiments with obstructed human bladder. This model may therefore used to assess the consequences of PUV in boys.

Cell turnover in the developing and obstructed fetal bladder.

N Thiruchelvam, P Nyirady, CH Fry[#], DM Peebles[*], PM Cuckow and AS Woolf *Nephro-urology Unit, Institute of Child Health, [#]Division of Applied Physiology, Institute of Urology and [*]Fetal Medicine Unit, Department of Obstetrics and Gynaecology, University College London, UK.*

Background : Posterior urethral valves (PUV) is a congenital anomaly that results in postnatal dysfunction of the urinary bladder, ureters and kidneys: PUV in the commonest cause of end-stage renal failure in children. We have established an experimental fetal model resembling human PUV; after 30 days in utero obstruction, we found impaired ex vivo bladder detrusor muscle contractility caused in part by defective innervation. In the current study, we have explored cell turnover in these fetal bladders. **Methods:** At mid-gestation, we produced partial bladder outflow obstruction in fetal male sheep (term is 145 days) by placement of an omega-shaped silver ring around the urethra and urachal ligation (n=6). Sham operated male fetuses had urethral and urachal exposure only (n=6). Pregnant ewes were sacrificed at 30 days following the procedure and fetal bladders collected at post-mortem. Basic histology was assessed by Masson's Trichrome staining. To assess proliferation, sections were immunostained for proliferationg cell nuclear

antigen (PCNA), a DNA polymerase associated protein expressed in high levels in the S phase of the cell cycle and used as a marker of cellular proliferation. Cell death was determined by the TUNEL method to assess apoptosis; the method employs a fluorescein-labelled nucleotide that attaches onto strand breaks in the digested DNA found in apoptotic nuclei. Nuclei were counted and expressed as the proportion of proliferating nuclei (stained brown by diaminobenzidine) per 1000 cells and as the proportion of apoptotic nuclei (fluorescent nuclei) per 1000 cells. **Results:** Versus sham-operated controls (n=6), obstructed urinary tracts had dysplastic kidneys and hydonephrosis, and their bladders (n=6) were significantly ($p<0.001$) longer and heavier (4.4±0.6 vs 0.8±0.2 g/kg, factored for fetal weight). Histologically, obstructed bladder urothelium was flattened, the lamina propria appeared more acellular and detrusor muscle bundles were separated by increased connective tissue. As assessed by proliferating cell nuclear antigen expression, we found a significant ($p<0.016$) increase in the proportion of proliferating cells in the detrusor layer of obstructed bladders (675±16 vs 437±165 per 1000 cells). By in-situ end-labeling (TUNEL method), we detected a significant ($p<0.001$) increase in the proportion of apoptotic cells within the obstructed detrusor (3.1±0.7 vs 1.4±0.9 per 1000 cells) and obstructed lamina propria (2.9±0.7 vs 1.1±0.6 per 1000 cells). Finally, we discovered a new cell population unique to obstructed bladders; this new population was located adjacent to obstructed detrusor muscle bundles with almost half the nuclei proliferating (447±99 per 1000 cells), as assessed by PCNA immunohistochemistry. **Conclusions :** We have shown that proliferation and apoptosis occur in the normal developing fetal bladder (at 105 days gestation); hence these opposing cellular processes have an important role in tissue modelling during detrusor development. In addition, pathology, in particular, partial urinary flow impairment in utero, results in significant perturbation of bladder cell turnover. There is an increase in proliferation and apoptosis in the obstructed fetal bladder detrusor and the development of a new proliferating cell population around obstructed muscle bundles. These results may in part account for the persistent postnatal bladder dysfunction found in boys with posterior urethral valves.

Electromechanical properties of detrusor smooth muscle in developing experimental animal model

P Nyirády[□], N Thiruchelvam[□], CH Fry[•], M Godley[□], PJD Winyard[□], DM Peebles[°], AS Woolf[□], PM Cuckow[□]

Nephro-Urology Unit, Institute of Child Health[□]; Division of Applied Physiology, Institute of Urology & Nephrology[•] and Department of Obstetric & Gynaecology[°], University College London, London, U.K.

Introduction & objectives: The ontogeny of bladder function has been already investigated in fetal calf and a protective system has been found which might be responsible for low sustained intravesical pressure, it is thought that this 'relaxation factor' prevents the bladder from reaching the maximal intravesical pressure. The developmental difference of bladder compliance is also well characterised as it was found that decreasing bladder compliance as gestation progresses. However, little is known about the electromechanical properties of detrusor muscle in the normal developing fetal sheep. However, only after understanding what occurs during normal fetal development can we then study and interpret the pathophysiology of experimental fetal models of

bladder disease. **Material & methods:** To examine bladder function in different gestational age, date-mated Romney Marsh ewes, bearing fetuses between 70 and 140 days of gestation (term in this breed is 145 days) were examined. We investigated fetal bladders from three different gestation age groups. The early gestation group were fetuses of 70 days of gestation (n=6). The mid-gestation group were aged between 105 and 110 days of gestation (n=10). The late gestation group consist of fetuses between 135 and 140 days of gestation (n=6). None of the fetuses underwent urogenital instrumentation. Smooth muscle function was characterised by: i) constructing nerve-mediated (1μM tetrodotoxin-sensitive) force-frequency relationships in the presence and absence of atropine (1μM), or α,β-methylene ATP (ABMA, 10μM) and ii) contractures elicited by KCl (120mM), carbachol (10μM) and ABMA (10μM). **Results:** There was little atropine-resistance to the nerve-mediated contractions in all groups. The absolute force developed electrical stimulation (mN*mg-1) showed a statistically significant increase as fetuses developed in age between the different groups. The same trend was found when stimulation was compared in 16 Hz frequency or by the calculated maximal tension. However there was a smaller increase between the early- and mid-gestation groups in tension measured by 16 Hz frequency (T16Hz mean 2.525 mN*mg-1 vs. 3.641 mN*mg-1, p=0.005) than between the mid- and late gestation groups (T16Hz mean 3.641 mN*mg-1 vs. 4.377 mN*mg-1, p=0.041). KCl response showed a similar trend with 16Hz stimulation. Contractions recorded in the presence of carbachol for one minute increased between the early- and mid-gestation groups but remained the same between the mid- and late-gestation groups (Tcarbachol mean 3.915 mN*mg-1 vs. 9.096 mN*mg-1; p=5.26*10-7 and 9.096 mN*mg-1 vs. 8.647 mN*mg-1; p=0.605). The same trend was seen by introducing ABMA (TABMA mean 1.039 mN*mg-1 vs. 2.638 mN*mg-1; p=0.059 and 2.638 mN*mg-1 vs. 2.451mN*mg-1; p=0.734). Paired measurements in the same strips also showed that the ratio of tension generated by carbachol and KCl or tension generated by 16 Hz frequency electrical stimulation was significantly ($p<0.05$) greater in strips from mid- than in early- gestation fetuses. However the same ratio between carbachol and KCl did not show a difference with the ratio between carbachol and T16Hz decreasing significantly ($p<0.05$) between the same age groups. There was no significant difference in the carbachol/ ABMA ratios between the different age groups. **Conclusions:** We found a continuous increase in nerve mediated contractions e.g. T16Hz, Tmax and in the presence of KCl, with increasing gestational age. These findings suggest that there is a continuous increase in the sensitivity, and absolute number of nerves existing in the detrusor smooth muscle during development. However, it appears that receptor mediated contractions don't change between mid- and late gestation. For example, Tcarbachol contractions remain stable in this later period, suggesting that receptors involved in bladder smooth muscle excitation develop earlier than nerves.

Effect of bladder outflow obstruction on the carbachol-induced $[Ca^{2+}]_i$ rise in a foetal sheep model

C Wu, N Thiruchelvam*, G Sui, CH Fry
*Department of Medicine and Institute of Urology, *Institute of Child Health, University College London, London W1W 7EY*

Introduction. Posterior urethral valves (PUV) result in congenital bladder outflow obstruction exclusively affecting boys (Woolf & Thiruchelvam 2001). As a consequence

of this pre-natal obstruction, these boys often have persistent post-natal bladder dysfunction in later life, with resultant end-stage renal failure and delayed achievement of urinary continence. To understand the pathophysiology of PUV, this study examined the role of intracellular Ca^{2+} ($[Ca^{2+}]_i$) regulation in altered contractility using a foetal lamb model with induced in utero bladder outflow obstruction. **Methods.** Partial bladder outflow obstruction was induced in male foetal sheep by placement of an omega-shaped urethral ring and urachal ligation midway through gestation, at 75 days (full-term 150 days) and animals sacrificed 30 days after surgery (105 days). Sham-operated control foetuses underwent urethral and urachal exposure only. Detrusor smooth muscle was obtained from the mid-region of bladders after removal of mucosa and serosa. Isometric twitch tension was measured from small muscle strips (less than 1mm in diameter) and $[Ca^{2+}]_i$ measured in single dissociated myocytes loaded with the fluorescent indicator Fura-2 (Wu & Fry 1998). Contraction and $[Ca^{2+}]_i$ rise were elicited by carbachol, an analogue of the functional neurotransmitter acetylcholine. Data were expressed as means±SE and Student's *t*-test used to test the statistical significance between ~~the~~ data sets. **Results.** In multicellular preparations, the force of contraction in response to carbachol (10 μM) was significantly reduced in obstructed foetal bladders (obstructed: 2.4±0.5 mN/mg, n=4; sham-operated control: 4.7±0.2 mN/mg, n=3; $p<0.05$). In isolated detrusor cells, 10 μM carbachol elicited a $[Ca^{2+}]_i$ transient from a resting value of 118±8 nM with an net increase of 629±86 nM (n=16), whilst in cells from obstructed bladders, the net rise was only 414±59 nM from a resting value of 144±2 nM (n=20, $p<0.05$). Further experiments determined the concentration-dependence of the carbachol-induced $[Ca^{2+}]_i$ rise over a range from 0.03 to 100 μM. The minimal effective concentration was around 0.1μM and the maximal effect around 10μM. An EC_{50} of 0.8±0.2 μM (n=6) was obtained from the dose-response relationship for the control group, whilst the relationship was shifted to the right in the obstruction group (EC_{50}: 2.4±0.5 μM, n=6; $p<0.05$). **Conclusion.** These results demonstrate that bladder outflow obstruction during foetal development results in a reduced mucarinic receptor efficacy and sensitivity in detrusor myocytes. The impaired Ca^{2+} regulation coupled to the receptor activation in these cells may in part account for the reduced bladder contractility found after in utero bladder obstruction.**References.** Woolf AS and Thiruchelvam N (2001). Adv Ren Replace Ther 8: 157-163. Wu C and Fry C H (1998). J Physiol 508: 131-143.

Experimental fetal urinary flow impairment disrupts cell turnover, extracellular matrix and innervation in the developing urinary bladder.

*N. Thiruchelvam, P. Nyirady, *D. Peebles, P.M. Cuckow and A.S. Woolf, Nephro-Urology Unit, Institute of Child Health and *Fetal Medicine Unit, Department of Obstetrics and Gynaecology, University College London, London, UK*

Posterior urethral valves (PUV) is associated with congenital malformation and postnatal dysfunction of the urinary bladder, ureters and kidneys: PUV accounts for 25% of boys with end-stage renal failure. We recently established a model resembling human PUV using surgical urethral partial obstruction and urachal complete ligation in male fetal sheep at 70 days gestation (term being 145 days) when bladder and metanephros are still developing: after 40 days in utero obstruction, we found impaired ex vivo bladder detrusor muscle contractility. In the current study, we explored cell turnover, extracellular matrix and innervation of these fetal bladders. Versus sham-operated controls (n=6),

obstructed urinary tracts had dysplastic kidneys and hydonephrosis, and their bladders (n=6) were significantly longer and heavier. Histologically, obstructed bladder urothelium was flattened, lamina propria vasculature was attenuated and detrusor muscle bundles were separated by increased connective tissue. As assessed by proliferating cell nuclear antigen expression, we found a significant ($p<0.016$) increase in the proportion of proliferating cells in the detrusor layer of obstructed bladders (mean 68% versus 44% cells in controls). By in-situ end-labeling, we detected a significant ($p<0.001$) increase in the proportion of apoptotic cells within the obstructed detrusor (0.31% versus 0.14%) and lamina propria (0.29% versus 0.11%). By immunohistochemistry, obstructed bladders exhibited increased collagen I and elastin in lamina propria and between detrusor muscle bundles, with less collagen III expression. Finally, a profound decrease of bladder innervation was noted, especially in the lamina propria, using S100 and PGP 9.5 immunostaining. Hence, relatively short-term partial urinary flow impairment in utero causes significant perturbation of bladder morphogenesis and cell turnover. We postulate that the previously observed decrease in ex vivo detrusor contractility is in part caused by a combination of defective innervation and an imbalance of extracellular matrix.

Biochemical Outcomes In A Fetal Sheep Model Of Bladder Outlet Obstruction

C.Taylor, N.Thiruchelvam*, P.Nyirady*, P.Cuckow*, P.Foxall, Institute of Urology and Nephrology and * Nephro-Urology unit, Institute of Child Health,University College London, UK

Introduction. Posterior urethral valves (PUV) affects 1 in 5000 male births and is the commonest cause of end-stage renal failure in children. We have established an experimental model of fetal bladder outflow obstruction to study the potential effects of PUV on the developing urinary tract[1]. We have previously documented that increased cell turnover, decreased detrusor contractility and reduced bladder innervation occurs in this model. The aim of the current work was to study the biochemical response of bladder outflow obstruction by measurement of urine biochemistry. **Method.** Partial bladder outflow obstruction was created at 75 days gestation (term is 145 days) by placement of an omega-shaped silver ring around the urethra and urachal ligation. Sham operated fetuses had urethral and urachal exposure only. Fetal urine was collected at initial operation and at 105 days gestation. Nineteen urine samples were available for analysis; 7 baseline samples taken at 75 days and 6 samples from both sham and obstructed fetuses at 105 days. Conventional urinalysis was carried out on all samples using flame photometry and micro-osmometry. Selected samples were also analysed using high resolution ^{1}H nuclear magnetic resonance (NMR) spectroscopy[2]. Statistical significance between sham and obstructed fetuses was assumed if $p< 0.05$ using Student's t test. **Results.** The table below shows mean urinary values obtained for the 3 study groups.

	Control 75d	Sham 105d	Obs 105d
U. Sodium (mM)	50 (n=7)	30 (n=6)	79 (n=6)*
U. Potassium (mM)	6.3 (n=7)	7.5 (n=6)	7.8 (n=6)^{ns}
U. Osmolality (mOsm)	124 (n=7)	107 (n=6)	182 (n=6)*
U. Creatinine (mM)	0.30 (n=5)	0.67 (n=4)	1.23 (n=5)$^{\#}$
U. Lactate (mM)	0.69 (n=5)	0.50 (n=4)	0.95 (n=5)^{ns}

*p=<0.005, $^{\#}$p=<0.05, ^{ns}p=not significant, when obstructed fetuses were compared with shams at 105 days.

Discussion. Our data shows that urine sodium and osmolality decreases and urine creatinine increases with gestational age in normal (sham) fetuses in parallel with renal maturation. Conversely, urine sodium and osmolality increases in obstructed fetuses with gestational age as observed in human fetuses with urinary tract obstruction[3]. We also observed an increase in urine creatinine with obstruction, this possibly being due to increased renal blood flow[4]. Only one obstructed fetus showed evidence of renal damage as identified by NMR[2]. Taken together, our data suggest that fetal bladder outflow obstruction results in delayed renal maturation but renal function is preserved. The work described here demonstrates the validity of this animal model for PUV and will form the basis of further investigations into the biochemical sequelae of bladder outflow obstruction *in utero*. **References**. 1. Nyirady P, Fry CH, Peebles, DM, Godley ML *et al.* Electromechanical properties of detrusor smooth muscle in developing and obstructed bladders – animal model. Presented at the Urological Research Society Meeting, London, January 5th 2001. 2. Foxall PJD, Bewley S, Neild GH, Rodeck, CH, Nicholson, JK. Analysis of neonatal and fetal urine using proton nuclear magnetic resonance spectroscopy. *Arch Dis Child* 1995;73: F153-7. 3.Nicolini U, Fisk NM, Rodeck CH, Beacham J. Fetal urine biochemistry: an index of renal maturation and dysfunction. *Br J Obstet Gynaecol* 1992; 99(1):46-50. 4.Bogaert GA, Gluckman GR, Mevorach RA, Kogan BA. Renal preservation despite 35 days of partial obstruction in the fetal lamb. *J Urol* 1995; 154: 694-9.

Natural fill, radiotelemetered fetal sheep cystometry

N Thiruchelvam, M Godley, M Farrugia, P Cuckow
Nephro-Urology Unit, Institute of Child Health, University College London, London, UK

Introduction. In utero bladder outflow obstruction, such as that caused by posterior urethral valves, can result in bladder and renal morbidity post-natally; however, the affects on developing bladder function in utero are poorly understood. Published studies of experimental fetal urodynamics have used external catheters with artificial filling of the bladder, or by forced pharmacological diuresis; or else cystometry in excised whole fetal bladders or cystometry in fetuses at post-mortem. This results in numerous difficulties. Radiotelemetered cystometry in the adult bladder has been used successfully but has not been applied to fetal animals. The aim of our study was to determine if fetal cystometric studies by radiotelemetry is feasible thus providing a means of monitoring the influence over time of in utero experimental bladder outflow obstruction. **Methods.** The procedure required fetal sheep surgery and anesthesia. Radiotelemetry implants (PhysioTel ® Multiplus ™ TL Series Implants, Data Sciences International, MN, USA)

employ two fluid-filled catheters that transmit pressure fluctuations to the implant body. Data transmitted from the implant is transferred using radio waves to a receiver that passes this information onto a Data Exchange Matrix and stored in the Dataquest A.R.T. system (a computer-based data acquisition system). The latter allows visualization of pressure recordings, accurate measurement of parameters and export of data to Microsoft Office Excel to derive traces by subtraction. We used four fetuses and used different methods of catheter placement to optimize the technique. **Results.** Recordings were possible in three of the four experiments. In two experiments, ex vivo filling cystometry showed identical pressure recordings comparing the radiotelemetry method with the conventional method using a chart recorder and water filled external transducer. During observation, we noted: 1) Quiet periods with no pressure rises, 2) Synchronous activity in the bladder and abdomen and 3) Discriminate activity, only associated with bladder activity. We observed four patterns of discriminate bladder activity, defined as: 1) *Void* (105-140 days gestation): sustained elevations of detrusor pressure with superimposed high frequency, low amplitude activity, 2) *Immature void* (75-105 days gestation): episodes of high frequency, low amplitude activity with or without elevations of baseline pressure, 3) *Staccato activity*: short (20-40 seconds) phasic elevations of pressure that were a) discrete, b) in trains or c) observed pre- and post-void and 4) *'Unstable' type activity*: very short (<5 seconds) elevations of pressure. **Discussion.** Radiotelemetry cystometry for long-term monitoring is feasible in the experimental fetus without inducing mortality nor any morbidity or inhibition of growth. There seems to be excellent synchrony between bladder and abdominal pressures. The method currently does not allow detection of urine flow, but can discriminate reproducible patterns of detrusor activity. Recorded 'voiding' types were consistent between experiments and as reported in other animal studies. The method appeared to differentiate between genders and during development in the frequency and duration of the 'voiding' pattern.

Perturbation of (cholinergic, purinergic and nitrergic) neurotransmission in the ovine fetal bladder after in utero bladder outflow obstruction.

N Thiruchelvam, PM Cuckow, C Wu, A David, AS Woolf, CH Fry

Introduction & objectives. In an attempt to investigate the effects of in utero bladder outflow obstruction on the developing fetal bladder, we have developed an experimental ovine model; we have previously described how this fetal bladder becomes hypocontractile and denervated following intravesical obstruction. The current study was designed to investigate neurotransmission in the developing fetal bladder and to determine, if any, perturbation of neurotransmission that may occur after bladder outflow obstruction. **Material & methods.** In utero intravesical obstruction was induced by placement of an omega shaped silver ring around the ovine male abdominal urethra and ligation of the urachus (n=5). Sham procedure in ovine male fetuses was by urethral and urachal exposure only (n=5). Detrusor smooth muscle function was assessed using bladder strips (diameter <1mm) after removal of the urothelium and adventitia by microdissection. Muscle strips were electrically-stimulated and also electrically stimulated in the presence of tetrodotoxin (1 mM); atropine (1 mM), adenosine (1mM), carbachol (10 μM) or carbachol (10 μM) with 1H-[1,2,4]oxadiazolo[4,3-a]quinoxalinme-1-one (1 μM) (ODQ) or exposed unstimulated to carbachol (1 μM, 3 μM,10 μM and 30 μM) or adenosine (1mM) with carbachol (1 μM). To determine the effect, if any, of the

urothelium, whole wall bladder strips (diameter <1mm) were also studied with electrical filed stimulation in the presence or absence of ODQ (1 μM). **Results.** Force-frequency relations revealed the obstructed bladder to be hypocontractile to electrical filed stimulation and to carbachol; carbachol dose-response revealed no difference to muscarinic sensitivity implying no supersensitivity. Adenosine reduced significantly tension produced by electrical field stimulation in both groups but 1 mM adenosine had no significant effect on the magnitude of the carbachol contracture implying that adenosine has no direct effect on muscle contractility but on earlier steps in the generation of contraction. Atropine-resistant contractions were recorded in three obstructed bladders and no sham bladders (numbers insufficient for statistics). Relaxant responses were evident in both groups and in the presence of ODQ, were significantly diminished. The effect of ODQ was variable in different preparations in either group.The presence of mucosa had a significant dampening effect on muscle contractility in the sham group only and this effect was nitrergic in nature as tested by ODQ. **Conclusions.** In the current study, we have reproduced anatomical and physiological features of fetal ovine bladder outflow obstruction suggesting our model is reliable and reproducible. Furthermore, we have shown the existence of cholinergic, purinergic and nitrergic systems in the normal ovine fetal bladder and perturbation to some extent of these systems after in utero bladder outflow obstruction.